





This is to certify that the

thesis entitled

INDUCED ELECTROMAGNETIC FIELDS IN CONDUCTING BODIES IRRADIATED BY MAGNETIC FIELDS

AND MICROWAVES

presented by

Jen-Hwang Lee

has been accepted towards fulfillment of the requirements for

Ph. D. degree in Elect. Engr. & Sys. Sci.

Major professor

Date 7/17/79

O-7639



OVERDUE FINES ARE 25¢ PER DAY PER ITEM

Return to book drop to remove this checkout from your record.

INDUCE

BOD

in part

Depa

INDUCED ELECTROMAGNETIC FIELDS IN CONDUCTING BODIES IRRADIATED BY MAGNETIC FIELDS AND MICROWAVES

By

Jen-Hwang Lee

A DISSERTATION

Submitted to
Michigan State University
in partial fulfillment of the requirements
for the degree of

DOCTOR OF PHILOSOPHY

Department of Electrical Engineering and Systems Science

A new theo:

radii and cross-radii and cros

ABSTRACT

INDUCED ELECTROMAGNETIC FIELDS IN CONDUCTING BODIES IRRADIATED BY MAGNETIC FIELDS AND MICROWAVES

By

Jen-Hwang Lee

A new theoretical method for determining the eddy current induced by a uniform RF magnetic field or a beam of RF magnetic field in a biological body is developed in this research. This study was motivated by the fact that more biological research and medical applications utilize the irradiation of RF magnetic fields, and by the need for an efficient method of determining the magnetic mode of the induced electric field in a thick biological body irradiated by HF-VHF EM waves. The body of rotational symmetry is subdivided into a number of circular rings with various radii and cross-sectional areas. The eddy current induced by the impressed magnetic field can be considered, physically, as induced by a circulatory impressed electric field associated with the uniform impressed magnetic field. Induced eddy currents in all the rings maintain a scattered electric field which can be added to the impressed electric field to yield the total induced electric field in the body.

At the same ti complex conduc these relations simultaneous eq be obtained, an With the presen magnetic fields bodies have been tionally used, o fails to yield a 20 MHz, while th accurately and e biological bodie Also includ Quantifying the irradiated biolog integral equation the quantification diated body has b equation methods. the human body is

Tange, the body but field concentrate MITAGE. A volume imadequate or inefit wore efficient

At the same time, the eddy current is the product of the complex conductivity and the induced electric field. Using these relations and the point-matching method, a set of simultaneous equations for the induced electric fields can be obtained, and they are subsequently solved numerically. With the present method, the eddy currents induced by magnetic fields of 1 to 200 MHz in various biological bodies have been obtained. It was found that the conventionally used, quasi-static solution for the eddy current fails to yield accurate results for frequencies higher than 20 MHz, while the present method can be used to determine accurately and efficiently the induced eddy currents in biological bodies for frequencies higher than 20 MHz.

Also included in this thesis is a numerical method for quantifying the induced EM field on the surface of an irradiated biological body based on two coupled, surface integral equations. In the field of theoretical dosimetry, the quantification of the induced EM field inside an irradiated body has been performed mainly by volume integral equation methods. When a large biological body such as the human body is irradiated by an EM wave of microwave range, the body becomes electrically large and the induced EM field concentrates mainly in a thin layer of the body surface. A volume integral equation method then becomes inadequate or inefficient to handle this problem, and it is more efficient to quantify the induced EM field on the

body surface ba induced electri are determined,

for this case.

To check the ac bodies are cons.

surface integral obtained from th

integral equatio

cases, the surfa tages in accurac integral equation body surface based on a surface integral equation method for this case. After the tangential components of the induced electric and magnetic fields on the body surface are determined, the internal EM field can be calculated. To check the accuracy of this method, electrically small bodies are considered first, and results obtained from the surface integral equation method are compared with that obtained from the tensor integral equation method, a volume integral equation method. It was learned that, in some cases, the surface integral equation method showed advantages in accuracy and computational cost over the volume integral equation method.

To my mother, Kim-Chu Hong Lee,
my wife, Ai-Chih,
and my son, Yueh.

research advisor
and guidance th
also wish to th
ments and encou
ciation is also

I wish to

for their valuable $I \text{ want to } \epsilon$ excellent job in

Poundation under U.S. Army Resear

This resear

Finally, I stand love, Which I

ACKNOWLEDGMENTS

I wish to express my sincere appreciation to my research advisor, Dr. K. M. Chen, for his constant support and guidance throughout the course of this research. I also wish to thank Dr. D. P. Nyquist for his helpful comments and encouragement about this study. Sincere appreciation is also extended to Dr. M. Siegel and Dr. D. Riska for their valuable help.

I want to express my gratitude to Sue Cooley for her excellent job in typing the manuscript.

This research was supported by the National Science Foundation under Grant ENG 74-12603, and, in part, by U.S. Army Research Office under Grant DAAG 29-76-G-0201.

Finally, I thank my wife and my son for their patience and love, which made completion of this work possible.

II. EDDY CURRENT INSIDE A FIN SYMMETRY ...

2.1. Intro
2.2. Theor
2.3. Numer.
2.4. Conver
2.5. Closec
Compa
2.6. Experi
Theore
2.8. Discus

III.SURFACE INTEG OF MICROWAVE

3.1.

Introd The Pr The Ge in an Deriva Equation The Sp Interfa Review Review Mumeric 3.3. 3.4.

3.5. 3.6.

3.7. 3.8

TABLE OF CONTENTS

TTCT OF T	77770	Page
	ABLES	vi
LIST OF F	GURES	
		vii
T. INTRO	DUCTION	1
TIANTE	CURRENTS INDUCED BY RF MACRETIC FIELDS E A FINITE CONDUCTING BODY WITH ROTATIONAL TRY	
2.1.		5
2.1.	Introduction	6
2.3.	Theory	8
2.4.	Numerical Results	20
2.5.	Convergence of Numerical Results Closed Form Solution for Sphere and	29
2.6.	Comparison with Present Numerical Popults	31
2.7.	Experimental Setup	38
2.8.	meoretical Results	40
2.0.	Discussion	46
III.SURFAC	E INTEGRAL EQUATION METHOD FOR INTERACTION	
OF. WIG	ROWAVE WITH BIOLOGICAL BODY	48
3.1.	Introduction	49
3.2.	The Preliminary Theorems	52
3.3.	The General Solution of Maxwell's Equations	32
3.4.	in an Unbounded Homogeneous Space	53
3.4.	Derivation of the Coupled Surface Integral	
3.5.	Equations The Special Case of an Infinite Plane	56
2.6	Interface	75
3.6.	Review of Moment-Method	85
3.7.	The Numerical Technique	86
3.8.	Numerical Results	110

IV. PART 1 A U INI CON

4.1 4.2 4.3 4.4 4.5 4.6

PART 2 A US INDO FINI SHAF

4.7. 4.8. 4.9. 4.10 4.11 4.12

V. SUMMARY BIBLIOGRAPHY

			Page
IV.	PART 1	II GDEAT D GOLDED TO GOLD CHEMIT THOUSAND	
		INDUCED EDDY CURRENT INSIDE A FINITE	
		CONDUCTING BODY WITH ROTATIONAL SYMMETRY	124
		4.1. Formulation of the Problem	124
		4.2. Description of Computer Program	127
		4.3. Data Structure and Input Variables	128
		4.4 An Example to Use the Program	132
		4.5 Printed Output	134
		4.6. Listing of the Program	135
	PART 2	A USER'S GUIDE TO COMPUTER PROGRAM FOR	
		INDUCED EM FIELD ON THE SURFACE OF A	
		FINITE CONDUCTING BODY WITH ARBITRARY	
		SHAPE	141
		4.7. Formulation of the Problem	141
		4.8. Description of Computer Program	144
		4.9. Data Structure and Input Variables	146
		4.10. An Example to Use the Program	152
		4.11. Printed Output	158
		4.12. Listing of the Program	164
v.	SUMMARY		230
BIB	LIOGRAPH	ť	233

4.1. The sy corres files gram "

4.2. 4.3.

4.4.

The syn corresp files n gram "8

Printe

First o 4.5.

Second 4.6.

Third o

4.7. Fourth (4.8. Printed

LIST OF TABLES

Table		Page
2.1.	Comparison of the present solutions and a closed form solution for the electric fields induced in a conducting sphere with a conductivity of 8.0 S/m and a dielectric constant of 50 by a 300 MHz magnetic field with an intensity of 1 A/m. Also listed are the solutions obtained by the quasi-static approximation	37
4.1.	The symbolic names of input variables and corresponding specifications for the data files used in data structure for the program "EDDY"	130
4.2.	Printed output of program "EDDY"	136
4.3.	The symbolic names of input variables and corresponding specifications for the data files used in data structure for the program "SURFLDS"	148
4.4.	First output file of program "SURFLDS"	160
4.5.	Second output file of program "SURFIDS"	161
4.6.	Third output file of program "SURFLDS"	162
4.7.	Fourth output file of program "SURFLDS"	163
4.8.	Printed output of program "COMBINE"	165

LIST OF FIGURES

Figure		Page
2.1.	A biological body is exposed to a uniformly impressed RF magnetic field	10
2.2.	A biological body is irradiated by a beam of RF magnetic field	12
2.3.	A biological body of rotational symmetry irradiated by a uniform RF magnetic field is subdivided into a number of rings of various radii	13
2.4.	Geometries of two rings in the subdivided biological body	14
2.5.	Geometries of a single ring inside the subdivided biological body	16
2.6.	Distributions of amplitudes and phase angles of electric fields induced by a 100 MHz magnetic field of l A/m in a cylindrical biological body with a diameter of 15 cm and a height of 30 cm	21
2.7.	Distributions of amplitudes and phase angles of electric fields induced by a 100 MHz magnetic field of 1 A/m in a cylindrical biological body with a diameter of 36 cm and a height of 90 cm	23
2.8.	Distributions of amplitudes and phase angles of electric fields induced by magnetic fields of various frequencies in a muscle disk with a diameter of 30 cm and a thickness of 1 cm	24
2.9.	Distributions of amplitudes and phase angles of electric fields induced by a 100 MHz mag- netic field in the central section of a cylindrical biological body of diameter 36 cm with various heights	26
2.10.	Distributions of amplitudes and phase angles of electric fields induced in a cylindrical biological body with a diameter of 32 cm and a height of 20 cm by a beam of 100 MHz mag-	

2,18.

Comparison results for induced in 22.2 cm, m magnetic f

Figure		Page
	netic field with a diameter of 8 cm and an intensity of 1 $\mbox{A/m}$	28
2.11.	Distributions of amplitudes and phase angles of electric fields induced by a uniform magnetic field of 100 MHz in a model of man $(\sigma=0.889~\mathrm{S/m},~\epsilon_\mathrm{r}=71.7)$	30
2.12.	Comparison of 81-ring solutions and 9-ring solutions for the electric fields induced in a cylindrical biological body with a diameter of 36 cm and a height of 18 cm by a 100 MHz magnetic field with an intensity of $1\mathrm{A/m}$	32
2.13.	A finite conducting sphere with radius R is immersed in a uniform magnetic field polarized in the +z direction	34
2.14.	A finite conducting sphere with a radius of 2 cm is simulated by a "ring sphere" constructed with 30 circular rings of two different cross-sectional areas. The sphere is assumed to have a conductivity of 8.0 S/m and a dielectric constant of 50, and is immersed in a 300 MHz oscillating magnetic field with an intensity of 1 A/m.	36
2.15.	Experimental setup for measuring the electric fields inside the phantom biological bodies induced by RF magnetic fields	39
2.16.	Comparison of theoretical and experimental results for the amplitudes of electric fields induced in a phantom biological cylinder of 4 cm diameter with various heights by a 750 MHz magnetic field	41
2.17.	Comparison of theoretical and experimental results for the amplitudes of electric fields induced in a phantom biological cylinder with a diameter of 3.8 cm, a height of 3.8 cm and various conductivities by a 750 MHz magnetic field	43
2.18.	Comparison of theoretical and experimental results for the amplitudes of electric fields induced in a phantom model of man (height = 22.2 cm, max. diameter = 3.8 cm) by a 750 MHz	
	magnetic field	45

A sou chara (Je, sitie into and p (E, H

A fin

The sc origin existing replace source current

The sca of the of the surface in term The bod space .

3.4.

3,5,

3.6.

The indi the body the body equivale defined surface by a med permitti

The indu
the body
exterior
gative o
(je, jm)
incident
permeabi

Figure	Page

3.1. A source region G_S enclosed by surface F_S is characterized by volume current densities $(\vec{J}_{\ell}, \vec{J}_{m})$ and equivalent surface current densities $(\vec{J}_{\ell}, \vec{J}_{m})$. These current sources radiate into a homogeneous space with permeability μ and permittivity ϵ , and maintain an EM field (\vec{E}, \vec{H}) at point \vec{r} .

3.2. A finite conducting body G, immersed in free space and enclosed by surface F, with a permeability μ and a complex permittivity ϵ_{cd} is irradiated by the incident field (E^1, H^1) radiated from the source region G where the equivalent surface current densities (J_e, J_m) are defined on the surface F_g . The PM fields scattered from and induced in the body are denoted as (E^2, H^3) and (E^1, H^3) , respectively 57

3.3. The scattered field (E^S, H̄^S) can be consider as originated from an equivalent current source J̄^C^Q existing inside the body region which has been replaced by free space. This equivalent current source consists of two components, the conduction current and the polarization current

3.4. The scattered field (\vec{E}^S, \vec{H}^S) in the exterior of the body and a zero field in the interior of the body are maintained by the equivalent surface currents (j_S^1, j_M^2) , which are defined in terms of the scattered field on surface F. The body region G has been replaced by free space

3.5. The induced field (E^d, H^d) in the interior of the body and a zero field in the exterior of the body are maintained by the negative of the equivalent surface currents (I^d_e, I^d_o), which are defined in terms of the induced field on surface F. The region external to F is replaced by a medium with permeability μ_o and complex permittivity ε_d

62

3.6. The induced field (E^d, fi^d) in the interior of the body and the scattered field (E^s, fi^s) in the exterior of the body are maintained by the negative of the equivalent surface currents (fi, fi), which are defined in terms of the incident field on surface F. The body G with permeability µ_O and complex permittivity ε_d

An in a fin µ_o an a plan

3.8.

3.9.

3.10.

The co

Divisi square using functi 3.11.

A simulincider direction The book tivity a number equival ferent obtained integral.

3.12. The symmof the i

3.13.

3.14.

The x-condeterminal ation method ...

The z-con determine ation met method ..

Figure		Page
	is immersed in free space	67
3.7.	With the body region G replaced by free space, the incident field (\vec{E}^1,\vec{H}^1) in the interior of the body and a zero field in the exterior of the body are maintained by the negative of the equivalent surface currents $(\vec{J}_0^1,\vec{J}_{11}^1)$, which are defined in terms of the incident field on surface F	e 68
3.8.	An infinite interface between free space and a finite conducting medium with permeability $_{\rm D}$ and complex permittivity $_{\rm S}$ is impinged by a plane wave propagating in the +z direction	76
3.9.	The coordinate system utilized in the infinite interface problem	81
3.10.	Division of the surface of a cubic body into square surface cells for moment-method solution using two-dimensional flat pulses as expansion functions and δ functions as testing functions	87
3.11.	A simulated human body is irradiated by an incident plane wave propagating in the +z direction with a x-polarized electric field. The body is characterized by complex permittivity ϵ_{d} , and its surface is subdivided into a number of square surface cells. The induced equivalent surface currents $(\vec{j}_{d}, \vec{j}_{m})$ at different locations on the surface can be obtained by solving two coupled, surface integral equations	89
3.12.	The symmetrical properties of various modes of the induced equivalent surface currents $(\vec{J}_e,\ \vec{J}_m)$ on the surface of a cubic body	109
3.13.	The x-components of the induced electric fields determined based on the surface integral equation method and the volume integral equation method. $ \frac{1}{2} \frac$	111
3.14.	The z-components of the induced electric fields determined based on the surface integral equ- ation method and the volume integral equation method.	112

Ampl: x-cor the x

Ampli y-com the x 11.25 figure

3.18. Amplit induce simula 3.19.

Phase of induced simulat

4.1.

4.2.

4.3.

A rotat symmetr irradia intensi number

A cyling ter of divided divided section body is 0.889 S/ and is i netic fi

A cubic 1 47) with irradiate a frequer x-polariz face is s dimension

Figure		Page
3.15.	Amplitude and phase distributions of the x-component of induced electric field along the x direction in various layers at y = 3.75 cm	115
3.16.	Amplitude and phase distributions of the x-component of induced electric field along the x direction in various layers at y = $11.25\ cm$	118
3.17.	Amplitude and phase distributions of the y-component of induced electric field along the x direction in various layers at y = 11.25 cm (top figure) and y = 3.75 cm (bottom figure)	120
3.18.	Amplitude distribution of the x-component of induced electric field on the surface of a simulated human body	122
3.19.	Phase distribution of the x-component of induced electric field on the surface of a simulated human body	123
4.1.	A rotationally symmetrical body with the symmetrical axis in the +z direction is irradiated by a magnetic field with unit intensity. The body is subdivided into a number of circular rings of various radii	126
4.2.	A cylindrical biological body with a diameter of 6 cm and a height of 2 cm is subdivided into 6 circular rings with a cross-section of 1 cm x 1 cm for each ring. The body is assumed to have a conductivity of 0.889 S/m and a dielectric constant of 71.7, and is immersed in a 100 MHz uniform magnetic field with an intensity of 1 A/m	129
4.3.	A cubic biological body (σ = 2.21 S/m, ϵ_{r} = 47) with dimensions of 2 cm x 2 cm x 2 cm is irradiated by an incident plane wave which has a frequency of 2.45 GHz and a unit intensity, x-polarized electric field. The body surface is subdivided into 95 surface cells with dimensions of 0.5 cm x 0.5 cm	147

these highly according to the service of the servic

Since ele

CHAPTER I

INTRODUCTION

Since electromagnetic radiation and propagation were discovered more than a century ago, electromagnetic waves of various frequencies have been utilized in many ways to benefit the human society. Especially, due to the ingenious contributions of engineers and scientists, such incredible dreams as satellite communications, long-range radar detection, high power-rating microwave ovens, and many other products related to EM technology have been realized. Moreover, high-level beamed microwave power is proposed as a new scheme for transporting energy in the future, and the use of electromagnetically induced hyperthermia as an adjunct in cancer treatment is receiving increased attention from many medical researchers. Indeed, these highly advanced techniques of utilizing energy in EM form do benefit us in many respects; unfortunately, they also bring us certain unwanted potential hazards.

Over a decade ago, medical personnel and public health officials began to suspect that low-level, long-term ionizing radiation could be one of the major causes for several different cancers. Even more astonishingly, it is found

since it exis either man-ma possible haza in high inter be harmful to ciated with s burns, catara effects have especially fo term or highthere is stro of the biolog therefore a de the safe power correct applic ing high-inter However, based area, many que of fact, there groups about w exposure shoul haximum allowa exposure varie as 0.01 mW/cm²

impossible to

impossible to completely avoid this low-level radiation since it exists everywhere in space, originating from either man-made or natural sources. Besides the above possible hazards due to low-level radiation, EM radiation in high intensities, under an uncontrolled condition, can be harmful to living systems. The thermal effects associated with such high-intensity radiation can produce burns, cataracts, and chemical changes, etc. All these effects have become the major concerns of the public, especially for those who are subject to possible longterm or high-intensity radiation exposure. As a result, there is strong demand for a more thorough understanding of the biological effects of EM radiation. There is therefore a demonstrated need to determine, for example, the safe power density for long-term human exposure, the correct applications methodology and techniques in utilizing high-intensity EM radiation for medical treatment, etc. However, based on the present state of knowledge in this area, many questions still remain unanswered. As a matter of fact, there exist strong arguments between involved groups about where realistic safety levels for microwave exposure should lie. It is surprising to observe that the maximum allowable safe power density for long-term human exposure varies from 10 mW/cm² in this country to as low as 0.01 mW/cm² in the USSR.

Under the research for t standing of EV study the eddy inside biologi field has receital usefulnes

bodies; further the current dis been accomplish we study the mi through the sol

about the mecha

equations. Thi quantify the EM trarily shaped

expect to obtain $e_{\text{Valuation}}$ of m.

To clarify these uncertainties, electromagnetic engineers should assume the responsibility for providing more complete, accurate, quantitative data on biological effects of EM radiation; they belong to the professional groups having adequate knowledge and ability to analyze this problem both theoretically and experimentally.

Under these circumstances, we complete the present research for the purpose of seeking for a better understanding of EM interactions with biological bodies. We study the eddy currents induced by RF magnetic fields inside biological bodies in Chapter II. The RF magnetic field has received increased attention due to its potential usefulness for local heating in cancer treatment. Based on our research, we obtain a better understanding about the mechanism exciting induced currents inside the bodies; furthermore, we are able to predict accurately the current distributions inside the bodies, which has not been accomplished by previous methods. In Chapter III, we study the microwave interactions with biological bodies through the solutions of two coupled, surface integral equations. This numerical technique can be applied to quantify the EM fields induced on the surfaces of arbitrarily shaped biological bodies. Through this study, we expect to obtain a more complete, accurate, quantitative evaluation of microwave interactions. Chapter IV describes

in detail th

problems. T

in detail the computer programs used for the above two problems. Then, Chapter V summarizes this research.

rotational sym

CHAPTER II

EDDY CURRENTS INDUCED BY RF MAGNETIC FIELDS INSIDE A FINITE CONDUCTING BODY WITH ROTATIONAL SYMMETRY

In this chapter, we will present a new theoretical method for determining the electric field or the eddy current induced by a uniform RF magnetic field or a beam of RF magnetic field in a finite conducting body with rotational symmetry.

The body being considered is divided into a number of circular rings with various radii and cross-sectional areas. The induced electric field in each ring is then numerically determined based on the theory of vector potential and the moment method. Numerical examples are given and the results based on the present theory are found to deviate significantly from the often-used quasi-static solutions. An experiment was conducted to measure the electric fields induced by a UHF magnetic field in finite conducting phantom models. Experimental results were found to be in a good agreement with the theory. The accuracy of the present theory was also verified by the

existing the in a conduct 2.1. Introd Due to j area, the rad important new

attention fro

electric fiel

field inside quasi-static s ${\tt approximation}$

is relatively magnetic field trically large

RF magnetic fi quasi-static a desirable to so

 $^{
m effectively.}$ Based on M quasi-static so

field induced b

Man. Their the to a spherical)

static solution

the magnetic fie

existing theoretical results on the induced eddy current in a conducting sphere.

2.1. Introduction

Due to its increasing applications in the biomedical area, the radiation of RF magnetic field is becoming an important new technique which has drawn a large amount of attention from many investigators. Conventionally, the electric field or the eddy current induced by a magnetic field inside a finite conducting body is estimated by the quasi-static solution. Unfortunately, the quasi-static approximation can give accurate results only when the body is relatively small or when the frequency of the applied magnetic field is lower than about 20 MHz. If an electrically large body such as human body is exposed to a RF magnetic field with a frequency higher than 20 MHz, the quasi-static approximation becomes inadequate. It is desirable to solve this practical problem accurately and effectively.

Based on Mie theory, Lin et al. [1] have obtained a quasi-static solution for the magnetic mode of the electric field induced by a HF EM wave inside a spherical model of man. Their theory is valid up to 20 MHz and restricted to a spherical body. Spiegel [2] has used the same quasi-static solution to estimate the electric field induced by the magnetic field of an EHV power line inside a simplified

low frequenc by an ac uni Was presented approximation (see Section method which or the eddy c to VHF range : More complex t Another m for improving [4] developed electric field When a thick by HF-VHF range, t be divided into electric mode b the body shape method. However strongly depende of this magnetic

biological body i

model of man

ters the difficu theoretical method Magnetic mode of model of man. His solution is valid only for the very low frequency range. A theory on the eddy current induced by an ac uniform magnetic field in a conducting sphere was presented by Van Bladel [3]. This theory imposes less approximations but only applies to a spherical geometry (see Section 2.5). There is a need for a new theoretical method which can be used to quantify the electric fields or the eddy currents induced by RF magnetic fields of up to VHF range in finite conducting bodies with geometries more complex than a sphere.

Another motivation of the present study is the need for improving the efficiency of a recent numerical method [4] developed by our group for quantifying the internal electric field induced by an EM wave in a human body. When a thick biological body is exposed to an EM wave of HF-VHF range, the induced electric field or current can be divided into the electric and magnetic modes. The electric mode being linear and relatively independent of the body shape is easily determined by the numerical method. However, the magnetic mode is circulatory and strongly dependent on the body shape. The determination of this magnetic mode with a numerical method often encounters the difficulty of numerical convergence. Thus, a new theoretical method which can efficiently determine the magnetic mode of the induced current in an irradiated biological body is desired.

in Section 2.3 discussed in S

The the

solution with in Section 2.5 tion 2.6, and a theoretical res

2.2. Theory

When a fin metry is exposed field $\mathring{H}^{\dot{1}}$, the i:

is conventional!

 $\int_{\bar{E}}^{\vec{r}}\cdot\vec{d\ell}$ The induced elec

equation is circulinearly with the of the body and i

interaction betwe

The theoretical method presented in this chapter is capable of predicting the electric field or the eddy current induced by a uniform RF magnetic field or a beam of RF magnetic field in a finite conducting body with rotational symmetry. The development of the theory is presented in Section 2.2. Some numerical examples are given in Section 2.3. The convergence of numerical results is discussed in Section 2.4. The comparison of the present solution with a closed form solution for a sphere is made in Section 2.5. The experimental setup is described in Section 2.6, and experimental results are compared with theoretical results in Section 2.7.

2.2. Theory

When a finite conducting body with rotational symmetry is exposed to a uniformly impressed, RF magnetic field $\vec{H}^{\dot{1}}$, the induced electric field \vec{E} inside the body is conventionally estimated by Maxwell equation of

$$\oint \vec{E} \cdot \vec{dk} = -j\omega\mu_0 \int \vec{H}^i \cdot \vec{ds}. \qquad (2.1)$$

The induced electric field \vec{E} determined from the above equation is circulatory and its amplitude increases linearly with the radial distance from the central axis of the body and its phase is 90° out of that of impressed magnetic field \vec{H}^i . In this quasi-static solution, the interaction between the induced currents at different

the induced or

quasi-static a
for frequencie
which can be u
finite conduct
by a RF magnet
is developed b
We consid
finite conduct
MR magnetic fi
drical beam of

Physically in the body is is associated w For the ca field \ddot{H}^{i} as sho

locations is rate results,

electric field

āS

where r is the r the body.

locations is completely ignored. However, to obtain accurate results, the scattered magnetic field produced by the induced current must be taken into consideration. The quasi-static approximation can predict good results only for frequencies lower than 20 MHz. A theoretical method which can be used to quantify the electric field in a finite conducting body with a rotational symmetry induced by a RF magnetic field with a frequency higher than 20 MHz is developed below.

We consider two different cases separately: (1) a finite conducting body immersed in an impressed, uniform RF magnetic field, and (2) the body irradiated by a cylindrical beam of RF magnetic field.

Physically, we may consider that the electric field in the body is induced by an impressed electric field which is associated with the impressed RF magnetic field.

For the case of an impressed, uniform RF magnetic field \vec{H}^i as shown in Figure 2.1, the associated, impressed electric field \vec{E}^i can be obtained from

$$\oint \vec{E}^{i} \cdot \vec{dl} = -j\omega\mu_{o} \int \vec{H}^{i} \cdot \vec{ds}$$

as

$$\dot{\vec{E}}^{\dot{i}} = -\frac{j}{2}\omega\mu_{o} H^{\dot{i}}r \hat{\phi}$$
 (2.2)

where r is the radial distance from the central axis of the body.



Figure 2.1

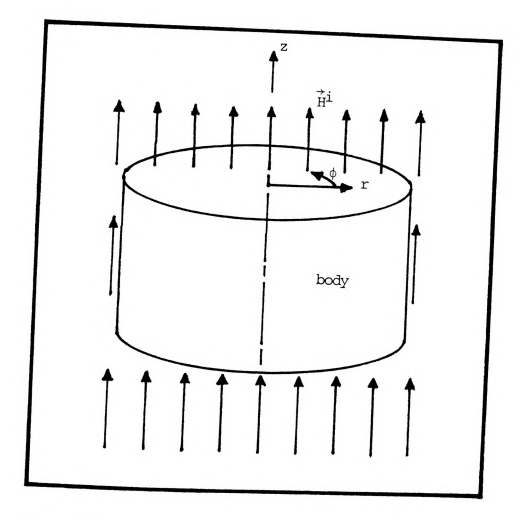


Figure 2.1. A biological body is exposed to a uniformly impressed RF magnetic field.

Figure 2.2, t be found to b $\vec{E}^{\dot{1}} = \begin{pmatrix} - & & \\ & \dot{E}^{\dot{1}} & \\ & & - & \\ & & & - & \\ \end{pmatrix}$

For the netic field

impressed magn tion and they the finite con-

These impresse

If the rot geometry and th body can be sub

of various radi.
Pigure 2.3. We
field within each

ring to ring. I Rigure 2.3; name Sectional area S the mth ring with

a reference point ings are depicte points of the rin

Nth ring, $\frac{1}{r_{h}}$, and

For the case of a cylindrical beam of uniform magnetic field $\dot{\vec{H}}^i$ with a beam radius of "b" as shown in Figure 2.2, the associated, impressed electric field can be found to be

$$\vec{E}^{\dot{1}} = \begin{cases} -\frac{\dot{1}}{2}\omega\mu_{O} & \text{H}^{\dot{1}}r & \hat{\phi} & \text{for } 0 \leq r < b \\ \\ -\frac{\dot{1}}{2}\omega\mu_{O} & \text{H}^{\dot{1}} & \frac{b^{2}}{r} & \hat{\phi} & \text{for } b \leq r \end{cases}$$
 (2.3)

These impressed electric fields \vec{E}^i associated with the impressed magnetic fields \vec{H}^i are in the azimuthal direction and they induce circulatory electric fields inside the finite conducting body.

If the rotational symmetry is assumed for the body geometry and the electrical properties of the body, the body can be subdivided into a number (N) of circular rings of various radii and cross-sectional areas as shown in Figure 2.3. We further assume that the induced electric field within each ring is uniform, but it can vary from ring to ring. Let's consider two sample rings shown in Figure 2.3; namely, the nth ring with radius \mathbf{r}_n , crosssectional area \mathbf{S}_n and a reference point $(\mathbf{r}_n, 0, \mathbf{z}_n)$, and the mth ring with radius \mathbf{r}_m , cross-sectional area \mathbf{S}_m and a reference point $(\mathbf{r}_m, 0, \mathbf{z}_m)$. The geometries of these two rings are depicted in Figure 2.4, where the reference points of the rings, $\hat{\mathbf{r}}_n$ and $\hat{\mathbf{r}}_m$, the source point in the nth ring, $\hat{\mathbf{r}}_n$, and the distance between the source point



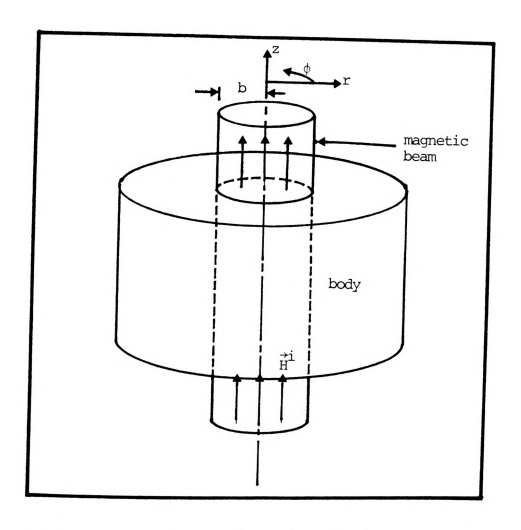


Figure 2.2. A biological body is irradiated by a beam of RF magnetic field.

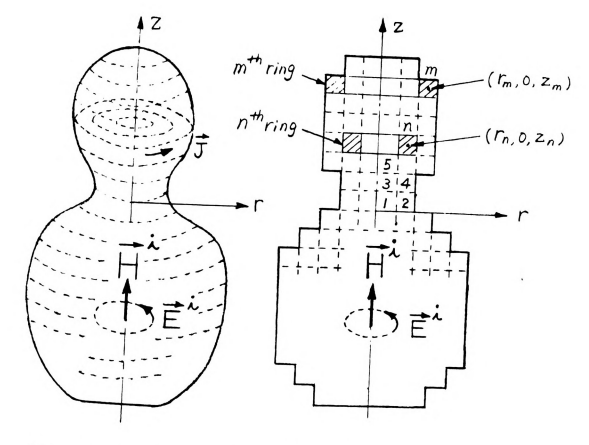
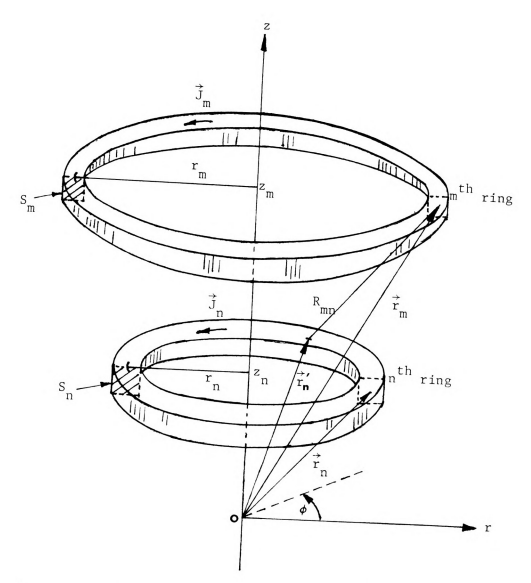


Figure 2.3. A biological body of rotational symmetry irradiated by a uniform RF magnetic field is subdivided into a number of rings of various radii.

 $\vec{r} = (r, 0, 0, r, 0$

Figure 2.4.



$$\begin{array}{l} \vec{r}_{n}=\left(r_{n},\;0,\;z_{n}\right)=\text{reference point of the }n^{th}\;\text{ring}\\ \vec{r}_{m}=\left(r_{m},\;0,\;z_{m}\right)=\text{reference point of the }m^{th}\;\text{ring}\\ \vec{r}_{n}'=\left(r_{n},\;\phi,\;z_{n}\right)=\text{source point in the }n^{th}\;\text{ring}\\ R_{mn}=\left|\vec{r}_{m}-\vec{r}_{n}'\right|=\left[r_{m}^{2}+r_{n}^{2}-2r_{m}r_{n}\cos\phi+\left(z_{m}-z_{n}\right)^{2}\right]^{\frac{1}{2}}\\ &=\text{distance between the source point in the }n^{th}\;\text{ring,} \end{aligned}$$

Figure 2.4. Geometries of two rings in the subdivided biological body.

 R_{mn} , are shown if the nth ring is the mth ring be determined $\vec{A}_{mn} =$

in the nth

where $R_{mn} = k_0 = 0$ Using $dv = s_n$

eq. (2.4) can

where $K_{mn} =$

Å_{mn} =

To determi With ring mainta

ring, we conside

cross-section by to the following in the nth ring and the reference point of the mth ring, $\mathbf{R}_{\mathrm{mn}},$ are shown.

If the volume density of the induced current in the nth ring is denoted as \vec{J}_n , the vector potential at \vec{r}_m of the mth ring maintained by \vec{J}_n of the nth ring, \vec{A}_{mn} , can be determined as

$$\vec{A}_{mn} = \frac{\mu_O}{4\pi} \int_{\text{nth ring}} \vec{J}_n \frac{e^{-jk} e^{R_{mn}}}{R_{mn}} dv \qquad (2.4)$$

where $R_{mn} = [r_m^2 + r_n^2 - 2 r_m r_n \cos \phi + (z_m - z_n)^2]^{\frac{1}{2}}$ $k_0 = \omega \sqrt{\mu_0 \epsilon_0}$.

Using $\mathrm{d} v = {\bf S}_{\rm n} \ {\bf r}_{\rm n} \ \mathrm{d} \phi$ and because of the rotational symmetry, eq. (2.4) can be evaluated as

$$\vec{A}_{mn} = \hat{\phi} \frac{\mu_o}{2\pi} J_n S_n r_n K_{mn}$$
 (2.5)

where
$$K_{mn} = \int_0^{\pi} d\phi \cos\phi \frac{e^{-jk_0R_{mn}}}{R_{mn}}$$
 (2.6)

To determine the vector potential \vec{A}_{m_m} at \vec{r}_m of the mth ring maintained by \vec{J}_m , the induced current in the mth ring, we consider the geometry of the mth ring shown in Figure 2.5. Note that we approximate the square ring cross-section by a circle with the same area. This leads to the following relationship:

top view the mth ring

side view of the mt ring

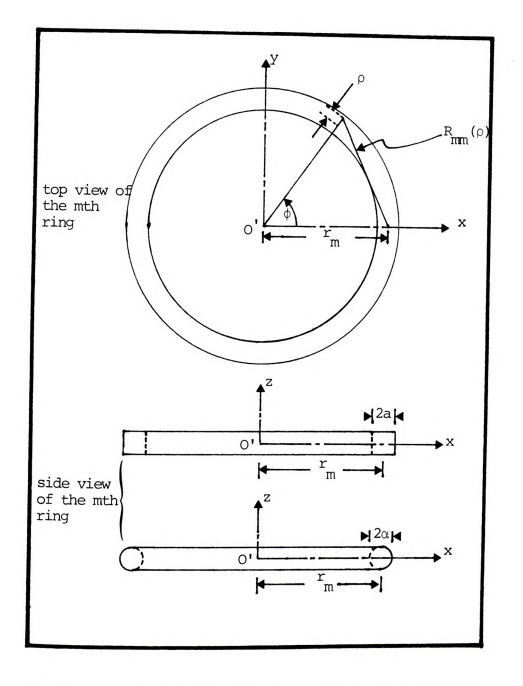


Figure 2.5. Geometries of a single ring inside the subdivided biological body.

where 2a is While α is t The dis

mth ring and as

The vector po

After substitu forward manipu

above equation

where $K_{mm} =$

The total

induced current às

 $\overset{\dagger}{A}_{m} = \Sigma \\
 & n$

$$\alpha = \frac{2a}{\sqrt{\pi}}$$

where 2a is the dimension of the square cross-section, while α is the radius of the circular cross-section.

The distance between the source point $\,$ inside the mth ring and the reference point $\overset{\star}{r}_m,\ R_{mm},$ can be expressed as

$$R_{mm}$$
 (p) $\doteq r_{m}[2 \ (1-\cos\phi) + \frac{\rho^{2}}{r_{m}^{2}}]^{\frac{1}{2}}$.

The vector potential $\overline{A}_{mm}^{\bullet}$ can be written in terms of $R_{mm}^{}$ as

$$\vec{A}_{mm} \,=\, \frac{\mu_{o}}{4\pi} \,\, \int_{\substack{\text{mth} \\ \text{ring}}} \,\, \vec{J}_{m} \,\, \frac{e^{-j\,k_{o}R_{mm}\,(\rho)}}{R_{mm}\,(\rho)} \,\, \text{dv.} \label{eq:Amm}$$

After substituting the expression of \mathbf{R}_{mm} and some straightforward manipulations, we have the following form for the above equation:

$$\vec{A}_{mm} = \hat{\phi} \frac{\mu_O}{2\pi} J_m S_m r_m K_{mm}$$
 (2.7)

where
$$K_{mm} = \frac{2\pi}{S_m} [R_{mm}(\alpha) - R_{mm}(0)] \int_0^{\pi} \cos \phi e^{-jk_0 R_{mm}(0)} d\phi$$
. (2.8)

The total vector potential at \vec{r}_m maintained by the induced currents in all the rings, \vec{A}_m , can then be obtained as

$$\vec{A}_{m} = \sum_{n} \vec{A}_{mn} = \hat{\phi} \sum_{n} \frac{\mu_{o}}{2\pi} S_{n} r_{n} K_{mn} J_{n}. \qquad (2.9)$$

At the ring can be in the nth :

j_n :

Equation (2. current and sidered as t

With eq

 $\vec{A}_{m} =$

This $\vec{A}_{\underline{m}}$ is re the mth ring

in all the rin

Where f is the since the indu

symmetrical, n

quently, no sc.

The total is the sum of t

ring and the sc

eq. (2.12):

At the same time, the induced current \vec{J}_n in the nth ring can be related to the total induced electric field in the nth ring, \vec{E}_n , as

$$\vec{J}_n = [\sigma_n + j \omega (\varepsilon_n - \varepsilon_0)] \vec{E}_n = \tau_n \vec{E}_n.$$
 (2.10)

Equation (2.10) expresses \vec{J}_n as the sum of the conduction current and the polarization current, and τ_n can be considered as the complex conductivity of the nth ring.

With eq. (2.10), \vec{A}_m can be rewritten as

$$\vec{A}_{m} = \hat{\phi} \sum_{n} \frac{\mu_{O}}{2\pi} S_{n} r_{n} K_{mn} \tau_{n} E_{n}. \qquad (2.11)$$

This \vec{A}_m is related to the scattered electric field \vec{E}_m^s in the mth ring which is maintained by the induced currents in all the rings:

$$\vec{E}_{m}^{S} = -j\omega \vec{A}_{m} = -\hat{\phi} \sum_{n} jf \mu_{o} S_{n} r_{n} K_{mn} \tau_{n} E_{n}$$
 (2.12)

where f is the frequency. It should be emphasized that since the induced current in each ring is rotationally symmetrical, no electric charge is induced and, consequently, no scalar potential is maintained.

The total induced electric field \vec{E}_m in the mth ring is the sum of the impressed electric field \vec{E}_m^i at the mth ring and the scattered electric field \vec{E}_m^s obtained in eq. (2.12):

$$\vec{E}_{m} = \vec{E}_{m}^{i} + \vec{E}_{m}^{s} \tag{2.13}$$

Equation (2. of the N rin

M₁₁ M₂₁ ...

Where

Mnn

M mn

The total indurings can be dinversion tech

rent is needed (2.10).

A compute method to calcu finite conducti

cassed in the r

38

With eq. (2.12), eq. (2.13) can be rearranged as

$$E_{m} + \sum_{n} jf \mu_{o} S_{n} r_{n} K_{mn} \tau_{n} E_{n} = E_{m}^{i}$$
 (2.14)

Equation (2.14) can be point-matched at N reference points of the N rings to yield N simultaneous equations in a matrix form as

$$\begin{bmatrix} M_{11}, & M_{12}, & \dots & M_{1N} \\ M_{21}, & M_{22}, & \dots & M_{2N} \\ \dots & \dots & \dots & \dots \\ M_{N1}, & M_{N2}, & \dots & M_{NN} \end{bmatrix} \cdot \begin{bmatrix} E_1 \\ E_2 \\ \vdots \\ E_N \end{bmatrix} = \begin{bmatrix} E_1^i \\ E_2^i \\ \vdots \\ E_N^i \end{bmatrix}$$
 (2.15)

where

$$M_{nn} = 1 + jf \mu_0 S_n r_n K_{nn} \tau_n$$
 (2.16)

$$M_{mn} = jf \mu_{o} S_{n} r_{n} K_{mn} \tau_{n}. \qquad (2.17)$$

The total induced electric fields, E_1 to E_n , in all the rings can be determined from eq. (2.15) by the matrix inversion technique. Note that if the induced eddy current is needed, it can be obtained readily from eq. (2.10).

A computer program has been developed based on this method to calculate induced electric fields in various finite conducting bodies. Some numerical results are discussed in the next section.

2.3. Numeri The fir biological b 30 cm being MHz with an have a condu stant (ϵ_r) o body is subd With a square The amplitude field \vec{E} in ea tions of thes radial distan ferent section is observed i induced elect: radial distanc solution as ca angle of the i -110° and -150 field $\mathring{\mathrm{H}}^{\dot{1}}$) whil be -90° at any body, the ofte

> estimate the an not its phase a drical body is

2.3. Numerical Results

The first numerical example deals with a cylindrical biological body with a diameter of 15 cm and a height of 30 cm being exposed to a uniform magnetic field of 100 MHz with an intensity of 1 Amp/m. The body is assumed to have a conductivity (o) of 0.889 S/m and a dielectric constant (ε_r) of 71.7. In the numerical calculation, the body is subdivided into 100 rings of various radii and with a square cross-sectional area of 1.5 cm x 1.5 cm. The amplitude and phase angle of the induced electric field E in each ring were calculated, and the distributions of these quantities are plotted as functions of the radial distance from the cylindrical axis r for 10 different sections of the body as shown in Figure 2.6. It is observed in Figure 2.6 that the amplitude of the induced electric field | E | increases linearly with the radial distance; this result is close to the quasi-static solution as can be obtained from eq. (2.1). The phase angle of the induced electric field varies between around -110° and -150° (with respect to the impressed magnetic field \vec{H}^{i}) while the quasi-static solution predicts it to be -90° at any point in the body. For this cylindrical body, the often-used quasi-static solution can be used to estimate the amplitude of the induced electric field but not its phase angle. However, as the size of the cylindrical body is increased, the quasi-static solution is

→ / (**) 7.5 cm

1 = 1 A/m 1 = 100MHz 1 = 0.889 S/m Pha oi È (degr

Pigure 2.6. Dis of net cal of

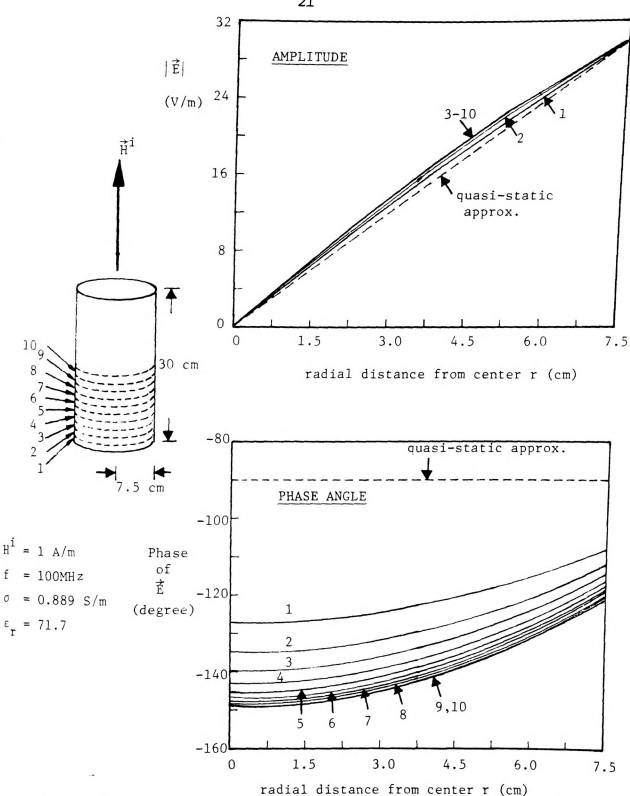


Figure 2.6. Distributions of amplitudes and phase angles of electric fields induced by a 100 MHz magnetic field of 1 $\rm A/m$ in a cylindrical biological body with a diameter of 15 cm and a height of 30 cm.

found to be the next exa In the biological b $(\sigma = 0.889 \text{ S})$ with a diame in Figure 2. an intensity distributions induced elect present resul solutions: t is two or thr While the pha the quasi-sta example, that field of VHF becomes compl The next

> the electric f intensity (1 P 100 and 200 MH and a thicknes

the disk are a

ε = 160 to 56

The amplitudes

found to be completely inadequate, as can be observed in the next example.

In the second example, we consider a cylindrical biological body with the same electric properties (σ = 0.889 S/m and ϵ_r = 71.7) as the first example, but with a diameter of 36 cm and a height of 90 cm as shown in Figure 2.7. The same magnetic field of 100 MHz with an intensity of 1 Amp/m is impressed on the body. The distributions of the amplitudes and phase angles of the induced electric fields in Figure 2.7 show that the present results deviate greatly from the quasi-static solutions: the amplitude of the induced electric field is two or three times lower than the quasi-static solution. while the phase angles vary between -120° and -290° against the quasi-static solution of -90°. It is clear, from this example, that when a human body is exposed to a magnetic field of VHF range, the often-used, quasi-static solution becomes completely invalid.

The next example as shown in Figure 2.8 deals with the electric fields induced by magnetic fields of unit intensity (1 Amp/m) and of various frequencies (10, 40, 100 and 200 MHz) in a muscle disk with a diameter of 30 cm and a thickness of 1 cm. The electrical properties of the disk are assumed to have σ = 0.625 to 1.28 S/m and $\epsilon_{\rm T}$ = 160 to 56.5 for the frequency range of 10 to 200 MHz. The amplitudes of the induced electric fields are found to

18 i = 1 A/m P i = 100MHz 0 = 0.889 S/m (de t = 71.7

rigure 2.7.
n.
1c
hr

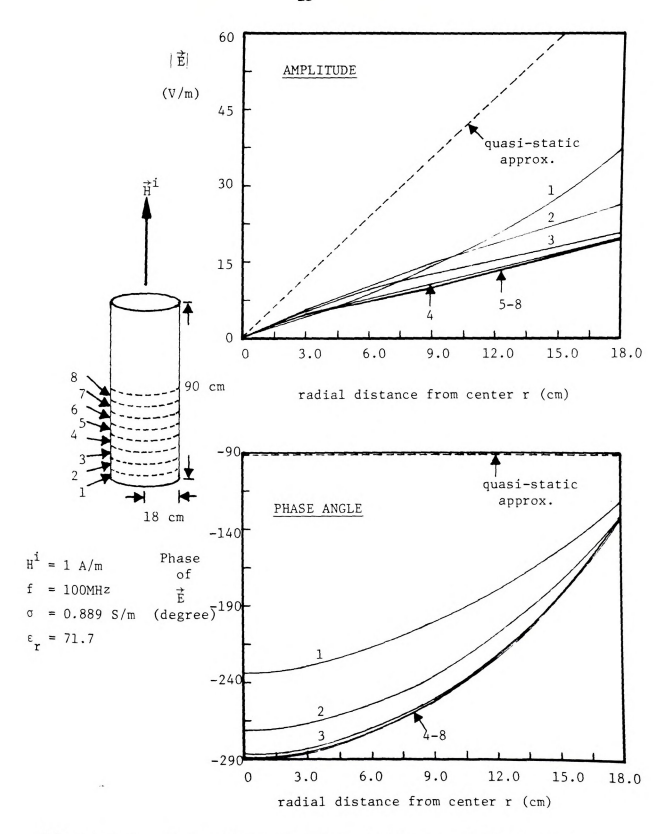


Figure 2.7. Distributions of amplitudes and phase angles of electric fields induced by a 100 MHz magnetic field of 1 A/m in a cylindrical biological body with a diameter of 36 cm and a height of 90 cm.

1 cm 🛨

Eⁱ = 1 A/n 0.625 to 1.28 S/m

(4

for 10-200 MH z E, = 160 to 56.

for 10-200 MHz rigure 2.8.

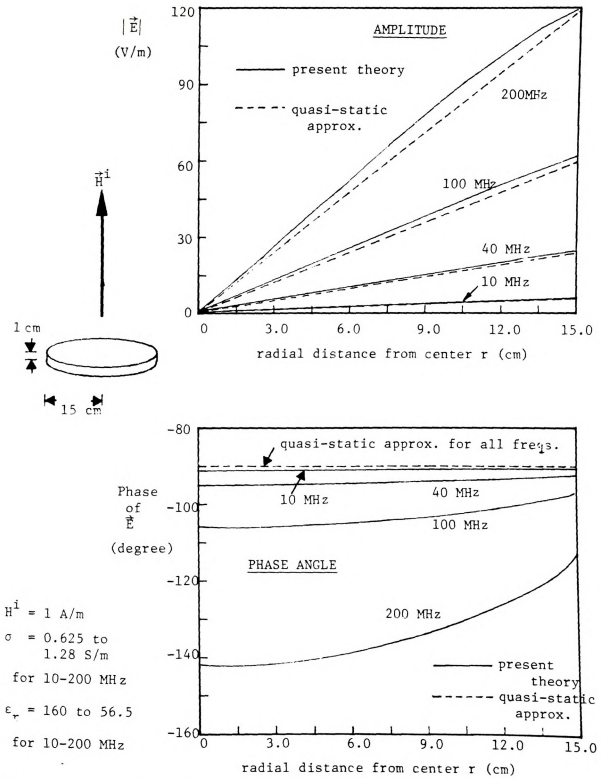


Figure 2.8. Distributions of amplitudes and phase angles of electric fields induced by magnetic fields of various frequencies in a muscle disk with a diameter of 30 cm and a thickness of 1 cm.

increase 1 distance fr slightly fr results for fields, how static solu In the effect of t field at the drical body from 6 cm to MHz has an i ties of the 0 = 0.889 S/ at the centr the distribu are plotted

12, 18, 30 a
as the cyling
the induced of
cylinder decr
drastically i
example indice
Magnetic fiel
dependent on

increase linearly with the frequency and with the radial distance from the cylindrical axis; these results deviate slightly from the quasi-static solutions. The present results for the phase angles of the induced electric fields, however, deviate significantly from the quasi-static solutions, especially, for the high frequency cases.

In the example shown in Figure 2.9, we study the effect of the cylindrical height on the induced electric field at the central section of the cylinder. The cylindrical body has a diameter of 36 cm, but its height varies from 6 cm to 90 cm. The impressed magnetic field at 100 MHz has an intensity of 1 Amp/m. The electrical properties of the body at this frequency are assumed to have σ = 0.889 S/m and ε_r = 71.7. The induced electric fields at the central section of the cylinder are determined and the distributions of their amplitudes and phase angles are plotted for the cases of cylindrical heights; H = 6. 12, 18, 30 and 90 cm. It is observed in Figure 2.9 that as the cylindrical height is increased, the amplitude of the induced electric field at the central section of the cylinder decreases greatly, and its phase angle varies drastically from the quasi-static solution of -90°. This example indicates that the eddy current induced by a RF magnetic field in a cylindrical biological body is strongly dependent on the cylindrical height.



Phase of E (degree $H^1 \approx 1 \text{ A/m}$ $f \approx 100 \text{ MHz}$

° = 0.889 S/ Er = 71.7

Figure 2.9.

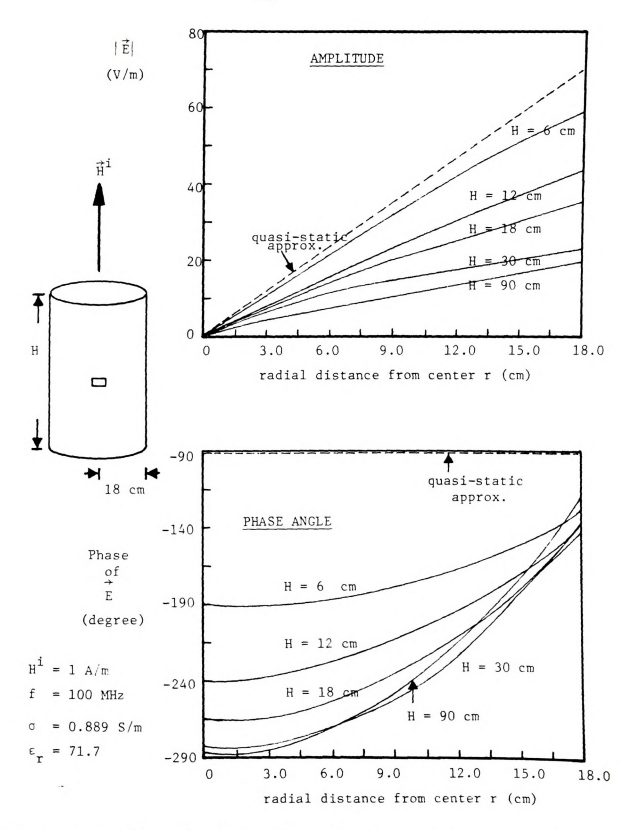


Figure 2.9. Distributions of amplitudes and phase angles of electric fields induced by a 100 MHz magnetic field in the central section of a cylindrical biological body of diameter 36 cm with various heights.

The last the electric with an inte

The c

The case of the eddy current induced by a beam of magnetic field in a biological body is studied next. Figure 2.10 shows the distributions of the amplitudes and phase angles of electric fields induced in a cylindrical body with a diameter of 32 cm and a height of 20 cm, by a beam of 100 MHz magnetic field with a beam diameter of 8 cm and an intensity of 1 Amp/m. The electrical properties of σ = 0.889 S/m and ϵ_{r} = 71.7 are assumed for the body. The impressed electric field for this case is calculated from eq. (2.3). The amplitudes and phase angles of the induced electric fields in five different sections of the cylinder are plotted in Figure 2.10. It is observed that the induced electric field or the induced eddy current is zero at the center of the magnetic beam and it increases linearly to a maximum value at the edge of the beam, and then decays down toward the edge of the body. The deviations between the present results and the quasistatic solutions are indicated in Figure 2.10. The application of a beam of RF magnetic field for the purpose of locally heating a biological body in a hyperthermia cancer therapy is feasible if the low heating at the beam center can be compensated by other means of EM heating.

The last numerical example is the quantification of the electric fields induced by a 100 MHz magnetic field with an intensity of 1 Amp/m in a cylindrical model of man with a height of 168 cm and a maximum diameter of



 $E^{i} = 1 \text{ A/m}$ i = 100 MHz $\sigma = 0.889 \text{ S/}$ $\tau = 71.7$

Pha o E (deg:

Figure 2.10.

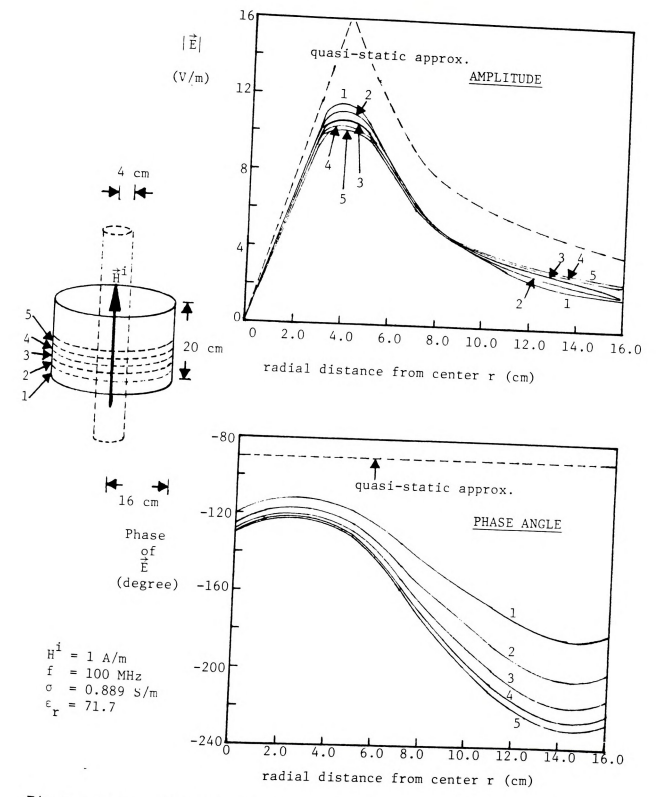


Figure 2.10. Distributions of amplitudes and phase angles of electric fields induced in a cylindrical biological body with a diameter of 32 cm and a height of 20 cm by a beam of 100 MH² magnetic field with a diameter of 8 cm and an intensity of 1 A/m.

36 cm as s and $\varepsilon_{\rm r}=7$ cal calcul of various of 6 cm x

induced ele Figure 2.11 greatly fro

the induced that in the radius of t

The phase a different for body.

2.4. Conver

sented in th of numerical increased.

excellent con demonstrated

of 18 cm is e With an inten of c = 0.889 36 cm as shown in Figure 2.11. Again, $\sigma=0.889~\text{s/m}$ and $\varepsilon_{_{\rm T}}=71.7$ are assumed for the body. In the numerical calculation, the body was subdivided into 66 rings of various radii and with a square cross-sectional area of 6 cm x 6 cm. The amplitudes and phase angles of the induced electric fields inside the body are indicated in Figure 2.11. It is noted that these results deviate greatly from the quasi-static solutions. For example, the induced electric field in the head can be greater than that in the middle section of the body even though the radius of the latter is greater than that of the former. The phase angles of the induced electric fields are very different from -90° and they vary widely throughout the body.

2.4. Convergence of Numerical Results

The accuracy and validity of numerical results presented in this chapter depend greatly on the convergence of numerical results as the number of subdivided rings is increased. Fortunately, the present theory gives an excellent convergence of numerical results. This fact is demonstrated in an example shown in Figure 2.12, in which a cylindrical body with a diameter of 36 cm and a height of 18 cm is exposed to a uniform magnetic field of 100 MHz with an intensity of 1 Amp/m. The electrical properties of σ = 0.889 S/m and ϵ_r = 71.7 are assumed for the body.

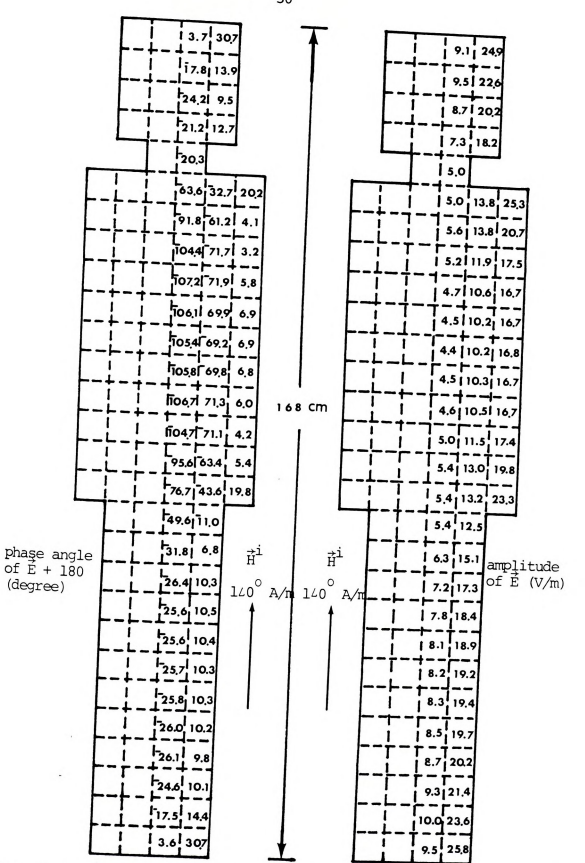


Figure 2.11. Distributions of amplitudes and phase angles of electric fields induced by a uniform magnetic field of 100 MHz in a model of man $(\sigma$ = 0.889 S/m, $\epsilon_{_{\rm T}}$ = 71.7).

In the fi:
divided in
cross-sect
numerical
%1 rings of
sectional
the induce
divisions
the agreem
is excelle
subdivisic
first subd
cal result
results on

without sul advantage p great savi

induced by

2.5. Close With To con

analytical ducting

ducting sph form time-1

μt

In the first numerical calculation, the body was subdivided into 9 rings of various radii and with a square cross-sectional area of 6 cm x 6 cm. In the second numerical calculation, the same body was subdivided into 81 rings of various radii and with a square crosssectional area of 2 cm \times 2 cm. The numerical results on the induced electric fields based on these two ring subdivisions are compared in Figure 2.12. It is observed that the agreement between these two sets of numerical results is excellent even though the number of rings in the second subdivision increases by a factor of 9 from that of the first subdivision. This excellent convergence of numerical results implies that it is possible to obtain accurate results on the electric fields or the eddy currents induced by a RF magnetic field in most biological bodies without subdividing the body into too many rings. This advantage provided by the present method can lead to a great saving in computer time and cost.

2.5. Closed Form Solution for Sphere and Comparison With Present Numerical Results

To compare our numerical results with the existing analytical solution [3], we consider the case of a conducting sphere with radius R which is immersed in a uniform time-harmonic magnetic field,

$$\vec{H}^{i} = \hat{z} H^{i} = \hat{r} H^{i} \cos \theta - \hat{\theta} H^{i} \sin \theta$$

H¹= 1 A/m f = 100 MHz 0 = 0.889 S/m f = 71.7

Figure 2.12.

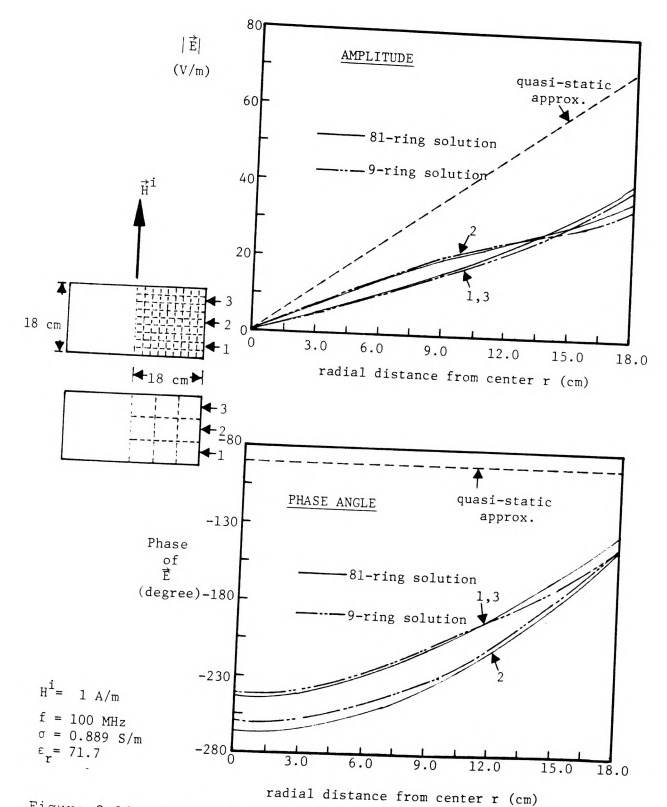


Figure 2.12. Comparison of 81-ring solutions and 9-ring solutions for the electric fields induced in a cylindrical biological body with a diameter of 36 cm and a height of 18 cm by a 100 MH^Z magnetic field with an intensity of 1 A/m.

as shown tained by

where \hat{r}

regions : ${\rm \check{A}_{in}}$

 ${}^{\stackrel{\rightarrow}{A}} \text{out}$

the conduc can be det tions at)

Where $I_{3/}$

1) A 2) -

After some spherical

c₂ = .

Where w = v

the sphere.

where \hat{f} and $\hat{\theta}$ are unit vectors in spherical coordinates, as shown in Figure 2.13. The vector potentials maintained by the induced currents and the sources for the regions inside and outside the sphere can be written as

$$\vec{A}_{in} = (1/2) \mu_0 H^i \sin \theta \frac{c_1}{\sqrt{r}} I_{3/2} [(j\omega \mu_0 \sigma)^{\frac{1}{2}} r] \hat{\phi}$$
when $r < R$ (2.18)

$$\vec{A}_{out} = (1/2) \mu_o H^i \sin\theta (r + \frac{C_2}{r^2}) \hat{\phi} \text{ when } r > R$$
 (2.19)

where ${\rm I}_{3/2}$ is the spherical Bessel function, and σ is the conductivity of the sphere. The constants ${\rm C}_1$ and ${\rm C}_2$ can be determined by use of the following boundary conditions at r = R,

1) A_{in} = A_{out}

2)
$$\frac{\partial}{\partial r}$$
 (r A_{out}) = $\frac{\partial}{\partial r}$ (r A_{in}).

After some manipulations and utilizing some identities of spherical Bessel functions we have

$$c_1 = \frac{3 R^{3/2}}{w I_{1/2}(w)}$$
 (2.20)

$$c_{2} = \frac{3 \text{ w I}_{-1/2}(\text{w}) - (3+\text{w}^{2}) \text{ I}_{1/2}(\text{w})}{\text{w}^{2} \text{ I}_{1/2}(\text{w})} \text{ R}^{3}$$
(2.21)

where $w=\sqrt{2}$ $\frac{R}{\delta}$, and $\delta=\left(\frac{2}{\omega\,\mu_{O}\,\sigma}\right)^{\frac{1}{2}}$ is the skin depth of the sphere. Combining eqs. (2.18) and (2.20), we obtain

Figure

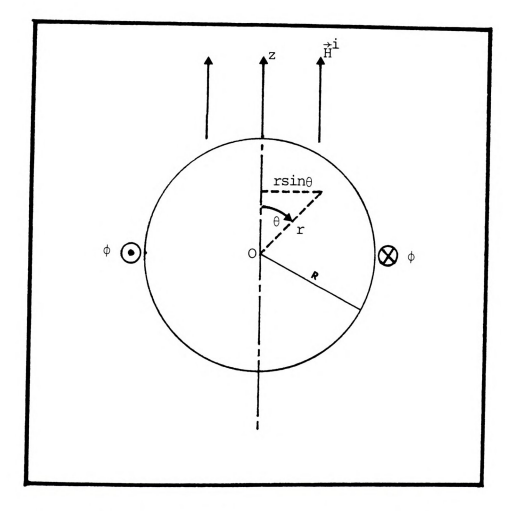


Figure 2.13. A finite conducting sphere with radius R is immersed in a uniform magnetic field polarized in the +z direction.

 $\vec{\mathbf{A}}_{\text{in}}$

To compare that the s $\ensuremath{\text{S/m}}\xspace,$ and a

a uniform (300 MHz. U

radius of t Now for the simulated by

different r evaluated re circular rir

from eq. (2. The comparis Table 2.1 ar approximation

It is ap $^{\rm cal}$ solution the complete expression for \vec{A}_{in} ,

$$\vec{\hat{A}}_{\text{in}} = (3/2) \ \mu_{\text{O}} \ \text{H}^{\text{i}} \ \text{sin} \theta \ \frac{\sqrt{Rr}}{wr} \ \frac{\textbf{I}_{3/2} \, (\text{wr/R})}{\textbf{I}_{1/2} \, (\text{w})} \ \hat{\phi}.$$

Then the electric field induced inside the sphere is given by

$$\vec{E} = -j\omega \vec{A}_{in} = - (3/2) j\omega \mu_0 H^i \sin\theta \sqrt{Rr} \frac{R}{wr} \frac{I_{3/2}(wr/R)}{I_{1/2}(w)} \hat{\phi}.$$
(2.22)

To compare eq. (2.22) with our numerical results, we assume that the sphere has a radius of 2 cm, a conductivity of 8.0 S/m, and a dielectric constant of 50, which is immersed in a uniform oscillating magnetic field with a frequency of 300 MHz. Under these assumptions the skin depth and the radius of the sphere are in the same order of magnitude. Now for the case of numerical evaluation, the sphere is simulated by a "ring sphere" which is constructed with 30 different rings, as shown in Figure 2.14. The numerically evaluated results of the induced electric fields in these circular rings are then compared with those values obtained from eq. (2.22) at corresponding points inside the sphere. The comparison is made in Table 2.1. Also listed in Table 2.1 are the results obtained by the quasi-static approximation.

It is apparent that the agreement between our numerical solution and the existing closed form solution is



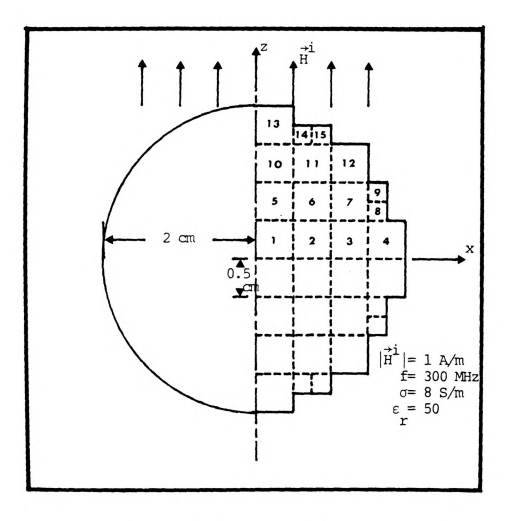


Figure 2.14. A finite conducting sphere with a radius of 2 cm is simulated by a "ring sphere" constructed with 30 circular rings of two different cross-sectional areas. The sphere is assumed to have a conductivity of 8.0 S/m and a dielectric constant of 50, and is immersed in a 300 MH² oscillating magnetic field with an intensity of 1 A/m.

Comparison of the present solutions and a closed form solution for the electric fields induced in a conducting sphere with a conductivity of θ .0 S/m and a distanctic constant of 50 by a 300 MHz magnetic field with an intensity of $1~\Lambda/m$. Also listed are the solutions obtained by the quasi-static approximation.

Table 2.1.

comparison of the present solutions and a closed form solution for the electric fields induced in a conducting sphere with a conductivity of 8.0 S/m and a dislectric constant of 50 by a 300 MHz magnetic field with an intensity of $1~\rm M/m$. Also listed are the solutions obtained by the quasi-static approximation. Table 2.1.

Ring.	Quasi-Static Approximation	tatic	Closed Form Solution	Form	Present Solution	olution
No.	Magnitude (10 V/m)	Phase (Degree)	Magnitude (10 V/m)	Phase (Degree)	Magnitude (10 V/m)	Phase (Degree)
1	0.296	06-	0.230	-25.6	0.259	-26.4
2	0.889	06-	0.689	-31.0	0.770	-31.7
e	1.480	06-	1.162	-41.8	1.269	-42.4
4	2.070	06-	1.681	-57.6	1.787	-58.3
2	0.296	06-	0.230	-30.9	0.256	-32.1
9	0.889	06-	0.692	-36.4	0.763	-37.3
7	1.480	06-	1.173	-47.2	1.264	-48.4
80	1.930	06-	1.557	-56.6	1.647	-58.2
6	1.930	06-	1.582	-60.7	1.658	-62.5
10	0.296	06-	0.232	-41.9	0.253	-43.4
11	0.889	06-	0.704	-47.1	0.759	-48.5
12	1.480	06-	1.206	-57.8	1.271	-59.0
13	0.296	06-	0.241	-57.6	0.255	-60.1
14	0.741	06-	0.600	-56.8	0.635	-59.0
15	1.040	06-	0.849	9.09-	0.894	-62.7

tions th lent agr techniqu static so cates tha usually i 2.6. Exp A se the elect some expe filled wi of substan presented The f Pigure 2.1 Microwave

excellen

Was create reflector.

horizontal ized. The of 500 to

location o field. If

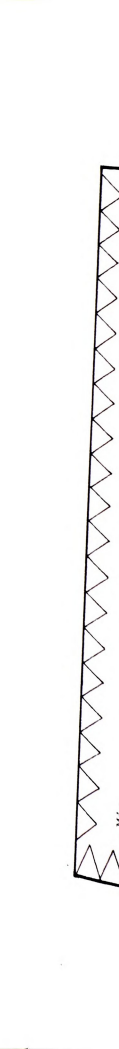
Propagatio:

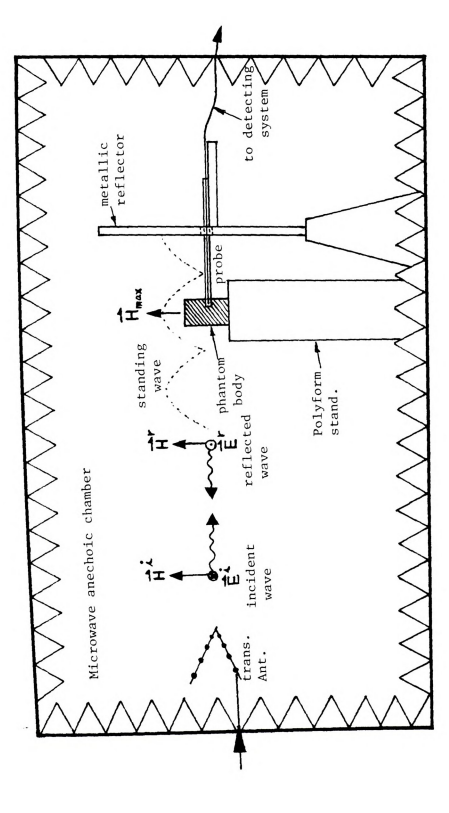
excellent for both the magnitude and the phase distributions throughout the interior of the sphere. This excellent agreement confirms the accuracy of our numerical technique. Furthermore, the deviation of the quasistatic solution from the other two sets of solutions indicates that the conventional quasi-static solution is usually inadequate.

2.6. Experimental Setup

A series of experiments has been conducted to measure the electric fields induced by UHF magnetic fields inside some experimental models constructed with plexiglass and filled with phantom biological materials for the purpose of substantiating the accuracy of theoretical results presented in this chapter.

The experimental setup is depicted schematically in Figure 2.15. The experiment was conducted inside a large microwave anechoic chamber in which a standing EM wave was created by radiating an EM wave upon a metallic reflector. The electric field of the wave was polarized horizontally and the magnetic field was vertically polarized. The experiment was conducted in the frequency range of 500 to 750 MHz. The phantom body was placed at the location of a maximum magnetic field or a minimum electric field. If the body dimension in the direction of wave propagation is small compared with the wavelength, the





Experimental setup for measuring the electric fields inside the phantom biological bodies induced by RF magnetic fields. Figure 2.15.

impresse body can field in able ele Wire sys The outpu tem outs: 2.7. <u>Exp</u> The phantom b The elect to be app ment was at the lo length (4) direction cylindrica

field prob tude of the

tral secti cylindrica amplitudes Figure 2.1 ponding th lines. It impressed magnetic field at any point inside the phantom body can be assumed to be uniform. The induced electric field inside the phantom body was measured by an implantable electric field probe with an interference-free leadwire system. This probe was described elsewhere [5]. The output of the probe was connected to a detecting system outside the anechoic chamber.

2.7. Experimental Results and Comparison With Theoretical Results

The first experiment was conducted on a cylindrical phantom body with a diameter of 4 cm and a variable height. The electric properties of the phantom body were estimated to be approximately $\sigma = 5.0 \text{ S/m}$ and $\varepsilon_{\text{m}} = 50$. The experiment was conducted at 750 MHz and the cylinder was placed at the location of a maximum magnetic field, one wavelength (40 cm) in front of the metallic reflector. The direction of the magnetic field was in parallel with the cylindrical axis. The induced electric field in the central section of the cylinder was probed for three cases of cylindrical heights; H = 2, 4 and 8 cm. The measured amplitudes of the induced electric fields are plotted in Figure 2.16 with dashed lines, in comparison with corresponding theoretical results which are indicated with solid lines. It is noted that with an implantable electric field probe loaded with a microwave diode, only the amplitude of the induced electric field could be measured. In

50 , \overline{z} , (V/n) 40

Figure 2.16.

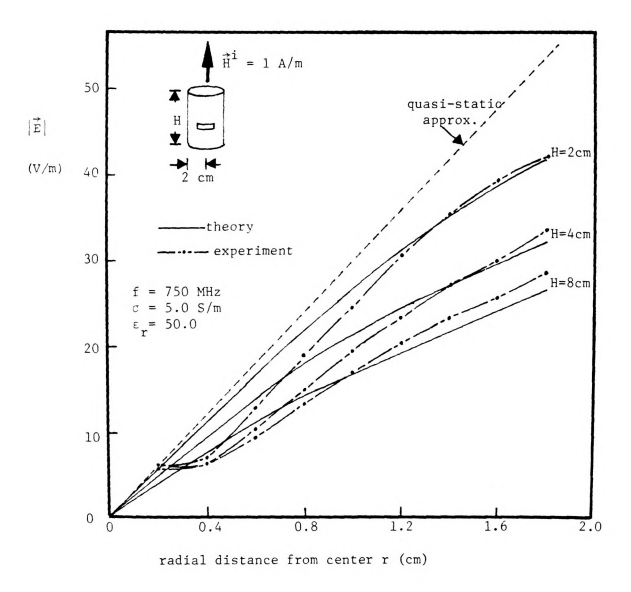


Figure 2.16. Comparison of theoretical and experimental results for the amplitudes of electric fields induced in a phantom biological cylinder of 4 cm diameter with various heights by a 750 MHz magnetic field.

Figure 2 theoretic near the probe (ab significa theory and effect of severe if is about o in Figure predicted . Was increas section of also found static solu The sea cylinder wit to study the electric fie ^{conductiviti}

The experiment was placed and in the previous at the central the distribut Nigure 2.17 i

Figure 2.16, the agreement between experimental and theoretical results is very good except in the region near the cylindrical axis where the perturbation of the probe (about 1 cm in size) on the induced current becomes significant. Another cause of discrepancy between the theory and the experiment can be attributed to the image effect of the metallic reflector; this effect is not severe if the distance between the body and the reflector is about one wavelength or greater. The important finding in Figure 2.16 is that it was observed experimentally and predicted theoretically that as the cylindrical height was increased, the induced electric field in the central section of the cylinder decreased. These results were also found to be significantly different from the quasistatic solutions.

The second experiment was conducted on a phantom cylinder with a diameter of 3.8 cm and a height of 3.8 cm to study the effect of body conductivity on the induced electric field. Three kinds of phantom materials with conductivities of $\sigma=2.2,\ 4.5$ and 6.0 S/m were used. The experiment was conducted at 750 MHz, and the cylinder was placed at the location of a maximum magnetic field as in the previous experiment. The induced electric fields at the central section of the cylinder were probed, and the distributions of their amplitudes are plotted in Figure 2.17 in comparison with corresponding theoretical

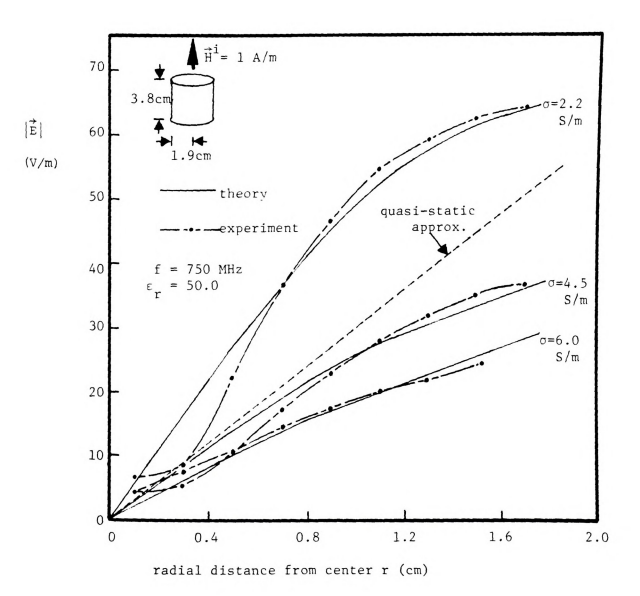


Figure 2.17. Comparison of theoretical and experimental results for the amplitudes of electric fields induced in a phantom biological cylinder with a diameter of 3.8 cm, a height of 3.8 cm and various conductivities by a 750 MHz magnetic field.

is increa effect wa by experi and exper quasi-sta experimen The induced e The phant and filler 22.2 cm an Figure 2. and electr are approx placed upr field with the long d fields at

measured and indicated ponding the and experi rather commental and very diffe

results.

results. It was observed that as the body conductivity is increased, the induced electric field decreases. This effect was accurately predicted by theory and confirmed by experiment. It is also noted that both theoretical and experimental results deviate significantly from the quasi-static solutions. The agreement between theory and experiment as shown in Figure 2.17 is very good.

The third experiment was conducted to measure the induced electric fields inside a phantom model of man. The phantom model of man was constructed with plexiqlass and filled with phantom material, and has a height of 22.2 cm and a maximum diameter of 3.8 cm as shown in Figure 2.18. The experiment was conducted at 750 MHz, and electrical properties of the model at this frequency are approximately σ = 5.0 S/m and ε_{r} = 50. The model was placed upright at the location of a maximum magnetic field with the impressed magnetic field in parallel with the long dimension of the body. The induced electric fields at 32 locations of the body were probed. The measured amplitudes of the induced electric fields are indicated in Figure 2.18 in comparison with the corresponding theoretical results. The agreement between theory and experiment is considered to be very good in this rather complicated body. It is to be noted that experimental and theoretical results shown in Figure 2.18 are very different from the quasi-static solutions.





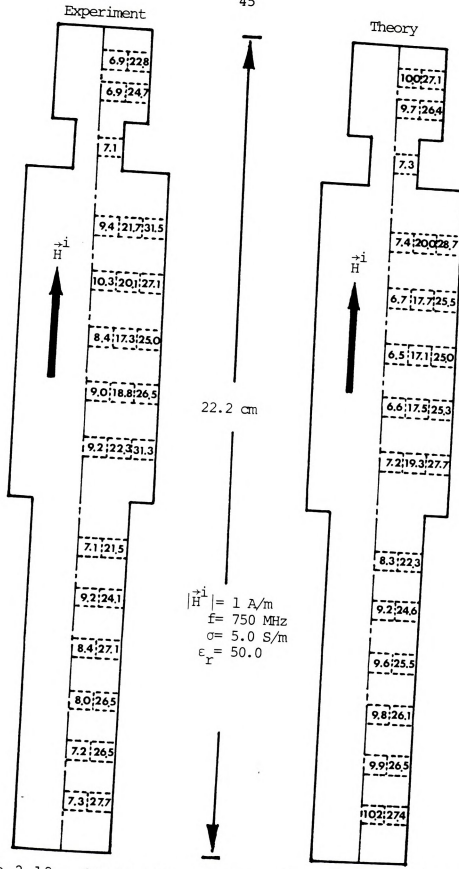


Figure 2.18. Comparison of theoretical and experimental results for the amplitudes of electric fields induced in a phantom model of man (height = 22.2 cm, max. diameter = 3.8 cm) by a 750 MHz magnetic field.

tion of a Since the

electric field was

cal calcu! body. From

experiment standing E

Was

μį

Where y =

A very good agreement between theory and experiment as demonstrated in Figures 2.16, 2.17 and 2.18 confirms the validity and accuracy of the theoretical method presented in this chapter.

2.8. Discussion

In the experiment, the body was placed at the location of a maximum magnetic field in a standing EM wave. Since the body dimension in the direction of wave propagation was small compared with the wavelength, the impressed magnetic field inside the body was assumed to be uniform. Under this approximation, the impressed electric field associated with the impressed magnetic field was

$$\vec{E}^{\dot{1}} = -\frac{j}{2} \omega \mu_{o} H^{\dot{1}} r \hat{\phi} \qquad (2.2)$$

as has been given before. This $\dot{\vec{E}}^i$ was used in the numerical calculation of the induced electric field inside the body.

From a different point of view, the body in the experiment was located at a minimum electric field of a standing EM wave, and the actual impressed electric field was

$$\dot{\vec{E}}^{\dot{i}} = \hat{x} \ j \sqrt{\frac{\mu_{o}}{\epsilon_{o}}} H^{\dot{i}} \ \text{sin ky} \ \dot{=} \ \hat{x} \ j \omega \mu_{o} \ H^{\dot{i}} \ y \tag{2.23}$$

where y = 0 corresponds to the center of the body.

 $\dot{\tilde{E}}^{i}$ in eq. (

amplitude the y axi It i

^{†i}'s can electric that, ind

results on This pheno experiment

chapter.

 \dot{E}^{i} given in eq. (2.2) is circulatory and that given in eq. (2.23) is linear and antisymmetrical. Also the amplitude of the latter is twice that of the former along the y axis.

It is important to ask whether these two different $\vec{E}^{\dot{1}}$'s can yield the same theoretical values for the induced electric fields in the body? We have numerically proved that, indeed, these two $\vec{E}^{\dot{1}}$'s give very similar numerical results on the induced electric fields in the same body. This phenomenon resulted in a very good agreement between experimental and theoretical results reported in this chapter.

Only

Volume int

CHAPTER III

SURFACE INTEGRAL EQUATION METHOD FOR INTERACTION OF MICROWAVE WITH BIOLOGICAL BODY

Only in recent years has beamed microwave power been proposed as a new technique in transporting high-level energy between two remote transmitting-receiving stations, and has microwave heating been considered as an effective method in hyperthermia cancer therapy. Although EM transmission and scattering phenomena have been major and classical topics in electrodynamics since the end of the last century, uncertainties about the potential hazards of these high-power microwave radiations are still major concerns relating to the acceptability of these newly developed technologies. In order to fully understand the biological effects of microwave radiation, it is necessary to quantify the electric fields induced in the biological bodies when they are irradiated by the incident EM waves.

Existing methods of quantifying the electric fields induced by EM waves are mostly based on the solutions of volume integral equations. Unfortunately, when the body is large compared with the wavelength of the incident

wave, t ficient mainly o it is be nique i In two coup between volume i 3.1. <u>In</u> Hig between nate sch the poter the beams fully cor Also, the are becom tive in h field int for the h to obtain interacti

> John Wave irra

wave, the volume integral equation method becomes inefficient. Since for this case, the induced electric field is mainly concentrated in the region near the body surface, it is believed that the surface integral equation technique is potentially more efficient.

In this chapter, we develop a new technique based on two coupled surface integral equations. A good agreement between our solutions and the existing results obtained by volume integral equation method has been verified.

3.1. Introduction

High-level, beamed-power microwave transmission between satellites and earth has been proposed as an alternate scheme for providing energy in the future. However, the potential hazards which exist in the interface between the beamed-power microwave and personnel should be carefully considered by the microwave systems design engineers. Also, the thermal-heating effects of intense microwaves are becoming well known, and have been demonstrated effective in hyperthermia cancer therapy. But the allowable field intensity and the permissible level of absorbed power for the human body still remain unknown. It is desirable to obtain some quantitative information about microwave interactions with human or other biological bodies.

Johnson and Durney [6] have investigated the plane wave irradiation of a prolate-spheroid model of man based

on the p Their th compared approach the inte an ellip developed equation, be used t arbitrari This volu tions tha small ele electrica: inside the face. Cor becomes in equation m $^{
m approach}.$ employed by induced ins only infinj surface int and Miller

tives of the

on the perturbation theory described by Van Bladel [7]. Their theory is valid only when the wavelength is long compared to the dimensions of the spheroid. The same approach has been adopted by Massoudi [8] to solve for the internal electric field induced by a plane wave inside an ellipsoidal model of man. Livesay and Chen [9] have developed a theoretical method based on a volume integral equation, the so called Tensor Integral Equation, which can be used to quantify the electric field induced inside an arbitrarily shaped biological body by an incident EM wave. This volume integral equation method removes the restrictions that the irradiated bodies have simple shapes and small electrical dimensions. However, when the body is electrically large, the EM waves cannot penetrate deeply inside the body, and will concentrate near the body surface. Consequently, the volume integral equation method becomes inefficient. For this case, the surface integral equation method seems to be a reasonable alternative approach. A surface integral equation method has been employed by Wu et al. [10] to solve for the EM fields induced inside arbitrary cylinders of biological tissue; only infinitely long cylinders were considered. Another surface integral formulation has been developed by Poggio and Miller [11]; however, in their formulation the derivatives of the surface unknowns are involved in the integrands of the surface integrals. This makes the numerical

solution Wang [12 conducti divides cells, b It is de the field gral equa tries mor In t integral field on conducting field can field, onc Befor Section 3. tion of Ma and 3.3, r integral e interface : of solution in Section

for the sol Presented i are given i solutions difficult, if not impossible, to implement. Wang [12] has determined the scattering characteristics of conducting bodies by use of the moment-method, which divides the surface of the body into trilateral surface cells, but only results for sphere have been reported. It is desirable to obtain more complete information about the fields induced by EM waves, based on the surface integral equations, for finite conducting bodies with geometries more complicated than that of the sphere.

In this chapter, we will develop a new surface integral equation technique to quantify the induced EM field on the surface of an arbitrarily shaped, finite conducting body. It should be emphasized that the internal field can be readily determined in terms of the surface field, once it is found.

Before the surface integral equations are derived in Section 3.4, two preliminary theorems and a general solution of Maxwell's equations are described in Sections 3.2 and 3.3, respectively. The application of the coupled, surface integral equations to the special case of an infinite interface is considered in Section 3.5. The moment-method of solution of these integral equations is briefly reviewed in Section 3.6. The development of the numerical technique for the solutions of the surface integral equations is presented in Section 3.7. Finally, some numerical examples are given in Section 3.8.

3.2. <u>T</u>

Be:

derived, consist theorems

elsewhere The

describe

Let and U be

With the s

Where |s|

7

by contour exterior t

exterior to represents

del-operato

If the

. n̂ (ξ

3.2. The Preliminary Theorems

Before the coupled, surface integral equations are derived, we must introduce two preliminary theorems which consist of several vector integral identities. These theorems are necessary for the derivation, and will be described without proof. The related proof can be found elsewhere [13].

Theorem 1.

Let \vec{v} , $\overset{\rightarrow}{\circ}$, \vec{v} be continuous on the closed surface F, and U be a differentiable function. Then

$$\int_{\mathbf{F}} \mathbf{U} \nabla_{\mathbf{O}} \cdot \overrightarrow{\mathbf{v}} d\mathbf{F}' = -\int_{\mathbf{F}} \overrightarrow{\mathbf{v}} \cdot \nabla_{\mathbf{O}} \mathbf{U} d\mathbf{F}'$$

with the surface divergence $\nabla \cdot \vec{v}$ defined as

$$\nabla_{\mathbf{O}} \cdot \vec{\mathbf{v}} \equiv \begin{vmatrix} \lim_{|\mathbf{S}| \to 0} \frac{1}{|\mathbf{S}|} \int_{\mathbf{C}} (\hat{\mathbf{n}}_{\mathbf{O}} \cdot \vec{\mathbf{v}}) d\mathbf{1} \end{vmatrix}$$

where |S| is the area of a small surface element S enclosed by contour C, and \hat{n}_O is a unit normal vector on C directed exterior to S. It can be shown that $\nabla_O = \nabla - \hat{n} \frac{\partial}{\partial n}$, where ∇ represents the conventional three-dimensional differential del-operator.

Theorem 2.

If the surface field $\vec{j}(\vec{r}')$ is continuous on F, then

$$\hat{\mathbf{n}}(\vec{\xi}) \times \int_{\mathbf{F}_{i}} [\vec{\mathbf{r}}'(\vec{\mathbf{r}}') \times \nabla' \Phi(\vec{\mathbf{r}}, \vec{\mathbf{r}}')] d\mathbf{F}' = -2\pi \hat{\mathbf{r}}(\vec{\xi}) +$$

$$\hat{n}(\vec{\xi}) \times \int_{\mathbf{F}} [\vec{j}(\vec{r}') \times \nabla' \Phi(\vec{\xi}, \vec{r}')] d\mathbf{F}'.$$

The sign gration, Also

The sign gration,

are both limits wh

surface F

3.3. <u>The</u> in a

region G_s,

With volum

radiates i

and isotro

region G

Based

densities a

Q_e

The sign f_{F_1} implies that \dot{r} is the field point in the integration, and lying in the interior side of the surface F. Also

$$\begin{split} \hat{\mathbf{n}} \left(\overrightarrow{\xi} \right) & \times \int_{\mathbf{F}} \left[\overrightarrow{j} \left(\overrightarrow{\mathbf{r}}' \right) \right] \times \nabla^{\dagger} \phi \left(\overrightarrow{\mathbf{r}}, \overrightarrow{\mathbf{r}}' \right) \right] d\mathbf{F}' = 2\pi \overrightarrow{j} \left(\overrightarrow{\xi} \right) + \\ & \hat{\mathbf{n}} \left(\overrightarrow{\xi} \right) \times \int_{\mathbf{F}} \left[\overrightarrow{j} \left(\overrightarrow{\mathbf{r}}' \right) \right] \times \nabla^{\dagger} \phi \left(\overrightarrow{\xi}, \overrightarrow{\mathbf{r}}' \right) \right] d\mathbf{F}' \end{split}$$

The sign $f_{\stackrel{}{\to} e}$ implies that \mathring{r} is the field point in the integration, and lying in the exterior side of the surface F.

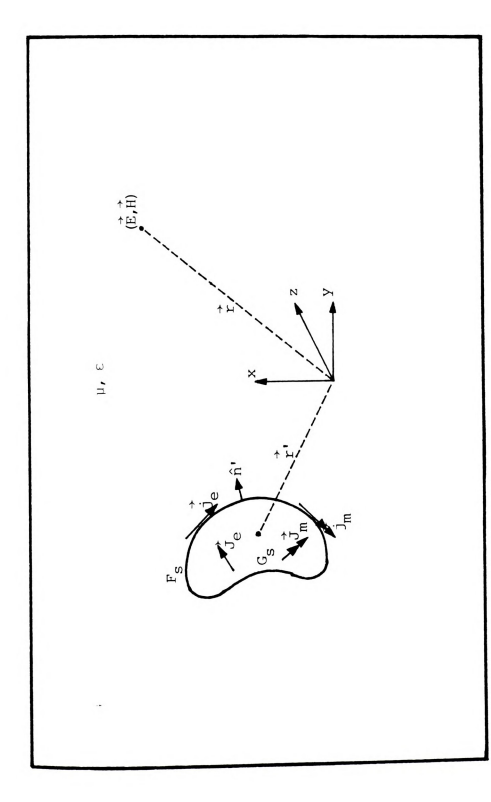
The eventual field point $\vec{\xi}$ and the source point \vec{r}' are both on the surface F. We denote with $\int_{\vec{F}_1}$ and $\int_{\vec{F}_2}$ the limits which we obtain if \vec{r} approaches the point $\vec{\xi}$ of the surface F from the interior or exterior, respectively.

3.3. The General Solution of Maxwell's Equations in an Unbounded Homogeneous Space

Let us consider the problem where a finite source region G_S , consisting of electric and magnetic sources with volume current densities of \mathring{J}_e and \mathring{J}_m , respectively, radiates into a lossless, unbounded, homogeneous, linear, and isotropic medium with permeability μ and permittivity ϵ , as shown in Figure 3.1 where we assume that the source region G_S is enclosed by surface F_S .

$$Q_e = \frac{j}{\omega} \nabla \cdot \vec{J}_e$$
 $Q_m = \frac{j}{\omega} \nabla \cdot \vec{J}_m$

U *11



A source region G_g enclosed by surface F_g is characterized by volume current densities (J_g, J_m) and equivalent surface current densities (J_g, J_m) . These current sources radiate into a momogeneous space with permeability μ and permittivity ε , and maintain an EM field (\vec{E}_r, \vec{H}) at point \vec{r} . Figure 3.1.

From the electric the above

where a

Ĕ(r

 Q_e , and

 $\stackrel{\rightarrow}{\text{H}}\stackrel{\rightarrow}{\text{(r)}}$ with φ =

ing the

ω√με is Now

the equip

where a time variation of $e^{\mathrm{j}\omega t}$ has been assumed, and ω is the angular frequency of the sources.

From the general solution of Maxwell's equations [14], the electromagnetic field at any point \vec{r} maintained by the above sources can be expressed in terms of \vec{J}_e , \vec{J}_m , Q_e , and Q_m as

$$\vec{E}(\vec{r}) = \frac{1}{4\pi} \int_{G_{S}} [-\vec{J}_{m} \times \nabla' \phi + \frac{Q_{e}}{\epsilon} \nabla' \phi - j\omega\mu \vec{J}_{e}' \phi] dG' \qquad (3.1)$$

$$\vec{H}(\vec{r}) = \frac{1}{4\pi} \int_{G_{\vec{S}}} [\vec{J}_{\vec{e}} \times \nabla \cdot \phi + \frac{Q_{\vec{m}}}{\mu} \nabla \cdot \phi - j\omega \epsilon \vec{J}_{\vec{m}} \phi] dG' \qquad (3.2)$$

with $\Phi=\frac{e^{-j\,k\left|\stackrel{\rightarrow}{r}-\stackrel{\rightarrow}{r}^{*}\right|}}{\left|\stackrel{\rightarrow}{r}-\stackrel{\rightarrow}{r}^{*}\right|}$, where $\stackrel{\rightarrow}{r}^{*}$ is the position vector locating the source point inside the source region $G_{_{S}}$, and $k=\omega\sqrt{\mu\epsilon}$ is the wavenumber in unbounded space.

Now let's define the following source densities of the equivalent surface currents and charges on the closed surface $F_{\rm c}$

$$\begin{aligned} &\vec{j}_{e} & \equiv \hat{\mathbf{n}} \cdot \mathbf{x} \cdot \vec{\mathbf{H}} \\ &\vec{j}_{m} & \equiv -\hat{\mathbf{n}} \cdot \mathbf{x} \cdot \vec{\mathbf{E}} / n_{o} \\ &\mathbf{q}_{e} & = \frac{\mathbf{j}}{\omega} \nabla_{o} \cdot \vec{j}_{e} \\ &\mathbf{q}_{m} & = \frac{\mathbf{j}}{\omega} \nabla_{o} \cdot \vec{j}_{m} \end{aligned}$$

where $\hat{n}^{\, \iota}$ is the outward unit normal vector on $\boldsymbol{F}_{_{\boldsymbol{S}}},$ and $\boldsymbol{\eta}_{_{\boldsymbol{O}}} = \sqrt{\mu_{_{\boldsymbol{O}}}/\epsilon_{_{\boldsymbol{O}}}} \text{ is the intrinsic wave impedance in free space.}$

can als [14] Ė(Ĥ (Where ¢ The last as the b 3.4. <u>De</u> To first con that a f irradiate region G assumed t mittivity With a ho

where ϵ_{r} i ${\tt ductivity}$

Th

 μ_0 and co $^{\ell_{\mbox{\scriptsize d}}}$ is def The above electromagnetic field (\vec{E}, \vec{H}) at position \vec{r} can also be expressed in terms of \vec{j}_e , \vec{j}_m , q_e , and q_m as [14]

$$\vec{E}(\vec{r}) = \frac{1}{4\pi} \int_{F_S} \left[-\eta_O \vec{j}_m \ X \ \nabla' \phi + \frac{q_e}{\epsilon} \nabla' \phi - j\omega \mu_{j_e}^{\dagger} \phi \right] \ dF' \ (3.3)$$

$$\vec{H}(\vec{r}) = \frac{1}{4\pi} \int_{F_g} \left[\vec{j}_e \ X \ \nabla^{\dagger} \phi + \frac{q_m}{\mu} \nabla^{\dagger} \phi - j \omega \epsilon \eta_o \vec{j}_m \phi \right] \ dF' \ (3.4)$$

where ϕ has the same form as that of eqs. (3.1) and (3.2). The last two equations are very important, and will serve as the basic tool in the following derivation.

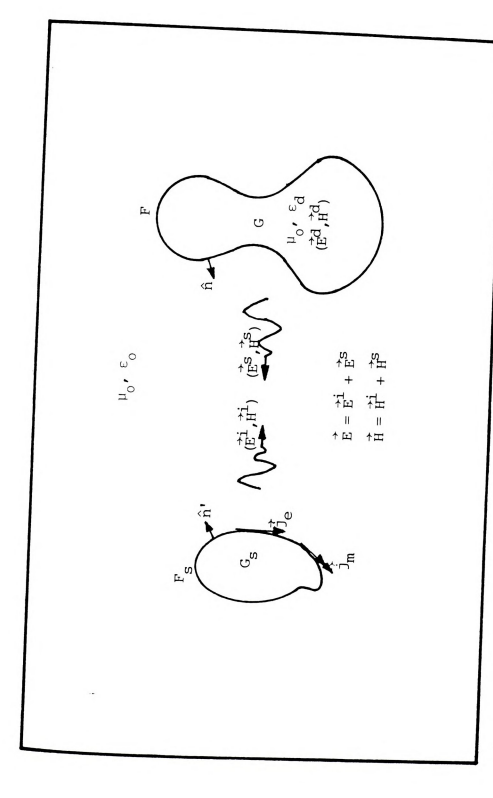
3.4. Derivation of the Coupled Surface Integral Equations

To derive the coupled, surface integral equations, we first consider the geometry shown in Figure 3.2. We assume that a finite conducting body G enclosed by surface F is irradiated by the electromagnetic wave from the source region G_S . The medium in the region external to F is assumed to be free space with permeability $\nu_{_{\hbox{\scriptsize O}}}$ and permittivity $\epsilon_{_{\hbox{\scriptsize O}}}$. The finite conducting body is constructed with a homogeneous material characterized by permeability $\nu_{_{\hbox{\scriptsize O}}}$ and complex permittivity $\epsilon_{_{\hbox{\scriptsize d}}}$. The complex permittivity $\epsilon_{_{\hbox{\scriptsize d}}}$ is defined by

$$\varepsilon_{\tilde{d}} = \varepsilon_{o} (\varepsilon_{r} - j \frac{\sigma}{\omega \varepsilon_{o}})$$

where $\epsilon_{_{\bf T}}$ is the dielectric constant, and σ is the conductivity of the body. The source region ${\rm G}_{_{\bf S}}$ is





A finite conducting body G, immersed in free space and enclosed by surface F, with a permeability we and a complex permittivity to a sirradiated by the incident field (E., #1) radiated from sities (Ge, #1) are defined on the surface current denscattered from and induced in the surface Fs. The DM fields and (Ed, #d), respectively. Figure 3.2.

charact $(\dot{j}_e,\dot{j}_m$

Le by the

body by fields s $(\vec{\mathbb{E}}^d, \vec{\mathbb{H}}^d)$

sider th I)

To

the regi ∇ X

7 X

Defining current d

7 X Where

After subs We may see

duction cu

of jeq e as

characterized by the equivalent surface current densities $(\mathring{J}_{\mu},\ \mathring{J}_{m})$ on surface F_{S} .

Let us denote the incident field which is radiated by the sources in the absence of the finite conducting body by (\vec{E}^i, \vec{H}^i) . With the body present, we denote the fields scattered from and induced in it as (\vec{E}^S, \vec{H}^S) and (\vec{E}^d, \vec{H}^d) , respectively. Now we are in a position to consider these three sets of EM fields separately.

I) The Scattered Field (\vec{E}^S, \vec{H}^S) :

To begin with, let's consider Maxwell's equations in the region internal to F. They are

$$\nabla \times \vec{H}^{d} = j\omega \varepsilon_{0} \vec{E}^{d} + j\omega (\varepsilon_{d} - \varepsilon_{0}) \vec{E}^{d}$$
 (3.5)

$$\nabla \times \vec{E}^{d} = -j\omega\mu_{O}\vec{H}^{d}. \tag{3.6}$$

Defining the last term of eq. (3.5) as an equivalent volume current density, then eq. (3.5) becomes

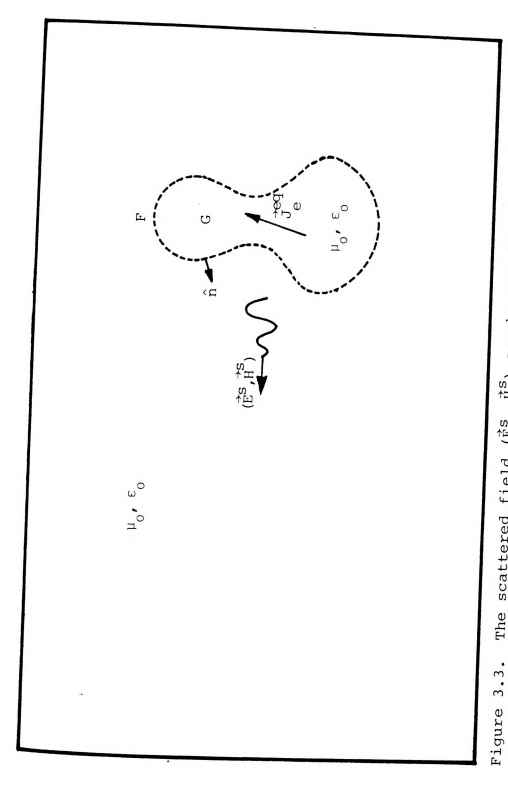
$$\nabla \times \vec{H}^{d} = j\omega \varepsilon_{o} \vec{E}^{d} + \vec{J}_{e}^{eq}$$
 (3.5')

where

$$\vec{J}_{e}^{eq} = j\omega(\varepsilon_{d} - \varepsilon_{o}) \vec{E}^{d}. \tag{3.7}$$

After substituting the expression for $\epsilon_{\rm d}$ into eq. (3.7), we may see that $J_{\rm e}^{\rm eq}$ consists of two components: the conduction current and the polarization current. We may think of $J_{\rm e}^{\rm eq}$ as a current existing in free space as shown in





The scattered field (\hat{b}_s , $\hat{\mu}_s$) can be considered as originated from an equivalent current source \hat{b}_e 0 existing inside the body current source consists of two components, the conduction current rent and the polarization current.

Figure and (3

Ι includ

the sc current Hence,

written

, H°

Ės

Where Q_{ϵ}^{ϵ}

and $k_0 =$

Now Sities in

face F as

js jm =

je s

qe =

Figure 3.3, since only $\boldsymbol{\mu}_{0}$ and $\boldsymbol{\epsilon}_{0}$ appear in eqs. (3.5') and (3.6).

It is to be noted that the source region G_s is not included in Figure 3.3, because \vec{J}_e^{eq} is the only source of the scattered field (\vec{E}^S, \vec{H}^S) . Furthermore, the equivalent current \vec{J}_e^{eq} radiates into an unbounded, homogeneous space. Hence, based on eqs. (3.1) and (3.2), \vec{E}^S and \vec{H}^S can be written as

$$\begin{split} & \dot{\vec{E}}^{S} = \frac{1}{4\pi} \int_{G} [\frac{Q_{e}^{eq}}{\epsilon_{o}} \nabla' \phi_{f} - j\omega\mu_{o} \dot{\vec{J}}_{e}^{eq} \phi_{f}] \ dG' \\ & \dot{\vec{H}}^{S} = \frac{1}{4\pi} \int_{G} [\dot{\vec{J}}_{e}^{eq} \times \nabla' \phi_{f}] \ dG' \end{split}$$

where $\textbf{Q}_{e}^{eq}=\frac{\textbf{j}}{\omega}\ \textbf{v}\cdot \textbf{J}_{e}^{eq}$ is the equivalent volume charge density,

$$\phi_{\rm f} = \frac{e^{-jk_{\rm O}|\vec{r}-\vec{r}^{\,\prime}|}}{|\vec{r}-\vec{r}^{\,\prime}|} \mbox{ is the Green's function for free space,}$$
 and $k_{\rm O} = \omega \sqrt{\mu_{\rm O} \epsilon_{\rm O}}$ is the wavenumber in free space.

Now let's define the equivalent surface current densities in terms of the scattered field (\vec{E}^S, \vec{H}^S) on the surface F as

$$\vec{J}_{e}^{s} = \hat{n} \times \hat{H}^{s}$$

$$\vec{J}_{m}^{s} = -\hat{n} \times \hat{E}^{s}/\eta_{o}$$

$$q_{e}^{s} = \frac{j}{m} \nabla_{o} \cdot \hat{J}_{e}^{s}$$

q. where f

Fr

the equ $(\stackrel{\scriptsize \downarrow}{\mathbb{E}}^{\mathtt{S}},\stackrel{\scriptsize \uparrow}{\mathbb{H}}^{\mathtt{S}}$ shown in

 j_{m}^{ts}) rad we can e

(3.3) an the EM f equivale

 $\dot{E}^{S} = \frac{1}{4\pi}$

 $\dot{H}^{S} = \frac{1}{4\pi}$

as the sc to F. In ^{Vanish}, i

 $0 = \frac{1}{4\pi} \int_{\mathbf{F}}$

 $0 = \frac{1}{4\pi} \int_{\mathbf{F}}$

because th

$$q_m^s = \frac{j}{\omega} \nabla_o \cdot j_m^s$$

where n is the outward unit normal vector on F.

From the equivalence theorem [15], [16], we know that the equivalent surface currents $(\vec{j}_e^S, \vec{j}_m^S)$ on F can support (\vec{E}^S, \vec{H}^S) external to F and zero field internal to F as shown in Figure 3.4. Since the surface currents $(\vec{j}_e^S, \vec{j}_m^S)$ radiate in an unbounded homogeneous space (free space), we can evaluate the EM fields supported by them with eqs. (3.3) and (3.4). From the uniqueness theorem, we know that the EM fields so calculated will be those postulated by the equivalence theorem. Hence we have

$$\vec{E}^{S} = \frac{1}{4\pi} \int_{F} \left[-\eta_{O} \dot{j}_{m}^{S} \times \nabla' \dot{\phi}_{f} + \frac{q_{e}^{S}}{\varepsilon} \nabla' \dot{\phi}_{f} - j\omega \mu_{O} \dot{j}_{e}^{S} \dot{\phi}_{f} \right] dF'$$

$$\vec{H}^{S} = \frac{1}{4\pi} \int_{F} \left[\dot{j}_{e}^{S} \times \nabla' \dot{\phi}_{f} + \frac{q_{m}^{S}}{\mu_{O}} \nabla' \dot{\phi}_{f} - j\omega \varepsilon_{O} \eta_{O} \dot{j}_{m}^{S} \dot{\phi}_{f} \right] dF'$$

$$(3.8)$$
external to F

$$(3.9)$$

as the scattered field at any point in the region external to F. In the region internal to F, the above two integrals vanish, i.e.,

$$0 = \frac{1}{4\pi} \int_{\mathbf{F}} \left[-\eta_{o} \overset{+}{J}_{m}^{s} \times \nabla' \varphi_{f} + \frac{q_{e}^{s}}{\varepsilon_{o}} \nabla' \varphi_{f} - j\omega \mu_{o} \overset{+}{J}_{e}^{s} \varphi_{f} \right] dF'$$

$$0 = \frac{1}{4\pi} \int_{\mathbf{F}} \left[\overset{+}{J}_{e}^{s} \times \nabla' \varphi_{f} + \frac{q_{m}^{s}}{\mu_{o}} \nabla' \varphi_{f} - j\omega \varepsilon_{o} \eta_{o} \overset{+}{J}_{m}^{s} \varphi_{f} \right] dF'$$

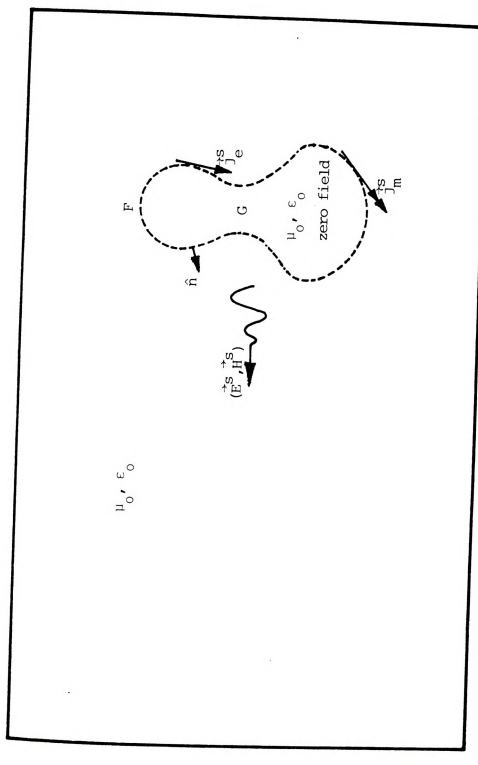
$$(3.10)$$

$$internal to \mathbf{F}$$

$$(3.11)$$

because there is a null field internal to F.





The scattered field (\vec{E}^s , \vec{H}^s) in the exterior of the body and a zero field in the interior of the body are maintained by the equivalent surface currents (\vec{J}^s , \vec{J}^s), which are defined in terms of the scattered field on surface \vec{H} . The body region G has been replaced by free space. Figure 3.4.

q^de

 $q_{\mathtt{m}}^{\mathrm{d}}$

Again, f

that, wi homogene

complex surface field $(\vec{E}$

in the r tions (3

fields;

II) The Induced Field (\vec{E}^d, \vec{H}^d) :

To investigate the induced field $(\stackrel{\rightarrow}{E}^d,\stackrel{\rightarrow}{H}^d)$, let us consider Figure 3.2 again. This time we treat the interior region of G as source free with the induced field $(\stackrel{\rightarrow}{E}^d,\stackrel{\rightarrow}{H}^d)$ maintained by the sources existing in the exterior region of G. As for the case of scattered field, we may define a set of equivalent surface current densities $(\stackrel{\uparrow}{\downarrow}^d_e,\stackrel{\uparrow}{\downarrow}^d_m)$ in terms of the surface value of $(\stackrel{\rightarrow}{E}^d,\stackrel{\rightarrow}{H}^d)$:

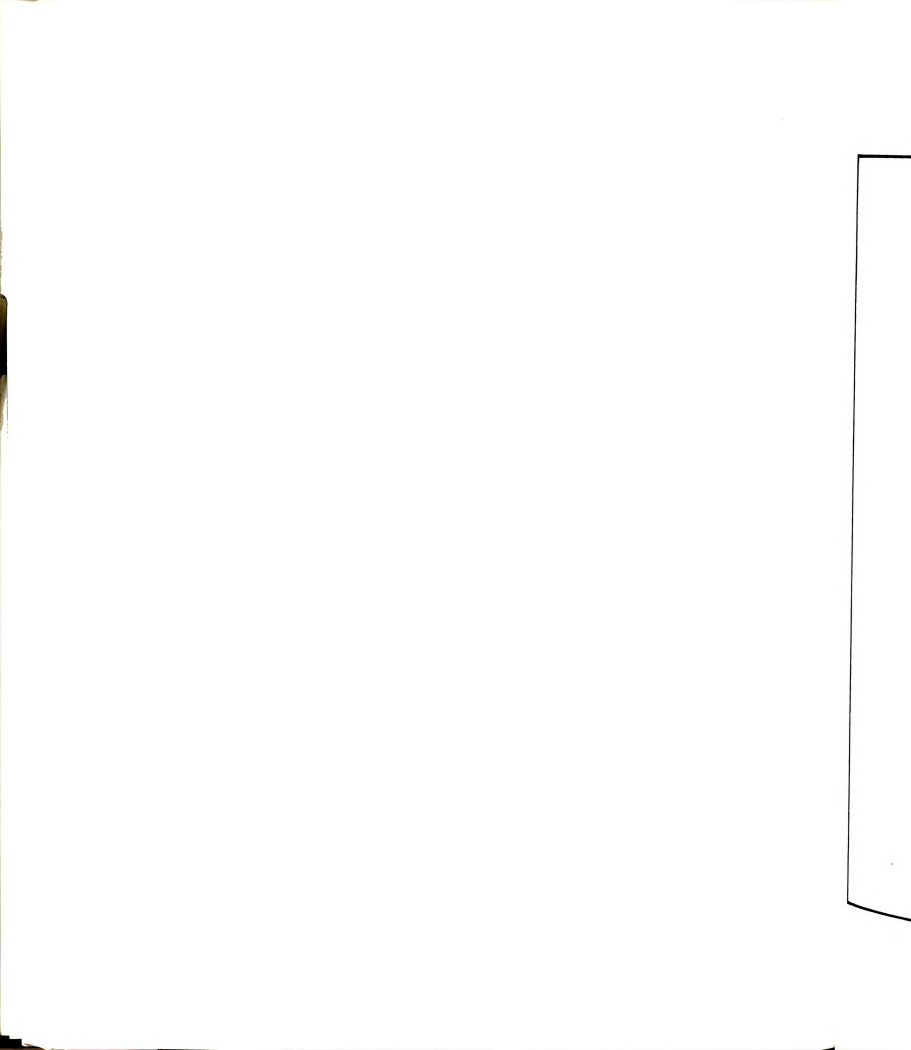
$$\vec{j}_{e}^{d} \equiv \hat{\mathbf{n}} \times \vec{\mathbf{H}}^{d}$$

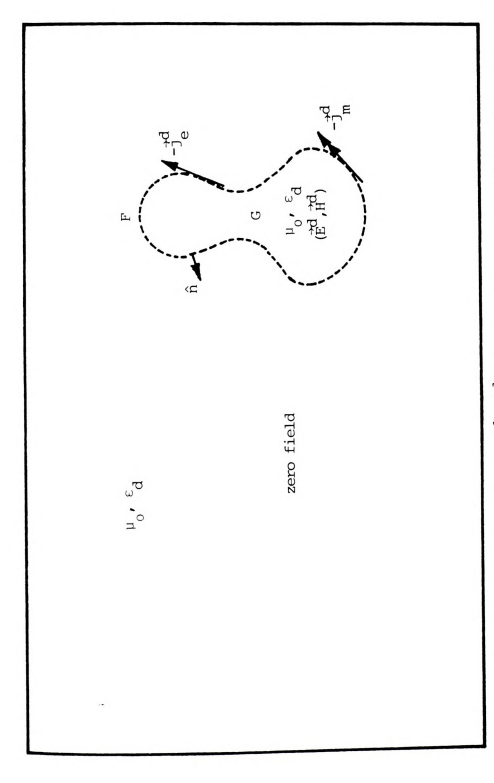
$$\vec{j}_{m}^{d} \equiv -\hat{\mathbf{n}} \times \vec{\mathbf{E}}^{d}/\eta_{o}$$

$$\mathbf{q}_{e}^{d} = \frac{\mathbf{j}}{\omega} \nabla_{o} \cdot \vec{\mathbf{j}}_{e}^{d}$$

$$\mathbf{q}_{m}^{d} = \frac{\mathbf{j}}{\omega} \nabla_{o} \cdot \vec{\mathbf{j}}_{m}^{d}$$

Again, from the equivalence theorem [15], [16], we know that, with the exterior region of G being replaced by a homogeneous source free region with permeability μ_{O} and complex permittivity ϵ_{d} , the negative of the equivalent surface currents $(\mathring{J}_{\text{e}}^{\text{d}},\mathring{J}_{\text{m}}^{\text{d}})$ will support the total induced field $(\mathring{E}^{\text{d}},\mathring{H}^{\text{d}})$ in the region internal to F and a null field in the region external to F, as shown in Figure 3.5. Equations (3.3) and (3.4) can be applied to determine these fields; a sign change is necessary since we define $(\mathring{J}_{\text{e}}^{\text{d}},\mathring{J}_{\text{m}}^{\text{d}})$





The induced field $(\vec{b}^d,\ \vec{h}^d)$ in the interior of the body and a zero field in the exterior of the body are maintained by the negative of the equivalent surface currents $(\vec{j}^d,\ \vec{h}^d)$, which are defined in terms of the induced field on surface F. The region external to F is replaced by a medium with permeability ν_0 and complex permittivity Ed. Figure 3.5.

in term the sou

 $\vec{E}^{d} = \frac{1}{4\pi}$

 $\mathring{H}^{d} = \frac{1}{4\pi}$

as the i to the s

tion for the comp nal to F,

 $0 = \frac{1}{4\pi} \int_{P}$

 $0 = \frac{1}{4\pi} \int_{\mathbf{F}}$

because th III)

To in consider t

(Ĕⁱ, Ħⁱ), 1 rents on th

 $j_e^i = \hat{n}$

in terms of the unit normal vector $\hat{\mathbf{n}}$ which is pointing into the source region. Hence we have

$$\begin{split} \vec{E}^{d} &= \frac{1}{4\pi} \int_{F} \left[\eta_{o} \vec{j}_{m}^{d} \times \nabla^{!} \phi_{d} - \frac{q_{e}^{d}}{\varepsilon_{d}} \nabla^{!} \phi_{d} + j \omega \mu_{o} \vec{j}_{e}^{d} \phi_{d} \right] dF' \\ \vec{H}^{d} &= \frac{1}{4\pi} \int_{F} \left[-\vec{j}_{e}^{d} \times \nabla^{!} \phi_{d} - \frac{q_{m}^{d}}{\mu_{o}} \nabla^{!} \phi_{d} + j \omega \varepsilon_{d} \eta_{o} \vec{j}_{m}^{d} \phi_{d} \right] dF' \end{split} \right] \end{aligned} \tag{3.12}$$

as the induced field at any point in the region internal to the surface F, where $\phi_d = \frac{e^{-jk}d|\vec{r}-\vec{r}'|}{|\vec{r}-\vec{r}'|}$ is the Green's function for the conducting body region, and $k_d = \omega \sqrt{\nu_0 \varepsilon_d}$ is the complex wavenumber in the body. In the region external to F, the above two integrals vanish. i.e..

$$0 = \frac{1}{4\pi} \int_{\mathbf{F}} \left[\eta_{0} \overset{?}{J}_{m}^{d} \times \nabla' \phi_{d} - \frac{q_{e}^{d}}{\varepsilon_{d}} \nabla' \phi_{d} + j\omega \mu_{0} \overset{?}{J}_{e}^{d} \phi_{d} \right] d\mathbf{F}'$$

$$0 = \frac{1}{4\pi} \int_{\mathbf{F}} \left[-\overset{?}{J}_{e}^{d} \times \nabla' \phi_{d} - \frac{q_{m}^{d}}{\mu_{0}} \nabla' \phi_{d} + j\omega \varepsilon_{d} \eta_{0} \overset{?}{J}_{m}^{d} \phi_{d} \right] d\mathbf{F}'$$

$$(3.14)$$

$$external to \mathbf{F}$$

$$(3.15)$$

because there is a null field external to F.

III) The Incident Field $(\stackrel{\rightarrow}{E}^i, \stackrel{\rightarrow}{H}^i)$:

To investigate the incident field (\vec{E}^i, \vec{H}^i) , let's consider the geometry shown in Figure 3.2 again. Based on (\vec{E}^i, \vec{H}^i) , we define the following equivalent surface currents on the body surface F:

$$\vec{j}_e^i = \hat{n} \times \vec{H}^i$$

Fr the nega ing in t the tota surface This is Supp the compl the free surface co (\vec{E}^i, \vec{H}^i) j the region homogeneou Obstaclefield. Thi Again, the EM field $\dot{\tilde{E}}^{\dot{1}} = \frac{1}{4\pi} \int_{\tilde{F}} [$

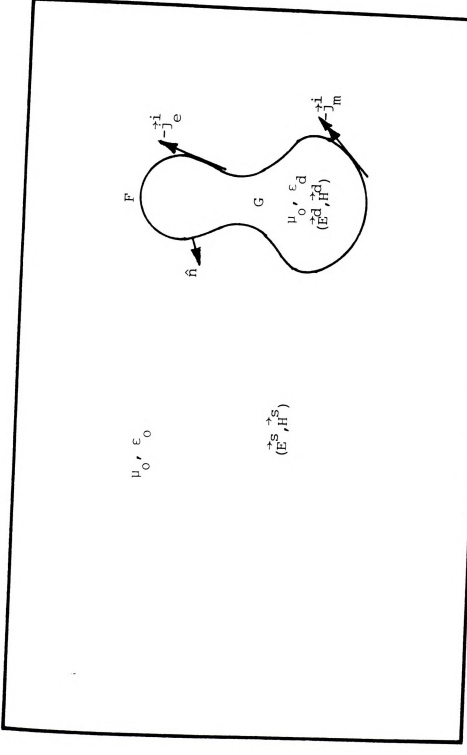
$$\begin{split} \vec{J}_{m}^{i} &= -\hat{n} \times \vec{E}^{i} / \eta_{o} \\ q_{e}^{i} &= \vec{J}_{\omega} \nabla_{o} \cdot \vec{J}_{e}^{i} \\ q_{m}^{i} &= \vec{J}_{\omega} \nabla_{o} \cdot \vec{J}_{m}^{i} \end{split}$$

From the induction theorem [15], [16], we know that the negative of these equivalent surface currents, radiating in the presence of the conducting body, will support the total induced field (\vec{E}^d, \vec{H}^d) in the region internal to surface F, and the scattered field (\vec{E}^S, \vec{H}^S) external to F. This is illustrated in Figure 3.6.

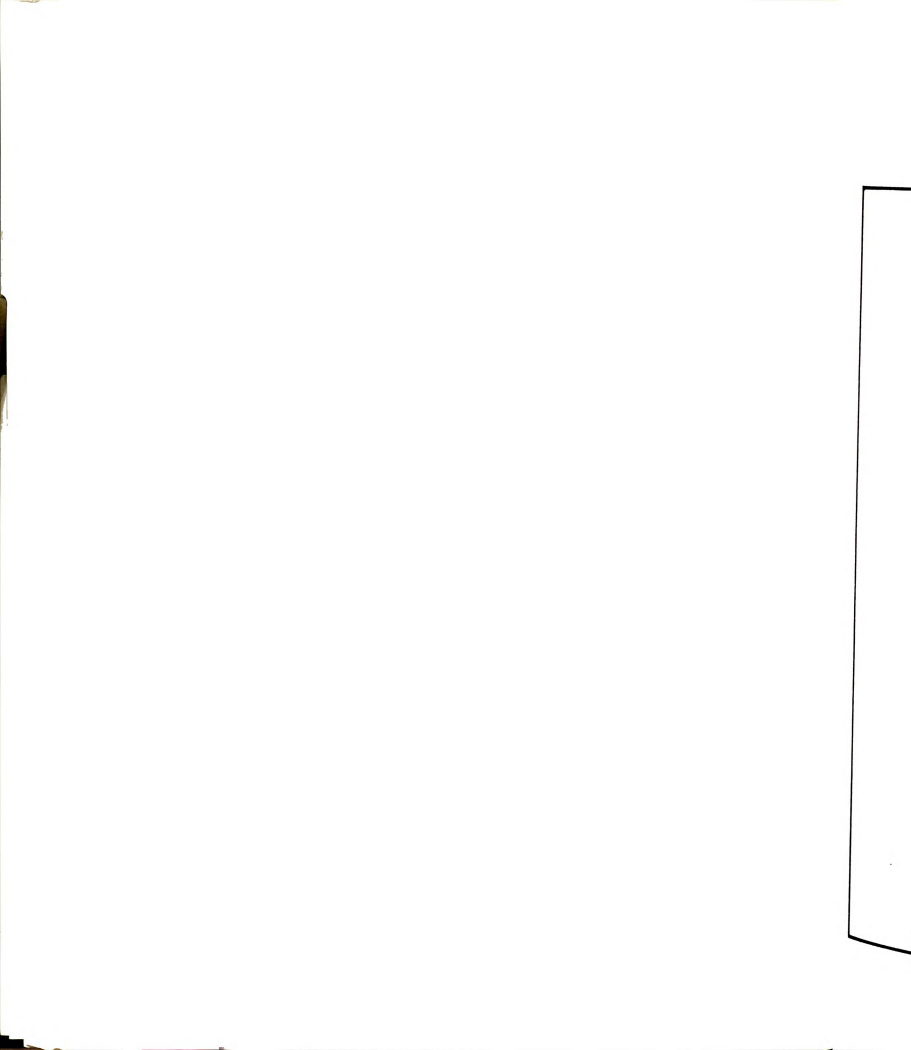
Suppose that we are considering an extreme case with the complex permittivity of the body $\varepsilon_{\hat{\mathbf{d}}}$ being replaced by the free space permittivity $\varepsilon_{\hat{\mathbf{O}}}$, then the negative of the surface currents $(\hat{\mathbf{J}}_{\hat{\mathbf{e}}}^{\hat{\mathbf{i}}},\hat{\mathbf{J}}_{\hat{\mathbf{m}}}^{\hat{\mathbf{i}}})$ will support the incident field $(\hat{\mathbf{E}}^{\hat{\mathbf{i}}},\hat{\mathbf{H}}^{\hat{\mathbf{i}}})$ in the region internal to F, and a null field in the region external to F. Because the entire space becomes homogeneous (free space), there exists no real scattering obstacle—the conducting body, so there is no scattered field. This situation is shown in Figure 3.7.

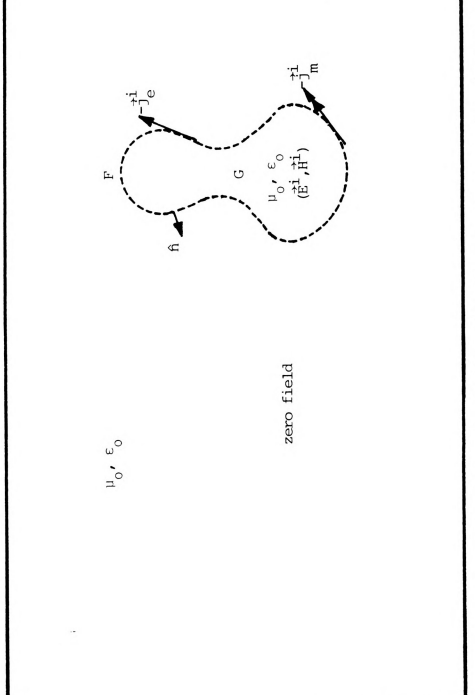
Again, eqs. (3.3) and (3.4) can be used to express the EM fields shown in Figure 3.7. We have

$$\vec{E}^{i} = \frac{1}{4\pi} \int_{F} \left[\eta_{o} \vec{j}_{m}^{i} \times \nabla' \phi_{f} - \frac{q_{e}^{i}}{\varepsilon_{o}} \nabla' \phi_{f} + j \omega \mu_{o} \vec{j}_{e}^{i} \phi_{f} \right] dF'$$
(3.16 internal to F



The induced field (\vec{E}^d , \vec{H}^d) in the interior of the body and the scattered field (\vec{E}^s , \vec{H}^s) in the exterior of the body are main-tained by the negative of the equivalent surface currents (\vec{J}^s , \vec{J}^s , \vec{J}^s , which are defined in terms of the incident field on mittivity \vec{e}_d is immersed in free space. Figure 3.6.





With the body region G replaced by free space, the incident field (\vec{E}_1 , \vec{H}_1) in the interior of the body and a zero field in exterior of the body are maintained by the negative of the equivalent surface currents (\vec{I}_2 , \vec{H}_1), which are defined in terms of the incident field on surface \vec{F}_1 . Figure 3.7.

∯i = <u>₹</u> as the to F.

exteri

U

field tered : derive

results Si

rior re Point ξ

the lim electri

may wri

 $\vec{\xi}^{\dot{1}}(\vec{\xi}) \; = \;$

Where Sp theorem

$$\vec{H}^{\dot{i}} = \frac{1}{4\pi} \int_{\mathbf{F}} \left[-\frac{1}{J_{\mathbf{e}}^{\dot{i}}} \times \nabla \cdot \phi_{\mathbf{f}} - \frac{q_{m_{\overline{V}}}^{\dot{i}}}{\mu_{\mathbf{O}}^{\dot{V}}} \phi_{\mathbf{f}} + j\omega \epsilon_{\mathbf{O}} \eta_{\mathbf{O}} J_{m_{\overline{V}}}^{\dot{i}} \phi_{\mathbf{f}} \right] d\mathbf{F}'$$
 internal to F (3.17)

as the incident field at any point in the region internal to F. However, the above two integrals vanish in the exterior region of the body, i.e.,

$$0 = \frac{1}{4\pi} \int_{\mathbf{F}} \left[\eta_{0} \overset{?}{j}_{m}^{i} \times \nabla^{i} \phi_{f} - \frac{q_{e}^{i}}{\epsilon_{0}^{i}} \nabla^{i} \phi_{f} + j \omega \mu_{0} \overset{?}{j}_{e}^{i} \phi_{f} \right] d\mathbf{F}'$$

$$0 = \frac{1}{4\pi} \int_{\mathbf{F}} \left[-\overset{?}{j}_{e}^{i} \times \nabla^{i} \phi_{f} - \frac{q_{m}^{i}}{\mu_{0}^{i}} \nabla^{i} \phi_{f} + j \omega \epsilon_{0} \eta_{0} \overset{?}{j}_{m}^{i} \phi_{f} \right] d\mathbf{F}'$$

$$(3.18)$$

$$external to \mathbf{F}$$

$$(3.19)$$

Up to this point, we have considered the incident field $(\vec{E}^{\dot{1}}, \vec{H}^{\dot{1}})$, the induced field $(\vec{E}^{\dot{d}}, \vec{H}^{\dot{d}})$, and the scattered field $(\vec{E}^{\dot{S}}, \vec{H}^{\dot{S}})$ individually. Now we are ready to derive the coupled surface integral equations based on the results we just obtained.

Since eq. (3.16) is true at any point \mathring{r} in the interior region of G, if we let the field point \mathring{r} approach a point $\mathring{\xi}$ on the surface F along the interior normal, then the limiting value of eq. (3.16) will be the incident electric field at the point $\mathring{\xi}$ on the surface F. Hence we may write

$$\vec{E}^{i}(\vec{\xi}) = \frac{1}{4\pi} \int_{\vec{\xi}_{i}} \left[\eta_{o} \vec{j}_{m}^{i} \times \nabla^{i} \phi_{f} - \frac{q_{e}^{i}}{\varepsilon_{o}} \nabla^{i} \phi_{f} + j \omega \mu_{o} \vec{j}_{e}^{i} \phi_{f} \right] dF'$$

where $f_{\mbox{\scriptsize F},i}$ has the same meaning as that described in theorem 2. After taking the cross-product of the above

equat. at the

 $\hat{n} \times \frac{1}{4}$

Applyi

-n x 1

A]

Ward to

 $\hat{n} \ \chi \ \frac{1}{4\pi}$

and

 $-\hat{n} \times \frac{1}{4\pi}$

Be:

boundary

F. The

componen

tinuous

equation with the unit normal vector $\hat{\mathbf{n}}(\vec{\xi})$, we will arrive at the following equation

$$\hat{\mathbf{n}} \times \frac{1}{4\pi} \int_{\tilde{\mathbf{F}}_{\underline{\mathbf{i}}}} \left[\eta_o \hat{\mathbf{j}}_m^{\underline{\mathbf{i}}} \times \nabla' \phi_{\underline{\mathbf{f}}} - \frac{q_{\underline{\mathbf{e}}}^i}{\varepsilon_o} \nabla' \phi_{\underline{\mathbf{f}}} + j \omega \mu_o \hat{\mathbf{j}}_{\underline{\mathbf{e}}}^i \phi_{\underline{\mathbf{f}}} \right] d\mathbf{F'}$$

$$= -\eta_o \hat{\mathbf{j}}_m^i . \tag{3.20}$$

Applying the same arguments to eq. (3.17), we have

$$-\hat{\mathbf{n}} \times \frac{1}{4\pi} \int_{\mathbf{F}_{\dot{\mathbf{i}}}} \left[-\dot{\mathbf{j}}_{\dot{\mathbf{e}}}^{\dot{\mathbf{i}}} \times \nabla \cdot \phi_{\mathbf{f}} - \frac{q_{\mathbf{m}}^{\dot{\mathbf{i}}}}{\nu_{o}} \nabla \cdot \phi_{\mathbf{f}} + j\omega \epsilon_{o} \eta_{o} \dot{\mathbf{j}}_{\mathbf{m}}^{\dot{\mathbf{i}}} \phi_{\mathbf{f}} \right] d\mathbf{F}'$$

$$= -\dot{\mathbf{j}}_{\dot{\mathbf{e}}}^{\dot{\mathbf{i}}} . \tag{3.21}$$

Also, from eqs. (3.10) and (3.11), it is straightforward to obtain

$$\hat{n} \times \frac{1}{4\pi} \int_{\vec{k}_{\perp}} \left[-n_{o} \hat{j}_{m}^{s} \times \nabla' \phi_{f} + \frac{q_{e}^{s}}{\varepsilon_{o}} \nabla' \phi_{f} - j\omega \mu_{o} \hat{j}_{e}^{s} \phi_{f} \right] dF' = 0$$

$$(3.22)$$

and

$$-\hat{n} \times \frac{1}{4\pi} \int_{\vec{E}_{1}} i \vec{j}_{e}^{s} \times \nabla' \phi_{f} + \frac{q_{m}^{s}}{\mu_{o}} \phi_{f} - j \omega \epsilon_{o} \eta_{o} \vec{j}_{m}^{s} \phi_{f} dF' = 0. \tag{3.23}$$

Before going any further, we should introduce the boundary conditions which must be satisfied at the surface F. The boundary conditions require that the tangential components of the electric and magnetic field must be continuous across F, or equivalently we may write

(3.22) $\hat{n} \ X \ \frac{1}{4\pi}$ Similar obtain On the tions f $\hat{n}~\chi~\frac{1}{4\pi}$ $-\hat{n} \times \frac{1}{4\pi}$ lowing p ${\tt regular}$

Ιt

$$j_e^s + j_e^i = j_e^d$$

$$\vec{j}_{m}^{s} + \vec{j}_{m}^{i} = \vec{j}_{m}^{d}$$

Now, take the difference between eqs. (3.20) and (3.22), and apply the above boundary conditions. We have

$$\hat{n} \times \frac{1}{4\pi} \int_{\bar{F}_{1}} \left[\eta_{o} \dot{J}_{m}^{d} \times \nabla' \phi_{f} - \frac{q_{e}^{d}}{\varepsilon_{o}} \nabla' \phi_{f} + j\omega \nu_{o} \dot{J}_{e}^{d} \phi_{f} \right] dF'$$

$$= -\eta_{o} \dot{J}_{m}^{i} .$$

$$(3.24)$$

Similarly, subtracting eq. (3.23) from eq. (3.21), we obtain

$$-\hat{\mathbf{n}} \times \frac{1}{4\pi} \int_{\mathbf{F}_{\dot{\mathbf{i}}}} \left[-\hat{\mathbf{j}}_{\dot{\mathbf{e}}}^{\dot{\mathbf{d}}} \times \nabla' \phi_{\mathbf{f}} - \frac{q_{\mathbf{m}}^{\dot{\mathbf{d}}}}{\mu_{o}} \nabla' \phi_{\mathbf{f}} + j \omega \epsilon_{o} \eta_{o} \hat{\mathbf{j}}_{\mathbf{m}}^{\dot{\mathbf{d}}} \phi_{\mathbf{f}} \right] d\mathbf{F}'$$

$$= -\hat{\mathbf{j}}_{\dot{\mathbf{e}}}^{\dot{\mathbf{i}}} \qquad (3.25)$$

On the other hand, we may derive the following two equations from eqs. (3.14) and (3.15):

$$\hat{\mathbf{n}} \ \mathbf{X} \ \frac{1}{4\pi} \ f_{\mbox{ξ}_e} \ [\eta_o \mbox{$\stackrel{\rightarrow}{J}_d$}^d \ \mathbf{X} \ \nabla^{\dagger} \phi_d \ - \ \frac{q_e^d}{\epsilon_d} \nabla^{\dagger} \phi_d \ + \ j \omega \nu_o \mbox{$\stackrel{\rightarrow}{J}_e$}^d \phi_d] \ d \mbox{†} \ = \ 0 \ (3.26)$$

$$-\hat{\mathbf{n}} \times \frac{1}{4\pi} \int_{\mathbf{E}_{\mathbf{e}}} \left[-\hat{\mathbf{j}}_{\mathbf{e}}^{\mathbf{d}} \times \nabla' \hat{\boldsymbol{\phi}}_{\mathbf{d}} - \frac{\mathbf{q}_{\mathbf{m}}^{\mathbf{d}}}{\nu_{\mathbf{o}}} \nabla' \hat{\boldsymbol{\phi}}_{\mathbf{d}} + \mathbf{j} \omega \epsilon_{\mathbf{d}} \eta_{\mathbf{o}} \hat{\mathbf{j}}_{\mathbf{m}}^{\mathbf{d}} \hat{\boldsymbol{\phi}}_{\mathbf{d}} \right] d\mathbf{F}' = 0 \tag{3.27}$$

It can be shown that equalities exist between the following limiting surface integrals and their corresponding regular surface integrals

î.

ñ

fi X

hand side

Applying equation,

It should

Fq

because 7' o

$$\hat{\mathbf{n}} \times \mathbf{f}_{\underline{\mathbf{f}}} \ \mathbf{q}_{\mathbf{e}}^{\mathbf{d}} \ \nabla^{\dagger} \mathbf{\phi}_{\mathbf{f}} \ \mathbf{d} \mathbf{F}^{\dagger} = \hat{\mathbf{n}} \times \mathbf{f}_{\mathbf{F}} \ \mathbf{q}_{\mathbf{e}}^{\mathbf{d}} \ \nabla^{\dagger} \mathbf{\phi}_{\mathbf{f}} \ \mathbf{d} \mathbf{F}^{\dagger}$$

$$\hat{\mathbf{n}} \times \mathbf{f}_{\underline{F}_{\mathbf{e}}} \mathbf{q}_{\mathbf{e}}^{\mathbf{d}} \nabla^{\mathbf{i}} \mathbf{\phi}_{\mathbf{d}} \mathbf{d} \mathbf{F}^{\mathbf{i}} = \hat{\mathbf{n}} \times \mathbf{f}_{\mathbf{F}} \mathbf{q}_{\mathbf{e}}^{\mathbf{d}} \nabla^{\mathbf{i}} \mathbf{\phi}_{\mathbf{d}} \mathbf{d} \mathbf{F}^{\mathbf{i}}.$$

Subtracting the second equation from the first equation, we find that $\begin{tabular}{ll} \end{tabular} \label{table_equation} % \begin{tabular}{ll} \end{tabular} \begin{tab$

$$\hat{\mathbf{n}} \times \mathcal{I}_{\mathbf{F}_{\hat{\mathbf{i}}}} \mathbf{q}_{\mathbf{e}}^{\mathbf{d}} \nabla' \hat{\mathbf{q}}_{\mathbf{f}} \mathbf{d} \mathbf{F}' - \hat{\mathbf{n}} \times \mathcal{I}_{\mathbf{F}_{\mathbf{e}}} \mathbf{q}_{\mathbf{e}}^{\mathbf{d}} \nabla' \hat{\mathbf{q}}_{\mathbf{d}} \mathbf{d} \mathbf{F}' =$$

$$\hat{\mathbf{n}} \ \mathbf{X} \ \mathbf{f}_{\mathbf{F}} \ \mathbf{q}_{\mathbf{e}}^{\mathbf{d}} \ \nabla''(\phi_{\mathbf{f}} \ - \ \phi_{\mathbf{d}}) \ \mathbf{d}\mathbf{F}' \ = \ -\hat{\mathbf{n}} \ \mathbf{X} \ \nabla \ \mathbf{f}_{\mathbf{F}} \ \mathbf{q}_{\mathbf{e}}^{\mathbf{d}}(\phi_{\mathbf{f}} \ - \ \phi_{\mathbf{d}}) \ \mathbf{d}\mathbf{F}'.$$

However, since $q_e^d=\frac{j}{\omega}\ \nabla_o^{\centerdot}\cdot\dot{J}_e^d,$ the integral on the right-hand side of the above equation can be rewritten as

$$\text{$\int_{F} \ q_{e}^{d}(\phi_{f}-\phi_{d})$ dF'=\frac{j}{\omega} \int_{F} \ (\nabla_{o}^{\prime}\cdot\mathring{J}_{e}^{d}) \ (\phi_{f}-\phi_{d})$ dF'.}$$

Applying theorem 1 to the right-hand side of the above equation, we can rewrite it as

$$\begin{split} & \int_{\mathbb{F}} q \overset{d}{\underset{e}{\circ}} (\phi_{f} - \phi_{d}) \ d\mathbb{F}' = - \overset{j}{\underset{\omega}{\smile}} \int_{\mathbb{F}} \overset{d}{\underset{e}{\circ}} \frac{1}{\underset{e}{\circ}} \cdot \nabla_{o}' (\phi_{f} - \phi_{d}) \ d\mathbb{F}' \\ & = - \overset{j}{\underset{\omega}{\smile}} \int_{\mathbb{F}} \overset{d}{\underset{e}{\circ}} \frac{1}{\underset{e}{\circ}} \cdot \nabla' (\phi_{f} - \phi_{d}) \ d\mathbb{F}'. \end{split}$$

It should be mentioned that the last equality is true, because $\nabla_0^1 = \nabla^1 - \hat{n}^1 \frac{\partial}{\partial n}$, and \hat{j}_e^d has no normal component. Then finally, we have

Based

it is n

Now, su multipl result

 $\epsilon_{o} \ \hat{n} \ \chi$

 $\epsilon_{d} \hat{n} \times \frac{1}{4}$

$$\begin{split} \hat{\mathbf{n}} \ x \ \mathcal{I}_{\mathbf{F}_{\underline{\mathbf{i}}}} \ q_{\mathbf{e}}^{\mathbf{d} \nabla^{\dagger} \phi_{\mathbf{f}}} \ \mathrm{d} \mathbf{F}^{\dagger} \ - \ \hat{\mathbf{n}} \ x \ \mathcal{I}_{\mathbf{F}_{\underline{\mathbf{e}}}} \ q_{\mathbf{e}}^{\mathbf{d}} \ \nabla^{\dagger} \phi_{\mathbf{d}} \ \mathrm{d} \mathbf{F}^{\dagger} \end{split}$$

$$= -\hat{\mathbf{n}} \ x \ \nabla \ [-\frac{\mathbf{j}}{\omega} \ \mathcal{I}_{\mathbf{F}} \ \tilde{\mathbf{J}}_{\mathbf{e}}^{\mathbf{d}} \ \cdot \ \nabla^{\dagger} (\phi_{\mathbf{f}} - \phi_{\mathbf{d}}) \ \mathrm{d} \mathbf{F}^{\dagger}]$$

$$= \frac{\mathbf{j}}{\omega} \ \hat{\mathbf{n}} \ x \ \mathcal{I}_{\mathbf{F}} \ \nabla [\tilde{\mathbf{j}}_{\mathbf{e}}^{\mathbf{d}} \ \cdot \ \nabla^{\dagger} (\phi_{\mathbf{f}} - \phi_{\mathbf{d}})] \ \mathrm{d} \mathbf{F}^{\dagger}. \end{split}$$

Based on the following vector identity

$$\nabla (\vec{A} \cdot \vec{B}) = (\vec{A} \cdot \nabla) \vec{B} + (\vec{B} \cdot \nabla) \vec{A} + \vec{A} \times (\nabla \times \vec{B}) + \vec{B} \times (\nabla \times \vec{A}),$$

it is easy to show that

$$\begin{split} \hat{\mathbf{n}} & \times \int_{\tilde{\mathbf{F}}_{\mathbf{d}}} \mathbf{q}_{\mathbf{e}}^{\mathbf{d}} & \nabla^{\dagger} \phi_{\mathbf{f}} & \mathrm{d} \mathbf{F}^{\dagger} - \hat{\mathbf{n}} \times \int_{\tilde{\mathbf{F}}_{\mathbf{e}}} \mathbf{q}_{\mathbf{e}}^{\mathbf{d}} & \nabla^{\dagger} \phi_{\mathbf{d}} & \mathrm{d} \mathbf{F}^{\dagger} \\ \\ & = -\frac{j}{\omega} \hat{\mathbf{n}} \times \int_{\mathbf{F}} \left[(\hat{\mathbf{j}}_{\mathbf{e}}^{\mathbf{d}} + \nabla^{\dagger}) \nabla^{\dagger} (\phi_{\mathbf{f}} - \phi_{\mathbf{d}}) \right] \mathrm{d} \mathbf{F}^{\dagger}. \end{split} \tag{3.28}$$

Now, subtracting eq. (3.26) from eq. (3.24) with the latter multiplied by $\epsilon_{\rm d}$, the result is

$$\begin{split} \varepsilon_{o} & \text{ fi } x \; \frac{1}{4\pi} \; \text{ } \int_{\xi_{\dot{\mathbf{i}}}} \; [\eta_{o}\dot{J}_{m}^{\dot{\mathbf{d}}} \; x \; \nabla' \varphi_{\dot{\mathbf{f}}} - \frac{q_{e}^{\dot{\mathbf{d}}}}{\varepsilon_{o}} \nabla' \varphi_{\dot{\mathbf{f}}} + j\omega\mu_{o}\dot{J}_{e}^{\dot{\mathbf{d}}} \varphi_{\dot{\mathbf{f}}}] \; \mathrm{d}\mathbf{F'} \; - \\ \varepsilon_{\dot{\mathbf{d}}} & \text{ fi } x \; \frac{1}{4\pi} \; \text{ } \int_{\xi_{\dot{\mathbf{e}}}} \; [\eta_{o}\dot{J}_{m}^{\dot{\mathbf{d}}} \; x \; \nabla' \varphi_{\dot{\mathbf{d}}} - \frac{q_{e}^{\dot{\mathbf{d}}}}{\varepsilon_{\dot{\mathbf{d}}}} \nabla' \varphi_{\dot{\mathbf{d}}} + j\omega\mu_{o}\dot{J}_{e}^{\dot{\mathbf{d}}} \varphi_{\dot{\mathbf{d}}}] \; \mathrm{d}\mathbf{F'} \\ & = -\varepsilon_{o}\eta_{o}\dot{J}_{m}^{\dot{\mathbf{d}}} \end{split}$$

or

 $\frac{1}{4\pi}$ {[î - [n̂ x [n̂ X]

В becomes

Similar

derived $j_e^{\dagger d} = j_e^{\dagger i}$

Where κ

We norma

of lengt equation:

have als

through .

$$\begin{split} \frac{1}{4\pi} & \{ [\hat{\mathbf{n}} \times \int_{\mathbf{E}_{\mathbf{i}}} \varepsilon_0 \eta_0 \mathring{J}_m^d \times \nabla^! \mathring{\phi}_f \ d\mathbf{F}' - \hat{\mathbf{n}} \times \int_{\mathbf{E}_{\mathbf{e}}} \varepsilon_d \eta_0 \mathring{J}_m^d \times \nabla^! \mathring{\phi}_d \ d\mathbf{F}'] \\ & - [\hat{\mathbf{n}} \times \int_{\mathbf{E}_{\mathbf{i}}} q_e^d \nabla^! \mathring{\phi}_f \ d\mathbf{F}' - \hat{\mathbf{n}} \times \int_{\mathbf{E}_{\mathbf{e}}} q_e^d \nabla^! \mathring{\phi}_d \ d\mathbf{F}'] + \\ [\hat{\mathbf{n}} \times \int_{\mathbf{E}_{\mathbf{i}}} j\omega \mu_0 \varepsilon_0 \mathring{J}_e^d \mathring{\phi}_f \ d\mathbf{F}' - \hat{\mathbf{n}} \times \int_{\mathbf{E}_{\mathbf{e}}} j\omega \mu_0 \varepsilon_d \mathring{J}_e^d \mathring{\phi}_d \ d\mathbf{F}'] \} \\ & = -\varepsilon_0 \eta_0 \mathring{J}_m^{\dagger} \ . \end{split}$$

Based on eq. (3.28) and theorem 2, the above equation becomes $\ensuremath{\mathsf{E}}$

$$\begin{split} \dot{\vec{j}}_m^d &= \frac{2}{\kappa^2 + 1} \ \dot{\vec{j}}_m^i - \frac{1}{2\pi \left(\kappa^2 + 1\right)} \ \hat{\mathbf{n}} \ \mathbf{x} \ f_F \ [jk_o \dot{\vec{j}}_e^d (\kappa^2 \phi_d - \phi_f) \ + \\ \\ \dot{\vec{j}}_m^d \ \mathbf{x} \ \nabla' \left(\kappa^2 \phi_d - \phi_f\right) \ + \frac{j}{k_o} (\dot{\vec{j}}_e^d \cdot \nabla') \ \nabla' \left(\phi_d - \phi_f\right)] \ d\mathbf{F'}. \end{split}$$

Similarly, the other surface integral equation can be derived from eqs. (3.25) and (3.27),

$$\begin{split} \vec{J}_{e}^{d} &= \vec{J}_{e}^{i} + \frac{1}{4\pi} \; \hat{n} \; x \; \mathcal{I}_{F} \; \left[\; j k_{o} \vec{J}_{m}^{d} (\kappa^{2} \phi_{d} - \phi_{f}) \; - \; \vec{J}_{e}^{d} \; x \; \nabla \cdot (\phi_{d} - \phi_{f}) \; + \\ & \frac{j}{k_{o}} (\vec{J}_{m}^{d} \cdot \nabla \cdot) \; \nabla \cdot (\phi_{d} - \phi_{f}) \right] \; dF' \end{split}$$

where $\kappa = \sqrt{\varepsilon_{\rm d}/\varepsilon_{\rm o}}$ is the refractive index of the body. If we normalize all the quantities concerning the dimension of length by $1/k_{\rm o}$, the above two coupled surface integral equations become (these two equations in similar forms have also been given by Müller [13] and Morita [19] through different derivations)

assume t

$$\begin{split} \mathring{J}_{m}^{d} &= \frac{2}{\kappa^{2}+1} \, \mathring{J}_{m}^{\dot{1}} - \frac{1}{2\pi \left(\kappa^{2}+1\right)} \, \, \hat{n} \, \, X \, \, \int_{F} \, \left[j \left(\kappa^{2} \phi_{d} - \phi_{f}\right) \, \mathring{J}_{e}^{\dot{d}} \, + \right. \\ \\ & \mathring{J}_{m}^{\dot{d}} \, X \, \, \nabla' \left(\kappa^{2} \phi_{d} - \phi_{f}\right) \, + \, j \left(\mathring{J}_{e}^{\dot{d}} \cdot \nabla'\right) \, \, \nabla' \left(\phi_{d} - \phi_{f}\right) \right] \, \, dF' \end{split} \tag{3.29}$$

and

$$\dot{j}_{e}^{d} = \dot{j}_{e}^{i} + \frac{1}{4\pi} \hat{n} \times \int_{F} \left[j \left(\kappa^{2} \phi_{d} - \phi_{f} \right) \dot{j}_{m}^{d} - \dot{j}_{e}^{d} \times \nabla' \left(\phi_{d} - \phi_{f} \right) + \right]$$

$$j \left(\dot{j}_{m}^{d} \cdot \nabla' \right) \nabla' \left(\phi_{d} - \phi_{f} \right) dF' .$$

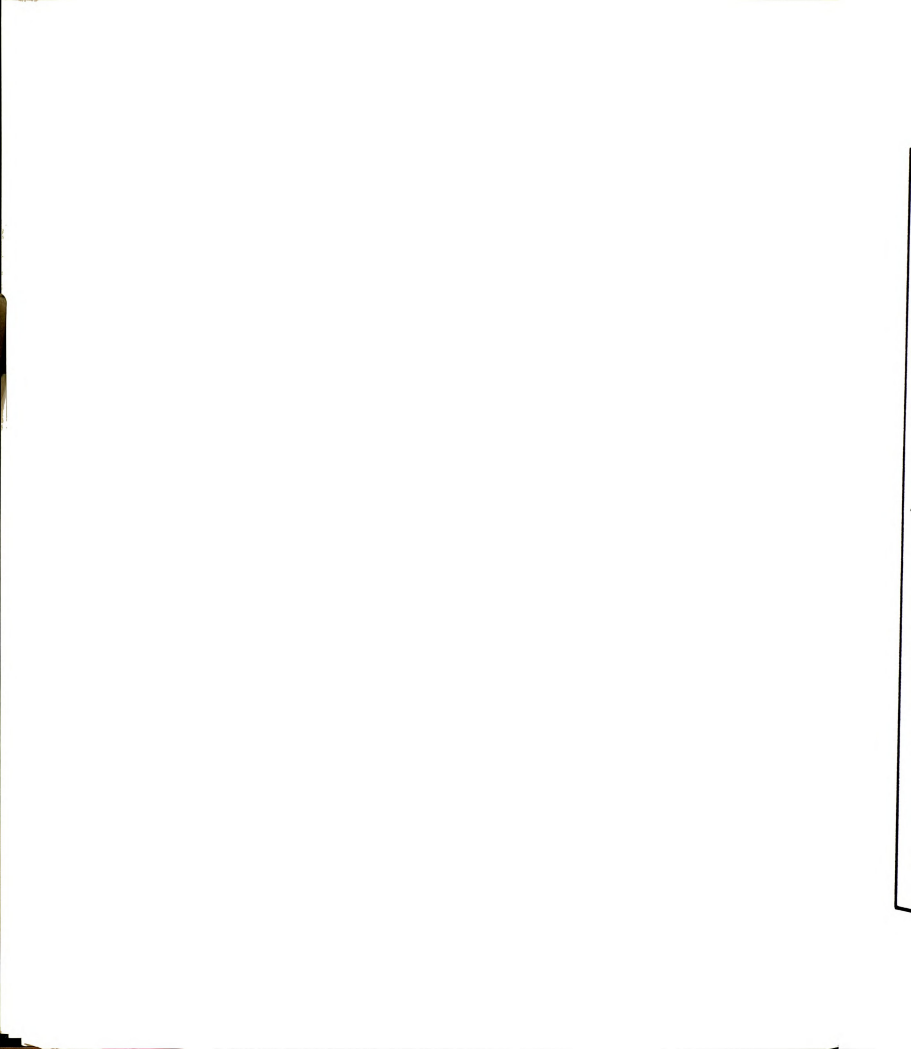
$$(3.30)$$

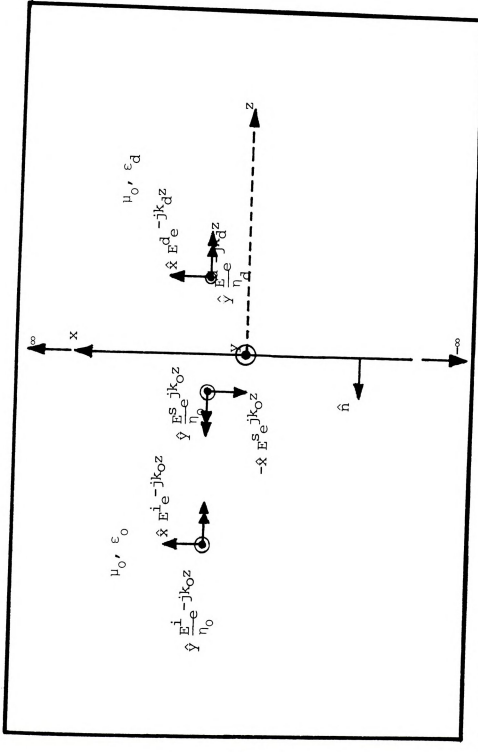
The induced equivalent surface currents $(\vec{j}_e^d, \vec{j}_m^d)$ (or the induced surface field (\vec{E}^d, \vec{H}^d)) can be calculated based on the above two coupled, surface integral equations. In these two equations, due to normalization with respect to $1/k_o$, the Green's functions ϕ_d and ϕ_f have the forms of

$$\phi_{d} = \frac{e^{-j\kappa \left| \stackrel{\rightarrow}{r} - \stackrel{\rightarrow}{r} \right|}}{\left| \stackrel{\rightarrow}{r} - \stackrel{\rightarrow}{r} \right|} \quad \text{and} \quad \phi_{f} = \frac{e^{-j\left| \stackrel{\rightarrow}{r} - \stackrel{\rightarrow}{r} \right|}}{\left| \stackrel{\rightarrow}{r} - \stackrel{\rightarrow}{r} \right|} \; .$$

3.5. The Special Case of an Infinite Plane Interface

In this section, we apply the surface integral equations to the special case of an infinite plane interface between two half spaces, a free-space in the region z < 0 with permeability $\mu_{\rm O}$ and permittivity $\epsilon_{\rm O}$ and a finite conducting medium in the region z > 0 with permeability $\mu_{\rm O}$ and complex permittivity $\epsilon_{\rm d}$, as shown in Figure 3.8. We assume that the incident plane wave, which propagates in





An infinite interface between free space and a finite conducting medium with permeability μ_0 and complex permittivity ϵ_d is impinged by a plane wave propagating in the +z direction. Figure 3.8.

the +y
the +y
and pr
field
ing me
can be

the +a

[→] H s

Ės

ıd ;

E

 $\vec{H}^{\hat{\alpha}}$ where $\eta_{\hat{\alpha}}$

conducti problem, transmit

field (E

H^d :

the +z direction with its electric field \vec{E}^i polarized in the +x direction and its magnetic field \vec{H}^i polarized in the +y direction, is normally impinging on the interface, and produces a reflected field (\vec{E}^S, \vec{H}^S) and a transmitted field (\vec{E}^d, \vec{H}^d) in the free space region and the conducting medium region, respectively. Intuitively, these fields can be expressed as

$$\begin{split} & \hat{E}^{\dot{i}} = \hat{x} \ E^{\dot{i}} \ e^{-jk}o^z \\ & \hat{H}^{\dot{i}} = \hat{y} \ H^{\dot{i}} \ e^{-jk}o^z = \hat{y} \ \frac{E^{\dot{i}}}{\eta_o} \ e^{-jk}o^z \ , \\ & \hat{E}^S = -\hat{x} \ E^S \ e^{jk}o^z \\ & \hat{H}^S = \hat{y} \ \frac{E^S}{\eta_o} \ e^{jk}o^z \end{split} \right\} \ \text{in the region } z < 0$$

and

$$\begin{split} & \hat{E}^{\hat{d}} = \hat{x} \ E^{\hat{d}} \ e^{-\hat{j}k} d^z \\ & \hat{H}^{\hat{G}} = \hat{y} \ H^{\hat{G}} \ e^{-\hat{j}k} d^z = \hat{y} \ \frac{E^{\hat{d}}}{\eta_{\hat{d}}} \ e^{-\hat{j}k} d^z \end{split} \right\} \text{ in the region } z > 0 \end{split}$$

where $\eta_{d}=\sqrt{\mu_{o}/\epsilon_{d}}$ is the complex wave impedance in the conducting medium. By solving a simple boundary value problem, it is easy to show that, on the interface, the transmitted field $(E^{d},\;H^{d})$ is related to the incident field $(E^{\dot{1}},\;H^{\dot{1}})$ by

$$E^{\dot{d}} = \frac{2}{1 + \kappa} E^{\dot{1}}$$

$$H^{\dot{d}} = \frac{2 \kappa}{1 + \kappa} H^{\dot{1}}.$$
(3.31)

eq. (face previ lowin

rent

also

where in the N

current last tv

ing to these t

I) first.

It would be interesting to show that the results of eq. (3.31) can be deduced from the rather complicated surface integral equations which have been derived in the previous section. To do that, let's start from the following definitions of the various equivalent surface current densities.

$$\vec{j}_{e}^{i} = \hat{n} \times \vec{H}^{i} = -\hat{z} \times \hat{y} + \vec{H}^{i} = \hat{x} \frac{E^{i}}{\eta_{O}}$$

$$\vec{j}_{m}^{i} = -\hat{n} \times \frac{\overline{E}^{i}}{\eta_{O}} = \hat{z} \times \hat{x} \frac{E^{i}}{\eta_{O}} = \hat{y} \frac{E^{i}}{\eta_{O}}$$
also
$$\vec{j}_{e}^{d} = \hat{n} \times \vec{H}^{d} = \hat{x} \vec{j}_{e}^{d}$$

$$\vec{j}_{m}^{d} = -\hat{n} \times \frac{\overline{E}^{d}}{\eta_{O}} = \hat{y} \vec{j}_{m}^{d}$$

where \hat{n} is the unit normal vector on the interface pointing in the -z direction.

Now, substituting the above expressions of surface current densities into eq. (3.29), we may show that the last two terms of the surface integration contribute nothing to the total surface integral. We should consider these two terms one by one as below.

I) Let us consider the term fix $f_F \stackrel{\uparrow d}{\to}_m x \ \nabla \cdot (\kappa^2 \phi_d - \phi_f) \, dF'$ first.

tively

is tr

7'(¢

expres

the sea

7

Combini express

(je · √

It is easy to show that

$$\hat{\mathbf{n}} \times \mathcal{T}_{\mathbf{F}} \hat{\mathbf{j}}_{\mathbf{m}}^{d} \times \nabla' (\kappa^{2} \phi_{\mathbf{d}} - \phi_{\mathbf{f}}) d\mathbf{F'} = (-\hat{\mathbf{z}}) \times \mathcal{T}_{\mathbf{F}} \hat{\mathbf{y}} \hat{\mathbf{j}}_{\mathbf{m}}^{d}$$

$$\times \nabla' (\kappa^{2} \phi_{\mathbf{d}} - \phi_{\mathbf{f}}) d\mathbf{F'} = 0$$

$$(3.32)$$

is true, since the term $\nabla^\intercal(\kappa^2\varphi_{\hat{\mathbf{d}}}-\varphi_{\hat{\mathbf{f}}})$ has only two components, x and y components but not z component (nothing is z-dependent in this problem), both of which vanish after cross-producting with unit vectors $\hat{\mathbf{y}}$ and $\hat{\mathbf{z}}$ consecutively.

II) Secondly, consider the term of \hat{n} X f_F $(\vec{j}_e^d \cdot \nabla')$ $\nabla'(\phi_{\vec{d}} - \phi_f)$ dF'.

Since the surface current \hat{J}_e^d is x-directed, we may express the first part of the integrand as

$$(j_e^{\dagger d} \cdot \nabla') = j_{ex}^{d} \frac{\partial}{\partial x'}$$
.

Because everything is z-independent, we may write the second part of the integrand as

$$\nabla^{\,\boldsymbol{\cdot}\,}(\boldsymbol{\varphi}_{\overset{}{\boldsymbol{d}}}\,-\,\boldsymbol{\varphi}_{\overset{}{\boldsymbol{f}}}) \ = \ \hat{\boldsymbol{x}}\ \frac{\partial}{\partial \boldsymbol{x}^{\,\boldsymbol{\cdot}}}(\boldsymbol{\varphi}_{\overset{}{\boldsymbol{d}}}\,-\,\boldsymbol{\varphi}_{\overset{}{\boldsymbol{f}}}) \ + \ \hat{\boldsymbol{y}}\ \frac{\partial}{\partial \boldsymbol{y}^{\,\boldsymbol{\cdot}}}(\boldsymbol{\varphi}_{\overset{}{\boldsymbol{d}}}\,-\,\boldsymbol{\varphi}_{\overset{}{\boldsymbol{f}}}) \ .$$

Combining the above two equations, we have the following expression for the integrand:

Hence, $\hat{\mathbf{n}} \ \mathbf{X} \ \mathbf{f}_{\mathbf{F}}$

If we d we may

Ŷ.

algebra $\frac{\delta^2}{\delta x'^2} (\phi_{\vec{G}})$

Where r

CC

Where θ

-3

vector larly,

Hence, the integral considered can be rewritten as

$$\hat{\mathbf{n}} \times \mathbf{f}_{\mathbf{F}} (\hat{\mathbf{j}}_{\mathbf{e}}^{\mathbf{d}} \cdot \nabla') \nabla' (\mathbf{\phi}_{\mathbf{d}} - \mathbf{\phi}_{\mathbf{f}}) d\mathbf{F}' = \hat{\mathbf{n}} \times \mathbf{f}_{\mathbf{F}} \hat{\mathbf{x}} \hat{\mathbf{j}}_{\mathbf{ex}}^{\mathbf{d}} \frac{\partial^{2}}{\partial \mathbf{x}'^{2}}$$

$$(\mathbf{\phi}_{\mathbf{d}} - \mathbf{\phi}_{\mathbf{f}}) d\mathbf{F}' + \hat{\mathbf{n}} \times \mathbf{f}_{\mathbf{F}} \hat{\mathbf{y}} \hat{\mathbf{j}}_{\mathbf{ex}}^{\mathbf{d}} \frac{\partial^{2}}{\partial \mathbf{x}'^{3} \mathbf{y}'} (\mathbf{\phi}_{\mathbf{d}} - \mathbf{\phi}_{\mathbf{f}}) d\mathbf{F}'.$$

$$(3.33)$$

If we choose the field point to be at origin; i.e., $\dot{\vec{r}}$ = 0, we may write the Green's functions $\phi_{\vec{d}}$ and $\phi_{\vec{f}}$ as

$$\phi_{d} = \frac{e^{-j\kappa r'}}{r'} , \quad \text{and} \quad \phi_{f} = \frac{e^{-jr'}}{r'}$$

where $r' = |\vec{r}'| = \sqrt{x'^2 + y'^2}$. With some straightforward algebraic manipulations, it can be shown that

where θ is the angle between the source-point position vector \vec{r}' and the x axis, as shown in Figure 3.9. Similarly, it can be shown that

$$\frac{\partial^2}{\partial x' \partial y'} (\phi_d - \phi_f) = \sin\theta \cos\theta \ [\frac{e^{-jr'} - \kappa^2 e^{-j\kappa r'}}{r'}$$

F.

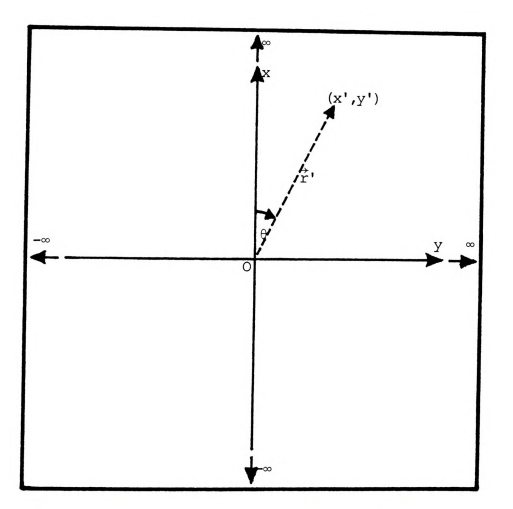


Figure 3.9. The coordinate system utilized in the infinite interface problem.

In the trari

face unifo

right last

F dx

It is

have

(3.33)

 $\int_{\mathbb{P}} \frac{\partial^2}{\partial x^1}$

- 3j
$$\frac{e^{-jr'} - \kappa e^{-j\kappa r'}}{r'^2}$$
 - 3 $\frac{e^{-jr'} - e^{-j\kappa r'}}{r'^3}$].

In the above derivation, the field point has been arbitrarily chosen at the origin. This assumption doesn't destroy the generality of this treatment, since the interface is infinitely large, and the field induced on it is uniformly distributed over it.

Now, we must show that both of the integrals on the right-hand side of eq. (3.33) vanish. Let us consider the last term of that equation first.

$$\begin{split} \int_{F} & \frac{\partial^{2}}{\partial x' \partial y'} (\phi_{\hat{\mathbf{d}}} - \phi_{\hat{\mathbf{f}}}) & \, \mathrm{d} F' = & \int_{O}^{2\pi} \sin \theta \, \cos \theta \, \, \mathrm{d} \theta \cdot \int_{O}^{\infty} \left[\, \mathrm{e}^{-\mathrm{j} \, \mathbf{r} \, \mathbf{r}} - \right. \\ & \left. \kappa^{2} \mathrm{e}^{-\mathrm{j} \, \kappa \, \mathbf{r}'} - 3\mathrm{j} \, \, \frac{\mathrm{e}^{-\mathrm{j} \, \mathbf{r}'} - \kappa \, \, \, \mathrm{e}^{-\mathrm{j} \, \kappa \, \mathbf{r}'}}{r'} - 3 \, \, \frac{\mathrm{e}^{-\mathrm{j} \, \mathbf{r}'} - \mathrm{e}^{-\mathrm{j} \, \kappa \, \mathbf{r}'}}{r'^{2}} \right] \, \mathrm{d} \mathbf{r}' \end{split}$$

It is clear that the first integral on the right-hand side of the above equation is equal to zero. Hence we have

$$\int_{\mathbf{F}} \frac{\partial^{2}}{\partial \mathbf{x}^{\dagger} \partial \mathbf{y}^{\dagger}} (\phi_{\mathbf{d}} - \phi_{\mathbf{f}}) d\mathbf{F}^{\dagger} = 0.$$
 (3.34)

For the first term on the right-hand side of eq. (3.33), we may write that

$$\int_{F} \frac{\partial^{2}}{\partial x^{\prime 2}} (\stackrel{\varphi}{d} - \stackrel{\varphi}{f}) dF' = 2\pi \int_{0}^{\infty} \left[j \frac{e^{-jr' - \kappa} e^{-j\kappa r'}}{r'} + \right]$$

radiati Af eq. (3.

= Note th

ĥ :

Then, su

We obtain $j_{n}^{d} = (\frac{1}{\kappa^{2}})^{d}$

The the resul

· ^f_F (

Hence, eq.

$$\frac{e^{-jr'} - e^{-j\kappa r'}}{r'^2} dr' + \int_0^{2\pi} \cos^2\theta d\theta \cdot \int_0^{\infty} [e^{-jr'} - \kappa^2 e^{-j\kappa r'}] dr'$$

$$-3j \frac{e^{-jr'} - \kappa e^{-j\kappa r'}}{r'} - 3 \frac{e^{-jr'} - e^{-j\kappa r'}}{r'^2} dr'$$

$$= -j\pi \int_0^{\infty} \frac{e^{-jr'} - \kappa e^{-j\kappa r'}}{r'} dr' - \pi \int_0^{\infty} \frac{e^{-jr'} - e^{-j\kappa r'}}{r'^2} dr'$$

$$+ j\kappa\pi - j\pi = \pi \int_0^{\infty} \frac{d}{dr'} \left(\frac{e^{-jr'} - e^{-j\kappa r'}}{r'} \right) dr' + j\kappa\pi - j\pi$$

$$= \pi \lim_{r' \to 0} \left[\frac{e^{-j\kappa r'} - e^{-jr'}}{r'} \right] + j\kappa\pi - j\pi = 0. \tag{3.35}$$

Note that for the last step in the above derivation, the radiation condition is applied.

After substitution of eqs. (3.34) and (3.35) into eq. (3.33), the result is

$$\hat{\mathbf{n}} \times \mathcal{I}_{\mathbf{F}} (\hat{\mathbf{J}}_{\mathbf{e}}^{\dagger \mathbf{d}} \cdot \nabla') \nabla'(\hat{\mathbf{q}}_{\mathbf{d}} - \hat{\mathbf{q}}_{\mathbf{f}}) d\mathbf{F}' = 0. \tag{3.36}$$

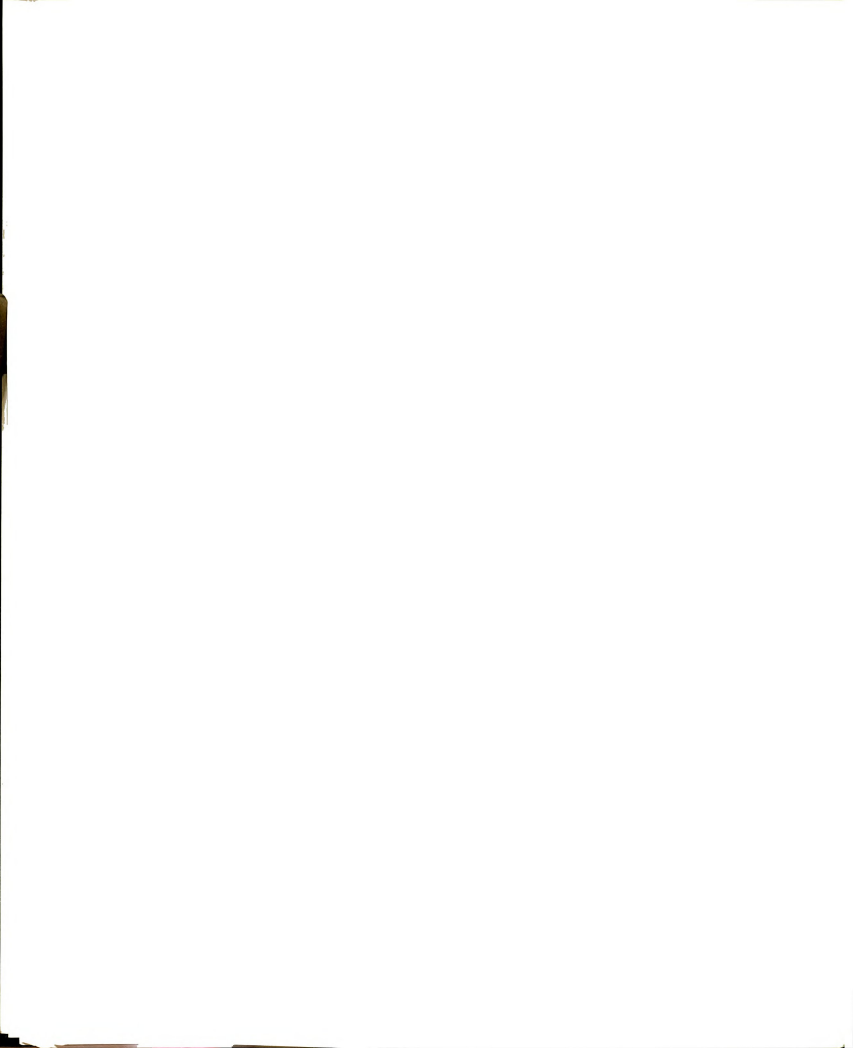
Then, substituting eqs. (3.32) and (3.36) into eq. (3.29), we obtain

$$j_{m}^{d} = (\frac{2}{\kappa^{2}+1}) \frac{E^{i}}{\eta_{o}} + \frac{j}{2\pi(\kappa^{2}+1)} j_{e}^{d} f_{F} (\kappa^{2} \phi_{d} - \phi_{f}) dF'.$$
 (3.37)

The integral term is easy to evaluate. We write down the result directly.

$$\int_{F} (\kappa^{2} \phi_{d} - \phi_{f}) dF' = j 2\pi (1 - \kappa)$$

Hence, eq. (3.37) becomes



$$j_{m}^{d} = \left(\frac{2}{\kappa^{2}+1}\right) \frac{E^{1}}{\eta_{o}} + \frac{\kappa^{-1}}{\kappa^{2}+1} j_{e}^{d}. \tag{3.38}$$

Following a similar procedure, we can obtain another equation from eq. (3.30), which is

$$j_{e}^{d} = \frac{E^{i}}{\eta_{0}} + \frac{\kappa - 1}{2} j_{m}^{d}. \tag{3.39}$$

Equations (3.29) and (3.30) have been simplified to become two linear equations with unknowns j_e^d and j_m^d . The solutions of these two unknowns are

$$j_e^d = (\frac{2\kappa}{\kappa+1}) \frac{E^i}{\eta_o}$$

and

$$j_m^d = (\frac{2}{\kappa + 1}) \frac{E^i}{\eta_0} ,$$

which also can be written as

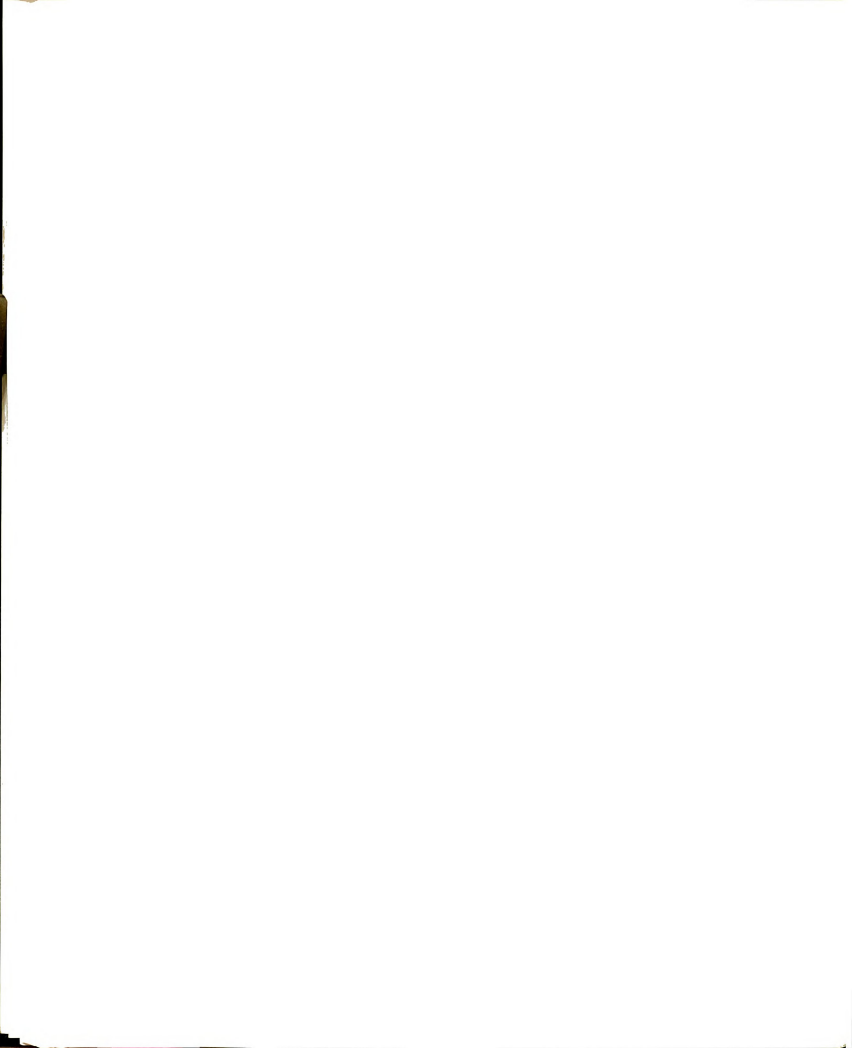
$$E^{d} = (\frac{2}{\kappa + 1}) E^{i}$$

and

$$H^d = (\frac{2\kappa}{\kappa+1}) H^i$$

which are exactly the same as eq. (3.31).

We have shown that the coupled, surface integral equations can predict correct results for the simplified special case of an infinite two-dimensional interface between a finite conducting medium and free space. This



example analytically proves the validity of the surface integral equations. In the following sections, we will develop a numerical technique for solving these surface integral equations for the cases of arbitrarily shaped, finite conducting bodies; after that, some numerical examples will be presented to discuss the accuracy of this numerical technique.

3.6. Review of Moment-Method

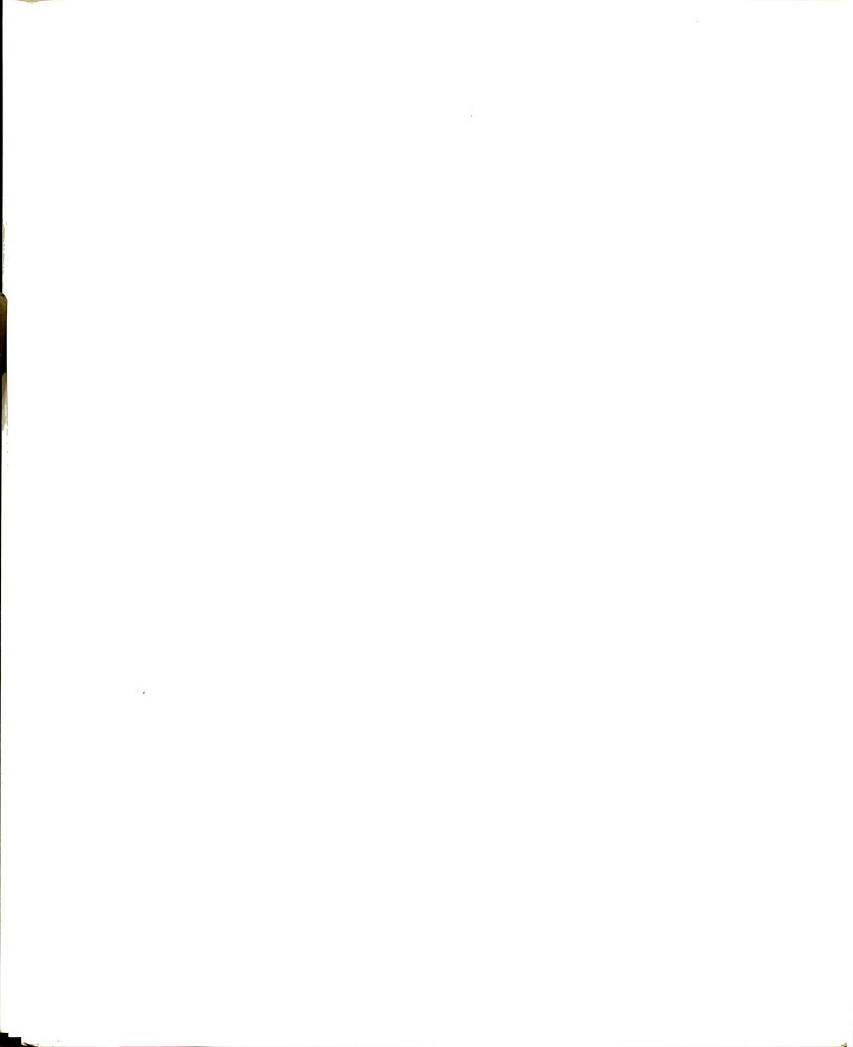
Before actually solving the surface integral equations, we should briefly review the basic steps involved in numerical implementation of such solutions, or the so-called Method of Moments (MOM) [17]. The idea of moment-method solutions is that the linear operator equation

$$L(f) = g ag{3.40}$$

where L is a linear operator, g is some known driving function, and f is to be determined, may be solved by first expanding f in a series of basis functions \mathbf{f}_n with unknown weighting coefficients α_n ,

$$f = \sum_{n} \alpha_{n} f_{n}$$
 (3.41)

Next, a set of weighting or testing functions w_m is chosen and an inner product (denoted by symbol < >) taken in eq. (3.40). After substitution of eq. (3.41) into eq. (3.40), the result is



$$\sum_{n} \alpha_{n} < w_{m}, L f_{n} > = < w_{m}, g >$$
 (3.42)

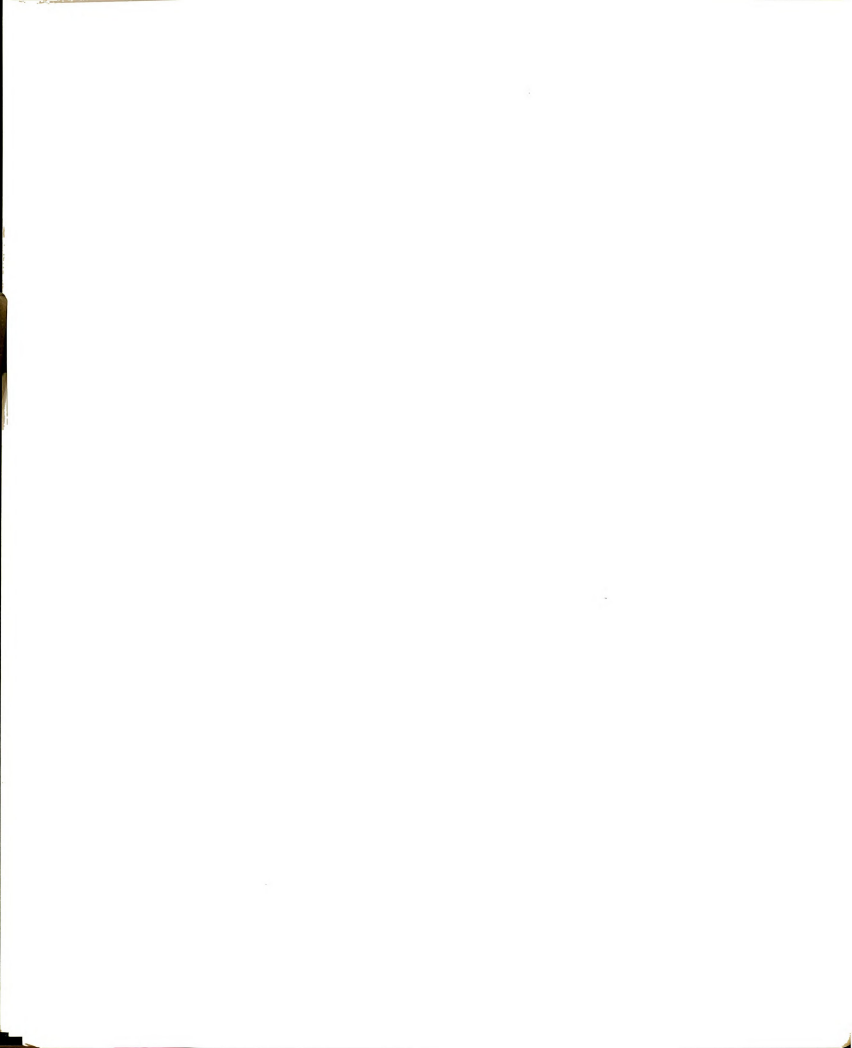
which may be written in matrix form as

$$[1_{mn}] [\alpha_n] = [g_m].$$

As illustrated in Figure 3.10, the idea when applied to the cubic box assumes that the box surface may be divided into square patches over each of which both components of surface current are assumed constant with unknown amplitudes (subdomain flat-top pulse-expansion functions). The testing functions chosen in this problem are δ functions at the patch centers (collocation or point matching). Thus, by successively enforcing the surface integral equations to be satisfied at these match points, a system of linear algebraic equations is generated. Matrix inversion then yields the solution for the unknown coefficients of the current samples.

3.7. The Numerical Technique

The validity of eqs. (3.29) and (3.30) has been checked in Section 3.5 through the consideration of a special case of a two-dimensional, infinite-plane interface between a finite conducting medium and free space. Since it is our goal to quantify the EM fields induced on the surfaces of arbitrarily shaped, finite conducting bodies, such as human bodies, it seems more realistic to consider a simulated human body with shape as shown in



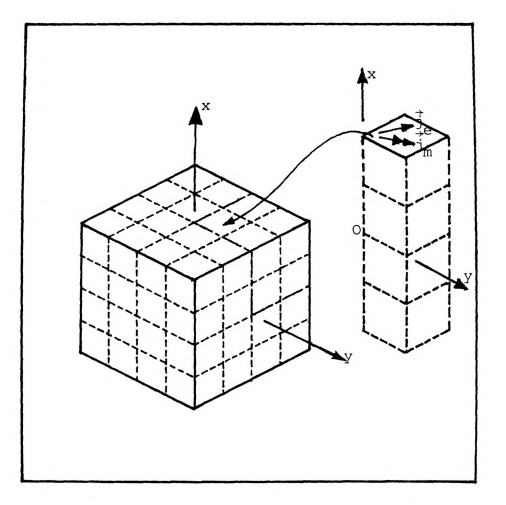


Figure 3.10. Division of the surface of a cubic body into square surface cells for moment-method solution using two-dimensional flat pulses as expansion functions and & functions as testing functions.



Figure 3.11. We assume that the body region G, being characterized by permeability μ_{0} and complex permittivity $\epsilon_{\vec{d}}$ and enclosed by surface F, is illuminated by an incident plane wave which is propagating in the +z direction with its electric field $\vec{E}^{\,i}$ polarized in the +x direction. The body is immersed in free space as shown in Figure 3.11.

It is easy to see from Figure 3.11 that, for a simulated body, the body surface F consists of a number of plane surface elements. If the body is described in a rectangular coordinate system, which is the one used in Figure 3.11, the problem can be simplified by constructing the body surface with surface elements having normal vectors pointing in one of the six possible along-axis directions, i.e., the $\pm \hat{x}$, the $\pm \hat{y}$, and the $\pm \hat{z}$ directions. For the purpose of clarity, we will name these surface elements according to the directions of their unit normal vectors. For example, the top surface element of the body head shown in Figure 3.11 will be considered as one of the +x surface elements, since its unit normal vector is pointing in the +x direction. It should be emphasized that a closed surface can consist of several surface elements with unit normal vectors pointing in the same direction, as can be seen from Figure 3.11.

Before going any further, we should mention that we choose a plane wave as the incident wave, because it is a realistic approximation when the body is distant from a



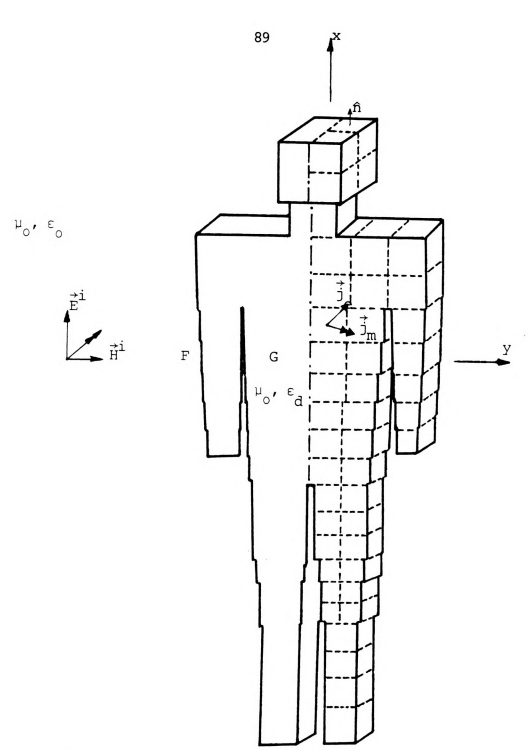
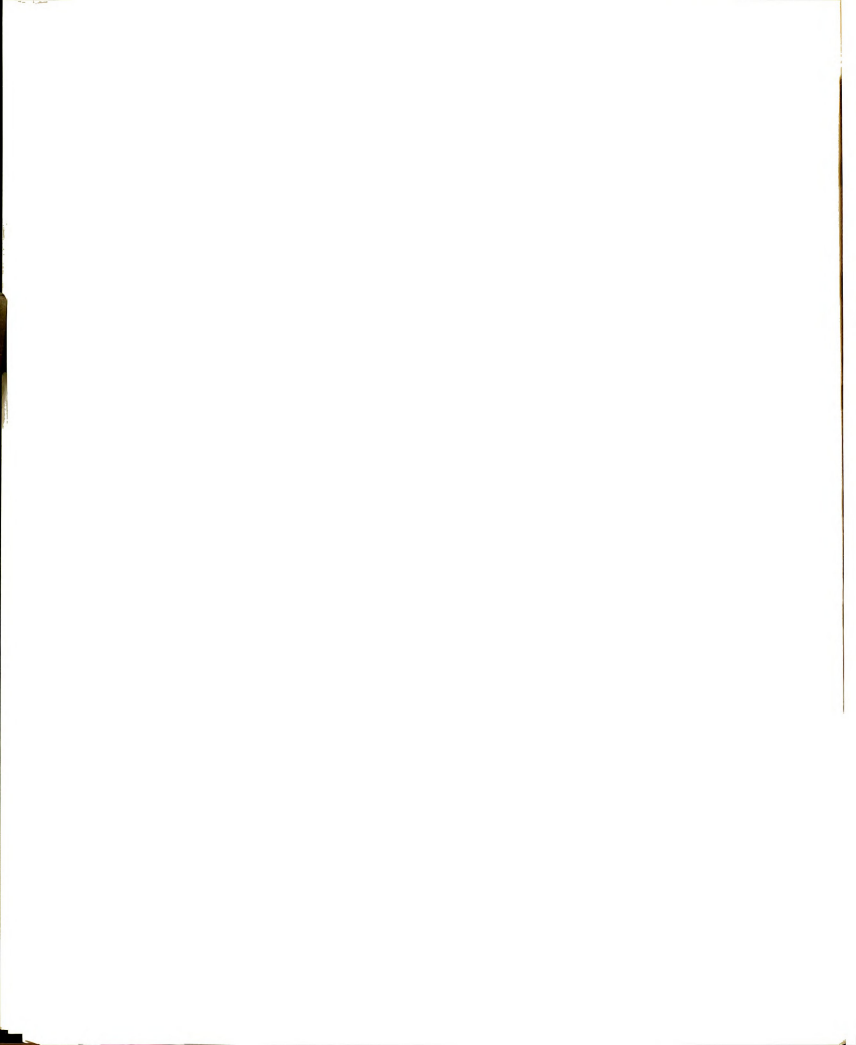


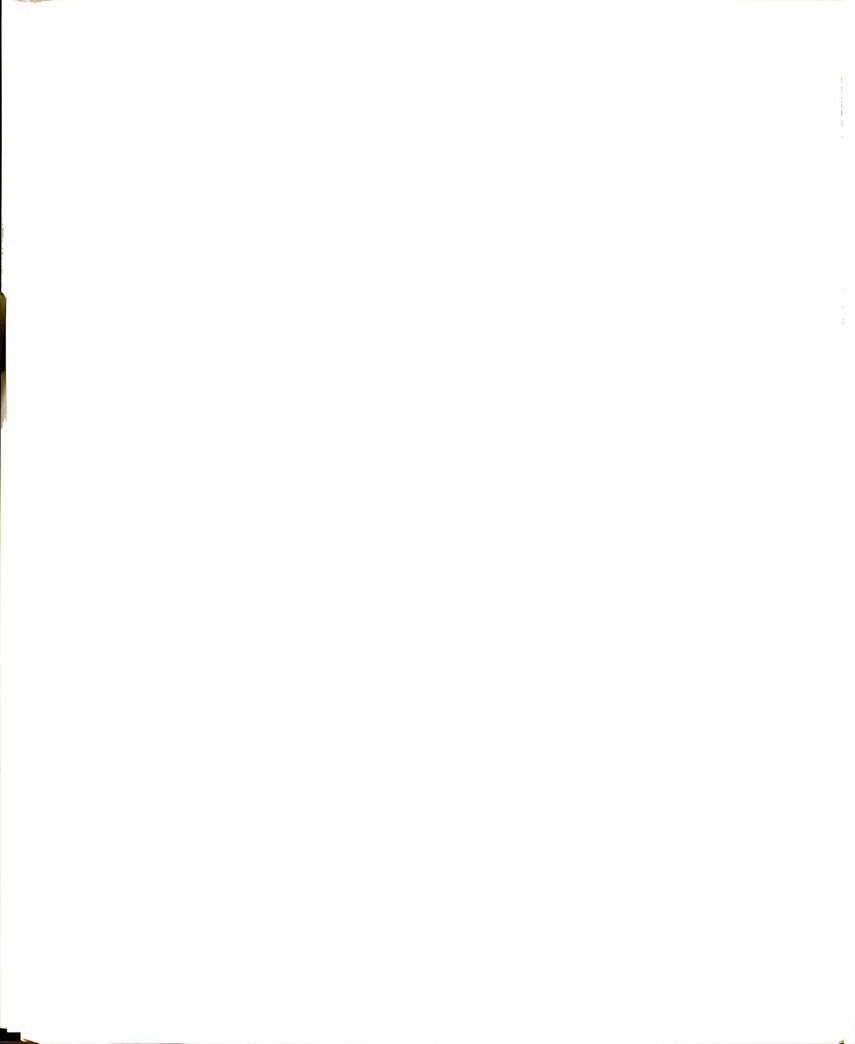
Figure 3.11. A simulated human body is irradiated by an incident plane wave propagating in the +z direction with a x-polarized electric field. The body is characterized by complex permittivity $\epsilon_{\rm d}$, and its surface is subdivided into a number of square surface cells. The induced equivalent surface currents $(\frac{1}{2}\epsilon_{\rm d},\frac{1}{2}m_{\rm d})$ at different locations on the surface can be obtained by solving two coupled, surface integral equations.



radiating source, and it facilitates the analysis. Also, we choose the rectangular coordinate system since it is the most adaptable to arbitrarily shaped bodies. However, it is to be noted that the surface integral equations derived previously are so general that they can be applied to any form of incident field, as well as any orthogonal coordinate system.

Now, let us consider Figure 3.11 again, where each surface element of F has been subdivided into several square subareas named surface cells. Each surface cell can have any arbitrary dimension which depends on the accuracy desired. Furthermore, the center point of each surface cell is considered as a reference point which could be either a field point or a source point or both. The EM field induced inside each surface cell is assumed to be uniform. We will use the notation $\boldsymbol{F}_{\boldsymbol{x}}$ to represent the combined surface of all the +x surface elements, and use the symbol $\mathbf{N}_{\mathbf{v}}$ to denote the total number of surface cells included in $\boldsymbol{F}_{\mathbf{x}}.$ Similar definitions will be applied to the notations, F_v , N_v ; F_z , N_z ; F_{-x} , N_{-x} ; F_{-y} , N_{-y} ; and $\mathbf{F_{-z}},~\mathbf{N_{-z}},$ etc. In other words, we may say that the body surface F has been divided into totally $^{\mathrm{N}}_{\mathrm{cell}}$ surface cells, where $\rm N_{cell}$ is the sum of $\rm N_{x},\ N_{v},\ N_{z},\ N_{-x},\ N_{-y},$ and N___.

To solve the surface integral equations numerically by use of the moment-method, we must decompose the integral



equations first and then point-match them at the reference point of each surface cell. By doing this, a system of simultaneous, scalar, linear algebraic equations will be obtained. After transforming these linear equations into a matrix form, it can be solved by conventional matrix inversion techniques. To describe the procedures in more detail, let's start with the following definitions:

m: the numbering index of the surface cells in each subsurface (F_x , F_y , F_z , F_{-x} , F_{-y} , F_{-z}), when center points of the surface cells are considered as field points.

n: the numbering index of the surface cells in each subsurface, when center points of the surface cells are considered as source points.

An: the area of the nth surface cell.

 \vec{r}^m : the position vector locating the mth field point, where $\vec{r}^m = (x^m, y^m, z^m)$.

 $\vec{r}^n\colon$ the position vector locating the nth source point, where \vec{r}^n = $(x^n$, y^n , $z^n)$.

Also,

$$\mathbf{r}^{nm} \equiv |\dot{\mathbf{r}}^n - \dot{\mathbf{r}}^m|, \mathbf{x}^{nm} \equiv \mathbf{x}^n - \mathbf{x}^m, \mathbf{y}^{nm} \equiv \mathbf{y}^n - \mathbf{y}^m,$$

$$\mathbf{z}^{nm} \equiv \mathbf{z}^n - \mathbf{z}^m.$$

and

 $a^{m} = \sqrt{A^{m}/\pi} : \quad \text{the equivalent radius of the mth surface}$ cell.



We also like to introduce the following associated Green's functions; the reasons behind these definitions will be clear when the surface integral equations are decomposed:

$$G_{1}^{nm} = j \, \frac{e^{-j r^{nm}} - \kappa \, \, e^{-j \kappa r^{nm}}}{r^{nm^{2}}} \ \ \, + \, \, \frac{e^{-j r^{nm}} - e^{-j \kappa r^{nm}}}{r^{nm^{3}}}$$

$$G_2^{nm} = \frac{e^{-jr^{nm}} - \kappa^2 e^{-j\kappa r^{nm}}}{r^{nm^3}} - 3j \frac{e^{-jr^{nm}} - \kappa e^{-j\kappa r^{nm}}}{r^{nm^4}} - 3 \frac{e^{-jr^{nm}} - e^{-j\kappa r^{nm}}}{r^{m^5}}$$

$$G_{3}^{nm} = j \frac{e^{-jr^{nm}} - \kappa^{3} e^{-j\kappa r^{nm}}}{r^{nm^{2}}} + \frac{e^{-jr^{nm}} - \kappa^{2} e^{-j\kappa r^{nm}}}{r^{nm^{3}}}$$

$$G_{4}^{nm} = -\frac{e^{-jr^{nm}} - \kappa^{2} e^{-j\kappa r^{nm}}}{r^{nm}}$$
(3.4)

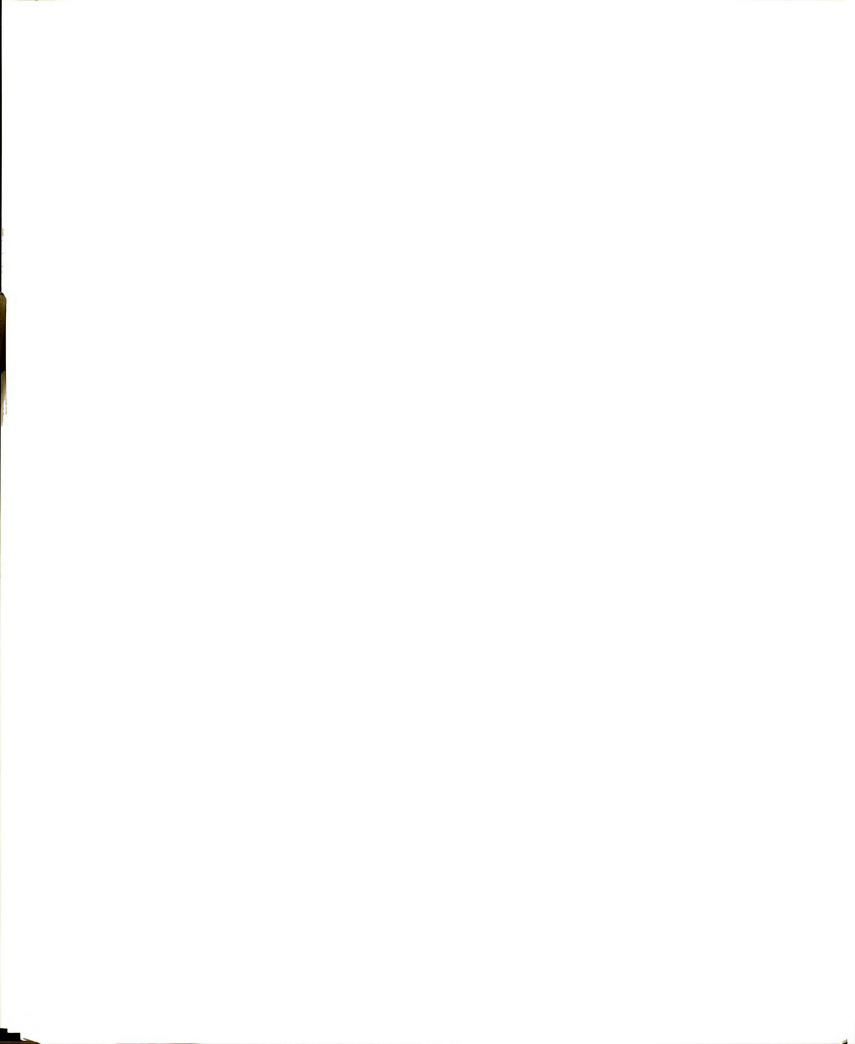
$$H_1^m = \pi (j e^{-ja^m} - j \kappa e^{-j\kappa a^m} + \frac{e^{-ja^m} - e^{-j\kappa a^m}}{a^m})$$

and

$$H_2^m = 2\pi (j\kappa e^{-j\kappa a^m} - je^{-ja^m} - j\kappa + j).$$

Now, we are in a position to decompose the coupled, surface integral equations, i.e., eqs. (3.29) and (3.30). For convenience, we repeat them here,

$$\vec{J}_{m} = \frac{1}{\kappa^{2}+1} \vec{J}_{m}^{i} - \frac{1}{2\pi(\kappa^{2}+1)} \hat{n} \times \int_{F} [j(\kappa^{2}\phi_{d} - \phi_{f}) \vec{J}_{e} + \vec{J}_{m} \times \nabla'(\kappa^{2}\phi_{d} - \phi_{f}) + j(\vec{J}_{e} \cdot \nabla') \nabla'(\phi_{d} - \phi_{f})] dF'$$
(3.29')



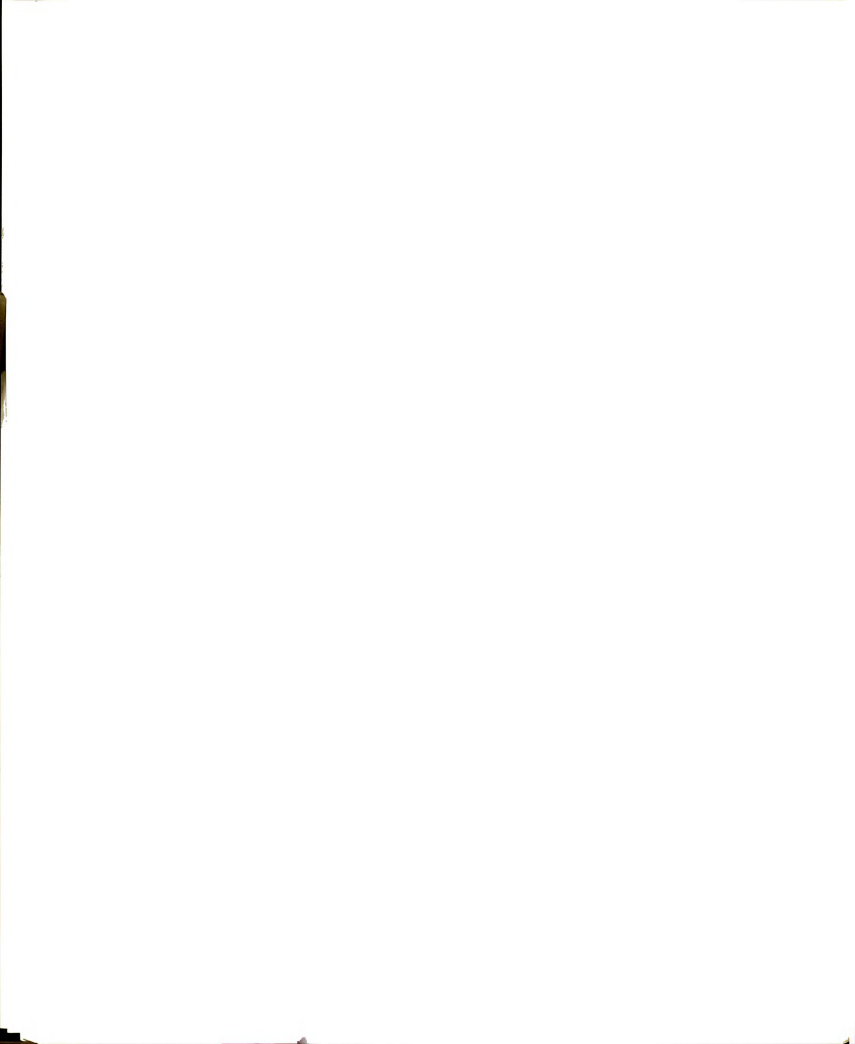
Note that, without any ambiguity, the superscript "d" for the induced equivalent surface current densities has been omitted in the above equations.

Let us consider eq. (3.29') first. To numerically implement the various surface integrals of this equation, we have to consider each possible case about the field point locations.

I) First of all, we consider the situation when the field point is located in one of the +x surface elements. Which means that the unit normal vector at field point, \hat{n} , is the same as the x-direction unit vector \hat{x} . For this case, we know that $1 \le m \le N_{\chi}$. Based on the previous definitions, it is easy to see that the last integral of eq. (3.29') can be written as

$$\hat{\mathbf{n}} \times \mathcal{I}_{\mathbf{F}}(\hat{\mathbf{j}}_{\mathbf{e}} \cdot \nabla') \nabla'(\phi_{\mathbf{d}} - \phi_{\mathbf{f}}) d\mathbf{F'} = \hat{\mathbf{x}} \times \{[\mathcal{I}_{\mathbf{F}_{\mathbf{X}}} + \mathcal{I}_{\mathbf{F}_{\mathbf{Y}}} + \mathcal{I}_{\mathbf{F}_{\mathbf{Z}}} + \mathcal{I}_{\mathbf{F}_{\mathbf{Z}} + \mathcal{I}_{\mathbf{Z}} + \mathcal{I}_{\mathbf{Z}}$$

where we have decomposed the total surface integral $f_{\rm F}$ into six different subintegrals, one for each subsurface. For example, $f_{\rm F_X}$ represents the integration of the integrand over all the surface elements having $\hat{\bf x}$ as the unit normal



vector. The remaining five subintegrals in eq. (3.44) have similar meanings. Now, as an example, let's carry out the first subintegral of eq. (3.44).

$$\begin{split} &\hat{x} \times \int_{F_{\mathbf{X}}} (\hat{\mathbf{j}}_{\mathbf{e}} \cdot \nabla^{\mathbf{i}}) \nabla^{\mathbf{i}} (\phi_{\mathbf{d}} - \phi_{\mathbf{f}}) \ d\mathbf{F}^{\mathbf{i}} = \hat{x} \times \int_{F_{\mathbf{X}}} [(j_{\mathbf{e}\mathbf{y}} \circ + j_{\mathbf{e}\mathbf{z}} \circ 2) \cdot (\hat{x} \cdot \frac{\partial}{\partial \mathbf{x}^{\mathbf{i}}} + \\ &\hat{y} \cdot \frac{\partial}{\partial \mathbf{y}^{\mathbf{i}}} + \hat{z} \cdot \frac{\partial}{\partial \mathbf{z}^{\mathbf{i}}})] \cdot [(\hat{x} \cdot \frac{\partial}{\partial \mathbf{x}^{\mathbf{i}}} + \hat{y} \cdot \frac{\partial}{\partial \mathbf{y}^{\mathbf{i}}} + \hat{z} \cdot \frac{\partial}{\partial \mathbf{z}^{\mathbf{i}}}) (\phi_{\mathbf{d}} - \phi_{\mathbf{f}})] \ d\mathbf{F}^{\mathbf{i}} \end{split}$$

$$&= \hat{x} \times \int_{F_{\mathbf{X}}} [\hat{x} (j_{\mathbf{e}\mathbf{y}} \cdot \frac{\partial^{2}}{\partial \mathbf{x}^{\mathbf{i}} \partial \mathbf{y}^{\mathbf{i}}} + j_{\mathbf{e}\mathbf{z}} \cdot \frac{\partial^{2}}{\partial \mathbf{x}^{\mathbf{i}} \partial \mathbf{z}^{\mathbf{i}}}) + \hat{y} (j_{\mathbf{e}\mathbf{y}} \cdot \frac{\partial^{2}}{\partial \mathbf{y}^{\mathbf{i}} 2} + j_{\mathbf{e}\mathbf{z}} \cdot \frac{\partial^{2}}{\partial \mathbf{y}^{\mathbf{i}} \partial \mathbf{z}^{\mathbf{i}}}) + \\ &\hat{z} (j_{\mathbf{e}\mathbf{y}} \cdot \frac{\partial^{2}}{\partial \mathbf{y}^{\mathbf{i}} \partial \mathbf{z}^{\mathbf{i}}} + j_{\mathbf{e}\mathbf{z}} \cdot \frac{\partial^{2}}{\partial \mathbf{z}^{\mathbf{i}} 2})] (\phi_{\mathbf{d}} - \phi_{\mathbf{f}}) \ d\mathbf{F}^{\mathbf{i}} \end{split}$$

$$&= \hat{x} \times \int_{F_{\mathbf{X}}} [\hat{y} (j_{\mathbf{e}\mathbf{y}} \cdot \frac{\partial^{2}}{\partial \mathbf{y}^{\mathbf{i}} 2} + j_{\mathbf{e}\mathbf{z}} \cdot \frac{\partial^{2}}{\partial \mathbf{y}^{\mathbf{i}} \partial \mathbf{z}^{\mathbf{i}}}) + \hat{z} (j_{\mathbf{e}\mathbf{y}} \cdot \frac{\partial^{2}}{\partial \mathbf{y}^{\mathbf{i}} \partial \mathbf{z}^{\mathbf{i}}} + j_{\mathbf{e}\mathbf{z}} \cdot \frac{\partial^{2}}{\partial \mathbf{z}^{\mathbf{i}} 2})]$$

$$&(\phi_{\mathbf{d}} - \phi_{\mathbf{f}}) \ d\mathbf{F}^{\mathbf{i}} \end{split}$$

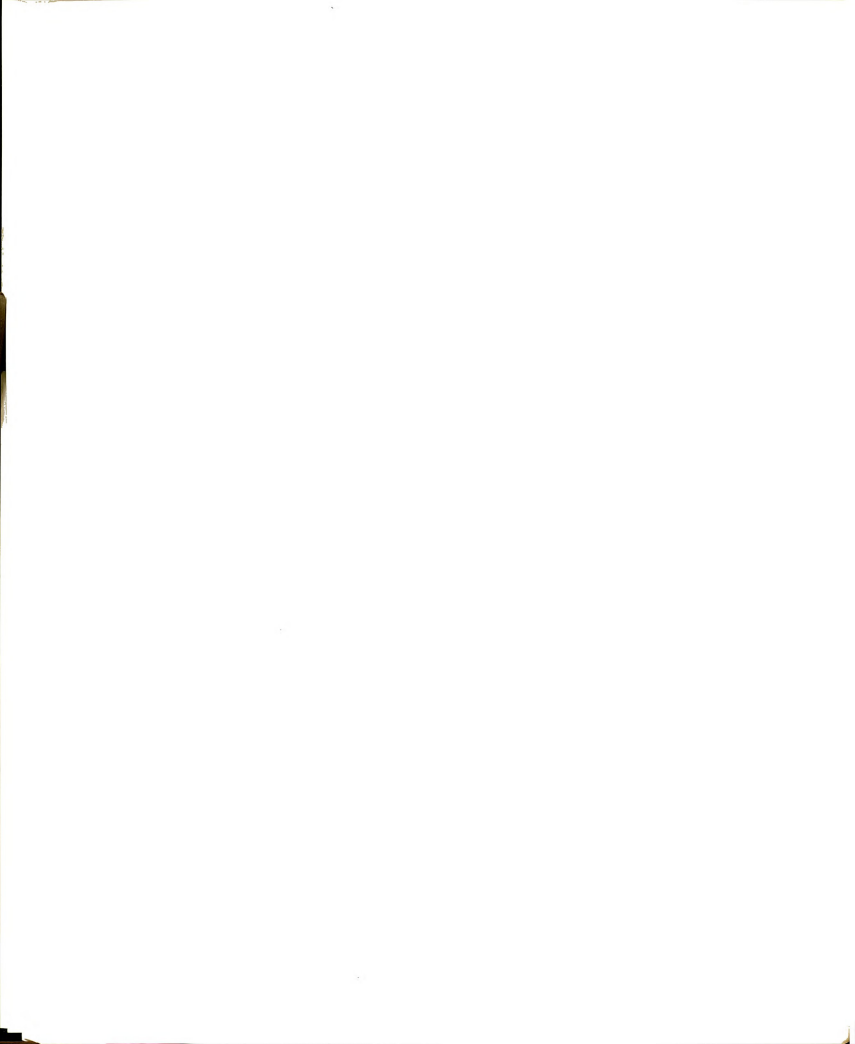
Since $\Phi_{d} = \frac{-j\kappa\underline{r}}{\underline{r}}$ and $\Phi_{f} = \frac{e^{-j}\underline{r}}{\underline{r}}$ where $\underline{r} = |\vec{r} - \vec{r}'|$, we may show that

$$\frac{\partial^2}{\partial y'^2} (\phi_d - \phi_f) = G_1 + (y' - y)^2 G_2$$

$$\frac{\partial^2}{\partial z'^2} (\phi_d - \phi_f) = G_1 + (z' - z)^2 G_2$$

and

$$\frac{\partial^2}{\partial y' \partial z'} (\Phi_d - \Phi_f) = (y' - y) (z' - z) G_2$$

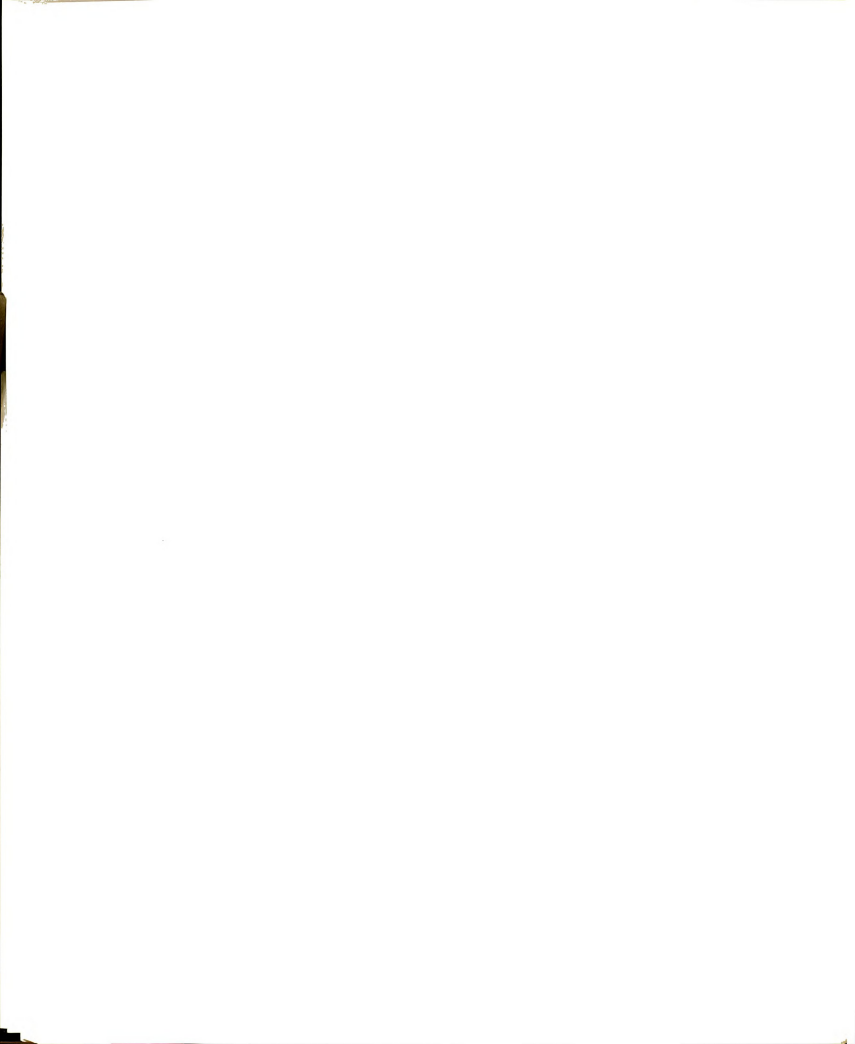


where ${\bf G}_1$ and ${\bf G}_2$ have the same expressions as that of ${\bf G}_1^{nm}$ and ${\bf G}_2^{nm}$ defined in eq. (3.43) except ${\bf r}^{nm}$ being replaced by $\underline{\bf r}$. Hence we have

$$\begin{split} \hat{x} \times \mathcal{I}_{F_{X}}(\hat{j}_{e} \cdot \nabla') & \nabla'(\phi_{d} - \phi_{f}) \ dF' = -\hat{y} \ \mathcal{I}_{F_{X}} \{ j_{ey}(y' - y)(z' - z) \ G_{2} + \\ & j_{ez}[G_{1} + (z' - z)^{2} \ G_{2}] \} \ dF' + \hat{z} \ \mathcal{I}_{F_{X}} \{ j_{ey}[G_{1} + (y' - y)^{2} \ G_{2}] + \\ & j_{ez}(y' - y)(z' - z) \ G_{2} \} \ dF'. \end{split}$$

The integrals on the right-hand side of the above equation can be numerically implemented by summing up the products of integrands and areas of the corresponding surface cells with a special consideration being paid to the singular terms which occur when the source point coincides with the field point. This process is completely based on the moment-method technique with two-dimensional pulse functions as the basis functions, and δ functions as the testing functions. So we may rewrite the above equation as

$$\hat{x} \times f_{\mathbf{r}} (\hat{\vec{j}}_{e} \cdot \vec{v}') \nabla' (\hat{\phi}_{d} - \hat{\phi}_{f}) d\mathbf{F}' = -\hat{y} \sum_{\substack{n=1 \\ n \neq m}}^{N_{x}} [j_{ey}^{n} \mathbf{A}^{n} \mathbf{y}^{nm} \mathbf{z}^{nm} \mathbf{G}_{2}^{nm} +$$



$$\begin{split} & j_{\text{ez}}^{n} \ \textbf{A}^{n} \ \textbf{y}^{nm} \ \textbf{z}^{nm} \ \textbf{G}_{2}^{nm}] - \hat{\textbf{y}} f_{\textbf{A}^{m}} \{ j_{\text{ey}}^{m} (\textbf{y'} - \textbf{y}) (\textbf{z'} - \textbf{z}) \textbf{G}_{2} + j_{\text{ez}}^{m} [\textbf{G}_{1} + (\textbf{z'} - \textbf{z})^{2} \textbf{G}_{2}] \} \ \textbf{dF'} + \hat{\textbf{z}} f_{\textbf{A}^{m}} \{ j_{\text{ey}}^{m} [\textbf{G}_{1} + (\textbf{y'} - \textbf{y})^{2} \textbf{G}_{2}] + j_{\text{ez}}^{m} (\textbf{y'} - \textbf{y}) (\textbf{z'} - \textbf{z}) \textbf{G}_{2} \} \ \textbf{dF'}, \ 1 \leq m \leq N_{\textbf{X}} \end{split}$$

$$(3.45)$$

where $j_{\mathrm{ey}}^{\mathrm{n}}$, $j_{\mathrm{ey}}^{\mathrm{n}}$, $j_{\mathrm{ey}}^{\mathrm{m}}$, and $j_{\mathrm{ez}}^{\mathrm{m}}$ are the unknown expansion coefficients of the equivalent surface current densities. Note that the above equation is satisfied at every field point location on the subsurface F_{x} . The notation $\frac{N_{\mathrm{x}}}{n+1}$ implies a summation with respect to all the source points on F_{x} excluding the one coinciding with the field point where the singularities of Green's functions occur. The contributions of the singular terms are accounted for by the last two terms in eq. (3.45), where the notation f_{x} means the integration of integrand over a circle centered at the field point with area A^{m} . Now, let's investigate these singular terms more specifically. It can be shown that

$$\begin{split} & \int_{\mathbb{A}^m} (\mathbf{y'} - \mathbf{y}) \, (\mathbf{z'} - \mathbf{z}) \, \mathbf{G}_2 \, \, \mathrm{d}\mathbf{F'} = \int_0^{\mathbb{A}^m} \int_0^{2\pi} \underline{\mathbf{r}}^2 \cos\theta \, \sin\theta \, \, \mathbf{G}_2 \, \, \mathrm{d}\theta \, \, \underline{\mathbf{r}} \, \, \mathrm{d}\underline{\mathbf{r}} \\ & = \int_0^{2\pi} \underbrace{\cos\theta \, \, \sin\theta \, \, \mathrm{d}\theta}_0 \, \int_0^{\mathbb{A}^m} \underline{\mathbf{r}}^3 \, \, \mathbf{G}_2 \, \, \mathrm{d}\underline{\mathbf{r}} = 0, \end{split} \tag{3.46}$$

also,

$$\int_{A} \!\! m [G_1 \, + \, (y^{\, \prime} \, - \, y)^{\, 2} \, G_2^{\, }] \ dF^{\, \prime} \, = \, \int_{O}^{2\pi} \int_{O}^{A^m} \, [G_1^{\, } \, + \, \underline{r}^2 \, \cos^2 \! \theta \, G_2^{\, }] \, \, \underline{r} \, \, d\underline{r} \, \, d\theta$$



and

After substituting the expressions of \mathbf{G}_1 and \mathbf{G}_2 into the above equations, we have

$$\int_{\mathbb{A}}^m [G_1 + (y' - y)^2 G_2] \ dF' = \int_{\mathbb{A}}^m [G_1 + (z' - z)^2 G_2] \ dF' = H_1^m,$$
 (3.47)

where ${\rm H}_1^{\rm m}$ is defined in eq. (3.43). Then, substituting eqs. (3.46) and (3.47) into eq. (3.45), finally we obtain

$$\hat{x} \times \mathcal{F}_{F_{x}}(\vec{j}_{e} \cdot \forall') \ \forall' (\phi_{d} - \phi_{f}) \ dF' = -\hat{y} \{ \sum_{\substack{n=1 \\ n \neq n}}^{N_{x}} \lambda^{n} [j_{ey}^{n} \ y^{nm} \ z^{nm} \ g_{2}^{nm} + (j_{ey}^{n} \ y^{nm} \ z^{nm} + (j_{ey}^{n} \ y^{nm} \ z^{nm} + (j_{ey}^{n} \ y^{nm} \ z^{nm} + (j_{ey}^{n} \ y^{nm} + (j_{ey}^{n} \ y^{nm} \ z^{nm} + (j_{ey}^{n} \ y^{nm} + (j_{ey}^{n} \ y^{$$

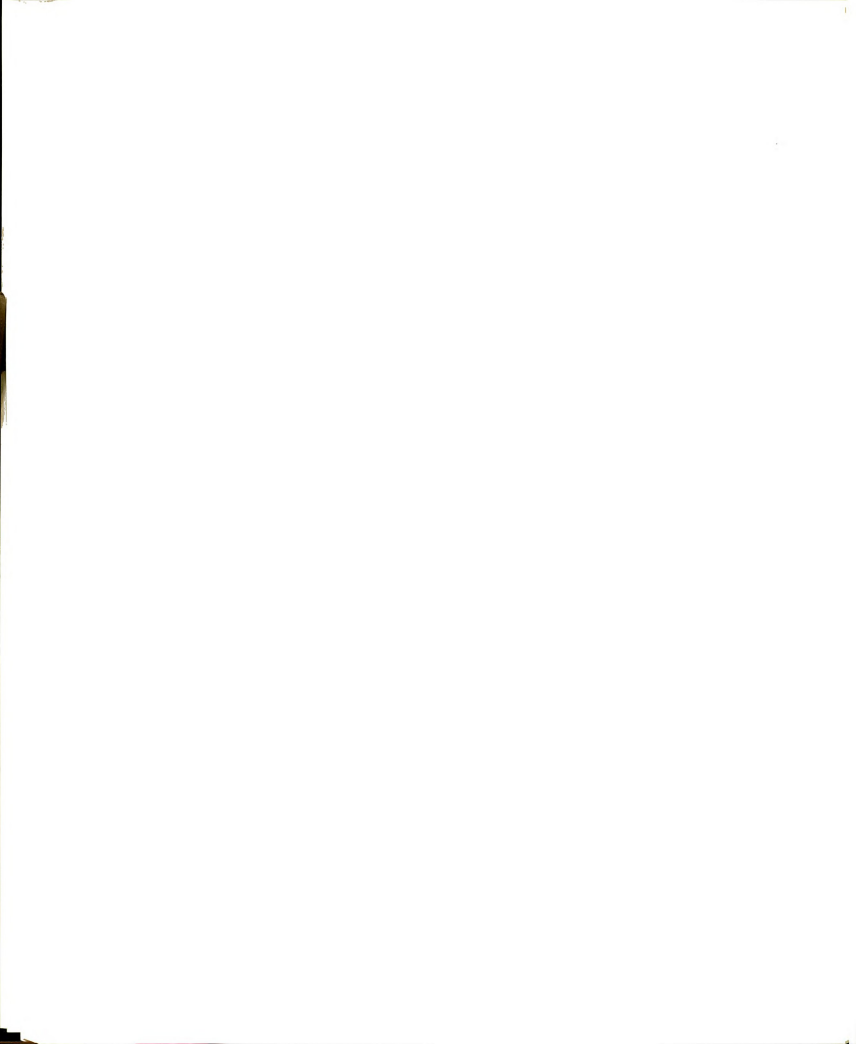
$$\mathtt{j}_{\mathrm{ez}}^{\mathrm{n}}(\mathtt{G}_{1}^{\mathrm{nm}} + \mathtt{z}^{\mathrm{nm}} \boldsymbol{\cdot} \mathtt{z}^{\mathrm{nm}} \ \mathtt{G}_{2}^{\mathrm{nm}}) \,] \, + \, \mathtt{j}_{\mathrm{ez}}^{\mathrm{m}} \ \mathtt{H}_{1}^{\mathrm{m}} \big\} \, + \,$$

$$\hat{z} \in \sum_{\substack{n=1 \\ n \neq m}}^{N_x} A^n [j_{ey}^n (G_1^{nm} + y^{nm} \cdot y^{nm} G_2^{nm}) +$$

$$j_{ez}^{n} \text{ y}^{nm} \text{ z}^{nm} \left(g_{2}^{nm} \right) + j_{ey}^{m} \text{ H}_{1}^{m} \right), \text{ where } 1 \leq \text{ m} \leq \text{ N}_{X} \text{ .} \tag{3.48}$$

This concludes the evaluation of the first subintegral in eq. (3.44). The remaining five subintegrals in that equation can be carried out similarly. Combining these results with eq. (3.44), the latter will become

$$\hat{x} \times f_{F}(\hat{j}_{e}^{+} + \nabla^{\dagger}) \ \nabla^{\dagger}(\phi_{d} - \phi_{f}) \ dF^{\dagger} = -\hat{y} \{ (\underbrace{n_{E}^{N_{x}}}_{n=1} + \underbrace{n_{E}^{N_{-x}}}_{n=1}) A^{n}[j_{ey}^{n} \ y^{nm} \ z^{nm} \ G_{2}^{nm} + \underbrace{n_{E}^{n}}_{n=1} + \underbrace{n_{E}^{N_{-x}}}_{n=1} A^{n}[j_{ey}^{n} \ y^{nm} \ z^{nm} \ G_{2}^{nm} + \underbrace{n_{E}^{N_{-x}}}_{n=1} + \underbrace{n_{E}^{N_{-x}}}_{n=1} A^{n}[j_{ey}^{n} \ y^{nm} \ z^{nm} \ G_{2}^{nm} + \underbrace{n_{E}^{N_{x}}}_{n=1} + \underbrace{n_{E}^{N_{x}}}_{n=1$$

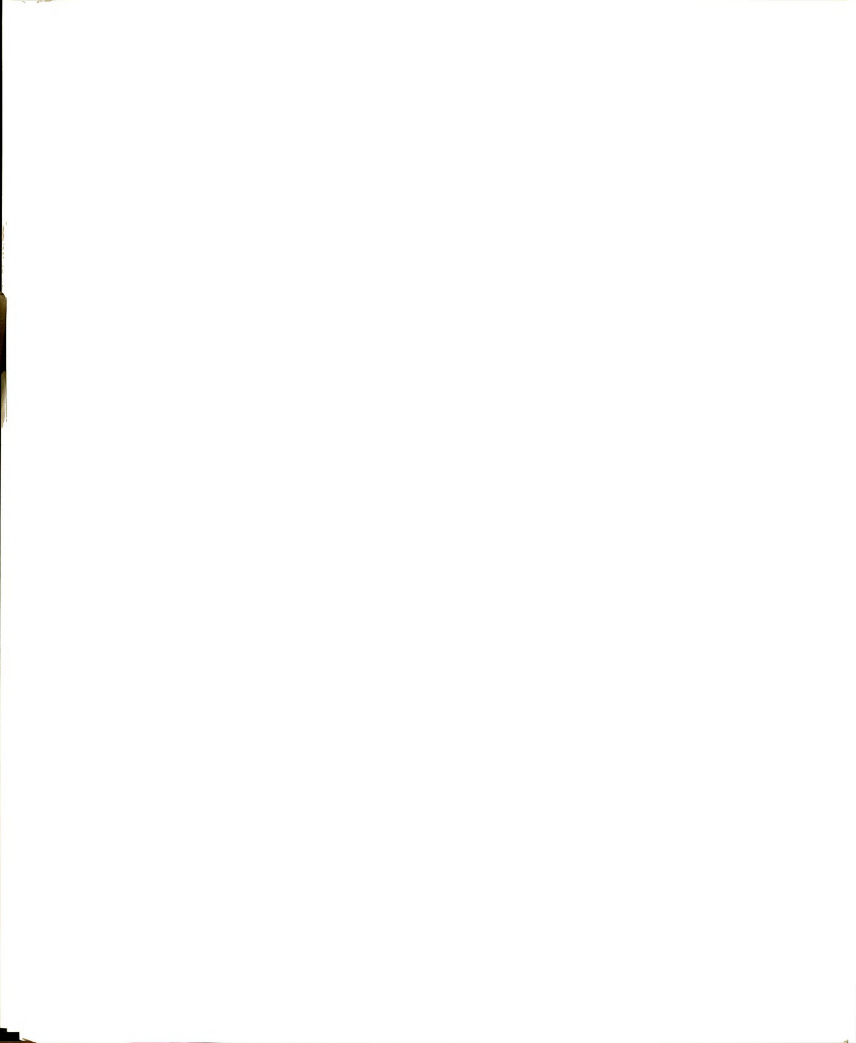


$$\begin{split} j_{ez}^{n} \left(G_{1}^{nm} + z^{nm} \cdot z^{nm} \; G_{2}^{nm} \right) + \left(\sum_{n=1}^{N_{y}} + \sum_{n=1}^{N_{-y}} \right) \; A^{n} [j_{ex}^{n} \; x^{nm} \; z^{nm} \; G_{2}^{nm} + \\ j_{ez}^{n} \left(G_{1}^{nm} + z^{nm} \cdot z^{nm} \; G_{2}^{nm} \right)] + \left(\sum_{n=1}^{N_{z}} + \sum_{n=1}^{N_{-z}} \right) \; A^{n} [j_{ex}^{n} \; x^{nm} \; z^{nm} \; G_{2}^{nm} + \\ j_{ey}^{n} \; y^{nm} \; z^{nm} \; G_{2}^{nm}] + j_{ez}^{m} \; H_{1}^{m} \} \; + \\ \hat{z} \; \left(\sum_{n=1}^{N_{x}} + \sum_{n=1}^{N_{-x}} \right) \; A^{n} [j_{ey}^{n} (G_{1}^{nm} + y^{nm} \cdot y^{nm} \; G_{2}^{nm}) + \\ \hat{z} \; \left(\sum_{n=1}^{N_{y}} + \sum_{n=1}^{N_{-x}} \right) \; A^{n} [j_{ex}^{n} \; x^{nm} \; y^{nm} \; G_{2}^{nm} + \\ \hat{z} \; \left(\sum_{n=1}^{N_{y}} + \sum_{n=1}^{N_{z}} \right) \; A^{n} [j_{ex}^{n} \; x^{nm} \; y^{nm} \; G_{2}^{nm} + \\ \hat{z} \; \left(\sum_{n=1}^{N_{z}} + \sum_{n=1}^{N_{z}} \right) \; A^{n} [j_{ex}^{n} \; x^{nm} \; y^{nm} \; G_{2}^{nm} + \\ \hat{z} \; \left(\sum_{n=1}^{N_{z}} + \sum_{n=1}^{N_{z}} \right) \; A^{n} [j_{ex}^{n} \; x^{nm} \; y^{nm} \; G_{2}^{nm} + \\ \hat{z} \; \left(\sum_{n=1}^{N_{z}} + \sum_{n=1}^{N_{z}} \right) \; A^{n} [j_{ex}^{n} \; x^{nm} \; y^{nm} \; G_{2}^{nm} + \\ \hat{z} \; \left(\sum_{n=1}^{N_{z}} + \sum_{n=1}^{N_{z}} \right) \; A^{n} [j_{ex}^{n} \; x^{nm} \; y^{nm} \; G_{2}^{nm} + \\ \hat{z} \; \left(\sum_{n=1}^{N_{z}} + \sum_{n=1}^{N_{z}} \right) \; A^{n} [j_{ex}^{n} \; x^{nm} \; y^{nm} \; G_{2}^{nm} + \\ \hat{z} \; \left(\sum_{n=1}^{N_{z}} + \sum_{n=1}^{N_{z}} \right) \; A^{n} [j_{ex}^{n} \; x^{nm} \; y^{nm} \; G_{2}^{nm} + \\ \hat{z} \; \left(\sum_{n=1}^{N_{z}} + \sum_{n=1}^{N_{z}} \right) \; A^{n} [j_{ex}^{n} \; x^{nm} \; y^{nm} \; G_{2}^{nm} + \\ \hat{z} \; \left(\sum_{n=1}^{N_{z}} + \sum_{n=1}^{N_{z}} \right) \; A^{n} [j_{ex}^{n} \; x^{nm} \; y^{nm} \; G_{2}^{nm} + \\ \hat{z} \; \left(\sum_{n=1}^{N_{z}} + \sum_{n=1}^{N_{z}} \right) \; A^{n} [j_{ex}^{n} \; x^{nm} \; y^{nm} \; G_{2}^{nm} + \\ \hat{z} \; \left(\sum_{n=1}^{N_{z}} + \sum_{n=1}^{N_{z}} \right) \; A^{n} [j_{ex}^{n} \; x^{nm} \; y^{nm} \; G_{2}^{nm} + \\ \hat{z} \; \left(\sum_{n=1}^{N_{z}} + \sum_{n=1}^{N_{z}} \right) \; A^{n} [j_{ex}^{n} \; x^{nm} \; y^{nm} \; G_{2}^{nm} + \\ \hat{z} \; \left(\sum_{n=1}^{N_{z}} + \sum_{n=1}^{N_{z}} \right) \; A^{n} [j_{ex}^{n} \; x^{nm} \; y^{nm} \; G_{2}^{nm} + \\ \hat{z} \; \left(\sum_{n=1}^{N_{z}} + \sum_{n=1}^{N_{z}} \right) \; A^{n} [j_{ex}^{n} \; x^{nm} \; y^{nm} \; G_{2}^{nm} + \\ \hat{$$

This concludes the investigation of the last integral on the right-hand side of eq. (3.29').

If we repeat the whole process for the second surface integration of eq. (3.29'), we will find that it can be decomposed into the following form:

$$\hat{x} \times \mathcal{I}_{F} \xrightarrow{\hat{J}_{m}} \times \nabla' (\kappa^{2} \varphi_{d} - \varphi_{f}) \text{ d}F' = \hat{y} \underbrace{\left(\sum\limits_{n=1}^{N_{x}} + \sum\limits_{n=1}^{N_{x}} + \sum\limits_{n=1}^{N_{x}} \right) A^{n} x^{nm} G_{3}^{nm} j_{my}^{n} - \underbrace{\left(\sum\limits_{n=1}^{N_{y}} + \sum\limits_{n=1}^{N_{y}} \right) A^{n} y^{nm} G_{3}^{nm} j_{my}^{n} - \underbrace{\left(\sum\limits_{n=1}^{N_{x}} + \sum\limits_{n=1}^{N_{x}} \right) A^{n} [j_{mx}^{n} y^{nm} G_{3}^{nm} - \underbrace{\left(\sum\limits_{n=1}^{N_{x}} + \sum\limits_{n=1}^{N_{x}} \right) A^{n} [j_{mx}^{n} y^{nm} G_{3}^{nm} - \underbrace{\left(\sum\limits_{n=1}^{N_{x}} + \sum\limits_{n=1}^{N_{x}} \right) A^{n} [j_{mx}^{n} y^{nm} G_{3}^{nm} - \underbrace{\left(\sum\limits_{n=1}^{N_{x}} + \sum\limits_{n=1}^{N_{x}} \right) A^{n} [j_{mx}^{n} y^{nm} G_{3}^{nm} - \underbrace{\left(\sum\limits_{n=1}^{N_{x}} + \sum\limits_{n=1}^{N_{x}} \right) A^{n} [j_{mx}^{n} y^{nm} G_{3}^{nm} - \underbrace{\left(\sum\limits_{n=1}^{N_{x}} + \sum\limits_{n=1}^{N_{x}} \right) A^{n} [j_{mx}^{n} y^{nm} G_{3}^{nm} - \underbrace{\left(\sum\limits_{n=1}^{N_{x}} + \sum\limits_{n=1}^{N_{x}} \right) A^{n} [j_{mx}^{n} y^{nm} G_{3}^{nm} - \underbrace{\left(\sum\limits_{n=1}^{N_{x}} + \sum\limits_{n=1}^{N_{x}} \right) A^{n} [j_{mx}^{n} y^{nm} G_{3}^{nm} - \underbrace{\left(\sum\limits_{n=1}^{N_{x}} + \sum\limits_{n=1}^{N_{x}} \right) A^{n} [j_{mx}^{n} y^{nm} G_{3}^{nm} - \underbrace{\left(\sum\limits_{n=1}^{N_{x}} + \sum\limits_{n=1}^{N_{x}} \right) A^{n} [j_{mx}^{n} y^{nm} G_{3}^{nm} - \underbrace{\left(\sum\limits_{n=1}^{N_{x}} + \sum\limits_{n=1}^{N_{x}} \right) A^{n} [j_{mx}^{n} y^{nm} G_{3}^{nm} - \underbrace{\left(\sum\limits_{n=1}^{N_{x}} + \sum\limits_{n=1}^{N_{x}} \right) A^{n} [j_{mx}^{n} y^{nm} G_{3}^{nm} - \underbrace{\left(\sum\limits_{n=1}^{N_{x}} + \sum\limits_{n=1}^{N_{x}} \right) A^{n} [j_{mx}^{n} y^{nm} G_{3}^{nm} - \underbrace{\left(\sum\limits_{n=1}^{N_{x}} + \sum\limits_{n=1}^{N_{x}} \right) A^{n} [j_{mx}^{n} y^{nm} G_{3}^{nm} - \underbrace{\left(\sum\limits_{n=1}^{N_{x}} + \sum\limits_{n=1}^{N_{x}} \right) A^{n} [j_{mx}^{n} y^{nm} G_{3}^{nm} - \underbrace{\left(\sum\limits_{n=1}^{N_{x}} + \sum\limits_{n=1}^{N_{x}} \right) A^{n} [j_{mx}^{n} y^{nm} G_{3}^{nm} - \underbrace{\left(\sum\limits_{n=1}^{N_{x}} + \sum\limits_{n=1}^{N_{x}} \right) A^{n} [j_{mx}^{n} y^{nm} G_{3}^{nm} - \underbrace{\left(\sum\limits_{n=1}^{N_{x}} + \sum\limits_{n=1}^{N_{x}} \right) A^{n} [j_{mx}^{n} y^{nm} G_{3}^{nm} - \underbrace{\left(\sum\limits_{n=1}^{N_{x}} + \sum\limits_{n=1}^{N_{x}} \right) A^{n} [j_{mx}^{n} y^{nm} G_{3}^{nm} - \underbrace{\left(\sum\limits_{n=1}^{N_{x}} + \sum\limits_{n=1}^{N_{x}} \right) A^{n} [j_{mx}^{n} y^{nm} G_{3}^{nm} - \underbrace{\left(\sum\limits_{n=1}^{N_{x}} + \sum\limits_{n=1}^{N_{x}} \right) A^{n} [j_{mx}^{n} y^{nm} G_{3}^{nm} - \underbrace{\left(\sum\limits_{n=1}^{N_{x}} + \sum\limits_{n=1}^{N_{x}} \right) A^{n} [j_{mx}^{n} y^{nm} G$$



$$\begin{pmatrix} N_y \\ (Z + Z) \\ n=1 \end{pmatrix} = \begin{pmatrix} N_{-y} \\ N_{-1} \end{pmatrix} A^n \left[j_{mz}^n \times^{nm} G_3^{nm} - j_{mx}^n Z^{nm} G_3^{nm} \right] - \begin{pmatrix} N_{-y} \\ N_{-y} \end{pmatrix} A^n \left[j_{mz}^n \times^{nm} G_3^{nm} - j_{mx}^n Z^{nm} G_3^{nm} \right] - \begin{pmatrix} N_{-y} \\ N_{-y} \end{pmatrix} A^n \left[j_{mz}^n \times^{nm} G_3^{nm} - j_{mx}^n Z^{nm} G_3^{nm} \right] - \begin{pmatrix} N_{-y} \\ N_{-y} \end{pmatrix} A^n \left[j_{mz}^n \times^{nm} G_3^{nm} - j_{mx}^n Z^{nm} G_3^{nm} \right] - \begin{pmatrix} N_{-y} \\ N_{-y} \end{pmatrix} A^n \left[j_{mz}^n \times^{nm} G_3^{nm} - j_{mx}^n Z^{nm} G_3^{nm} \right] - \begin{pmatrix} N_{-y} \\ N_{-y} \end{pmatrix} A^n \left[j_{mz}^n \times^{nm} G_3^{nm} - j_{mx}^n Z^{nm} G_3^{nm} \right] - \begin{pmatrix} N_{-y} \\ N_{-y} \end{pmatrix} A^n \left[j_{mz}^n \times^{nm} G_3^{nm} - j_{mx}^n Z^{nm} G_3^{nm} \right] - \begin{pmatrix} N_{-y} \\ N_{-y} \end{pmatrix} A^n \left[j_{mz}^n \times^{nm} G_3^{nm} - j_{mx}^n Z^{nm} G_3^{nm} \right] - \begin{pmatrix} N_{-y} \\ N_{-y} \end{pmatrix} A^n \left[j_{mz}^n \times^{nm} G_3^{nm} - j_{mx}^n Z^{nm} G_3^{nm} \right] - \begin{pmatrix} N_{-y} \\ N_{-y} \end{pmatrix} A^n \left[j_{mz}^n \times^{nm} G_3^{nm} - j_{mx}^n Z^{nm} G_3^{nm} \right] - \begin{pmatrix} N_{-y} \\ N_{-y} \end{pmatrix} A^n \left[j_{mz}^n \times^{nm} G_3^{nm} - j_{mx}^n Z^{nm} G_3^{nm} \right] - \begin{pmatrix} N_{-y} \\ N_{-y} \end{pmatrix} A^n \left[j_{mz}^n \times^{nm} G_3^{nm} - j_{mx}^n Z^{nm} G_3^{nm} \right] - \begin{pmatrix} N_{-y} \\ N_{-y} \end{pmatrix} A^n \left[j_{mz}^n \times^{nm} G_3^{nm} - j_{mx}^n Z^{nm} G_3^{nm} \right] - \begin{pmatrix} N_{-y} \\ N_{-y} \end{pmatrix} A^n \left[j_{mx}^n \times^{nm} G_3^{nm} - j_{mx}^n Z^{nm} G_3^{nm} \right] - \begin{pmatrix} N_{-y} \\ N_{-y} \end{pmatrix} A^n \left[j_{mx}^n \times^{nm} G_3^{nm} - j_{mx}^n Z^{nm} G_3^{nm} \right] - \begin{pmatrix} N_{-y} \\ N_{-y} \end{pmatrix} A^n \left[j_{mx}^n \times^{nm} G_3^{nm} - j_{mx}^n Z^{nm} G_3^{nm} \right] + \begin{pmatrix} N_{-y} \\ N_{-y} \end{pmatrix} A^n \left[j_{mx}^n \times^{nm} G_3^{nm} - j_{mx}^n Z^{nm} G_3^{nm} \right] + \begin{pmatrix} N_{-y} \\ N_{-y} \end{pmatrix} A^n \left[j_{mx}^n \times^{nm} G_3^{nm} - j_{mx}^n Z^{nm} G_3^{nm} \right] + \begin{pmatrix} N_{-y} \\ N_{-y} \end{pmatrix} A^n \left[j_{mx}^n \times^{nm} G_3^{nm} - j_{mx}^n Z^{nm} G_3^{nm} \right] + \begin{pmatrix} N_{-y} \\ N_{-y} \end{pmatrix} A^n \left[j_{mx}^n \times^{nm} G_3^{nm} - j_{mx}^n Z^{nm} G_3^{nm} \right] + \begin{pmatrix} N_{-y} \\ N_{-y} \end{pmatrix} A^n \left[j_{mx}^n \times^{nm} G_3^{nm} - j_{mx}^n Z^{nm} G_3^{nm} \right] + \begin{pmatrix} N_{-y} \\ N_{-y} \end{pmatrix} A^n \left[j_{mx}^n \times^{nm} G_3^{nm} - j_{mx}^n Z^{nm} G_3^{nm} \right] + \begin{pmatrix} N_{-y} \\ N_{-y} \end{pmatrix} A^n \left[j_{mx} \right] + \begin{pmatrix} N_{-y} \\ N_{-y} \end{pmatrix} A^n \left[j_{mx} \right] + \begin{pmatrix} N_{-y} \\ N_{-y} \end{pmatrix} A^n \left[j_{mx} \right] + \begin{pmatrix} N_{-y} \\ N_{-y} \end{pmatrix} A^n \left[j_{mx} \right] + \begin{pmatrix} N_{-y} \\ N_{$$

and G_3^{nm} is defined in eq. (3.43). It is noted that the singular terms have no contribution to eq. (3.50).

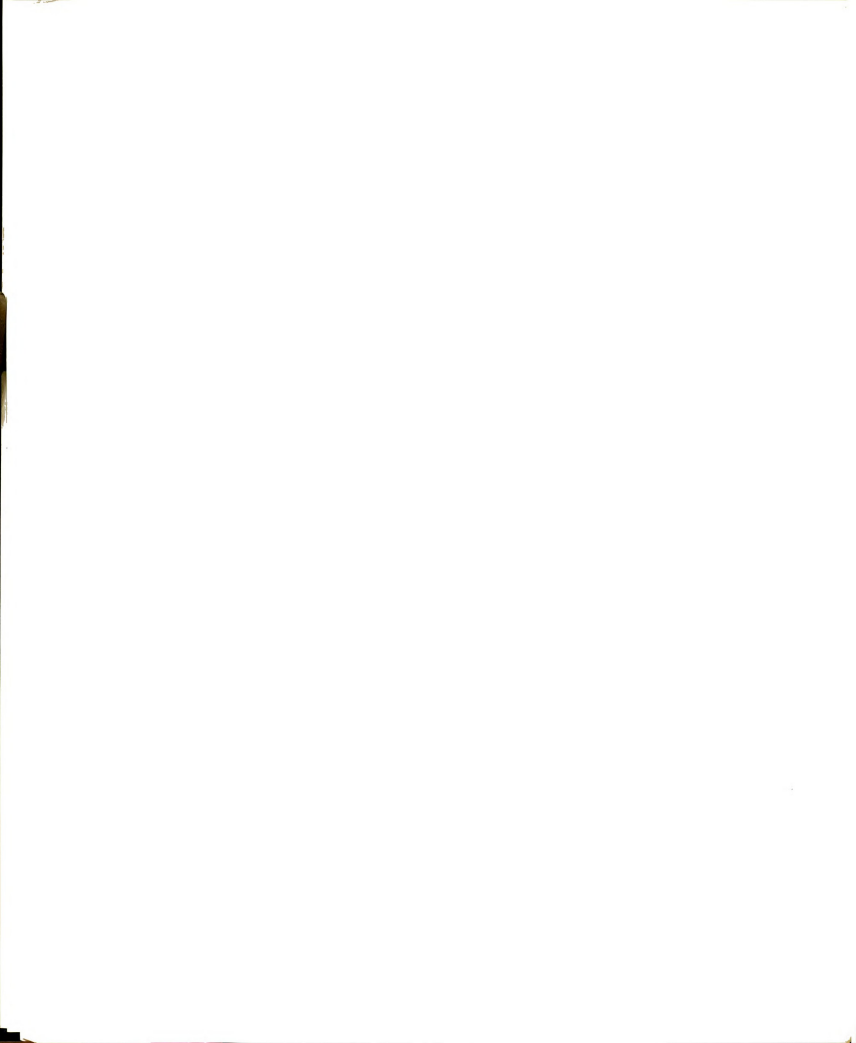
Similarly, the first integral term on the right-hand side of eq. (3.29') can be transformed to become

$$\hat{x} \times \mathcal{I}_{F} \vec{j}_{e} (\kappa^{2} \phi_{d} - \phi_{f}) dF' = -\hat{y} \cdot ((\sum_{\substack{n=1 \\ n \neq n}}^{N_{x}} + \sum_{n=1}^{N_{-x}}) A^{n} G_{4}^{nm} j_{ez}^{n} +$$

$$(\begin{smallmatrix} N_y \\ \Sigma \\ n=1 \end{smallmatrix} + \begin{smallmatrix} N-y \\ \Sigma \\ n=1 \end{smallmatrix}) \overset{A^n}{\overset{}{_{}}} \overset{G^{nn}}{\overset{}{_{}}} \overset{1}{\overset{}{_{}}} \overset{n}{\overset{}{_{}}} \overset{n}{\overset{}{_{}}} + \overset{m}{\overset{}{_{}}} \overset{n}{\overset{}{_{}}} \overset{n}{\overset{}{_{}}} + \overset{n}{\overset{}{_{}}} \overset{n}{\overset{}{_{}}} \overset{N_x}{\overset{}{_{}}} \times \overset{N_{-x}}{\overset{}{_{}}} \overset{N_x}{\overset{}{_{}}} \overset{N_x}{\overset{}{_{}}} \overset{N_x}{\overset{}{_{}}} \overset{N_x}{\overset{}{_{}}} \overset{N_{-x}}{\overset{}{_{}}} \overset{n}{\overset{}} \overset{n}{\overset{n}} \overset{n}{\overset{n}}$$

and $\textbf{G}_4^{\text{nm}},~\textbf{H}_2^{\text{m}}$ are defined in eq. (3.43).

If we enforce satisfaction of eq. (3.29') at each reference point on the subsurface F_X , with the help of eqs. (3.49), (3.50), and (3.51), we can obtain totally N_X vector equations, i.e., one equation for each matching point. Furthermore, it is possible to decompose these N_X vector equations into $2N_Y$ scalar, linear algebraic equations since



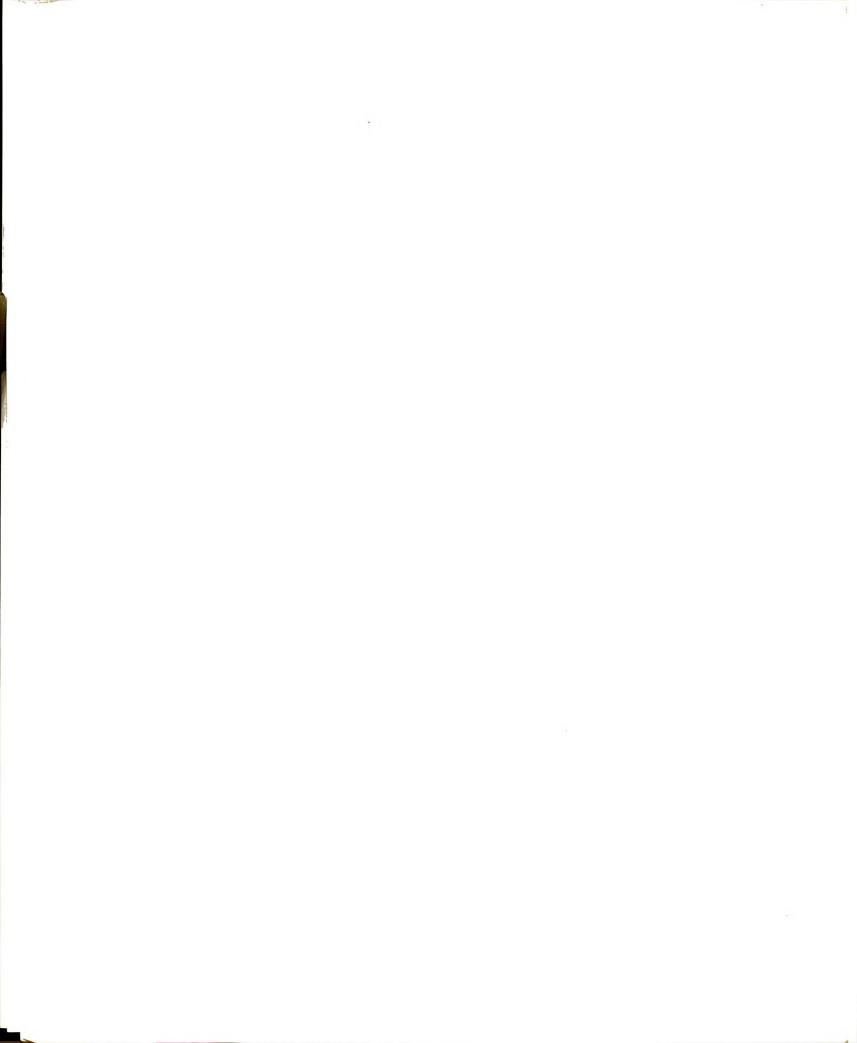
each surface current possesses two tangential components. Based on eqs. (3.29'), (3.49), (3.50), and (3.51), it can be shown that the following are those $2N_{_{\mathbf{Y}}}$ linear equations:

$$\left\{ \begin{array}{l} (\sum\limits_{n=1}^{N_{X}} + \sum\limits_{n=1}^{N_{-X}}) \cdot [-j_{\text{ey}}^{n} \ \psi_{1x}(n,m) \ - \ j_{\text{ez}}^{n} \ \psi_{2z}(n,m) \ + \ j_{\text{my}}^{n} \ \psi_{3x}(n,m)] \ - \\ \\ j_{\text{ez}}^{m} \ \text{H}(m) \ + \ j_{\text{my}}^{m} \ \text{C} \ - \ \left\{ \begin{array}{l} (\sum\limits_{n=1}^{N_{Y}} + \sum\limits_{n=1}^{N_{-Y}}) \cdot [j_{\text{ex}}^{n} \ \psi_{1y}(n,m) \ + \ j_{\text{ex}}^{n} \ \psi_{2z}(n,m) \ + \\ \\ j_{\text{mx}}^{n} \ \psi_{3y}(n,m)] \ \} \ - \ \left\{ \begin{array}{l} (\sum\limits_{n=1}^{N_{Z}} + \sum\limits_{n=1}^{N_{-Z}}) \cdot [j_{\text{ex}}^{n} \ \psi_{1y}(n,m) \ + \ j_{\text{ey}}^{n} \ \psi_{1x}(n,m) \ + \\ \\ j_{\text{mx}}^{n} \ \psi_{3y}(n,m) \ - \ j_{\text{my}}^{n} \ \psi_{3x}(n,m)] \ \} \ = \ 4\pi \ j_{\text{my}}^{mi} \end{array} \right.$$

also,

also,
$$\{ (\sum_{n=1}^{N_{X}} + \sum_{n=1}^{N_{-X}} \cdot [j_{ey}^{n} \psi_{2y}(n,m) + j_{ez}^{n} \psi_{1x}(n,m) + j_{mz}^{n} \psi_{3x}(n,m)] + j_{mz}^{m} \psi_{3x}(n,m) + j_{mz}^{m} \psi_{3x}(n,m)] + j_{mz}^{m} \psi_{3x}(n,m) + j_{mz}^{m} \psi_{3x}(n,m) + j_{mz}^{m} \psi_{3x}(n,m) + j_{mz}^{m} \psi_{3x}(n,m) + j_{mz}^{n} \psi_{3x}(n,m)] \} + \{ (\sum_{n=1}^{N_{Z}} + \sum_{n=1}^{N_{Z}} \cdot [j_{ex}^{n} \psi_{1z}(n,m) + j_{nz}^{n} \psi_{3x}(n,m)] \} + \{ (\sum_{n=1}^{N_{Z}} + \sum_{n=1}^{N_{Z}} \cdot [j_{ex}^{n} \psi_{1x}(n,m) + j_{nz}^{n} \psi_{3x}(n,m)] \} + \{ (\sum_{n=1}^{N_{Z}} + \sum_{n=1}^{N_{Z}} \cdot [j_{ex}^{n} \psi_{1x}(n,m) + j_{nz}^{n} \psi_{3x}(n,m)] \} + \{ (\sum_{n=1}^{N_{Z}} + \sum_{n=1}^{N_{Z}} \cdot [j_{ex}^{n} \psi_{1x}(n,m) + j_{nz}^{n} \psi_{3x}(n,m)] \} \}$$

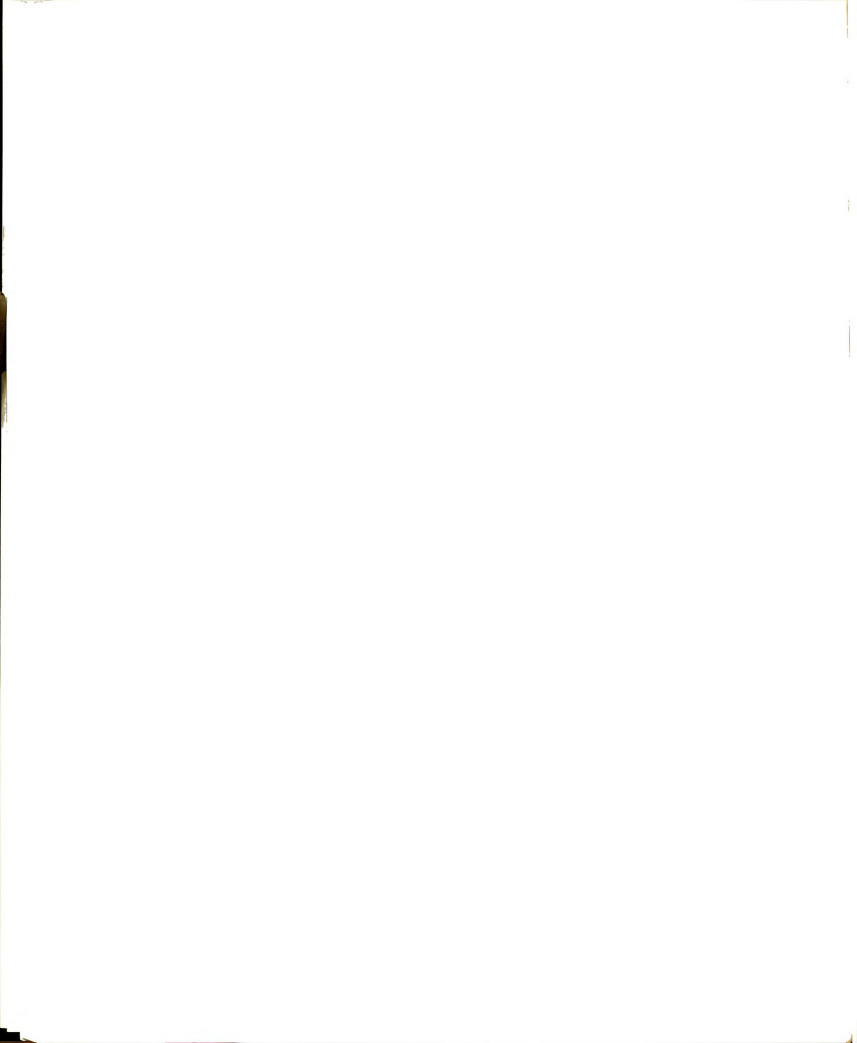
where 1 \leq $\,$ m \leq $\,$ N $_{_{{\bf X}}}$, and the various $\,$ $\,$ functions are defined as



$$\begin{array}{l} \Psi_{1x}(n,m) = j \ A^n \ y^{nm} \ z^{nm} \ G_2^{nm} \\ \\ \Psi_{1y}(n,m) = j \ A^n \ x^{nm} \ z^{nm} \ G_2^{nm} \\ \\ \Psi_{1z}(n,m) = j \ A^n \ x^{nm} \ y^{nm} \ G_2^{nm} \\ \\ \Psi_{2x}(n,m) = j \ A^n (G_1^{nm} + x^{nm} \cdot x^{nm} \ G_2^{nm} + G_4^{nm}) \\ \\ \Psi_{2y}(n,m) = j \ A^n (G_1^{nm} + y^{nm} \cdot y^{nm} \ G_2^{nm} + G_4^{nm}) \\ \\ \Psi_{2z}(n,m) = j \ A^n (G_1^{nm} + z^{nm} \cdot z^{nm} \ G_2^{nm} + G_4^{nm}) \\ \\ \Psi_{3x}(n,m) = A^n \ x^{nm} \ G_3^{nm} \\ \\ \Psi_{3y}(n,m) = A^n \ y^{nm} \ G_3^{nm} \\ \\ \Psi_{3z}(n,m) = A^n \ z^{nm} \ G_3^{nm} \\ \\ \\ \Psi_{3z}(n,m) = A^n \ z^{nm} \ G_3^{nm} \\ \\ \\ \Psi_{3z}(n,m) = A^n \ z^{nm} \ G_3^{nm} \\ \\ \\ \end{array}$$

This completes the whole analysis for the case of $\hat{n} = \hat{x}$.

II) If the field point is located in one of the +y-surface elements, i.e., when $\hat{n}=\hat{\gamma}$, other $2N_{\hat{\gamma}}$ linear equations can be obtained by following a similar procedure as that described in case I). We will present these equations without repeating the details of the derivations:



$$\{ (\sum_{n=1}^{N_{x}} + \sum_{n=1}^{N_{-x}}) \cdot [j_{ey}^{n} \psi_{1x}(n,m) + j_{ez}^{n} \psi_{2z}(n,m) - j_{my}^{n} \psi_{3x}(n,m)] \} +$$

$$\{ (\sum_{n=1}^{N_{y}} + \sum_{n=1}^{N_{-y}}) \cdot [j_{ex}^{n} \psi_{1y}(n,m) + j_{ez}^{n} \psi_{2z}(n,m) + j_{mx}^{n} \psi_{3y}(n,m)] \} +$$

$$j_{ez}^{m} H(m) + j_{mx}^{m} C \} + \{ (\sum_{n=1}^{N_{z}} + \sum_{n=1}^{N_{-z}}) \cdot [j_{ex}^{n} \psi_{1y}(n,m) + j_{ey}^{n} \psi_{1x}(n,m) +$$

$$j_{mx}^{n} \psi_{3y}(n,m) - j_{my}^{n} \psi_{3x}(n,m)] \} = 4 \pi j_{mx}^{mi}$$

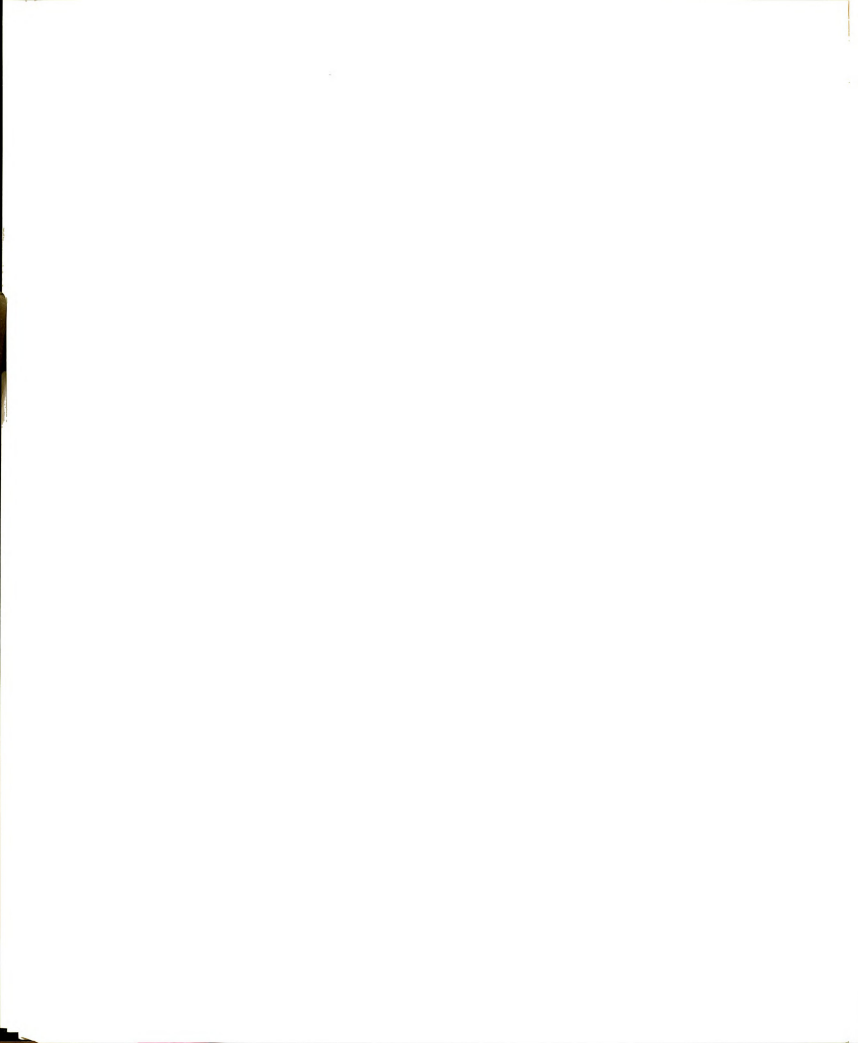
$$(3.54)$$

also.

(3.55)

 $j_{ey}^n~\Psi_{1z}(n,m)~+~j_{my}^n~\Psi_{3z}(n,m)\,\}~\}~=~4\pi~j_{mz}^m~i$ where $1~\leq~m~\leq~N_{_{\rm U}}.$

III) Next, let's consider the case where the field point is located in one of the +z-surface elements. As in the previous two cases, by use of the point-matching technique, we may obtain the following $2N_{_{\rm Z}}$ scalar, linear equations:



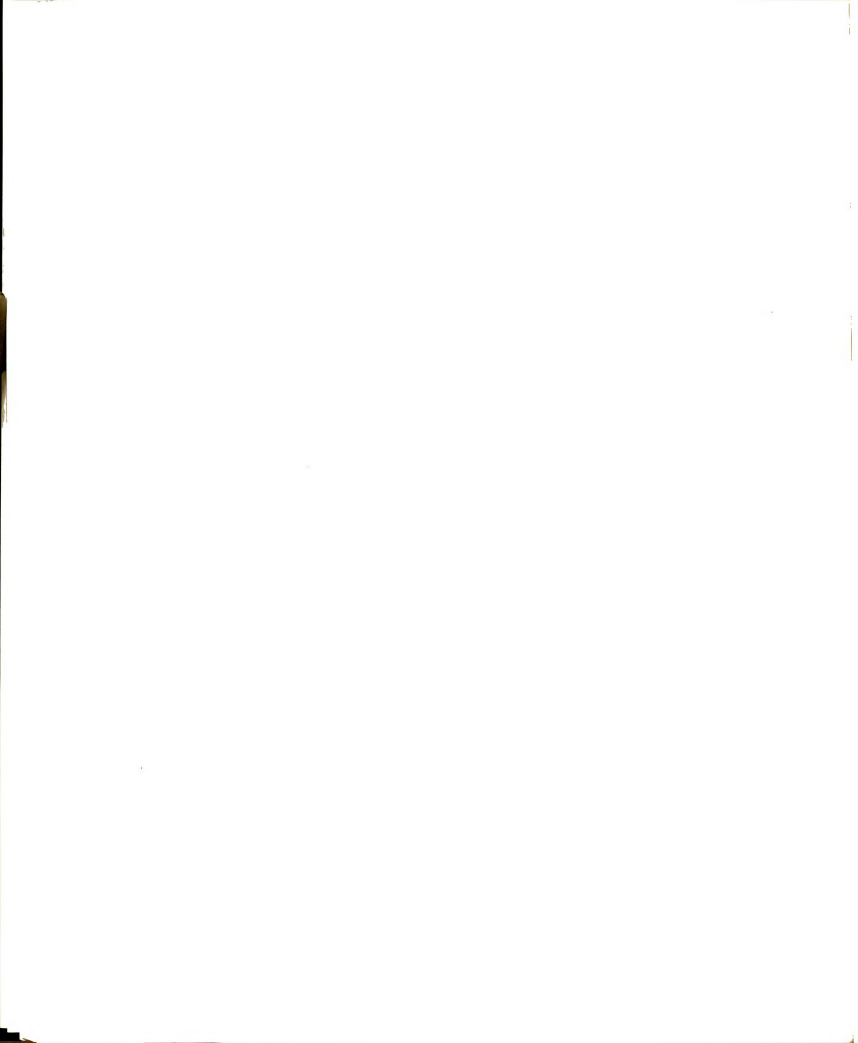
$$\begin{cases} \binom{N_{x}}{\Sigma} + \binom{N_{x}}{n=1} \cdot [-j_{ey}^{n} \ \Psi_{2y}(n,m) - j_{ez}^{n} \ \Psi_{1x}(n,m) - j_{mz}^{n} \ \Psi_{3x}(n,m)] \end{cases} - \\ \{ \binom{N_{y}}{\Sigma} + \binom{N_{x}}{n=1} \cdot [j_{ex}^{n} \ \Psi_{1z}(n,m) + j_{ez}^{n} \ \Psi_{1x}(n,m) - j_{mx}^{n} \ \Psi_{3z}(n,m) + j_{mx}^{n} \ \Psi_{3z}(n,m)] \} - \\ \{ \binom{N_{y}}{\Sigma} + \binom{N_{x}}{n=1} \cdot [j_{ex}^{n} \ \Psi_{1x}(n,m) - j_{mx}^{n} \ \Psi_{3z}(n,m)] \} - \\ \{ \binom{N_{x}}{\Sigma} + \binom{N_{x}}{n=1} \cdot [j_{ex}^{n} \ \Psi_{1z}(n,m) + j_{ey}^{n} \ \Psi_{2y}(n,m) - j_{mx}^{n} \ \Psi_{3z}(n,m)] \} - \\ \{ \binom{N_{x}}{\Sigma} + \binom{N_{x}}{\Sigma$$

$$\{ (\sum\limits_{n=1}^{N_{x}} + \sum\limits_{n=1}^{N_{-x}}) \cdot [j_{ey}^{n} \ \psi_{1z}(n,m) \ + \ j_{ez}^{n} \ \psi_{1y}(n,m) \ + \ j_{my}^{n} \ \psi_{3z}(n,m) \ - \\ \\ j_{mz}^{n} \ \psi_{3y}(n,m) \] \ \} \ + \ \{ (\sum\limits_{n=1}^{N_{z}} + \sum\limits_{n=1}^{N_{-y}}) \cdot [j_{ex}^{n} \ \psi_{2x}(n,m) \ + \ j_{ez}^{n} \ \psi_{1y}(n,m) \ - \\ \\ j_{mz}^{n} \ \psi_{3y}(n,m) \] \ \} \ + \ \{ (\sum\limits_{n=1}^{N_{z}} + \sum\limits_{n=1}^{N_{-z}}) \cdot [j_{ex}^{n} \ \psi_{2x}(n,m) \ + \ j_{ey}^{n} \ \psi_{1z}(n,m) \ + \$$

$$j_{my}^{n} \ \Psi_{3z}(n,m)] \ + \ j_{ex}^{m} \ H(m) \ + \ j_{my}^{m} \ C) = 4\pi \ j_{my}^{m\, \perp} \eqno(3.57)$$

where $1 \le m \le N_z$.

Similarly, we can obtain $2N_{-x}$, $2N_{-y}$, and $2N_{-z}$ linear equations by enforcing eq. (3.29') at various reference points on the subsurfaces F_{-x} , F_{-y} , and F_{-z} , respectively. We list all these equations as follows:



IV)
$$\hat{n} = -\hat{x}$$
:

$$\{ (\sum_{n=1}^{N_{X}} + \sum_{n=1}^{N_{-X}}) \cdot [-j_{ey}^{n} \psi_{lx}(n,m) - j_{ez}^{n} \psi_{2z}(n,m) + j_{my}^{n} \psi_{3x}(n,m)] - j_{ez}^{m} H(m) - j_{my}^{m} C \} - \{ (\sum_{n=1}^{N_{Y}} + \sum_{n=1}^{N_{-Y}}) \cdot [j_{ex}^{n} \psi_{ly}(n,m) + j_{ez}^{n} \psi_{2z}(n,m) + j_{ey}^{n} \psi_{3x}(n,m)] \} - \{ (\sum_{n=1}^{N_{Z}} + \sum_{n=1}^{N_{-Z}}) \cdot [j_{ex}^{n} \psi_{1y}(n,m) + j_{ey}^{n} \psi_{1x}(n,m) + j_{mx}^{n} \psi_{3y}(n,m)] \} - \{ (\sum_{n=1}^{N_{Z}} + \sum_{n=1}^{N_{-Z}}) \cdot [j_{ex}^{n} \psi_{1y}(n,m) + j_{ey}^{n} \psi_{1x}(n,m) + j_{mx}^{n} \psi_{3y}(n,m)] \} - \{ (\sum_{n=1}^{N_{Z}} + \sum_{n=1}^{N_{Z}}) \cdot [j_{ex}^{n} \psi_{1y}(n,m) + j_{ey}^{n} \psi_{1x}(n,m) + j_{mx}^{n} \psi_{3y}(n,m)] \} - \{ (\sum_{n=1}^{N_{Z}} + \sum_{n=1}^{N_{Z}}) \cdot [j_{ex}^{n} \psi_{1y}(n,m) + j_{ey}^{n} \psi_{1x}(n,m)] \} - \{ (\sum_{n=1}^{N_{Z}} + \sum_{n=1}^{N_{Z}}) \cdot [j_{ex}^{n} \psi_{1y}(n,m) + j_{ey}^{n} \psi_{1x}(n,m)] \} - \{ (\sum_{n=1}^{N_{Z}} + \sum_{n=1}^{N_{Z}}) \cdot [j_{ex}^{n} \psi_{1y}(n,m)] \} - \{ (\sum_{n=1}^{N_{Z}} + \sum_{n=1}^{N_{Z}}) \cdot [j_{ex}^{n} \psi_{1y}(n,m)] \} - \{ (\sum_{n=1}^{N_{Z}} + \sum_{n=1}^{N_{Z}}) \cdot [j_{ex}^{n} \psi_{1y}(n,m)] \} - \{ (\sum_{n=1}^{N_{Z}} + \sum_{n=1}^{N_{Z}}) \cdot [j_{ex}^{n} \psi_{1y}(n,m)] \} - \{ (\sum_{n=1}^{N_{Z}} + \sum_{n=1}^{N_{Z}}) \cdot [j_{ex}^{n} \psi_{1y}(n,m)] \} - \{ (\sum_{n=1}^{N_{Z}} + \sum_{n=1}^{N_{Z}}) \cdot [j_{ex}^{n} \psi_{1y}(n,m)] \} - \{ (\sum_{n=1}^{N_{Z}} + \sum_{n=1}^{N_{Z}}) \cdot [j_{ex}^{n} \psi_{1y}(n,m)] \} - \{ (\sum_{n=1}^{N_{Z}} + \sum_{n=1}^{N_{Z}}) \cdot [j_{ex}^{n} \psi_{1y}(n,m)] \} - \{ (\sum_{n=1}^{N_{Z}} + \sum_{n=1}^{N_{Z}}) \cdot [j_{ex}^{n} \psi_{1y}(n,m)] \} - \{ (\sum_{n=1}^{N_{Z}} + \sum_{n=1}^{N_{Z}}) \cdot [j_{ex}^{n} \psi_{1y}(n,m)] \} - \{ (\sum_{n=1}^{N_{Z}} + \sum_{n=1}^{N_{Z}}) \cdot [j_{ex}^{n} \psi_{1y}(n,m)] \} - \{ (\sum_{n=1}^{N_{Z}} + \sum_{n=1}^{N_{Z}}) \cdot [j_{ex}^{n} \psi_{1y}(n,m)] \} - \{ (\sum_{n=1}^{N_{Z}} + \sum_{n=1}^{N_{Z}}) \cdot [j_{ex}^{n} \psi_{1y}(n,m)] \} - \{ (\sum_{n=1}^{N_{Z}} + \sum_{n=1}^{N_{Z}}) \cdot [j_{ex}^{n} \psi_{1y}(n,m)] \} - \{ (\sum_{n=1}^{N_{Z}} + \sum_{n=1}^{N_{Z}}) \cdot [j_{ex}^{n} \psi_{1y}(n,m)] \} - \{ (\sum_{n=1}^{N_{Z}} + \sum_{n=1}^{N_{Z}}) \cdot [j_{ex}^{n} \psi_{1y}(n,m)] \} - \{ (\sum_{n=1}^{N_{Z}} + \sum_{n=1}^{N_{Z}}) \cdot [j_{ex}^{n} \psi_{1y}(n,m)] \} - \{ (\sum_{n=1}^{N_{Z}} + \sum_{n$$

$$\begin{cases} \sum_{n=1}^{N_{x}} + \sum_{n=1}^{N_{x}} \cdot \left[j_{ey}^{n} \psi_{2y}(n,m) + j_{ez}^{n} \psi_{1x}(n,m) + j_{mz}^{n} \psi_{3x}(n,m) \right] + j_{ey}^{m} H(m) - j_{mz}^{m} C \right] + \begin{cases} \sum_{n=1}^{N_{y}} + \sum_{n=1}^{N_{y}} \cdot \left[j_{ex}^{n} \psi_{1z}(n,m) + j_{ez}^{n} \psi_{1x}(n,m) - j_{mx}^{n} \psi_{3z}(n,m) + j_{mz}^{n} \psi_{3x}(n,m) \right] \right] + \begin{cases} \sum_{n=1}^{N_{y}} + \sum_{n=1}^{N_{y}} \cdot \left[j_{ex}^{n} \psi_{1z}(n,m) + j_{nz}^{n} \psi_{3z}(n,m) + j_{nz}^{n} \psi_{3z}(n,m) \right] \right] - 4\pi j_{mz}^{m} \end{cases}$$

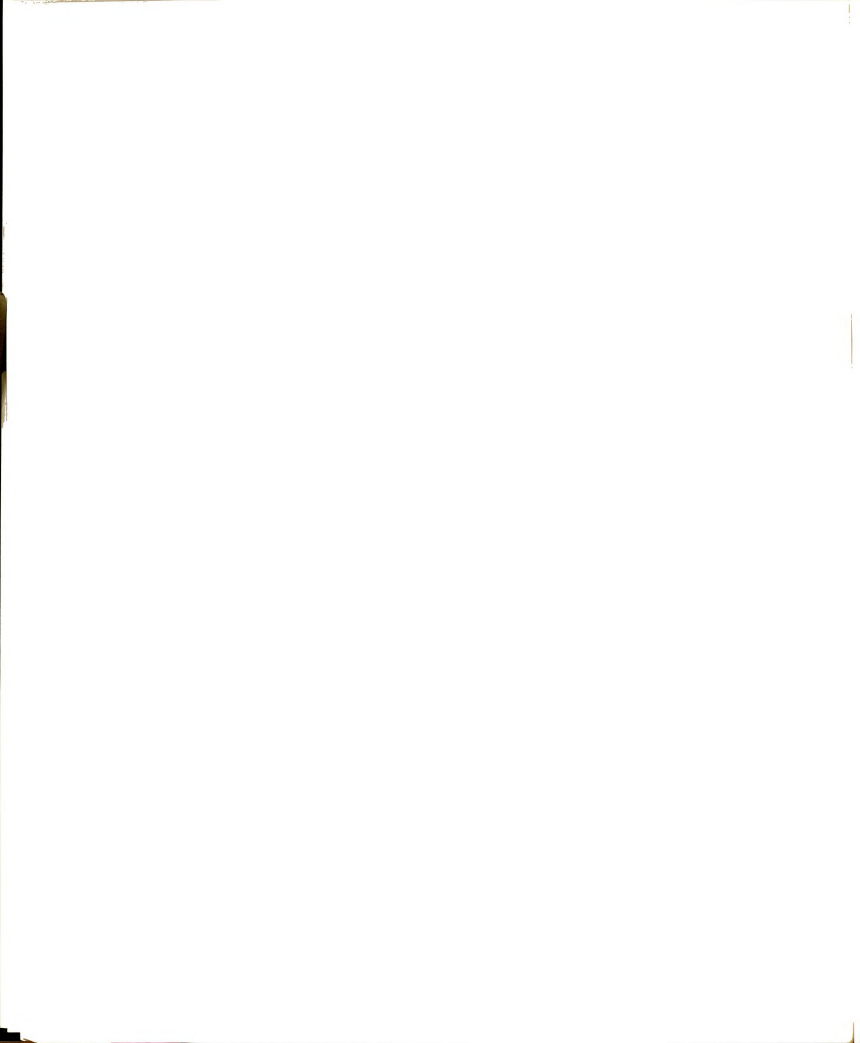
$$(3.59)$$

(3.59)

where $1 \le m \le N_{-x}$.

$$\vec{v}$$
) $\hat{n} = -\hat{y}$:

$$\{(\sum_{n=1}^{N_x}+\sum_{n=1}^{N_{-x}})\cdot[j_{\text{ey}}^n~\psi_{1x}(n,m)~+~j_{\text{ez}}^n~\psi_{2z}(n,m)~-~j_{my}^n~\psi_{3x}(n,m)]~\}~+$$



$$\left\{ \left(\sum_{n=1}^{N_{y}} + \sum_{\substack{n=1 \\ n \neq n}}^{N_{-y}} \cdot [j_{\text{ex}}^{n} \psi_{1y}(n,m) + j_{\text{ez}}^{n} \psi_{2z}(n,m) + j_{\text{mx}}^{n} \psi_{3y}(n,m)] + \right. \\ \left. j_{\text{ex}}^{m} H(m) - j_{\text{mx}}^{m} C \right\} + \left\{ \left(\sum_{n=1}^{\infty} + \sum_{n=1}^{N_{-z}} \right) \cdot [j_{\text{ex}}^{n} \psi_{1y}(n,m) + j_{\text{ey}}^{n} \psi_{1x}(n,m) + j_{\text{mx}}^{n} \psi_{1$$

$$\{ (\sum_{n=1}^{N_{x}} + \sum_{n=1}^{N_{-x}}) \cdot [-j_{\text{ey}}^{n} \psi_{1z}(n,m) - j_{\text{ez}}^{n} \psi_{1y}(n,m) - j_{\text{my}}^{n} \psi_{3z}(n,m) + \\ j_{\text{mz}}^{n} \psi_{3y}(n,m) \} \} - \{ (\sum_{n=1}^{N_{y}} + \sum_{n=1}^{N_{-y}}) \cdot [j_{\text{ex}}^{n} \psi_{2x}(n,m) + j_{\text{ez}}^{n} \psi_{1y}(n,m) - \\ j_{\text{mz}}^{n} \psi_{3y}(n,m) \} - j_{\text{ex}}^{m} H(m) - j_{\text{mz}}^{m} C \} - \{ (\sum_{n=1}^{N_{z}} + \sum_{n=1}^{N_{-z}}) \cdot [j_{\text{ex}}^{n} \psi_{2x}(n,m) + \\ j_{\text{ey}}^{n} \psi_{1z}(n,m) + j_{\text{my}}^{n} \psi_{3z}(n,m) \} \} = -4\pi j_{\text{mz}}^{m}$$
 (3.61)

where $1 \le m \le N_{-y}$.

VI)
$$\hat{n} = -\hat{z}$$
:

$$\{ \begin{pmatrix} \sum_{i=1}^{N} + \sum_{i=1}^{N} \cdot [-j_{ey}^{n} \ \psi_{2y}(n,m) \ - \ j_{ez}^{n} \ \psi_{1x}(n,m) \ - \ j_{mz}^{n} \ \psi_{3x}(n,m) \] \ \} \ - \\ \{ \begin{pmatrix} \sum_{i=1}^{N} + \sum_{i=1}^{N} \cdot [-j_{ey}^{n} \ \psi_{2y}(n,m) \ - \ j_{ez}^{n} \ \psi_{1x}(n,m) \ - \ j_{mx}^{n} \ \psi_{3z}(n,m) \] \ \} \ - \\ \{ \begin{pmatrix} \sum_{i=1}^{N} + \sum_{i=1}^{N} \cdot [-j_{ex}^{n} \ \psi_{1z}(n,m) \ + \ j_{ex}^{n} \ \psi_{1z}(n,m) \ - \ j_{ex}^{n} \ \psi_{2y}(n,m) \ + \ j_{ex}^{n} \ \psi_{2y}(n,m) \ - \ j_{ex}^{n} \ \psi_{2y}(n,m) \ + \ j_{$$



$$j_{mx}^{n} = y_{3z}(n,m) - j_{ey}^{m} H(m) - j_{mx}^{m} c = -4\pi j_{mx}^{mi}$$
 (3.62)

$$\{ (\sum_{n=1}^{N_{X}} + \sum_{n=1}^{N_{-X}}) \cdot [j_{ey}^{n} \psi_{1z}(n,m) + j_{ez}^{n} \psi_{1y}(n,m) + j_{my}^{n} \psi_{3z}(n,m) - j_{mz}^{n} \psi_{3y}(n,m)] \} + \{ (\sum_{n=1}^{N_{Y}} + \sum_{n=1}^{N_{-Y}}) \cdot [j_{ex}^{n} \psi_{2x}(n,m) + j_{ez}^{n} \psi_{1y}(n,m) - j_{mz}^{n} \psi_{3y}(n,m)] \} + \{ (\sum_{n=1}^{N_{Z}} + \sum_{n=1}^{N_{-Z}}) \cdot [j_{ex}^{n} \psi_{2x}(n,m) + j_{ey}^{n} \psi_{1z}(n,m) + j_{mx}^{n} \psi_{1z}(n,m) + j_{mx}^{n}$$

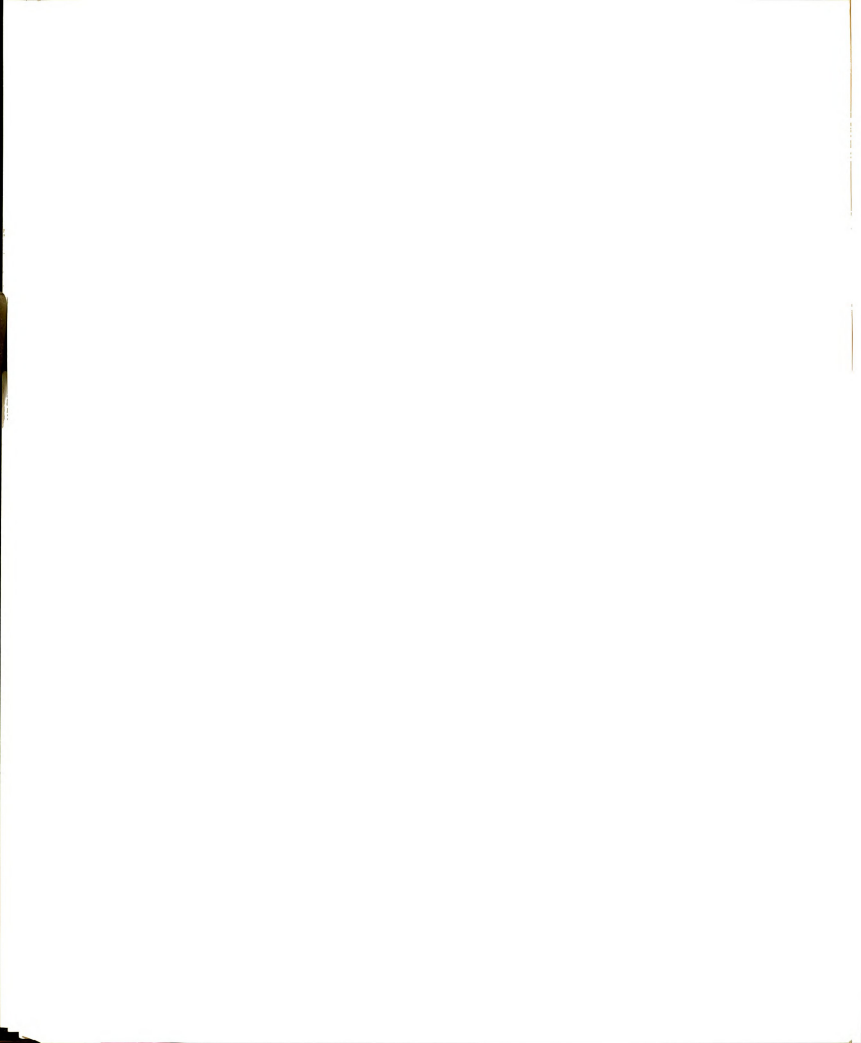
$$j_{my}^{n} \stackrel{\Psi}{}_{3z}(n,m)] + j_{ex}^{m} H(m) - j_{my}^{m} C = -4\pi j_{my}^{mi}$$
 (3.63)

where $1 \le m \le N_{-2}$.

Up to this point, we have obtained totally 2N cell $^{(N)}$ cell $^{=N}_{X} + ^{N}_{y} + ^{N}_{z} + ^{N}_{-X} + ^{N}_{-y} + ^{N}_{-z})$ scalar, linear algebraic equations based on eq. (3.29'). Repeating the same procedure for eq. (3.30'), we can obtain another 2N cell linear equations. We therefore have totally 4N cell equations, which are adequate to solve for the surface unknowns. For the purpose of saving space, we will not list the other 2N cell equations; however, since eqs. (3.29') and (3.30') have very similar forms, they can be carefully deduced from eqs. (3.52)-(3.63). The combination of these 4N cell linear equations can be transformed into a matrix form as shown in eq. (3.64), which then can be solved by a conventional

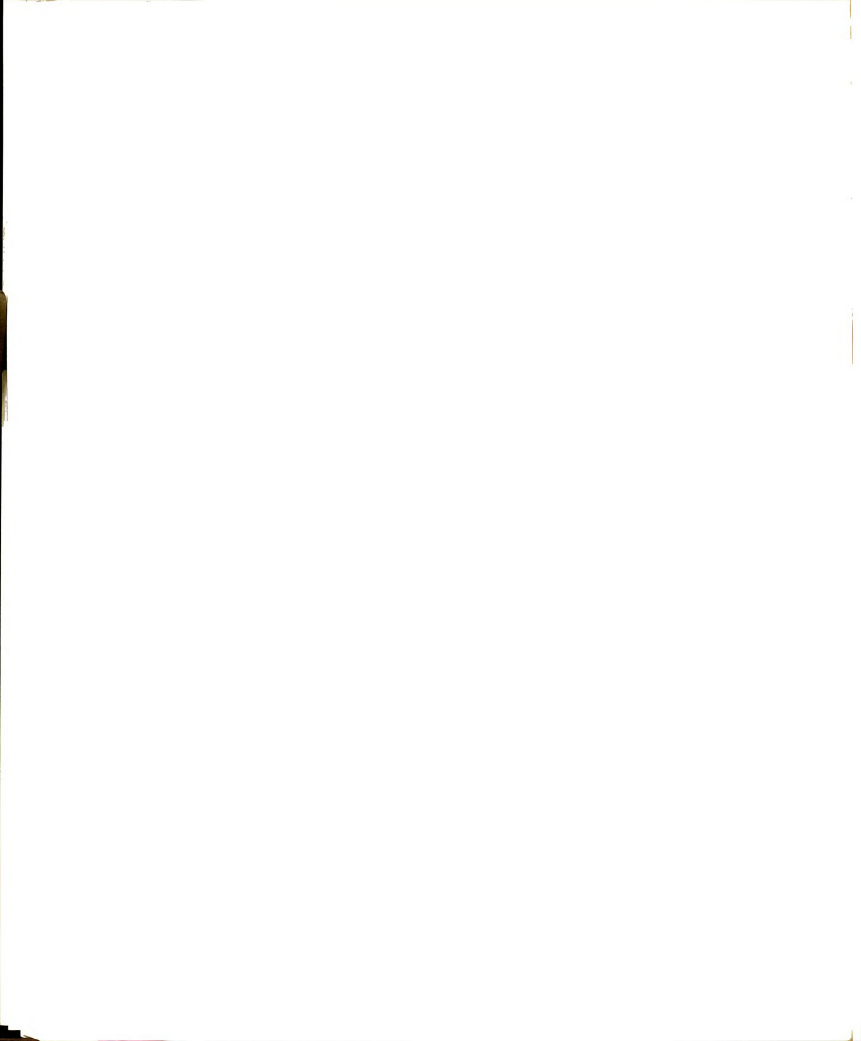


			(3.64)			
	Z×	<u>z</u> ^	A N	A X	å v	NA NA
(imi)	8 1 2 1 A 1 B	ENENE E	<u>Inivital</u>	int yer int int	ī a ī a ī k ī k	Jai Jai Jai
÷						
(")	و ال الله الله	" () " () " () " ()	-ggj	1912 TET	트워 트임 트ૉ 트ૉ	() () () ()
AP Z-Z	M Z-,x	Σ, γ,	, z, -z	Σ-'X-	[Z-,Y-Z]	2-, 2- M
A-Y-	[N, -y]	<u>κ</u> _γ-,γ	[M _{Z,-y}]		[M_y, _y]	<u>≅</u> _√-,∑-
¥*	Σ _χ ×	<u>~</u> , , ,	χ.	Σ. .×.	[X-',Y-	X, Z
N. N.	4, x, z,	(M, x, 4N, x, 4N	[M _{z,z}] 4N _z × 4N _z	[2,x,Z]	[M_y,z]	[2,2] W
₹ >	(N, X,	M Ly, y, X × AN y	$\begin{bmatrix} M \\ Z, y \end{bmatrix}$ $4 M \\ X \times 4 M \\ Y$	[M_x,y]	[M_Y,y_	(A,z,y)
₹×		[M, x, y, x,	[M, X,	[x,x,x]	[M,y,x]	[x,z,x]
	¥×			¥ X	AP V-	A S



matrix inversion technique. The matrix elements in eq. (3.64) may be obtained from the above linear equations.

It should be mentioned that the matrix [M] shown in eq. (3.64) possesses a four-fold symmetry, which is easy to see from the coefficients of the linear equations. These symmetry properties of the equations have been found very useful for the computer implementation of the numerical method. The initial version of the computer program is implemented directly based on eq. (3.64). Unfortunately, this program has only limited usefulness due to the prohibitive requirement of the matrix size needed to adequately sample current variations. However, if the incident plane wave is decomposed into four basic modes (cosine and sine variations of E and H fields), an eightfold symmetrical property can be found for each type of surface current. These symmetrical properties are shown in Figure 3.12. A final version of the computer program, with the above symmetry conditions imposed, is then developed. By use of this computer program, it is possible to reduce the matrix size by a factor of 8 when an eightfold symmetrical body is considered since it is sufficient to solve for the surface currents induced in only 1/8 of the biological body. The induced surface currents for the rest of the body can be readily obtained by intuition. Of course, since the original incident plane wave has been



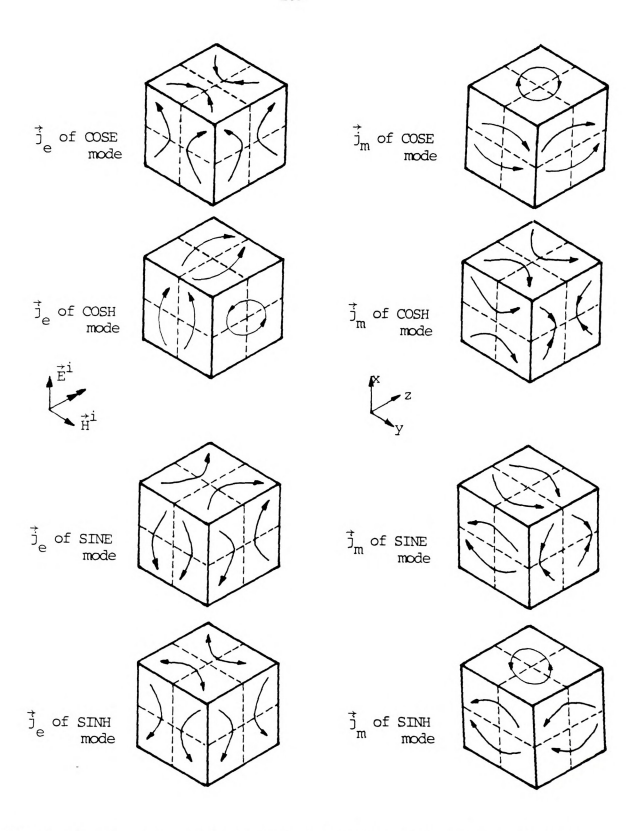
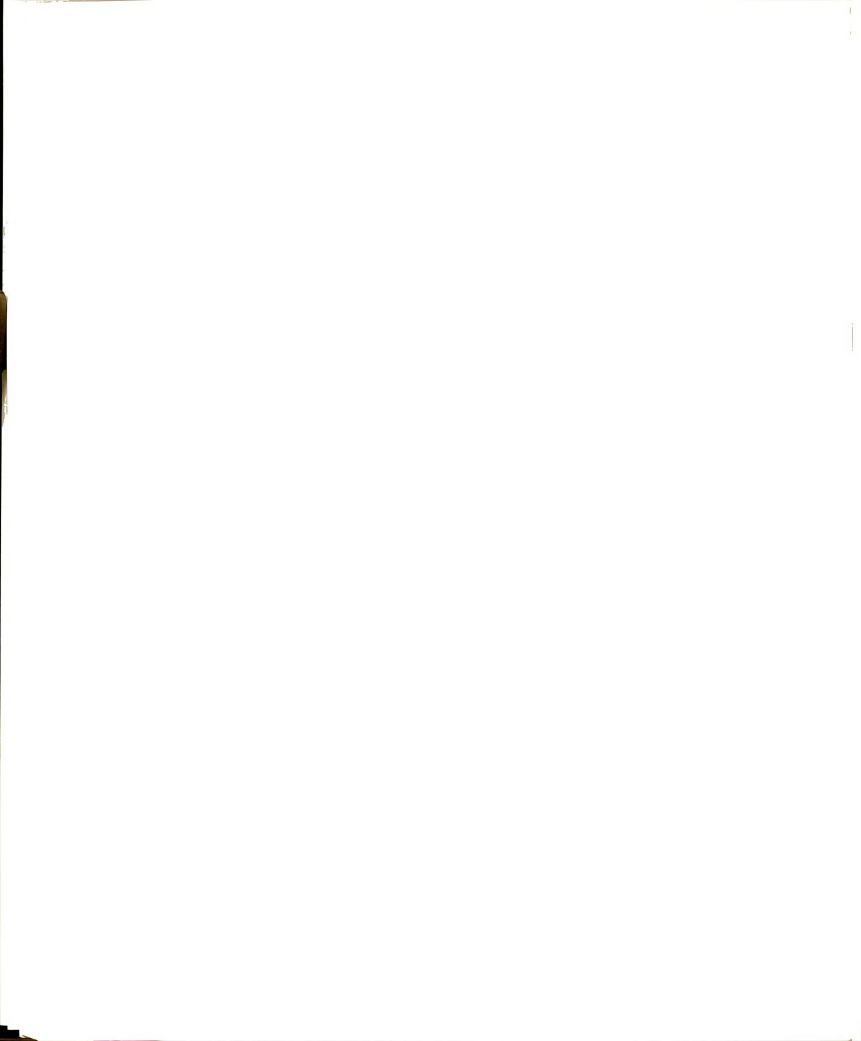


Figure 3.12. The symmetrical properties of various modes of the induced equivalent surface currents (\vec{j}_e , \vec{j}_m) on the surface of a cubic body.



separated into four different modes, the final solutions must be the combinations of results obtained for each basic mode. More details about the computer programs will be discussed in Chapter IV.

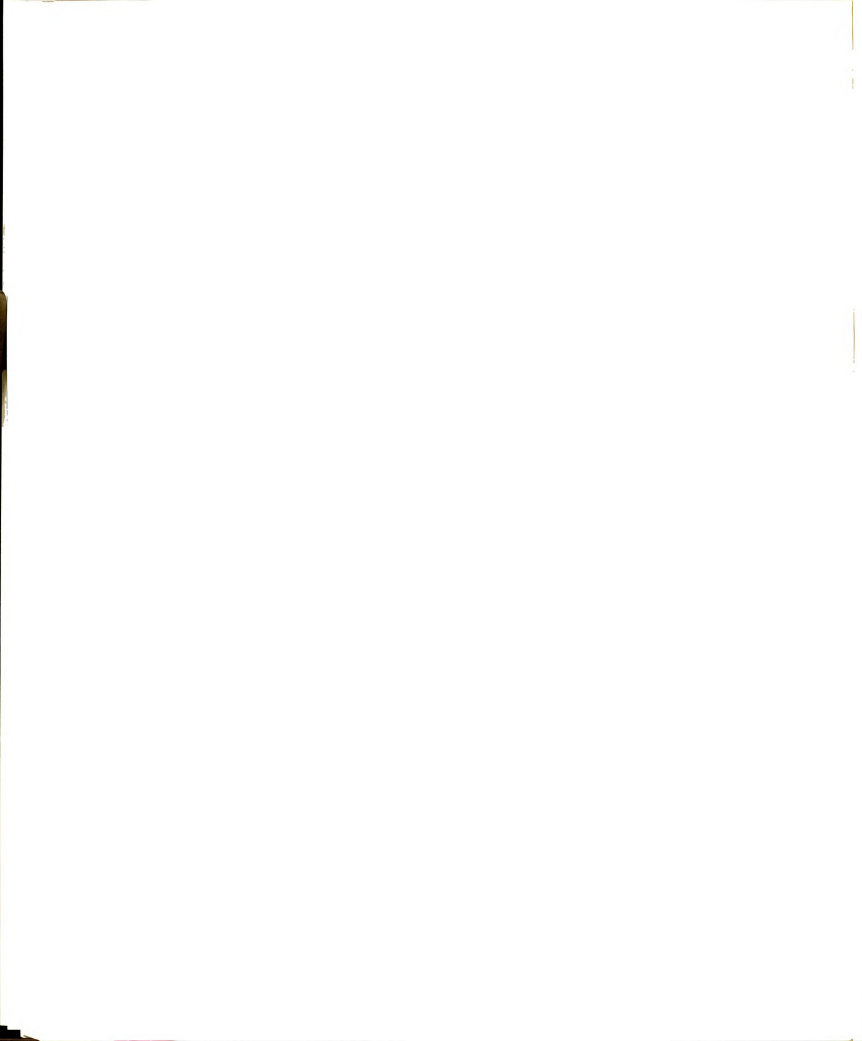
3.8. Numerical Results

The numerical technique developed in the previous section has been applied to solve for the EM fields induced on the surfaces of several finite conducting bodies.

These results of induced surface fields obtained by the surface integral equation method (SIEM), accompanied with the results of internal fields induced in the same bodies obtained by the volume integral equation method (VIEM)

[18], will be presented in this section. It should be mentioned that although SIEM gives solutions for both the induced electric field and induced magnetic field, for the purpose of simplifying the presentation we will only emphasize the induced electric fields, especially the component which predominates.

Figure 3.13 shows the vertical component of the induced electric field, $E_{\rm X}$, in a muscle layer of 6cm x 6cm x 1 cm irradiated by an EM wave of 100 MH $_{\rm Z}$ with a vertical incident electric field of 1 V/m at side-on incidence. The conductivity and dielectric constant of the body are assumed to be 0.889 S/m and 71.7. The top figure of Figure 3.13 shows the results for E $_{\rm X}$ (magnitude



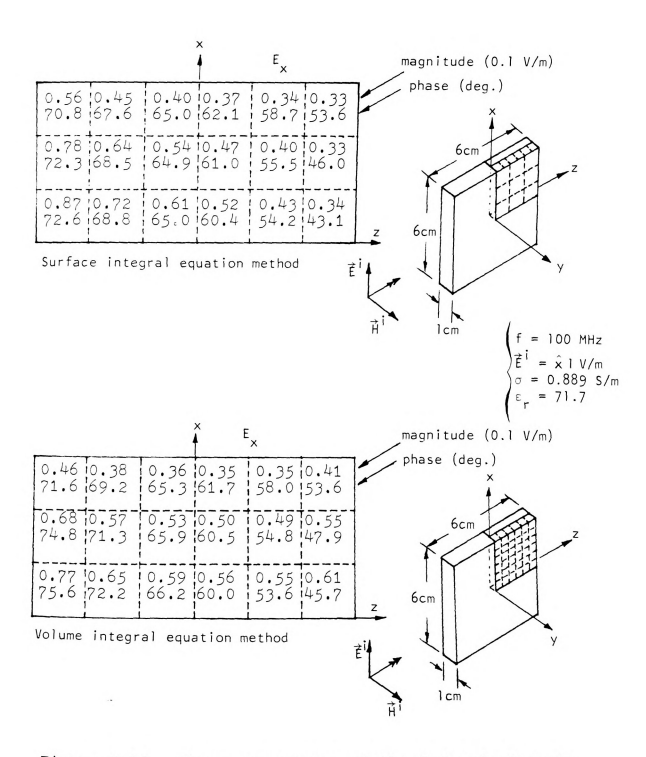
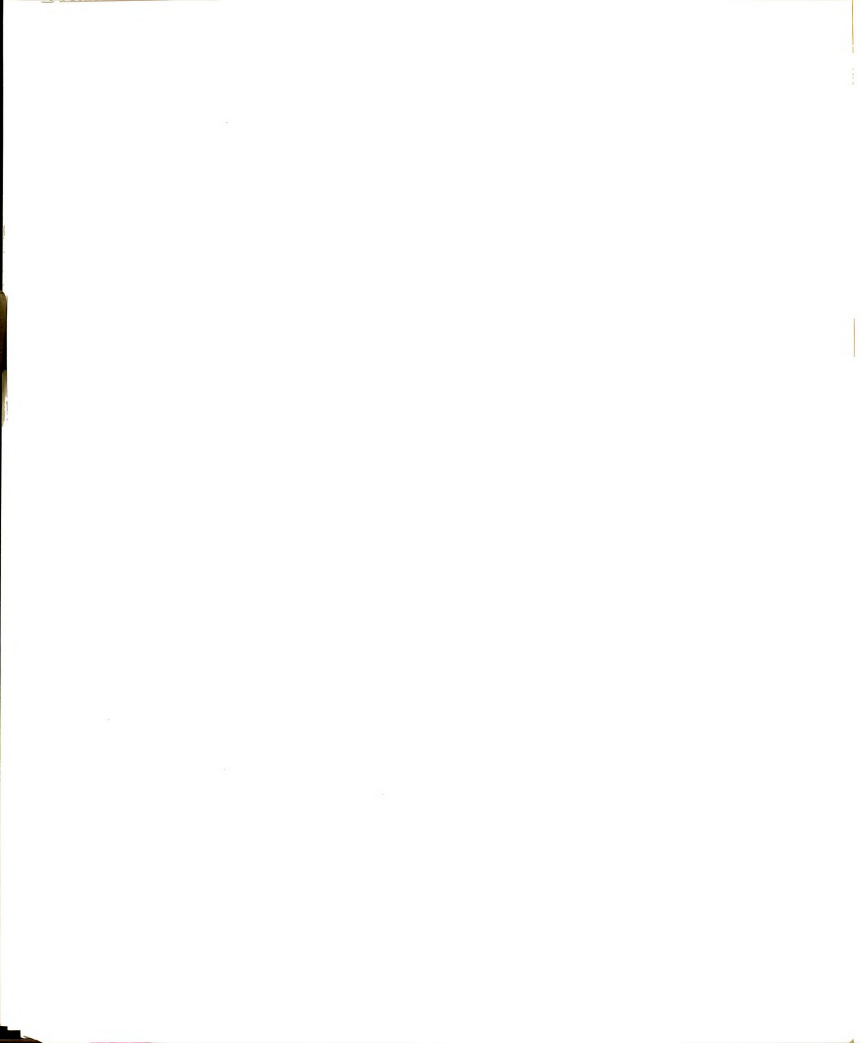


Figure 3.13. The x-components of the induced electric fields determined based on the surface integral equation method and the volume integral equation method.



and phase angle) on the surface of the body obtained with the surface integral equation method. In this numerical calculation, 1/8 of the body surface is divided into 21 subareas of two different sizes. The bottom figure of Figure 3.13 shows the results for $E_{_{\mathbf{x}}}$ (magnitude and phase angle) at the centers of the first layer cells, or at y = 0.25 cm plane, obtained with the tensor integral equation method. In this numerical calculation, 1/8 of the body is divided into 36 volume cells. Comparison of these two sets of results, obtained with a surface integral equation method and a volume integral equation method, shows a qualitatively good agreement. This comparison is possible because the body is electrically thin in the y-direction, and the induced EM field should remain quite uniform in that direction. The disagreement between the two sets of results occurs mainly over the vertical edges of the body where the circulatory magnetic mode of the induced electric field has a significant contribution; the volume integral equation method usually gives poor results for that circulatory magnetic mode of the induced electric field.

Figure 3.14 shows the horizontal component of the induced electric field, ${\rm E_{_{\rm Z}}}$, in the same body under the same irradiation as the case of Figure 3.13. ${\rm E_{_{\rm Z}}}$ near the central portion of the body, or the region near the x-axis, can be considered as mainly consisting of the

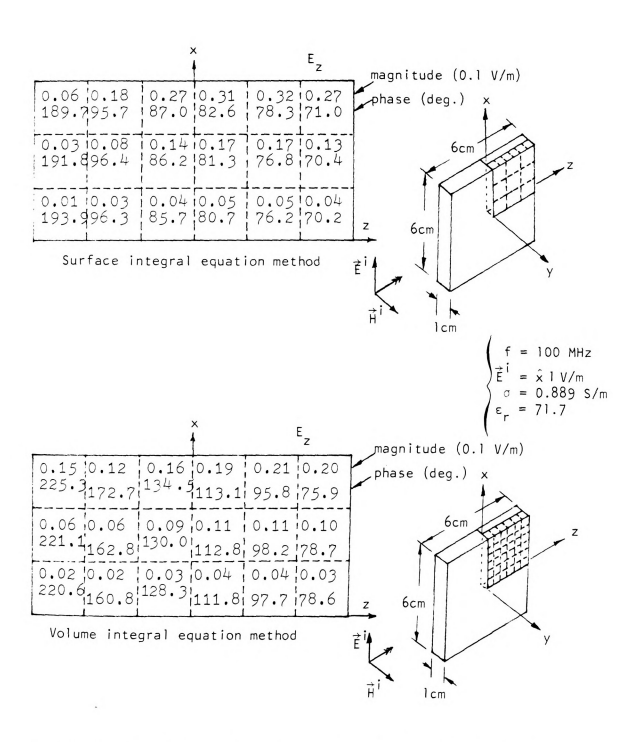
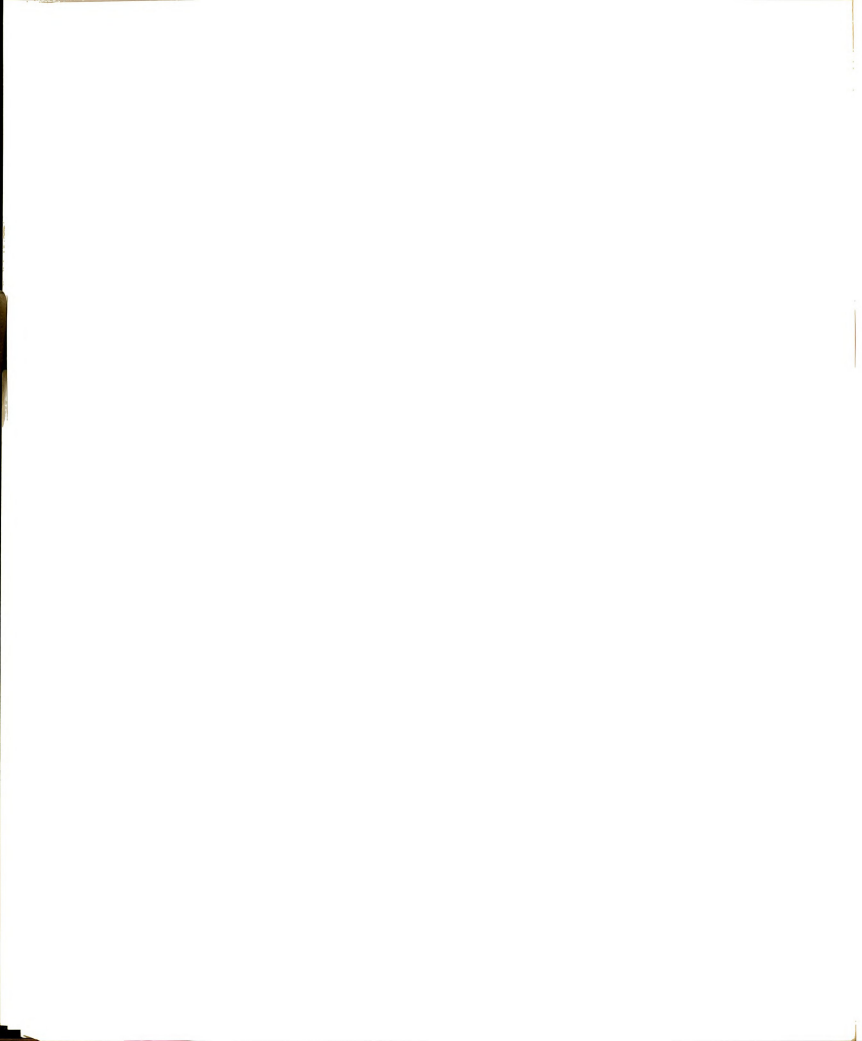
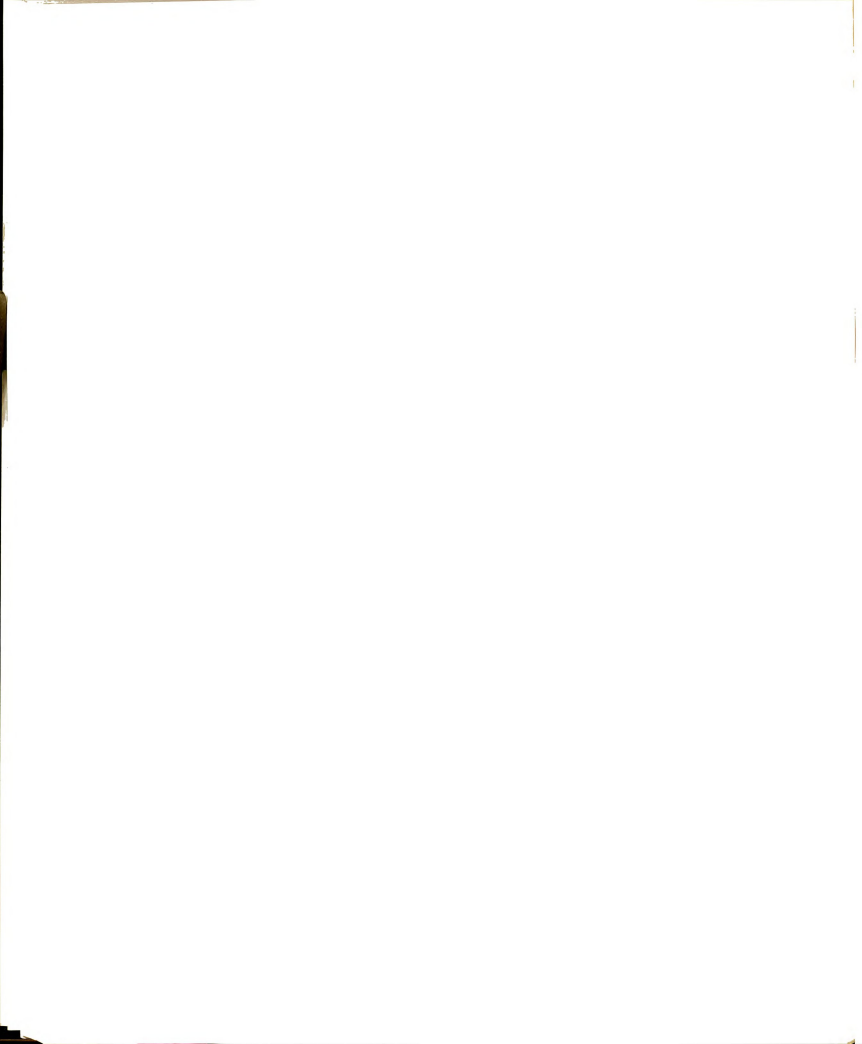


Figure 3.14. The z-components of the induced electric fields determined based on the surface integral equation method and the volume integral equation method.



circulatory magnetic mode of the induced electric field. For this component of induced electric field, only a fair agreement was obtained between the two sets of results obtained with the surface integral equation method and the volume integral equation method. The main reason for discrepancy is the inefficiency of a volume integral equation method in quantifying the circulatory magnetic mode of the induced electric field. The results obtained with the surface integral equation method appear to be more accurate for this case, because this set of results agrees with the results calculated by a method of quantifying the eddy current induced by a RF magnetic field as discussed in Chapter II.

As the second numerical example, we consider a rectangular body with a height of 180 cm, a width of 30 cm, and a thickness of 7.5 cm illuminated by a plane wave as shown in Figure 3.15. The incident wave is assumed to be x-polarized with a frequency of 10 MH $_2$ and an electric field intensity of 1 V/m, and the body is assumed to have a conductivity (σ) of 0.625 S/m and a dielectric constant ($\varepsilon_{\rm r}$) of 160. For the purpose of comparison, we plot the amplitude and phase distributions of the x-component of induced electric field in the top and bottom figures of Figure 3.15, where the results of both SIEM and VIEM are included. In the calculation by SIEM, 1/8 of the body surface is divided into 52 surface cells of two different



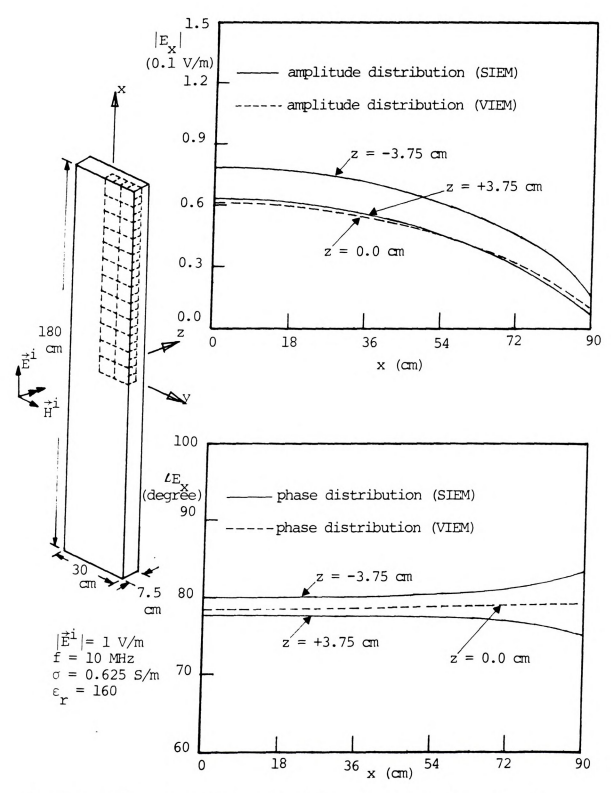
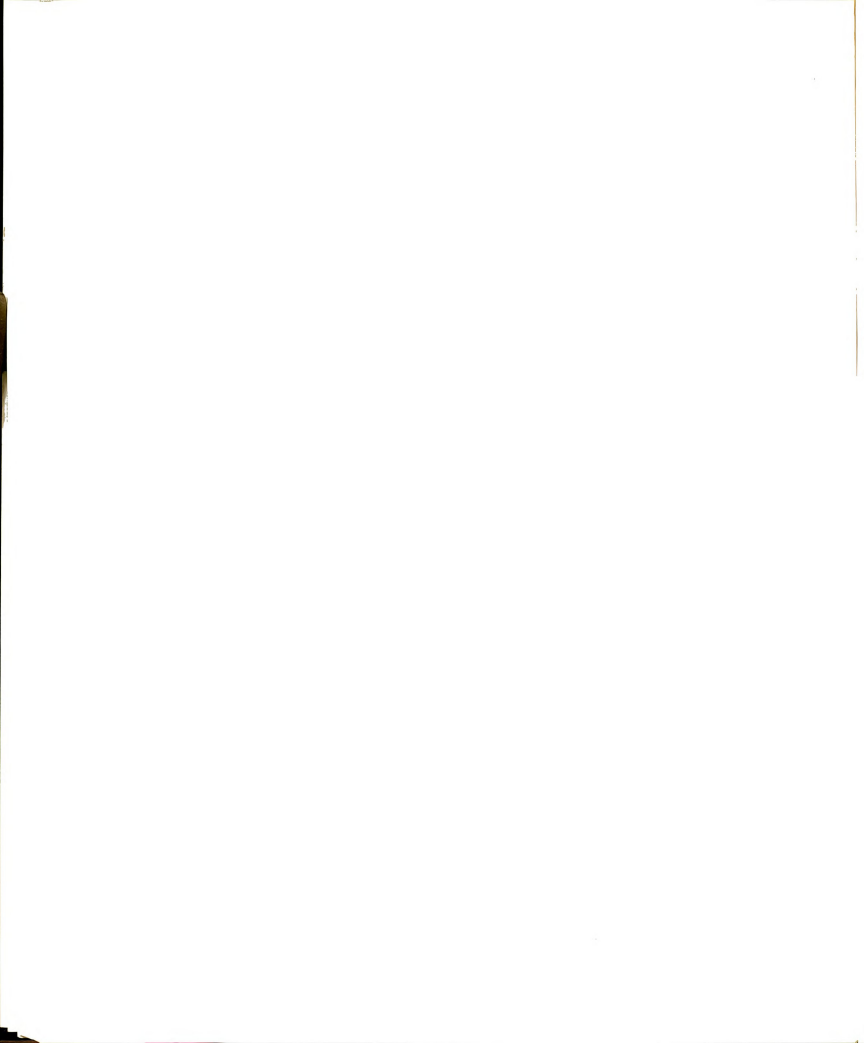
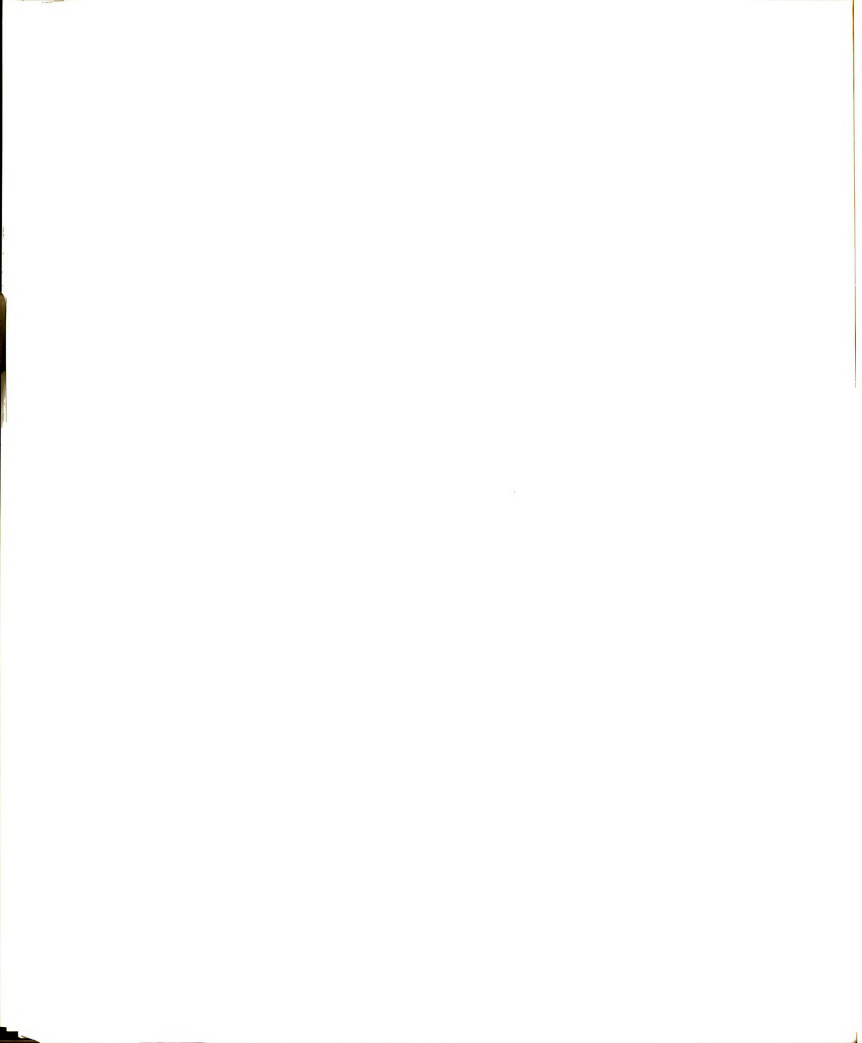


Figure 3.15. Amplitude and phase distributions of the x-component of induced electric field along the x direction in various layers at y = 3.75 cm.

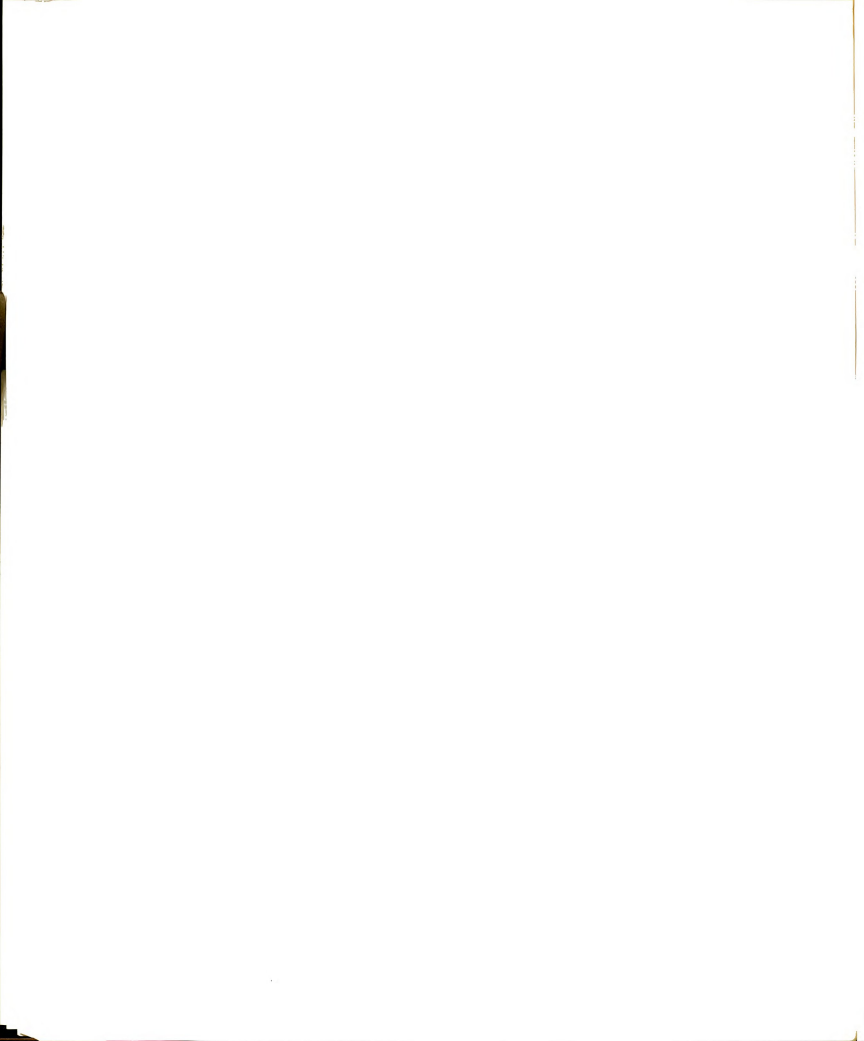


sizes. The EM fields induced at center points of the surface cells are numerically evaluated. In the top figure of Figure 3.15, we plot, in solid lines, the amplitude distributions of the x-component of electric field, $\mathbf{E}_{\mathbf{x}}$, induced at y = 3.75 cm on the front surface and the back surface as functions of the x-coordinate. The corresponding phase distributions are plotted in the bottom figure of Figure 3.15. For the numerical calculation by VIEM, 1/4 of the body is divided into 24 volume cells. The internal electric fields induced at center points of the volume cells are then numerically calculated. In Figure 3.15, we plot, in dashed lines, the amplitude and phase distributions of the x-component of internal electric field induced at y = 3.75 cm and z = 0.0 cm as functions of the x-coordinate. The comparison between these two sets of results, the results from SIEM and that from VIEM, shows a reasonably good agreement. However, we observe that the amplitude of the surface field induced on the front surface is almost 25% larger than that induced on the back surface, while the latter is very close to the results of VIEM as shown in Figure 3.15. Based on this observation, we would tend to conclude that the SIEM doesn't predict accurate results for the field induced on the front surface since we expect that the induced field is quite uniform along the z-direction. But, if we consider an extreme case with the assumption that the body



is extended to infinity in both transverse directions, we find that the surface field induced on the front surface of this infinite plane slab is about 40% larger than that induced on the back surface (based on solution of plane-wave reflection and transmission in multiple-layer region). This special case gives some qualitative explanations regarding the difference between the surface fields of the front surface and the back surface. Finally, we should emphasize that the comparison of the phase distributions obtained by SIEM and VIEM shows a very good agreement, especially in the central portion of the body.

Figure 3.16 shows the amplitude and phase distributions of the x-component of induced electric field along the x-direction in various layers at y = 11.25 cm for the same body illuminated by the same incident wave. The results shown in Figure 3.16 are very similar to those of Figure 3.15. This is understandable since for this case, the x-component of the induced electric field should be rather insensitive to the location along the y-direction. In Figure 3.16, the results obtained by SIEM are plotted in solid lines, while those obtained by VIEM are plotted in dashed lines. As we can see from the top figure of Figure 3.16, the amplitude distributions of the x-component of induced electric field decrease monotonically along the x-direction. On the other hand, we observe from the bottom figure of Figure 3.16 that the phase distributions are



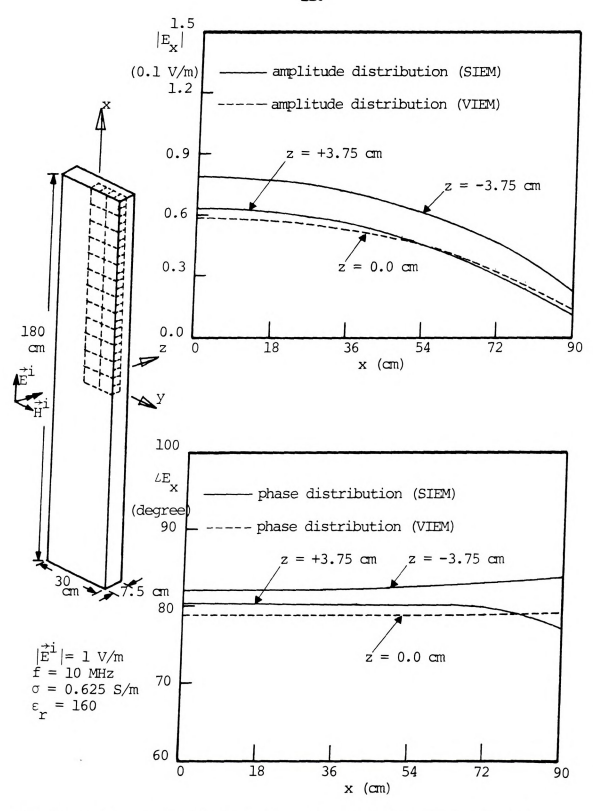
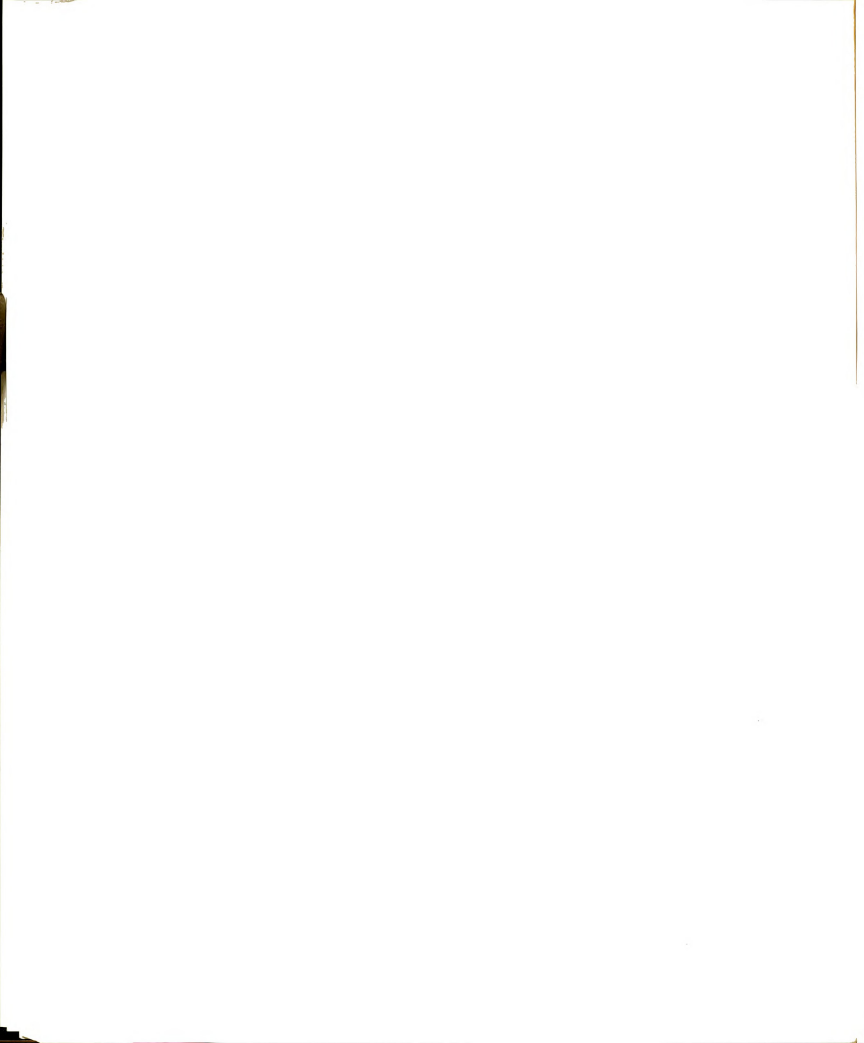


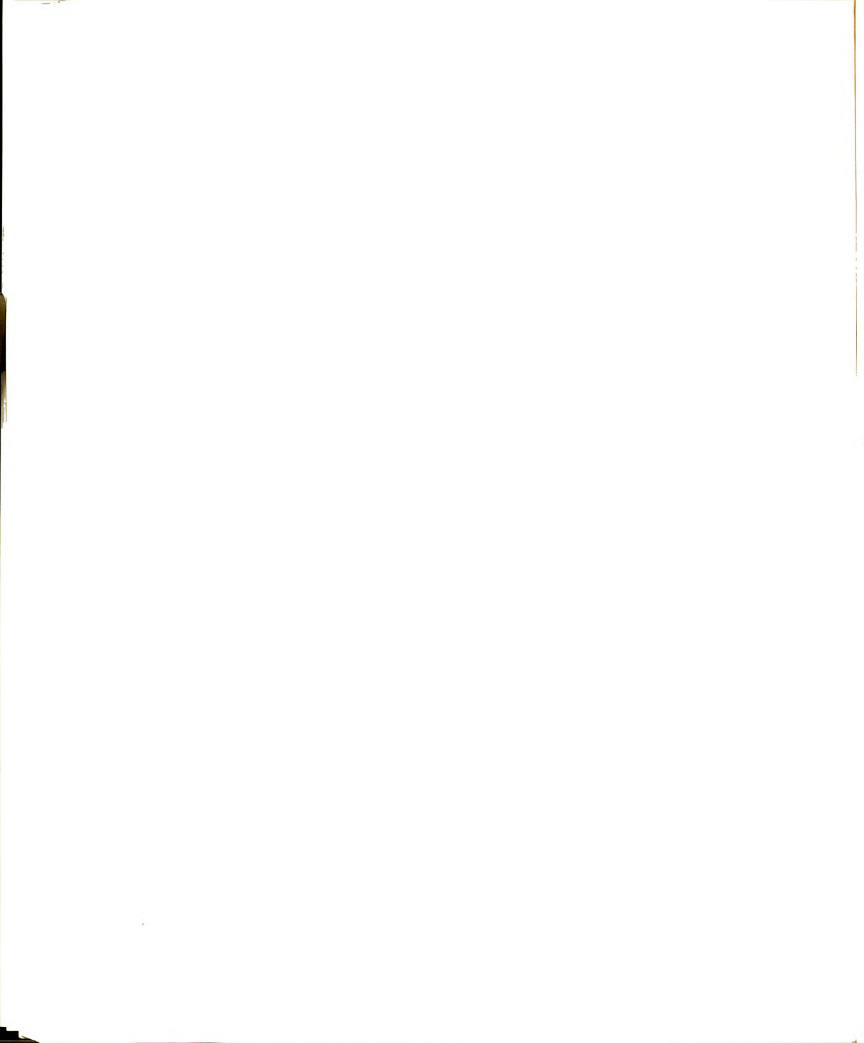
Figure 3.16. Amplitude and phase distributions of the x-component of induced electric field along the x direction in various layers at y = 11.25 cm.



nearly constant along the x-direction. Again, as in the case of Figure 3.15, the comparison between SIEM and VIEM shows reasonably good agreement, especially for the phase distributions.

The amplitude and phase distributions of the y-component of induced electric field along the x-direction in various layers at y = 11.25 cm and y = 3.75 cm are plotted in Figure 3.17. It is shown in Figure 3.17 that the field distributions at y = 11.25 cm (top figure) are very similar to those at y = 3.75 cm (bottom figure), except that the amplitude distributions of the former are three times as large as that of the latter. This is reasonable since the y-component of induced electric field must depend strongly on the locations along the y-direction. Figure 3.17 shows that the amplitude distributions of the V-component of induced electric field increase monotonically along the x-direction, while the phase distributions are nearly constant along the x-direction. It is to be noted that the y-component of induced electric field on the front surface and that on the back surface are exactly the same. This is quite different from what was observed in the previous two figures. Finally, it is clear from Figure 3.17 that the comparison between SIEM and VIEM demonstrates very good agreement for this case.

As the last example, we consider a more complicated geometry as shown in Figures 3.18 and 3.19. The body



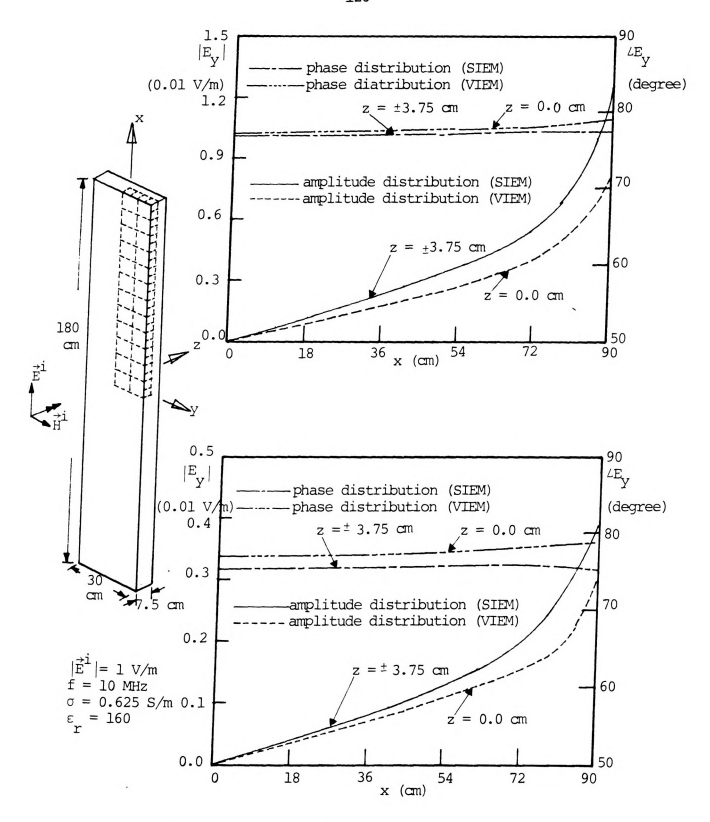
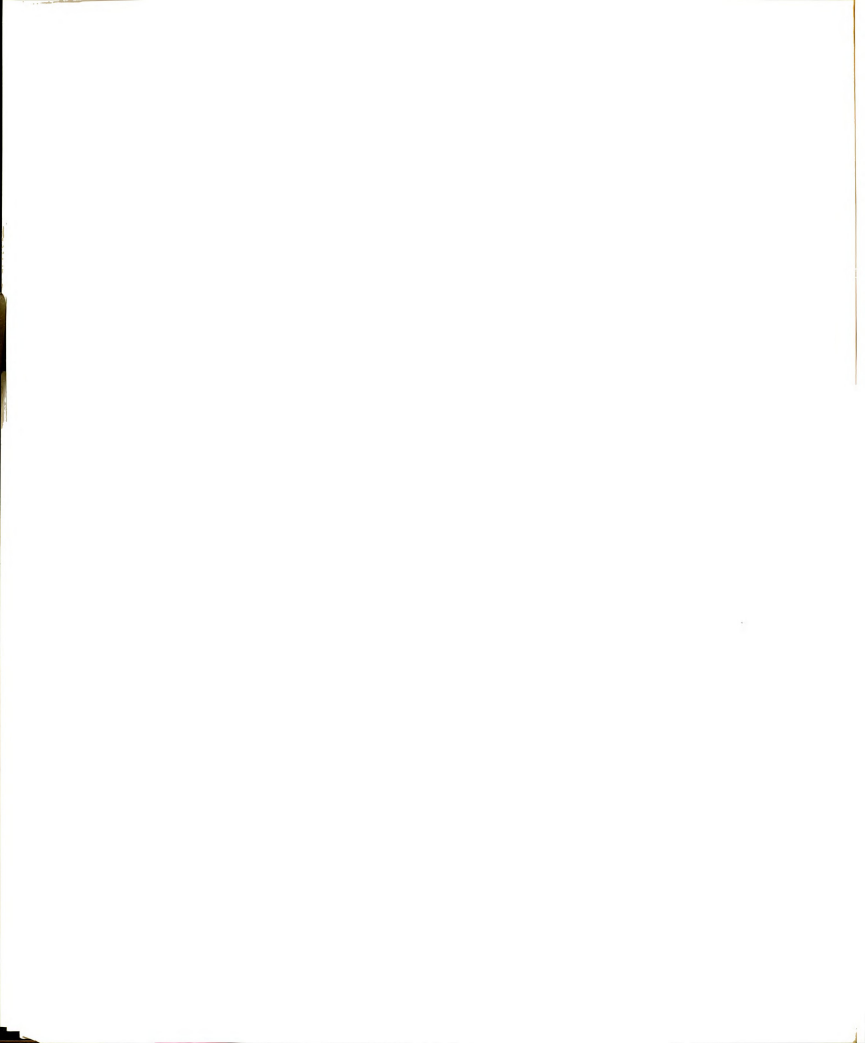
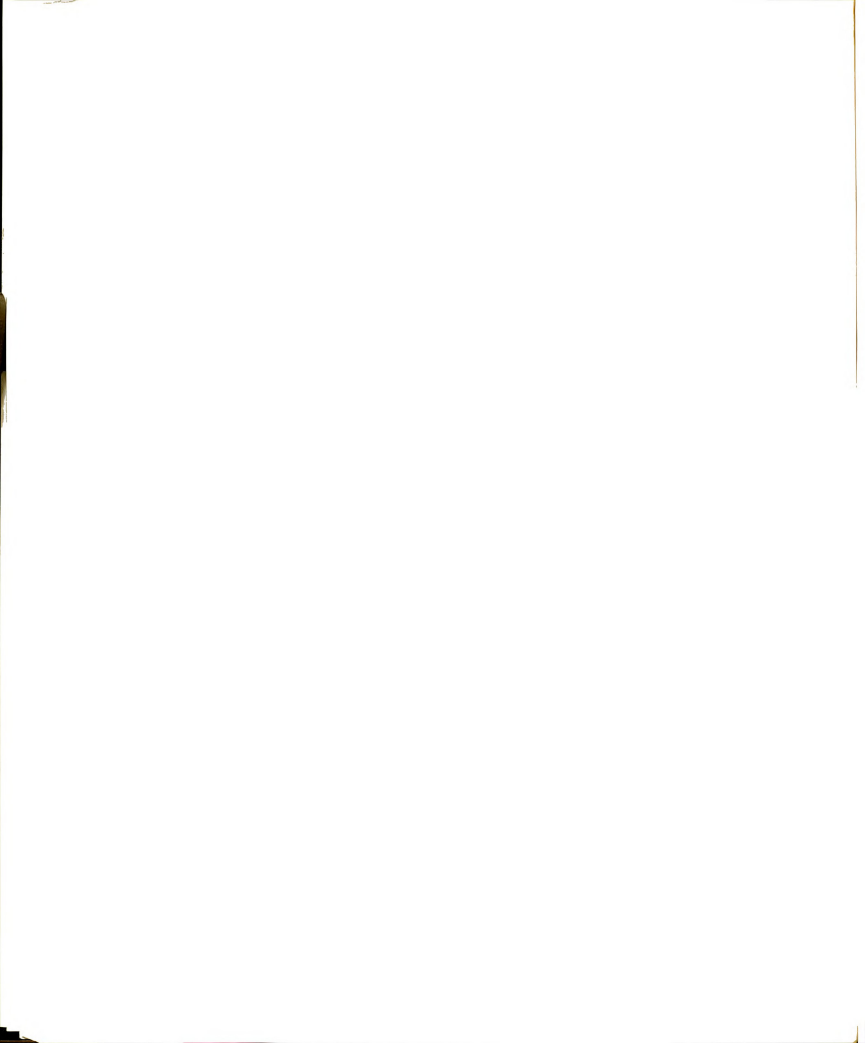


Figure 3.17. Amplitude and phase distributions of the y-component of induced electric field along the x direction in various layers at y = 11.25 cm (top figure) and y = 3.75 cm (bottom figure).



considered has a shape similar to that of a human body with the following dimensions: 70 cm in height, 20 cm in maximum width, and 10 cm in thickness. This situation can be considered as a simulation to the case of a twoyear-old child innocently exposed to a high-intensity EM wave. For the purpose of reducing the number of unknowns to keep the computational cost low, we still assume that the frequency is as low as 10 MHz. The electrical properties of the body are assumed to be σ = 0.625 S/m and ε_{r} = 160. In the calculation by SIEM, 1/4 of the body surface is divided into 29 surface cells of two different sizes. The amplitude distribution of the x-component of induced electric field is shown in Figure 3.18 for both the front surface and the back surface of the body. It is observed from Figure 3.18 that the electric field induced on the front surface is larger than that induced on the back surface. In Figure 3.19, the phase distribution of the x-component of induced electric field is shown. Unlike the amplitude distribution, the phase distribution is quite uniform over the entire body surface.



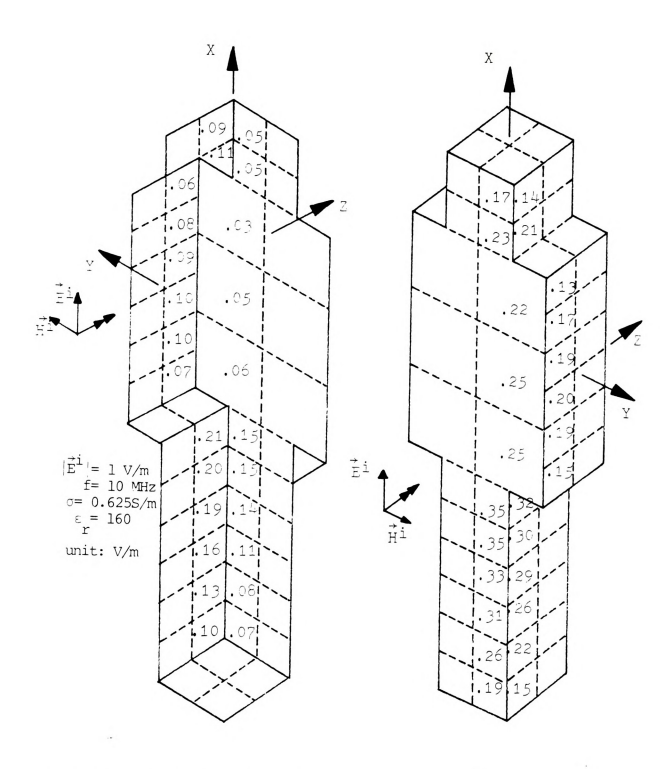
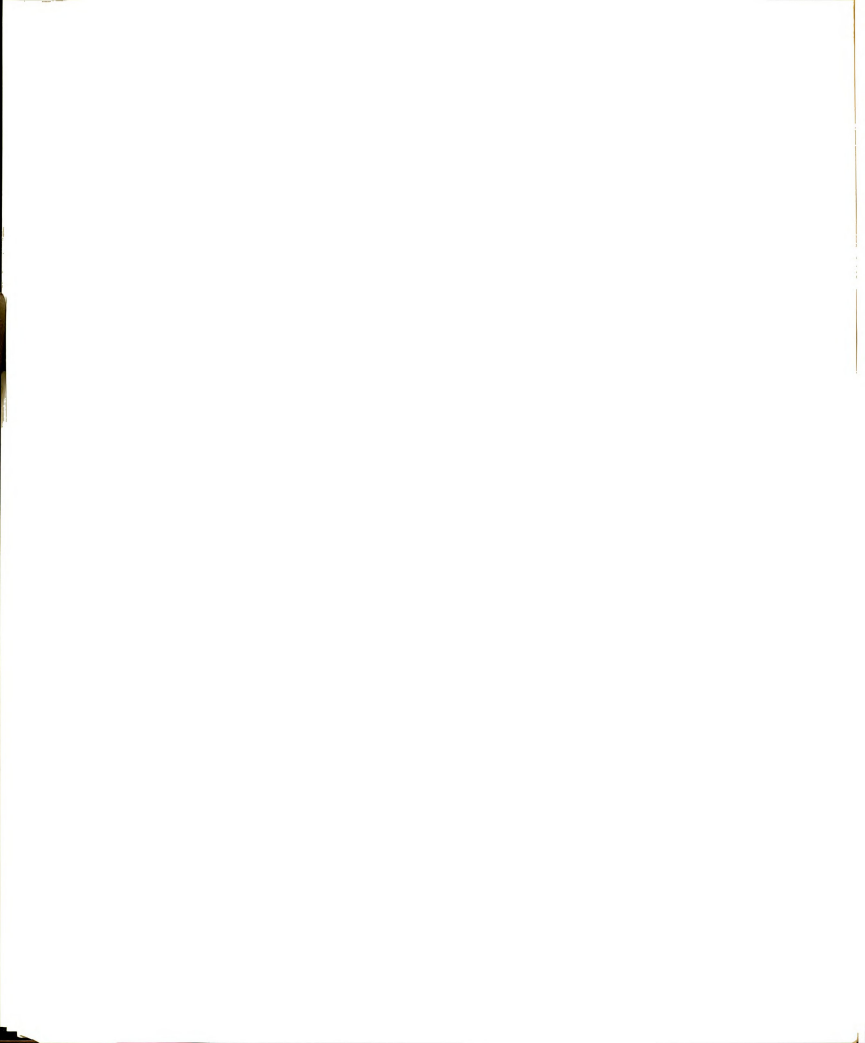


Figure 3.18. Amplitude distribution of the x-component of induced electric field on the surface of a simulated human body.



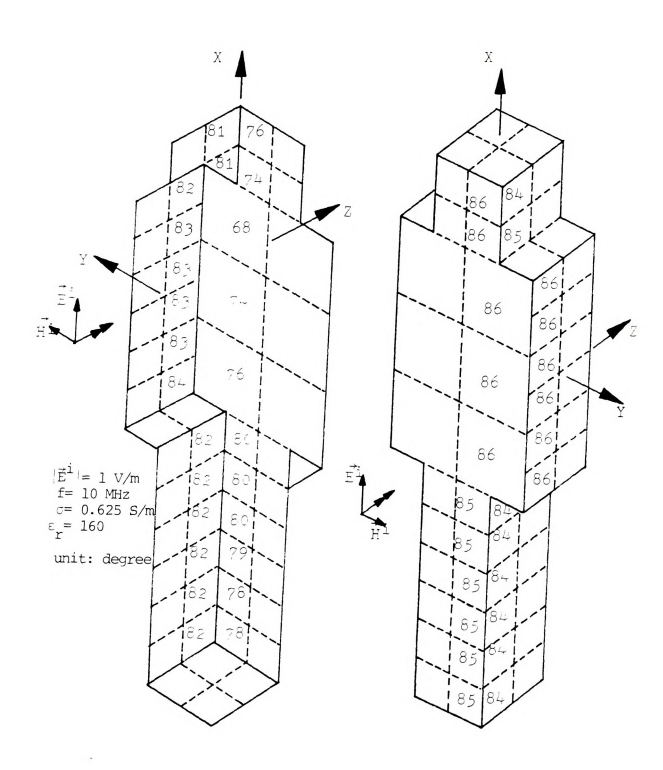
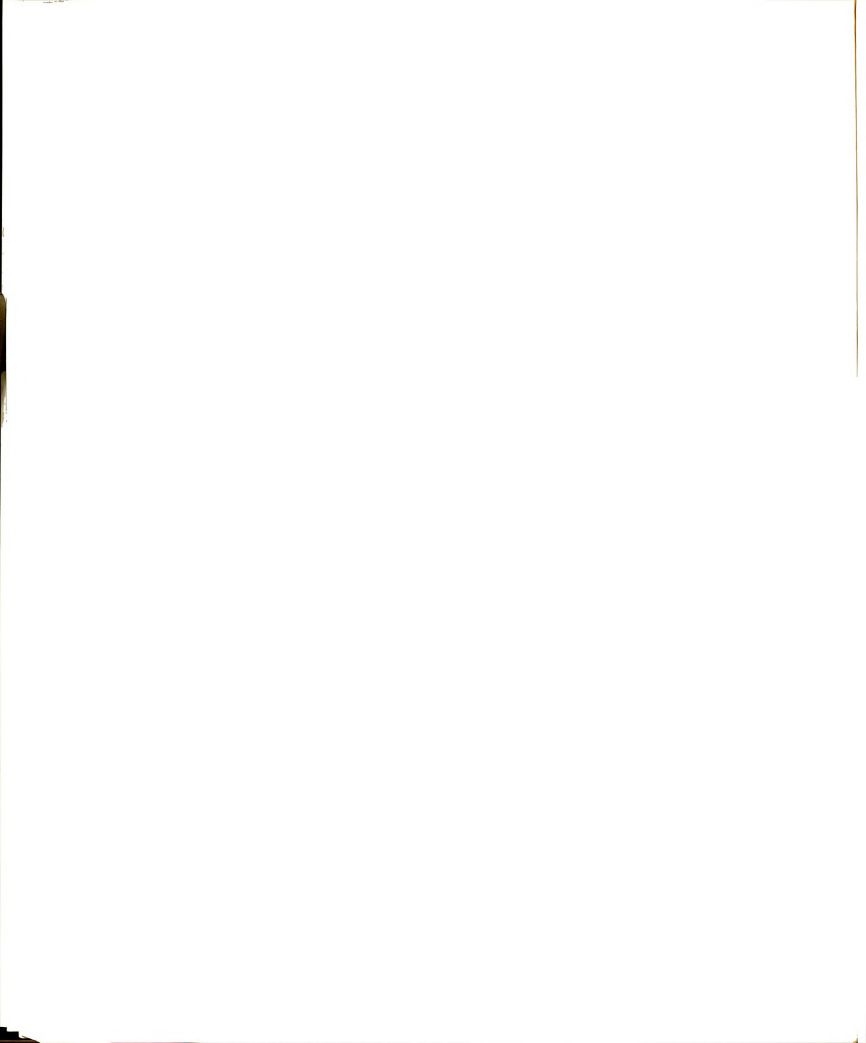


Figure 3.19. Phase distribution of the x-component of induced electric field on the surface of a simulated human body.



CHAPTER IV

PART 1

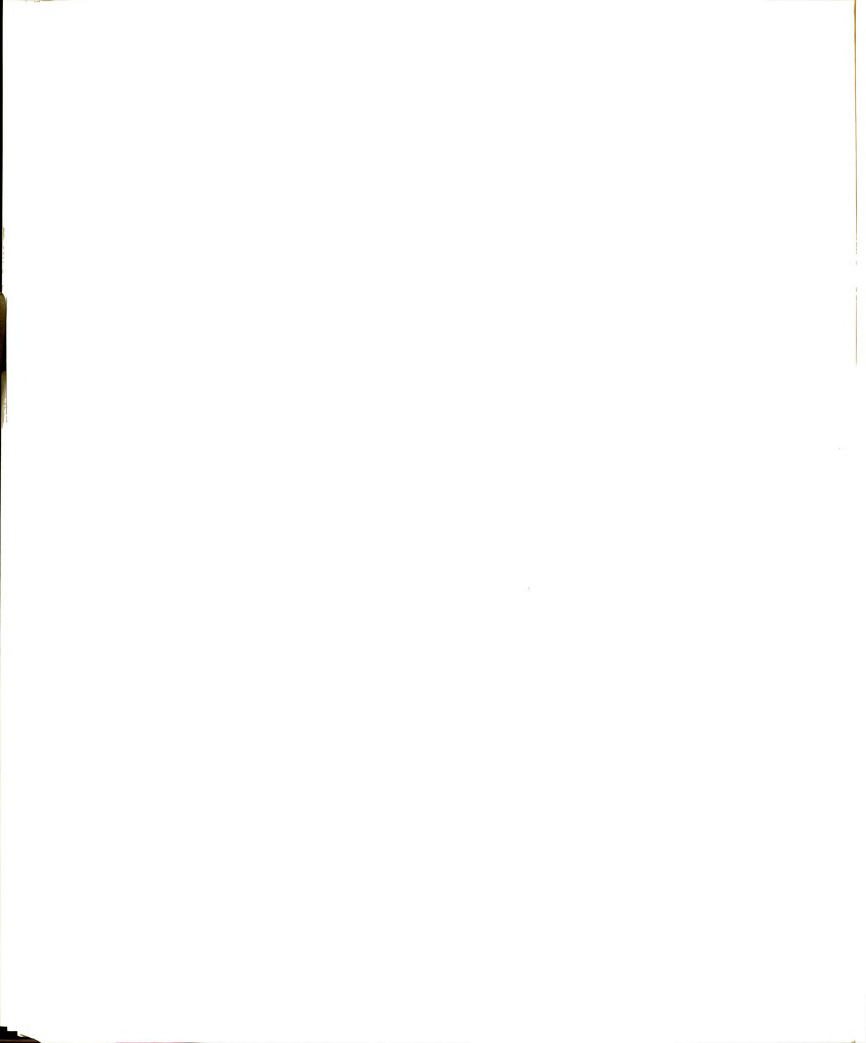
A USER'S GUIDE TO COMPUTER PROGRAM FOR INDUCED
EDDY CURRENT INSIDE A FINITE CONDUCTING BODY
WITH ROTATIONAL SYMMETRY

The first part of Chapter IV explains the computer program used to evaluate the eddy current induced at various locations within a finite conducting body with rotational symmetry. The theory behind this numerical technique has been presented in Chapter II. In addition to the listing of the program, an example will be worked out to help readers understand the sequential order of data files and the sample print out.

4.1. Formulation of the Problem

The program "EDDY" can handle two different cases:

(1) the case of a body immersed in a uniform magnetic field and (2) the case of a body irradiated by a uniform magnetic beam. The first step in utilizing this program is to divide a body with rotational symmetry into N circular rings with various dimensions and radii. Inside each circular ring the induced electric field (induced electric field and induced eddy current are interchangeable, since



they are only related by the conductivity) and the electrical properties are assumed to be uniformly distributed; however, they may be changed from ring to ring.

For the first case considered, the impressed magnetic field can be written as

$$\vec{H}^{i}(r) = \hat{z}H^{i}$$
.

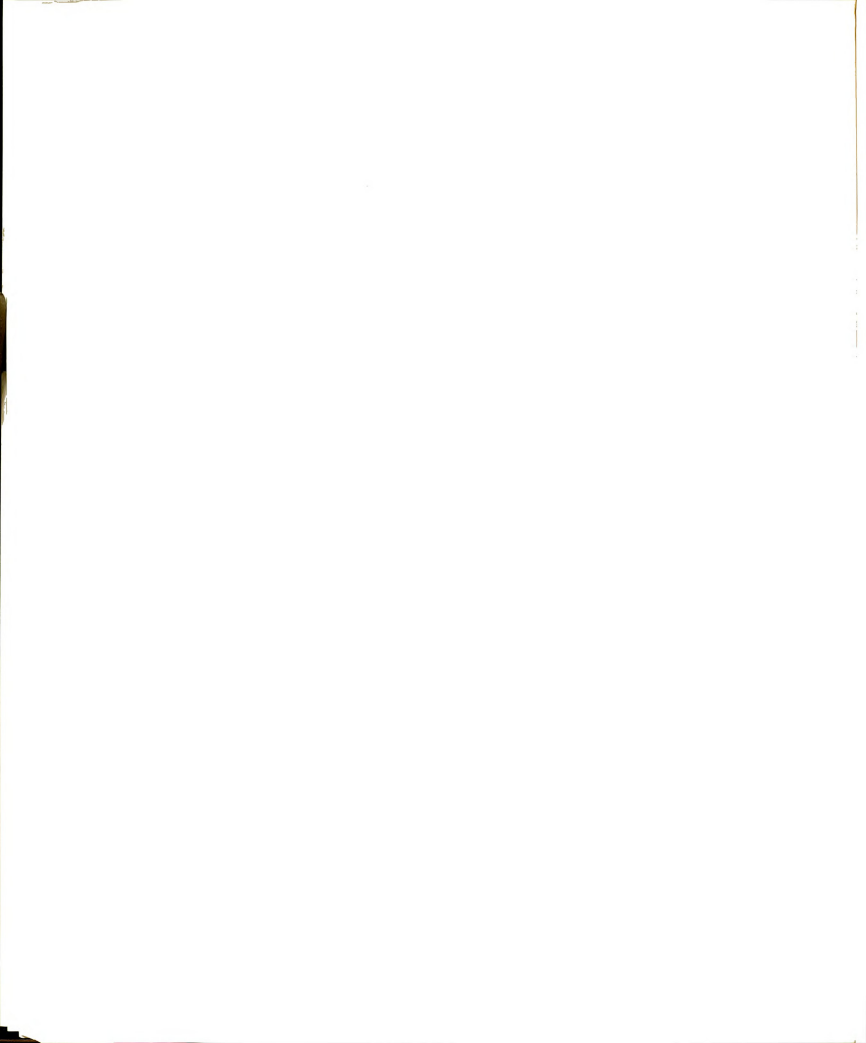
Similarly, for the second case, it can be expressed as

$$\vec{H}^{\dot{1}}(r) = \hat{z}H^{\dot{1}} \qquad \text{for } 0 \le r < b$$

$$= 0 \qquad \text{for } b \le r.$$

Here the time-varying factor $\exp(j\omega t)$ has been suppressed. Usually, we assume that the impressed magnetic field has unit intensity, $H^{\dot{1}}=1$ A/m. The body considered has a symmetrical axis in the +z direction, as shown in Figure 4.1. For convenience, we also assume that the cross-section of each ring is a square which is then approximated by a circle in the integration. Since the induced electric fields have only one component (in the + ϕ direction), we have N unknowns in total.

The second step in the numerical formulation of the problem is the specification of the location of each ring, its physical dimensions and its electrical parameters. As mentioned earlier, this program has been written for the case of uniformly impressed magnetic field or for the case of uniform magnetic beam. However, other types of



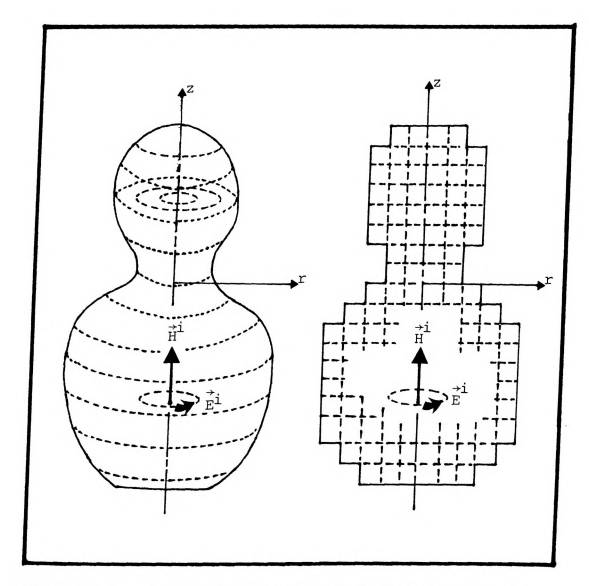
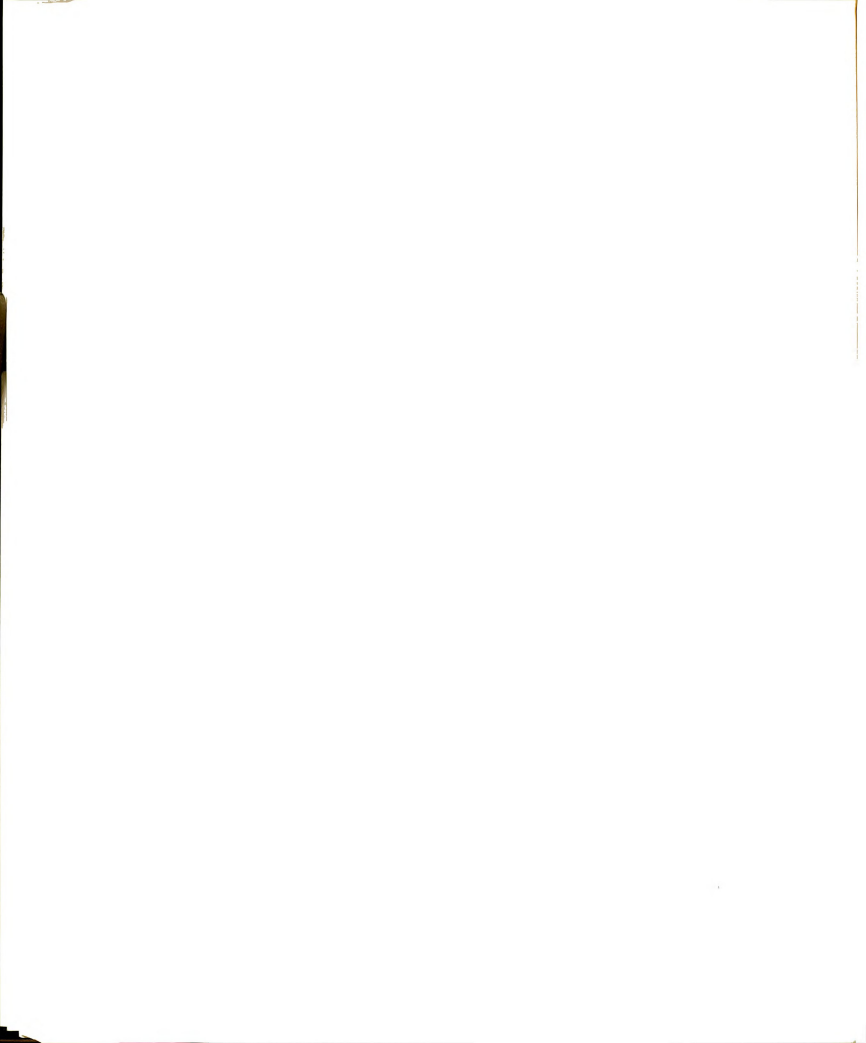


Figure 4.1. A rotationally symmetrical body with the symmetrical axis in the +z direction is irradiated by a magnetic field with unit intensity. The body is subdivided into a number of circular rings of various radii.

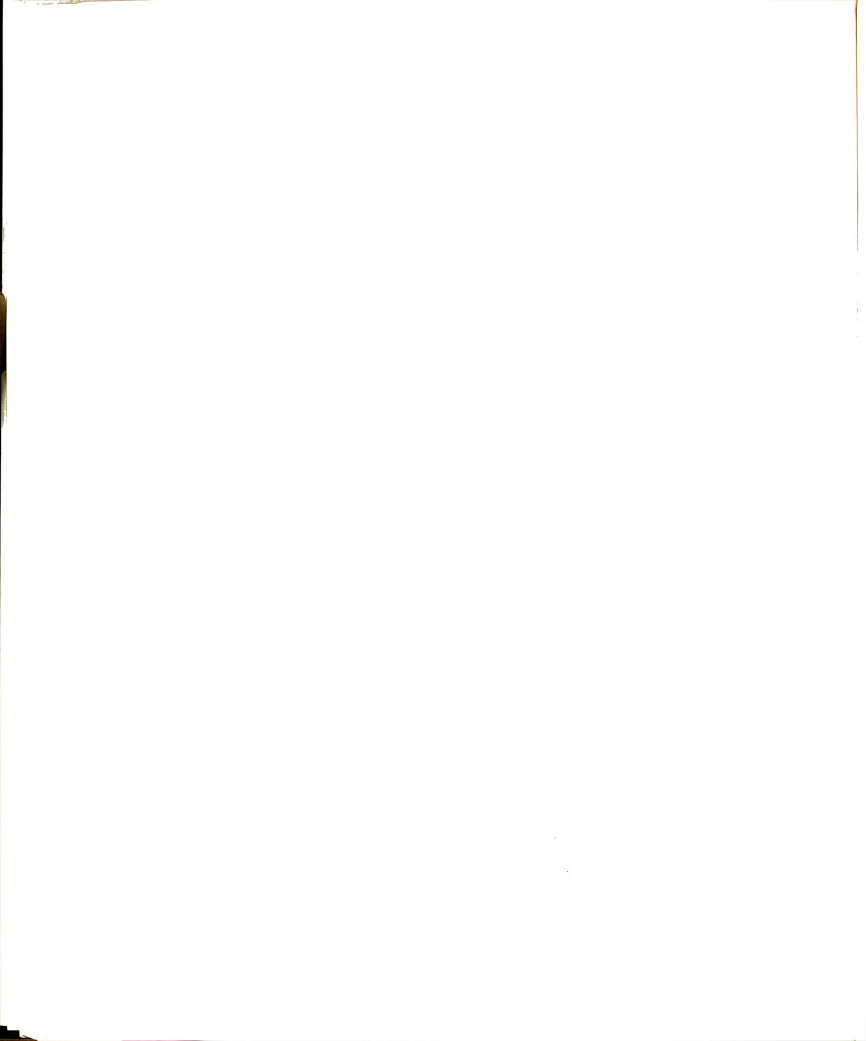


impressed magnetic fields may be used with few changes in the main program.

4.2. Description of Computer Program

The program "EDDY" is coded in FORTRAN. It used the following complex functions and subroutines:

- "LEEMAT"--is a subprogram which calculates the elements of [M] matrix based on eqs. (2.16) and (2.17).
- "FMM C," "FMMS," "FMNC," "FMNS"--are function subprograms which determine the integrands of integrals Kmn, and Kmm as expressed in eqs. (2.6) and (2.8). Note that we decompose each integrand into real and imaginary parts. Since these four functions are used as calling arguments for function subprogram "DCADRE," they must be declared external in subroutine "LEEMAT" which calls subprogram "DCADRE" for numerical integration.
- "DCADRE"--is an IMSL routine which integrates a function by using technique of Cautious Adaptive Romberg Extrapolation.
- "CMATP"--is a subprogram which calculates the induced electric field in each ring by solving N \times N matrix. It is actually a Gauss-Seidel



method for solving a system of N equations in N unknowns.

A CHARLESTON OF THE PARTY OF TH

"MAGPHA"--this subprogram, as the name suggests, determines magnitude and phase of the induced electric field in each ring.

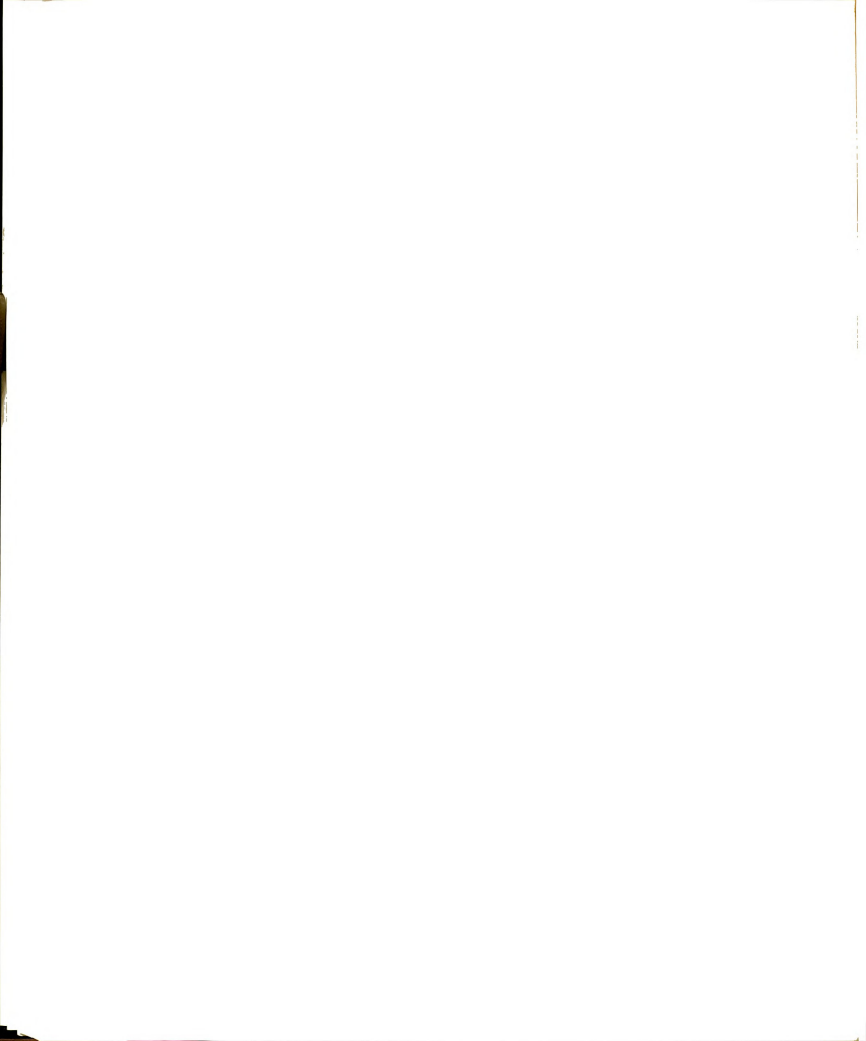
"MCURVE," "PCURVE"--these two subroutines plot the magnitude and phase distributions of the induced electric fields as functions of radial distance.

A listing of the program "EDDY" is given at the end of this chapter.

4.3. Data Structure and Input Variables

Figure 4.2 shows a typical example of a body with rotational symmetry we refer to from time to time. This body is divided into six circular rings. The origin of the coordinate system can be arbitrarily chosen at any point along the central axis of the body; then the location of each ring is determined with respect to this origin. In this example, it is assumed that all the rings have the same cross-sectional area and electrical parameters.

The sequential structure of the input data files, the format specifications and the symbolic names of the variables appearing on each file are outlined in Table 4.1. There are totally three input files; each of them consists



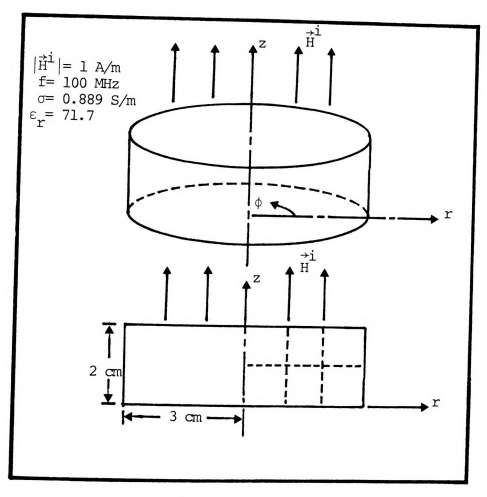


Figure 4.2. A cylindrical biological body with a diameter of 6 cm and a height of 2 cm is subdivided into 6 circular rings with a cross-section of 1 cm x 1 cm for each ring. The body is assumed to have a conductivity of 0.889 ${\rm S/m}$ and a dielectric constant of 71.7, and is immersed in a 100 MHz uniform magnetic field with an intensity of 1 ${\rm A/m}$.

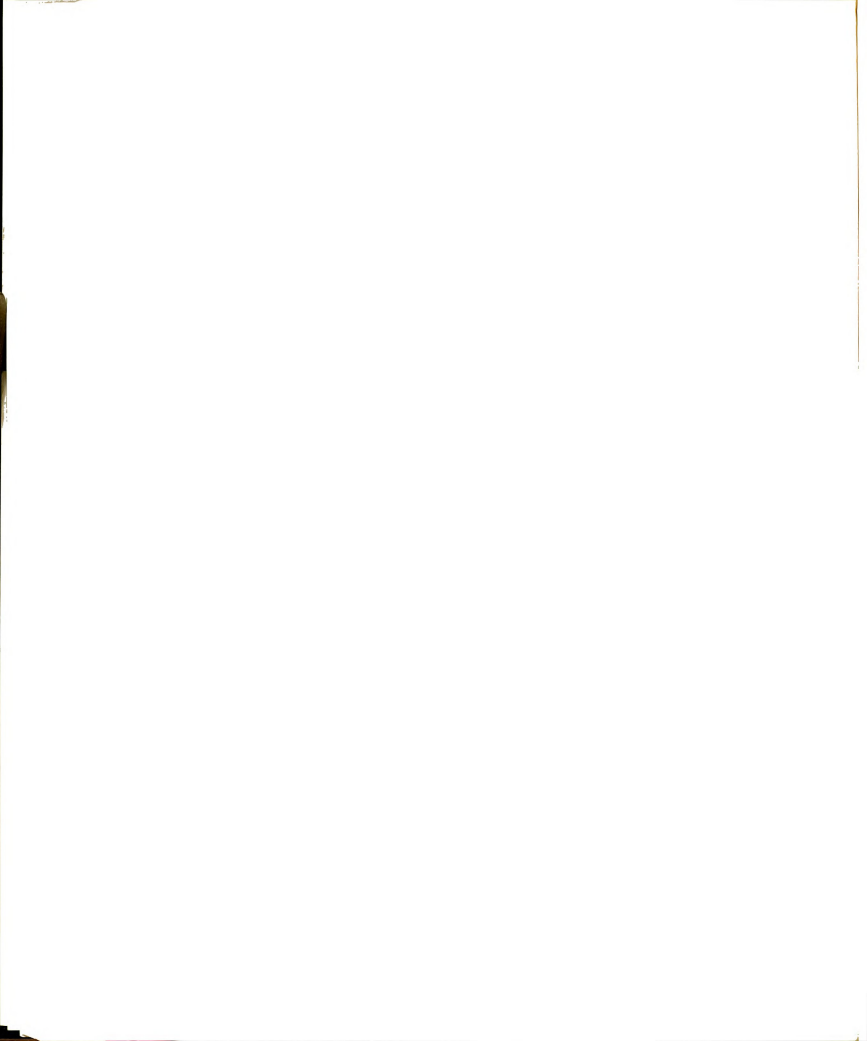
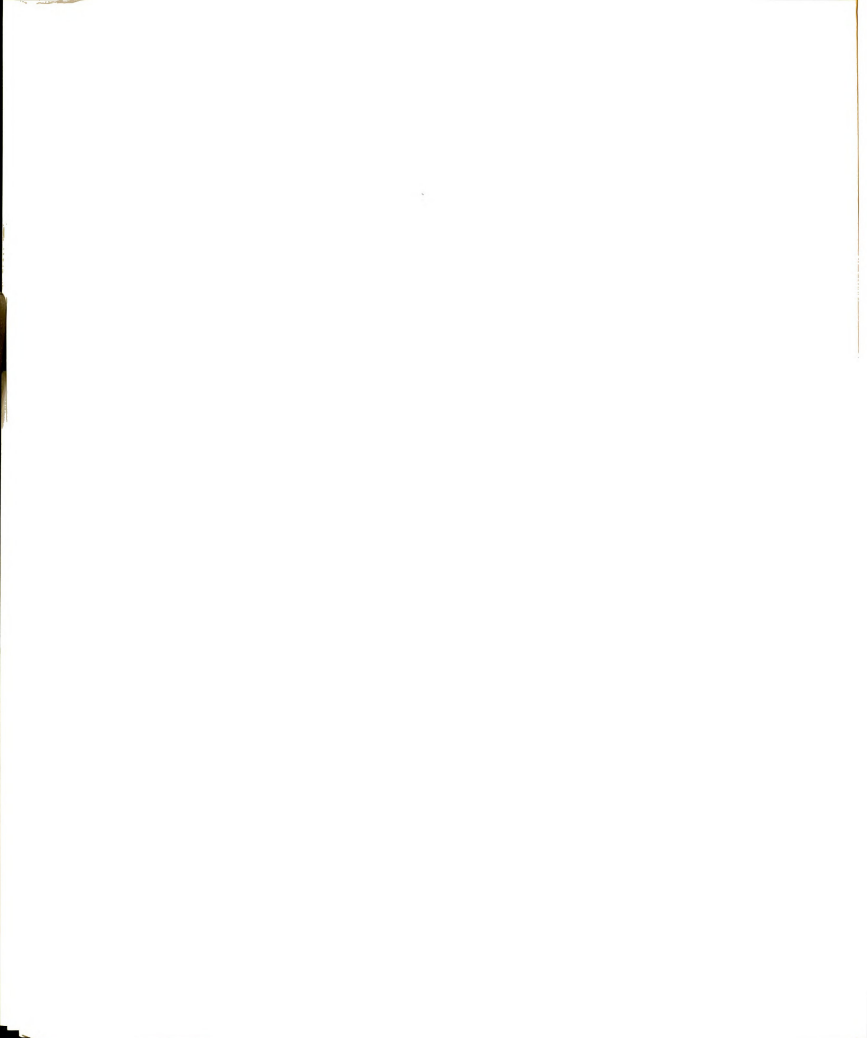


Table 4.1. The symbolic names of input variables and corresponding specifications for the data files used in data structure for the program "EDDY."

File No.	Card No.	Symbolic Name	Columns	Format
1	1	N	1-5	15
		FREINM	6-15	F10.5
		NX	16-20	15
		NXB	21-25	15
2	1	NPAR	1-5	15
		AERR	6-15	F10.5
3 1-N	RERR	16-25	F10.5	
	XEND	1-12	F12.5	
		ZEND	13-24	F12.5
		XAA	25-36	F12.5
		ZBB	37-48	F12.5
		REP	49-60	F12.5
		SIG	61-73	E13.6



of at least one data card. Specifically, the first two data files consist of only one data card each, while the third file consists of N data cards. The information on each data file is explained as below:

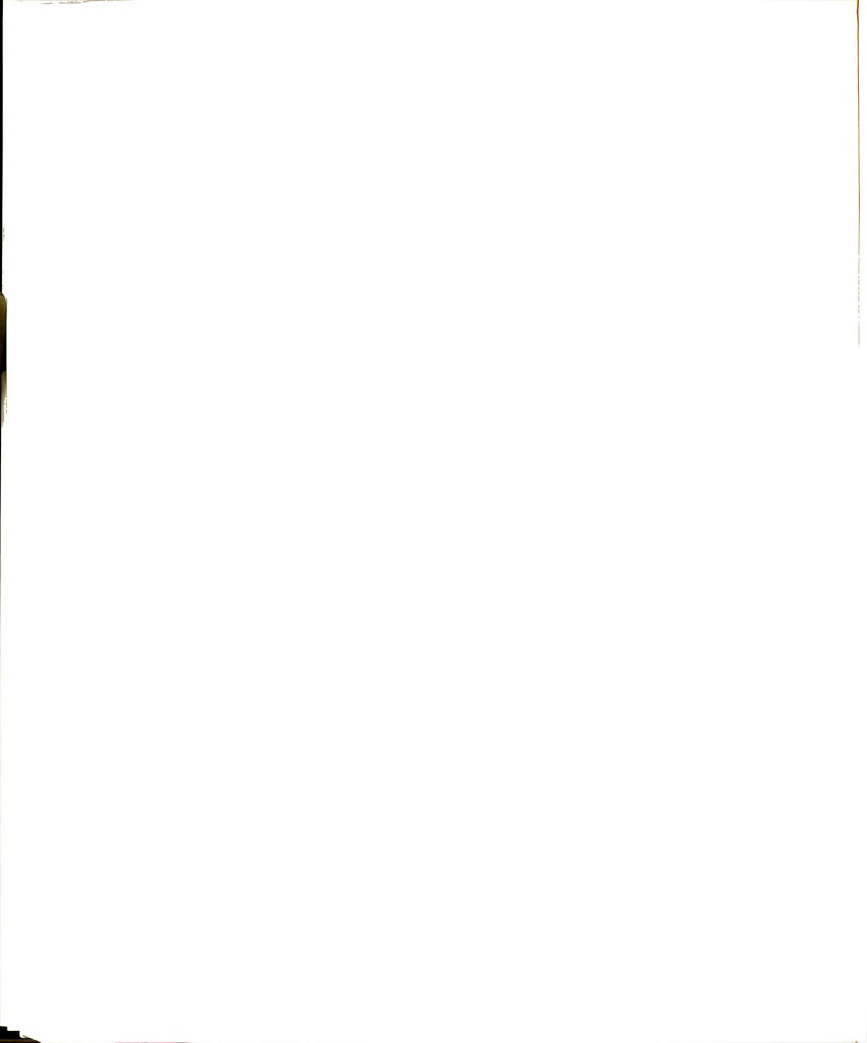
First Data File

This data file defines four variables with symbolic names N, FREINM, NX, and NXB. Where N is the total number of circular rings inside the body. NX is the number of rings per layer, and NXB is the number of rings per layer within the range of the magnetic beam. Finally FREINM is simply the frequency of the impressed magnetic field in MHz.

Second Data File

This file consists of only one data card and determines the following variables:

- "NPAR"--for the integrals Kmn and Kmm, the integration
 limits 0° and 180° will be divided into "NPAR"
 equal-size subintervals. The purpose of this partitioning is to save the computational cost.
- "AERR"--desired minimum absolute error for the numerical integration.
- "RERR"--desired minimum relative error for the numerical integration.



Third Data File

This data file consists of N data cards, one for each circular ring. This set of data cards helps simulate the finite conducting body being considered.

Each data card contains the following information:

- "XEND," and "ZEND"--these codes correspond to the maximum boundaries of a ring cross-section in the x-, and the z-directions with reference to the origin. This information is supplied by the user in centimeters.
- "XAA," and "ZBB"--are the symbolic names for the dimensions of the ring cross-section in the x-, and the z-directions. Since each ring cross-section is a square, the column for "XAA," and "ZBB" will contain the same information.
- "REP," and "SIG"--are the codes for dielectric constant and conductivity (S/m) of each circular ring.

This completes the structure of the input data files needed to specify all the necessary information for the quantification of induced electric fields inside a finite conducting body with rotational symmetry. An example is worked out in the next section.

4.4. An Example to Use the Program

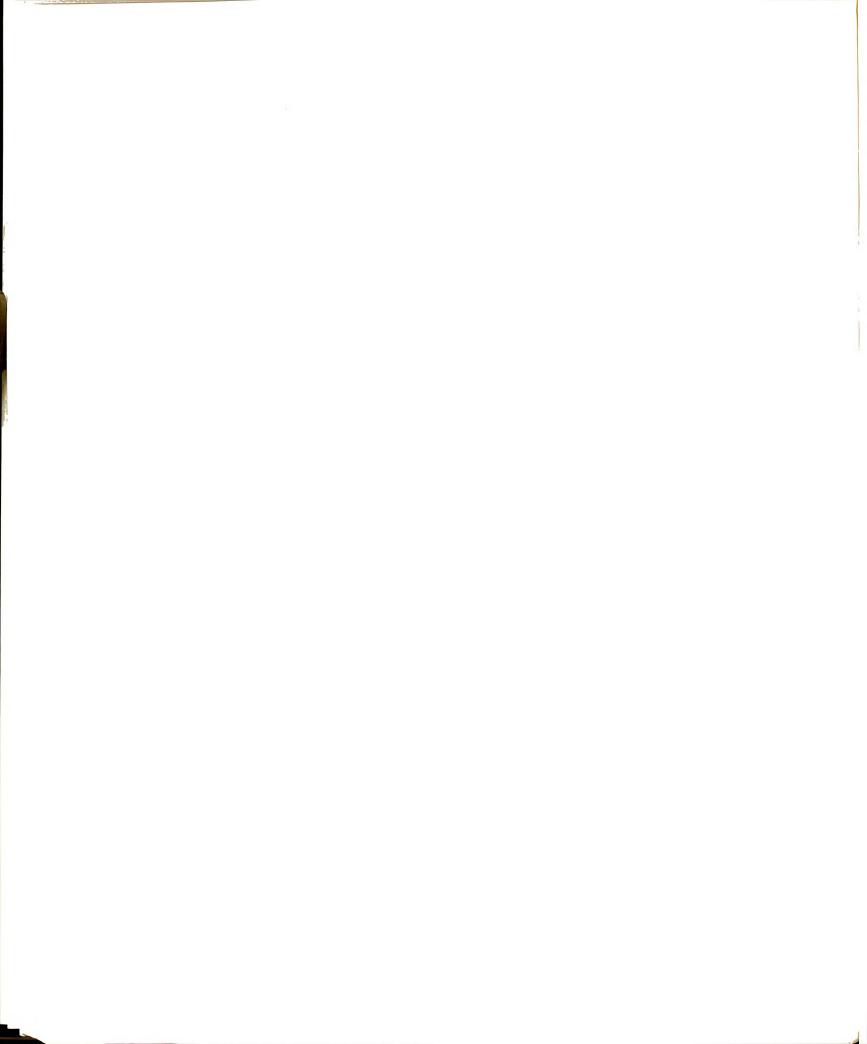
As an example, let us try to determine the electric field induced inside a circular cylinder, as shown in Figure 4.2. We assume that the body has radius 3 cm and



height 2 cm, and is immersed in a uniform magnetic field with an intensity of 1 A/m. Let us further assume that the frequency of the impressed magnetic field is 100 MHz, and the electrical parameters of the conducting body are $\varepsilon_{\rm r}$ = 71.7, σ = 0.889 S/m, and with a ring cross-section of 1 cm x 1 cm. With the aids of Section 4.3 and Table 4.1, the sequential order of the input data files is as follows:

File No.	Info	ormatio	on on	he Fi	Le	
1	6	100.0)		3 3	
2	18	0.0		0.	01	
3.1	1.0	1.0	1.0	1.0	71.7	0.88900E+00
3.2	2.0	1.0	1.0	1.0	71.7	0.88900E+00
3.3	3.0	1.0	1.0	1.0	71.7	0.88900E+00
3.4	1.0	2.0	1.0	1.0	71.7	0.88900E+00
3.5	2.0	2.0	1.0	1.0	71.7	0.88900E+00
3.6	3.0	2.0	1.0	1.0	71.7	0.88900E+00

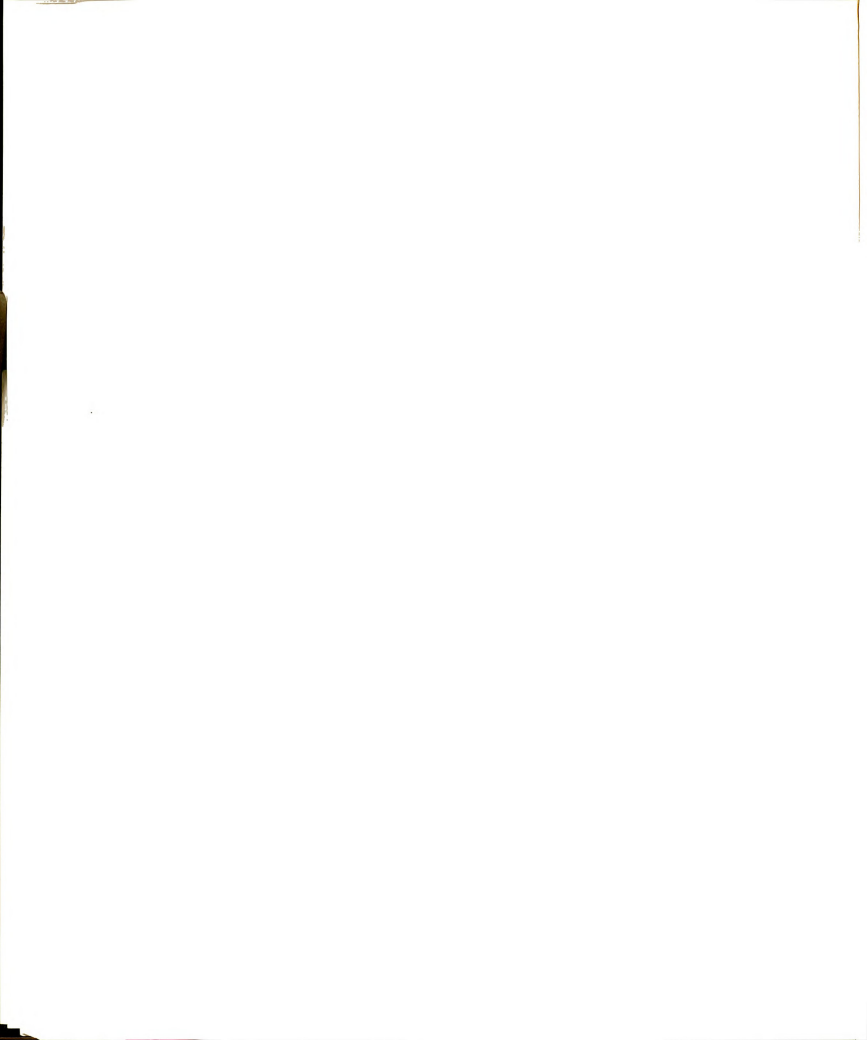
Now suppose that the program "EDDY" and the input data files are both stored on the magnetic disc under the permanent file names of "EDDYCURRENTEW" and "EDDYCURRENTDATA," respectively. In this case, the list of the commands needed for the execution of the program when submitted through a terminal interactively is as follows:



Statement No.	Its Purpose	Information in the Statement
1.	Job request	*JOBCARD*,CM170000, RG1,T600,JC1000.
2.	Dispose to engi- neering terminal	DISPOSE, **, V.
3.	Identification name	HAL, BANNER, LEE, EDDY, CURRENT.
4.	Calling subroutine DCADRE	HAL, LGO=DCADRE, UERTST.
5.	Calling the PF	ATTACH, EWFILE, EDDYCURRENTEW.
6.	Calling the EDITOR	EDITOR.
7.	Compile the program	FTN, I=Z, R, T.
8.	Return the EWFILE	RETURN, EWFILE.
9.	Calling the data	ATTACH, EWFILE, EDDYCURRENTDATA.
10.	Calling the EDITOR	EDITOR.
11.	Execute the program	LGO, W.
12.	End of Record	*EOR
13.	Change EWFILE to scope coded format	SAVE, Z.
14.	End of Record	*EOR
15.	Change EWFILE to scope coded format	SAVE, W, NS.
16.	End of file	*EOF

4.5. Printed Output

Now we would like to explain briefly the various sections of the output data files.



First, the coordinates of the maximum boundary limits on the x-z plane for each ring cross-section are listed, accompanied with the dimension and the cross-sectional area for each ring.

Then, the second output file contains the internally calculated coordinates for the central location of each ring cross-section, as well as the dielectric constant and the conductivity.

The third output file includes the information of the associated impressed electric field due to the impressed magnetic field of unit intensity. Also printed out is type of magnetic field applied.

The fourth output file has the information of the real and imaginary parts of the induced electric field inside each ring. Also included are the parameters used for numerical integrations, and the frequency of the impressed magnetic field.

The last output file is the induced electric field in magnitude and phase form, where the phase angles are in degrees.

An example print out of this program is shown in Table 4.2.

4.6. Listing of the Program

A FORTRAN listing of the program "EDDY" begins on page 175. Generally speaking, when compiled, the program "EDDY" requires about 46500B storage units of core memory.

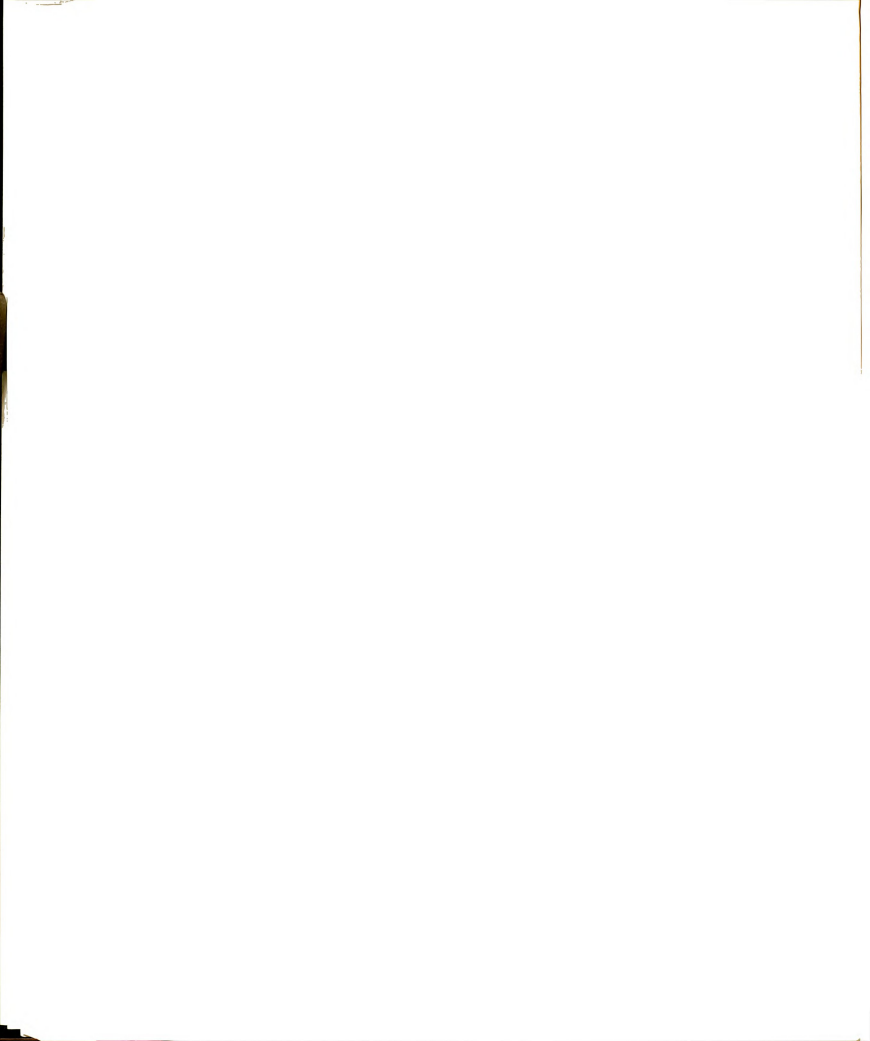


Table 4.2. Printed output of program "EDDY."

1 St. 4010 to 10 41 x	BN.AS WFLL AS	CR9-SIC ARTA OF	CACH PIYS ARE	THE COLUMN STORAGE WILL AS CRO-SEC ARTA OF CACH RIVS ARE SIVEN BELOW IN MERCAS
AF ND	25.15	V-01287910-X	7-0-10-10-10-1	
·10(603)01	1030301.	11.00011.	NOTS 1010-3	CRU-SEC AREA
.2000005-11	.1000001-01	1 - 1 - 1 - 1 - 1	10-10:0:	* 1 - 16 u 6 u . 1 *
.3300-21-41	.15.00001-11	- Transcr-	16-3665.01.	
.1000001-01	.2 GOUGE - 01	10-10-11	16-30.01-61	. 10-00 11-01
.2.6:0:51	10-1000012.		10-15-15-15-1	* 1 - 100 0 0 0 0 0 0 0 0 0 0 0 0 0 0 0 0
.36.0:0:1	.2 1 M9565-F1	11-1000-11	10-10-10-10-1	• 10-100E-03

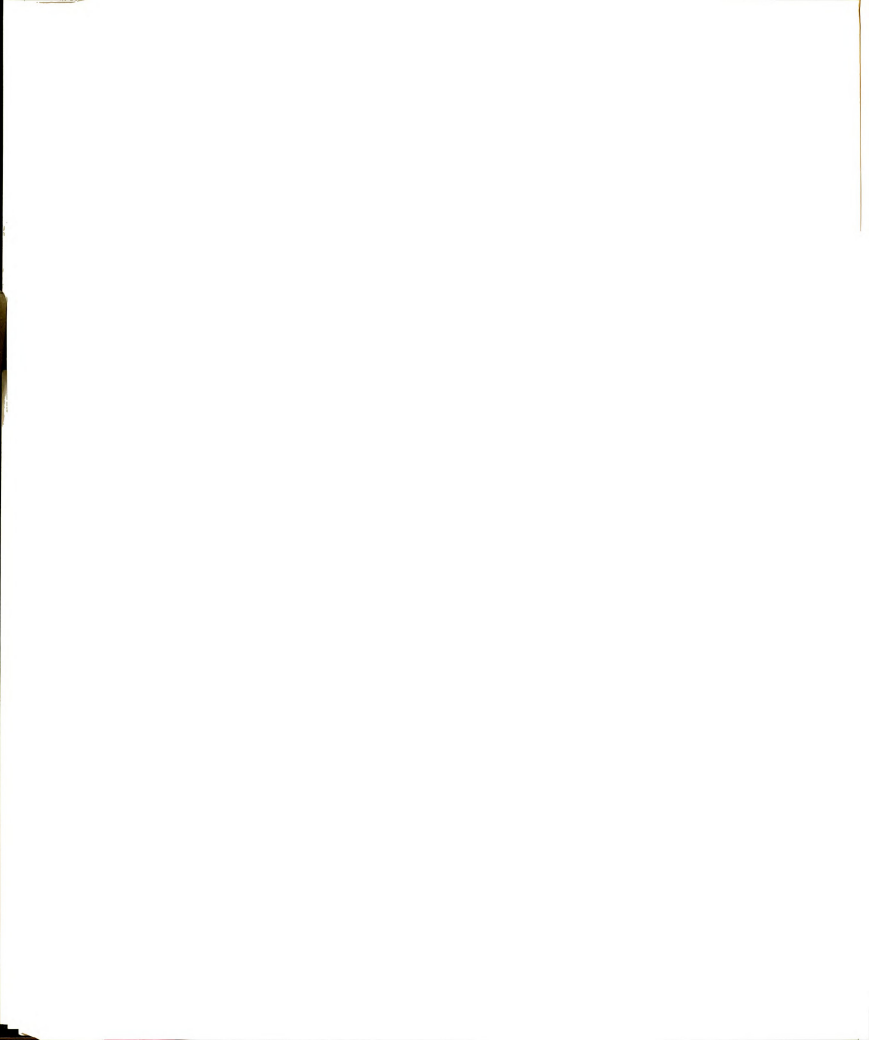


Table 4.2. (Cont'd.)

The Califold Incides As are as a control of fact the are all as a control of fact the are also as a control of fact the area of fact the are	AOF CIVIL	AUT or which are						
V KCKW	ACH RING							
V KTKN THESS TESS DILLIFORMERS V KTKN THESS DILLIFORMERS SECTION SEQUENCE TITON SECTION SECTION TITON SECTION SECTION TITON SECTION SECTION SECTION S	PPOPPRITES OF E	and an	**************************************	-883 E8 9E + 0 F	*869 C" BF +9 A	00+ 30 Jun 688*	*889 ** 21 * p.n	. 989 nn nr nn
	L AS TREETERS.	DIFLIT CONST.	-717cnar+:2	4717-9-18-32	\$ C+ 1.0 12 12 .	. 71 776 OE + #2	60.445.717.	
M XCFM HEIGES) - **RECFEEL** - **SECFEEL** - **S	LOCATION AS WEL	ZCLN (MF1ERS)	.5renege-02	.569639E-62	20-306001-02	115 1000 1	.150000-01	
	INE CENTRAL POINT	N XCFNC HETERS)	1 .500-000-02	35.00.01.	Cr-1006695.	5 .156299'- 1	6 .256(.001- 1	

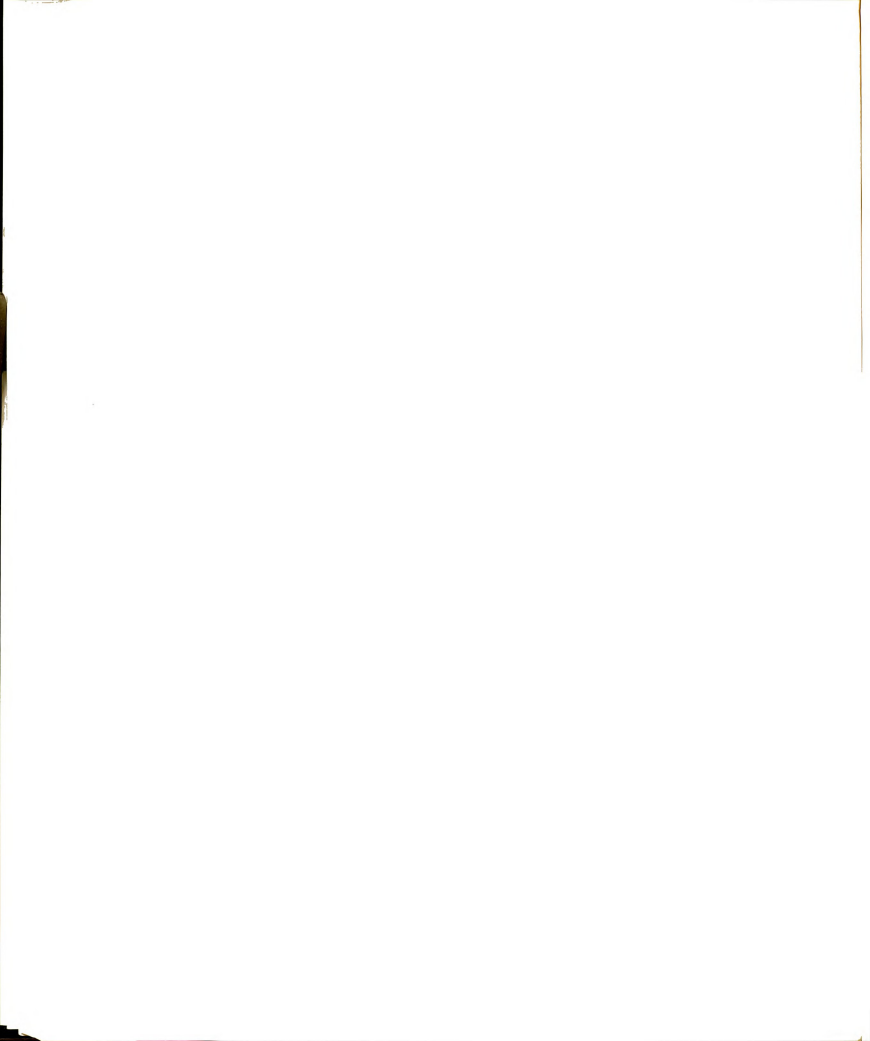


Table 4.2. (Cont'd.)

	2
	=
i	
	e e
	_
ć	-
-	
_	
2	
2	
-	
į	
2	
-	
2	
Ξ	
3	
6	
=======================================	
_	
E	
A G	28
Ξ.	=
12.0	137
25	7.
-	-
-	7
Ē	_
5	i a
=	5
10	T.
C.I.R	553
, LL	E.
ري د:	INFRESS ELECTRIC FIELD COLTS/METER)
P.R.E	
THE IMPRESS (LLEGIRIC FIFLD DUF TO TUCNOFUL MAGNETIC FIFLD CWITH UNIT TUCHDENT FLECIBLE FIFLDS, 15 15 55	
H	
	-

1836	5239448-62	1571876-1	13-30.6166	52 39565 52	15/1871- 1	
B! A!		• .	• _C	٠	٠	
	-	۲.	•	4	'n	,,

THE BODY IS IMMERSED IN AN UNIFORM MAGNETIC FIFED

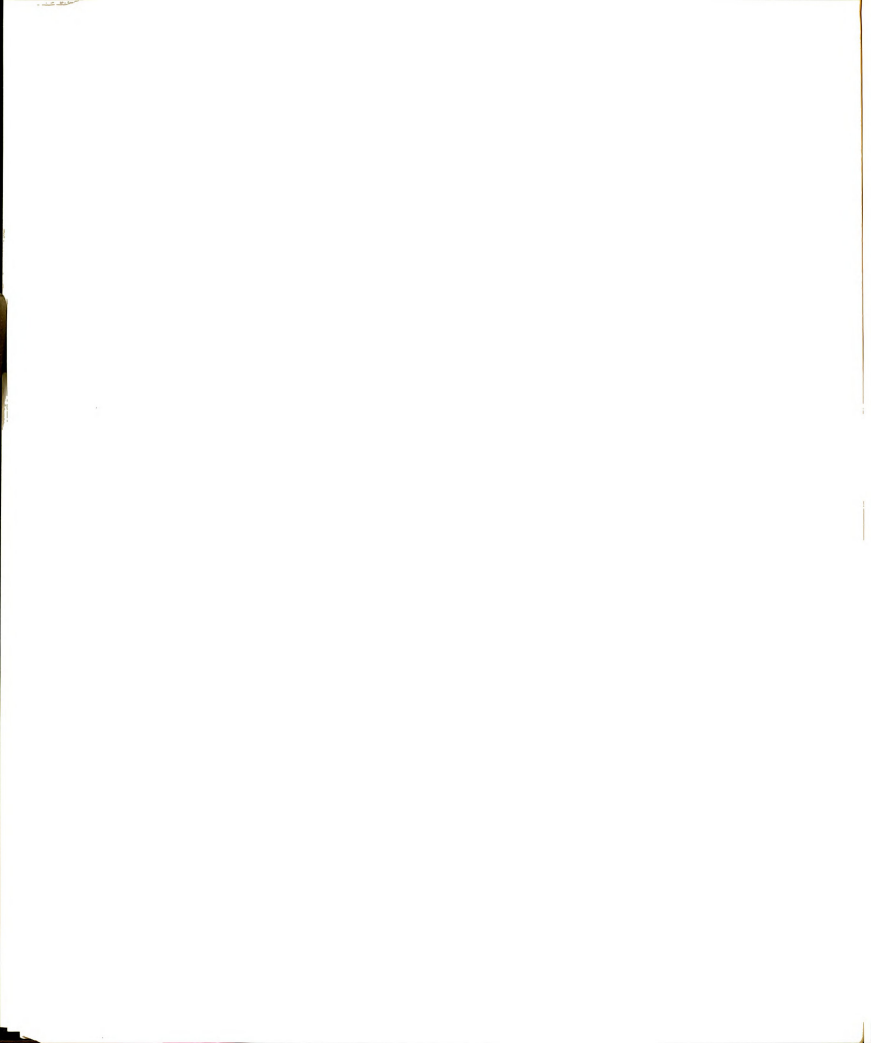
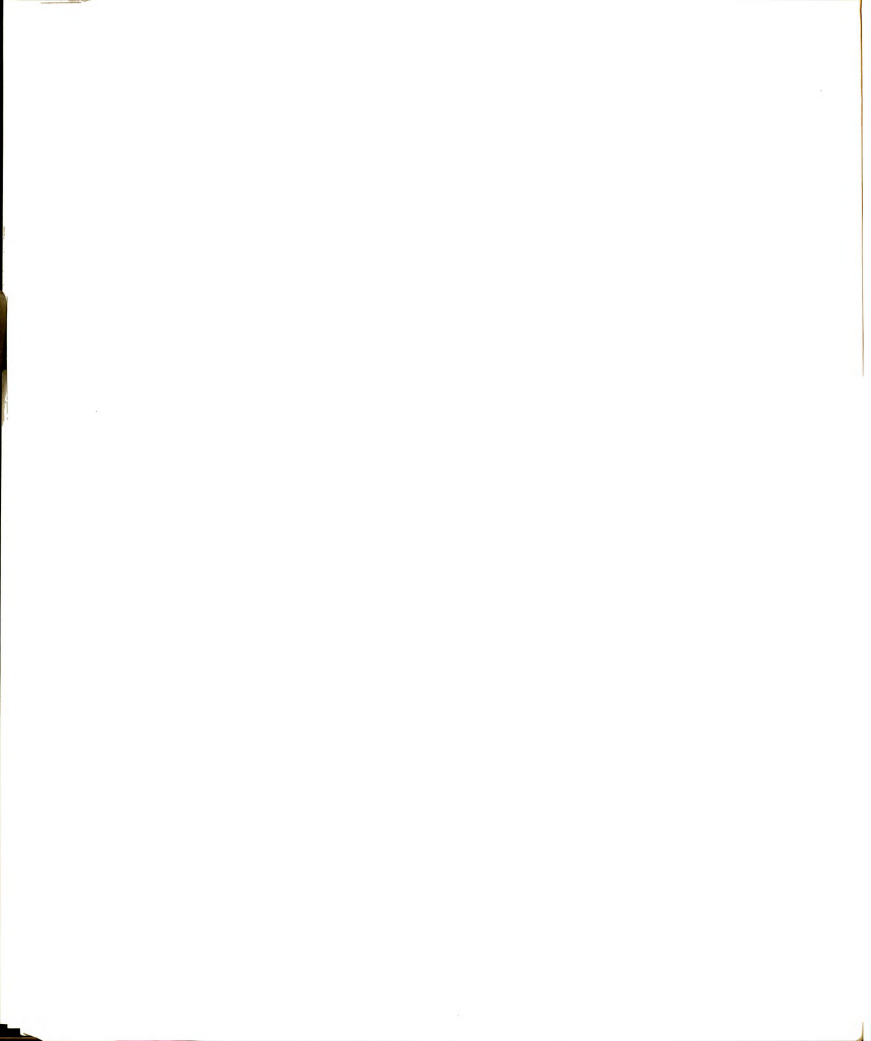


Table 4.2. (Cont'd.)

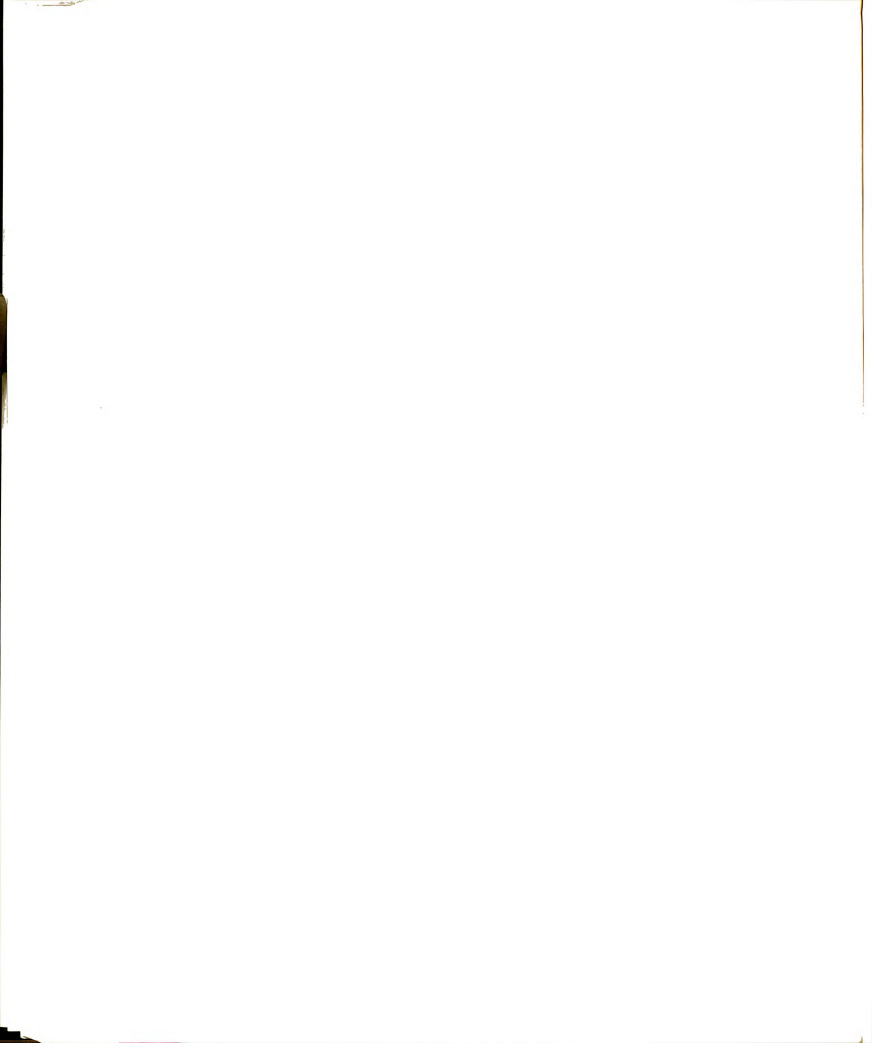
THE IMPULID ELECTRIC CITED IS 19 AZIMUTIAL DIRECTION. THE ESTIMATED VALUES AT COVIRAL OF FACH SUICREF FRE GIVEN SELVE THE FREQUENCY BEING USED IS TICK-RANGURMIZAZIRG TO PT GEING DIVIDID TOTAL TOSUCIUTENALS MURTO MUMERICAL INTEGRALITY *019' BEFLATIVE (3R)R CTRUUCED-TRAGENOLISZMETER) --5793565-02 -- 1c 1333F-31 Iu-1986995*---578379L-02 --1,1933--91 THE INTEGRATIONS INVOLVED RETAIN 5.0000AHSOLUTE FRROR AND ZOR FINDUCED-REAL CVOLTS/WLTLE) - TR4671 - 17 -- 1074701-12 -- 1174045-62 - 11 1 4 705 - 112 -.117494r- 2 - . - 37 HARTE - . 7



(Cont'd.) Table 4.2.

N ETHONGED-WAGDEVOLLS/HETER) FTHRUCEN-PHAS										
	2	2	- WA	110		:	-		-	
		0.1.	-		5					

	E IMDUCED-MACHEVELIS/HETER)	FINDUCID-PHASE(IN DESREES)
1	\$ 5376281-12	0441214E+60
~	1.13466-11	2-1257046+02
к.	.2468357-11	925240F+02
4	6 1867624*	c0+16I2.4c+-
r.	.1617467-1	735704F+02
١.	***************************************	-+ 925241 +112



PART 2

A USER'S GUIDE TO COMPUTER PROGRAM FOR INDUCED
EM FIELD ON THE SURFACE OF A FINITE CONDUCTING
BODY WITH ARBITRARY SHAPE

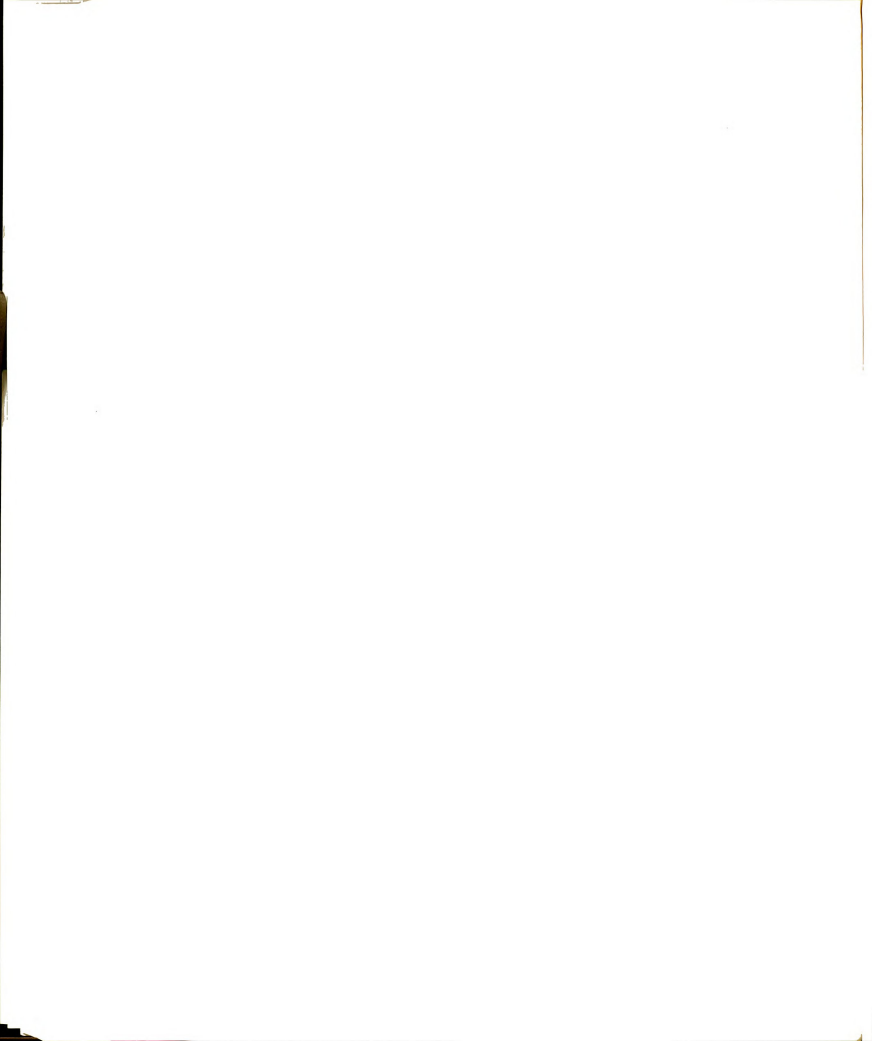
The purpose of Part 2 is to explain the computer program used for quantifying the EM field induced on the surface of a finite conducting body when illuminated by an incident plane wave. The theoretical derivation and the development of this numerical technique have been discussed in Chapter III. Besides explaining the usage of this program, we will also present an example accompanied with a sample print out for the purpose of better understanding.

4.7. Formulation of the Problem

We are considering a finite conducting body illuminated by an incident wave which, for the purpose of simplicity, has been assumed to be a plane wave. Mathematically, the incident plane wave can be expressed in the following form:

$$\begin{split} \dot{\vec{E}}^{i}(z) &= \hat{x}e^{-jz} = \hat{x} \; [\cos(z) - j \; \sin(z)] \\ \dot{\vec{H}}^{i}(z) &= \hat{y}\frac{1}{\eta_{o}}e^{-jz} = \hat{y}\frac{1}{\eta_{o}}[\cos(z) - j \; \sin(z)] \end{split} \tag{4.1}$$

We like to mention a few points concerning the above expressions:



- The wave is propagating in the +z direction, and has a time factor exp(jwt) which is suppressed.
- 2) All quantities with the dimension of length are normalized by $1/k_{_{\rm D}}$.
- The incident electric field has unit intensity,
 V/m.
- 4) η_0 is the intrinsic wave impedance of free space.

The first step in utilizing this program is the numerical formulation of the problem; hence, the first thing to do is to visualize the shape, dimensions and the orientation of the conducting body with respect to the incident electromagnetic wave. The incident wave may illuminate the body either at normal incidence or at end-on incidence. To begin with, the body surface is divided into NCELL surface cells with NX, NY, NZ, NNX, NNY, and NNZ cells facing the positive-x, positive-y, positive-z, negative-x, negative-y, and negative-z directions, respectively. Each surface cell is a square with suitable dimension in order to obtain optimum results.

The maximum number of unknowns that can be handled is about 150. Since there are four unknowns for each surface cell, the maximum number of surface cells, without any simplifications, can not be greater than 40. This imposes a restraint on the physical size of the body. But, due to the symmetrical properties which exist in most of the bodies we are considering, it seems adequate to

apply these properties and reduce the number of unknowns by a factor of 4 or 8. It must be mentioned here that in order to apply symmetrical conditions the incident wave has to be decomposed into four different modes named COSE, COSH, SINE, and SINH, respectively, as can be understood from eq. (4.1). The above-mentioned symmetry conditions are justifiable since most of the bodies considered (either biological bodies or other finite conducting materials encountered in engineering) possess four or eight similar-looking segments and hereafter called quadrants, such that it is sufficient merely to calculate the induced electromagnetic field at each surface cell of the first quadrant and then convert them into the induced field for the rest of the body.

After determining the symmetry conditions, the next step in the numerical formulation of the problem is the specification of the location of each surface cell, its physical dimensions, and the electrical parameters of the body. The size of each cell can vary but the electrical properties are assumed to be uniform throughout the body. Note that the central location of each surface cell is predetermined by the user; then the incident field intensities are automatically evaluated for each cell.

4.8. Description of Computer Program

This program is also coded in standard FORTRAN and can be compiled on either FTN or MNF compilers. The program is symbolically named as "SURFLDS" with input and output formats on any undefined logic units in conjunction with four magnetic tapes, "TAPE1," TAPE2," "TAPE3," and "TAPE4." "TAPE1"-"TAPE4" are the names of the local files which are used to temporarily store the computed results due to COSE, COSH, SINE, and SINH components of incident field.

Program "SURFLDS" makes use of the following sub-programs:

- "MNSB"--is a subroutine mainly used to print out the echo information which includes all the messages just read in from the input data files by the main program.
- "MATRI," "LEE"--are subroutines which generate the matrix of the linear equations set. The matrix elements are related to the associated Green's functions evaluated at various locations.
- "ELEMY," "ELEMY," and "ELEMZ"--are subroutines which evaluate the matrix elements when source points are in the ±x-, the ±y-, and the ±z-directed surfaces, respectively. In these

subroutines, the symmetry conditions have been imposed.

- "EXIM," "CEIM," "CHIM," "SEIM," and "SHIM"--are subroutines which calculate the incident electric
 and magnetic fields for EXPZ, COSE, COSH,
 SINE, and SINH modes, respectively. In these
 subroutines, the incident electric field is
 polarized in the +x direction and has unit
 intensity, 1 V/m.
- "T"--is a subroutine which converts the equivalent surface currents to surface field quantities.
- "PRNT"--this subroutine, as the name suggests, is a program used to generate the print out.
- "COEFX," "COEFY," "COEFZ," "FCNXX"-"FCNZZ," and
- "CEFXX,"-"CEFZZ," etc.--are subprograms which evaluate
 the elements of the Tensor Green's function.
- "CMATP"--is the program being used to solve a system

 of N equations in N unknowns. It is actually

 a Gauss-Seidel method of numerical technique.

A listing of the program "SURFLDS," including all the subprograms called, is given at the end of this chapter. In the next section, the structure of the input data files as well as the associated input variables are explained in detail.

4.9. Data Structure and Input Variables

Figure 4.3 shows a sample body with finite conductivity. With origin of the coordinate system being chosen at the center of the body, we divide it into eight different sections which are called quadrants. The numbering system used is also shown in Figure 4.3. Note that the symmetry conditions exist if the physical dimensions of each surface cell in the first quadrant are the same as their counterparts in other quadrants, which is the case for this sample body because we assume that all the surface cells have the same physical dimensions. Based on these existing symmetry conditions, we only intend to solve for the induced electromagnetic fields at various surface cells of the first quadrant and then convert them into the fields induced at the surface cells on the rest of the body. Now we like to introduce the input data files before we go any further in determining the induced surface field. First of all, the sequential structure of the data files, the format specifications and the symbolic names of the variables appearing on each file are outlined in Table 4.3.

There are totally five input data files. Only the fourth data file contains NCELL data cards, while the rest of the data files contain one data card each. The input variables associated with these input data files are discussed in detail as below:

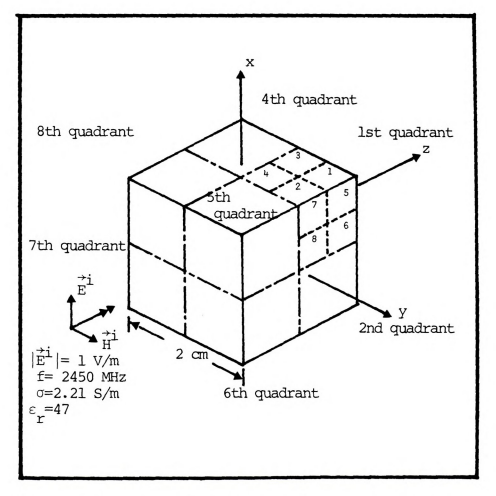


Figure 4.3. A cubic biological body (σ = 2.21 S/m, $\epsilon_{\rm Y}$ = 47) with dimensions of 2 cm x 2 cm x 2 cm is irradiated by an incident plane wave which has a frequency of 2.45 GHz and a unit intensity, x-polarized electric field. The body surface is subdivided into 95 surface cells with dimensions of 0.5 cm x 0.5 cm.

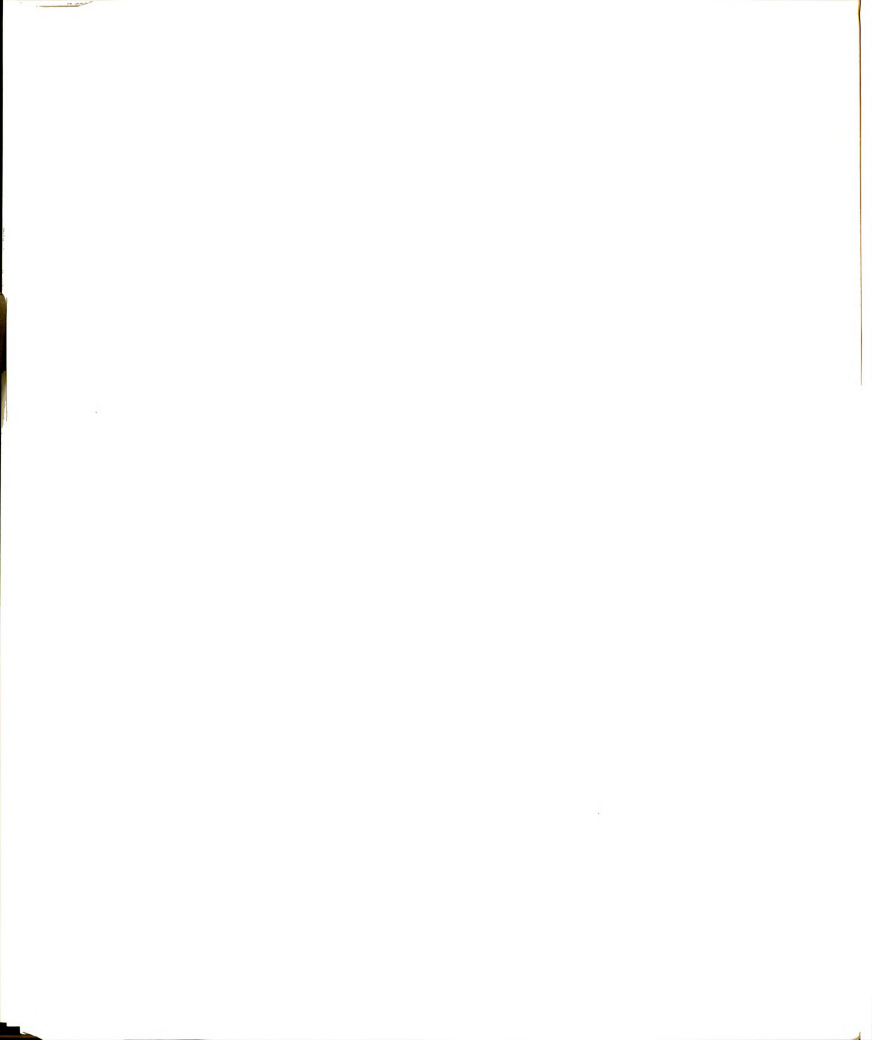
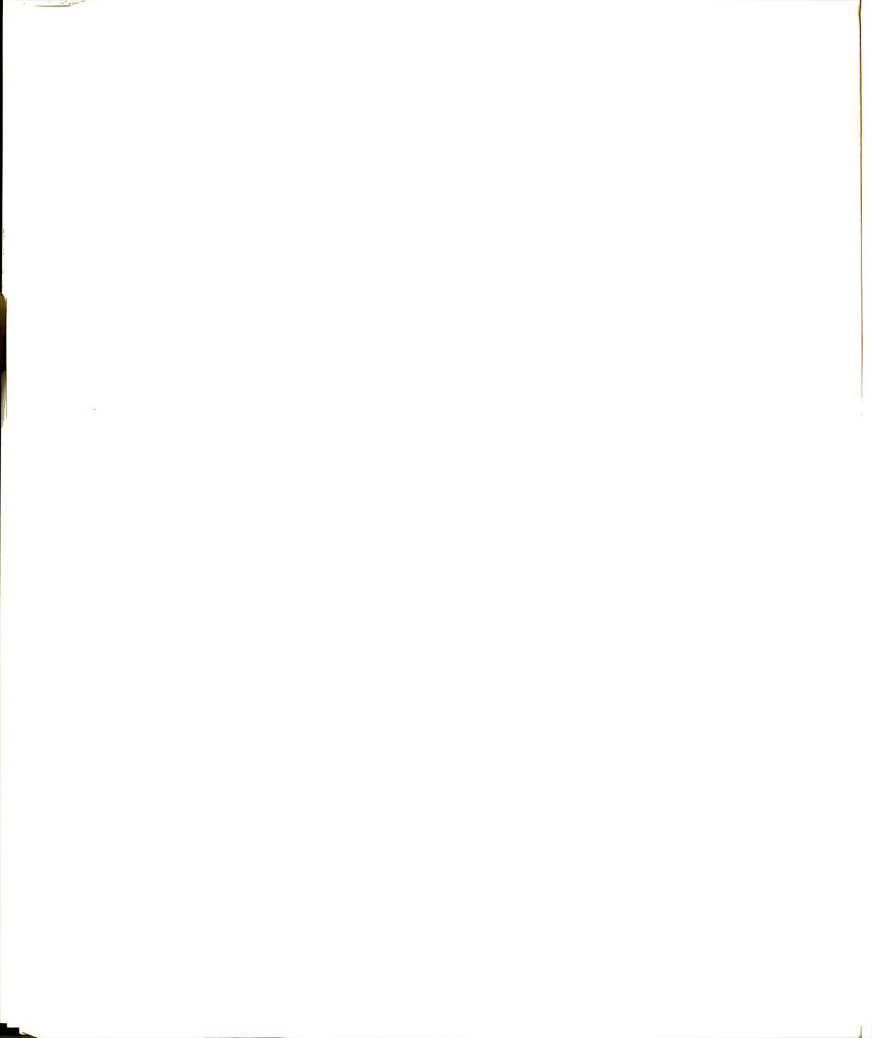


Table 4.3. The symbolic names of input variables and corresponding specifications for the data files used in data structure for the program "SURFLDS."

File No.	Card No.	Symbolic Name	Columns	Format
1	1	NDIV	1-2	12
2	1	IQ	1-4	I 4
3	1	NX	1-3	13
		NY	4-6	13
		NZ	7-9	13
		NNX	10-12	13
		NNY	13-15	13
		NNZ	16-18	I3
4	1-NCELL	Х	1-10	F10.5
		Y	11-20	F10.
		Z	21-30	F10.5
		DCELL	31-40	F10.5
5	1	RLEP	1-13	E13.6
		SIG	14-26	E13.6
		FMEG	27-39	E13.6
		MODE	40-43	A4



First Data File

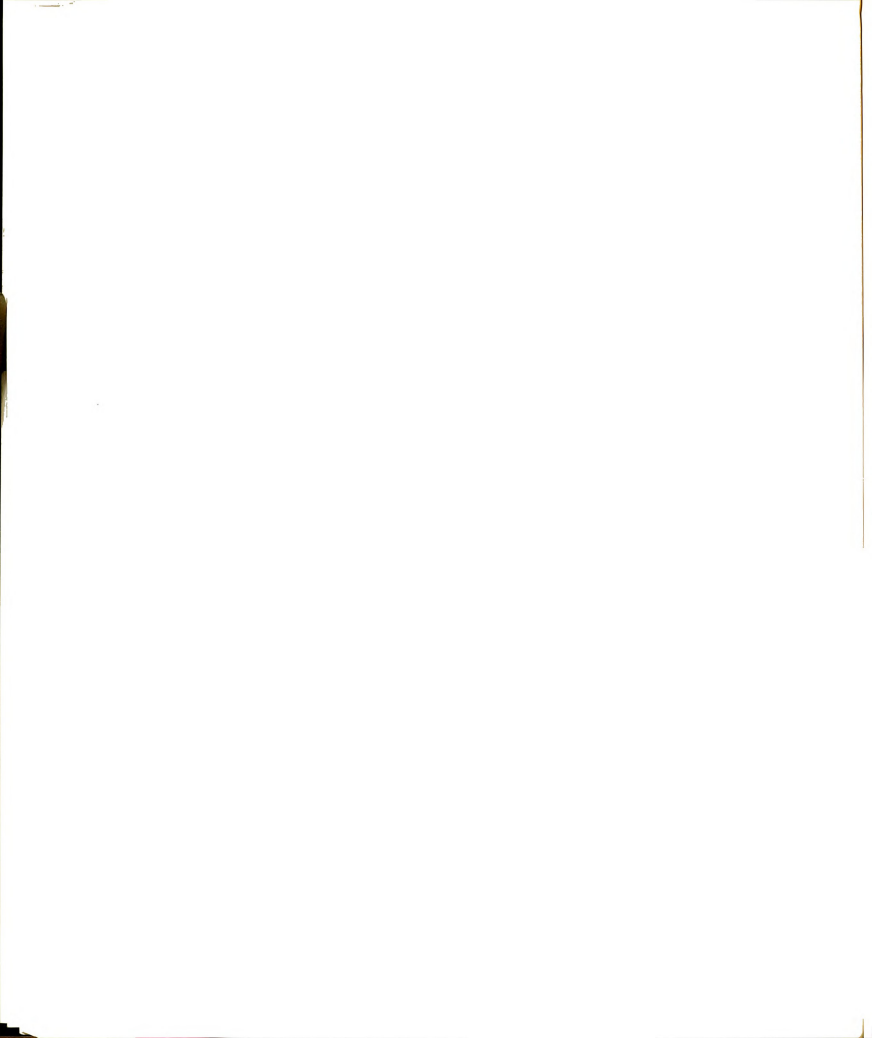
This file has only one data card with only one variable on it; namely, NDIV. NDIV is the number of subdivisions each side of the square surface cell will be divided into when the numerical integration over the surface cell is performed. The purpose of subdividing the surface cell is to improve the accuracy of the results. But the computational cost increases substantially when the value of NDIV goes up.

Usually, we find that NDIV with value 3 gives excellent results and still keeps the required CPU time reasonably low. For the case of NDIV=3, each surface cell is subdivided into nine subsurface cells when numerical integration is carried out by the computer.

Second Data File

This data file has only one data card which defines a variable with symbolic name IQ. IQ is a four-digit code of the symmetrical property used. There are four different types of symmetrical property that can be handled by this program, as described in the following:

- IQ = 0008 This is for the case of an eight-quadrants symmetrical body.
- IQ = 1234 This is used when the body has symmetry with respect to the y-z plane and the x-z plane.



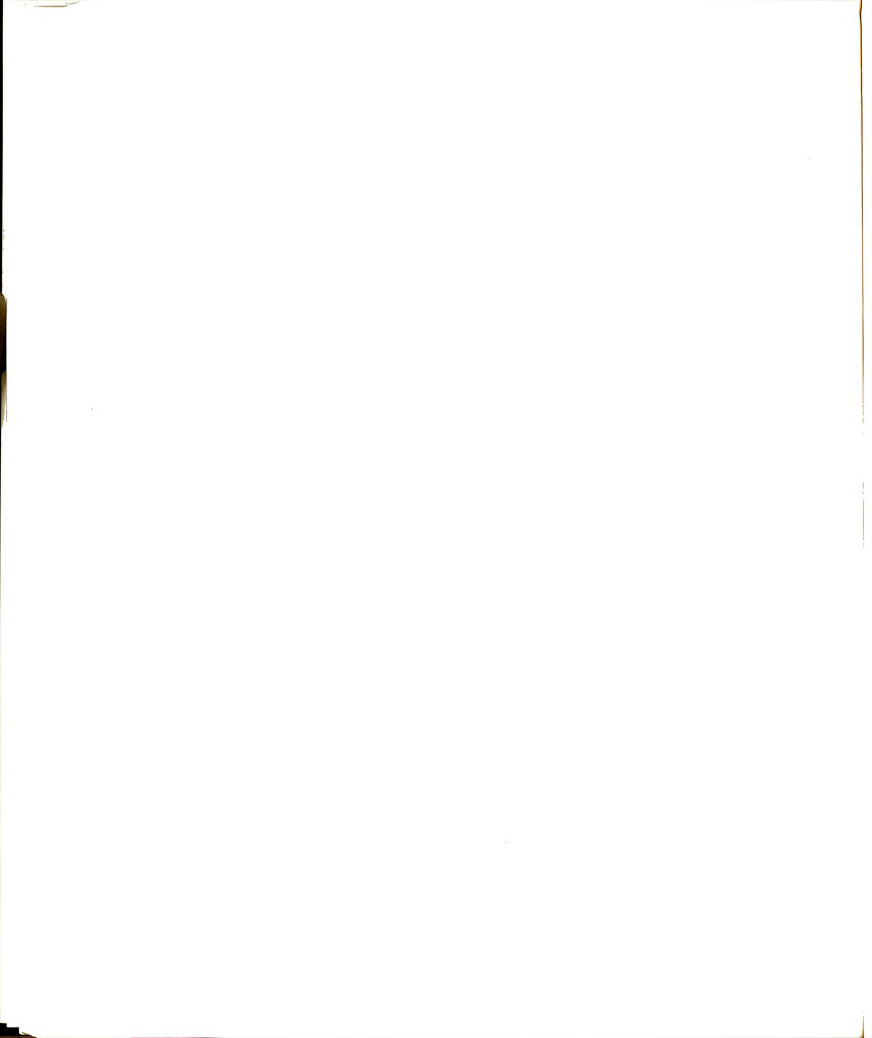
- IQ = 1458 This is used when the body considered has symmetry with respect to the x-y plane and the x-z plane.
- IQ = 1256 This is used when symmetry properties with respect to the x-y plane and the y-z plane exist.

Third Data File

This file has only one data card which defines six integer variables, NX, NY, NZ, NNX, NNY, and NNZ. These six integers are the numbers of surface cells on the +x, the +y, the +z, the -x, the -y, and the -z-directed surfaces of the first quadrant, respectively. The total number of surface cells of the first quadrant, NCELL, is obtained by summing up all these six integers.

Fourth Data File

This data file consists of NCELL data cards; i.e., one data card for each surface cell. On each data card, it defines four real variables, X, Y, Z, and DCELL. Where X, Y, Z are the coordinates of the central location for each corresponding surface cell with reference to the origin, while DCELL is the dimension of the corresponding surface cell. Note that these quantities are in centimeters.

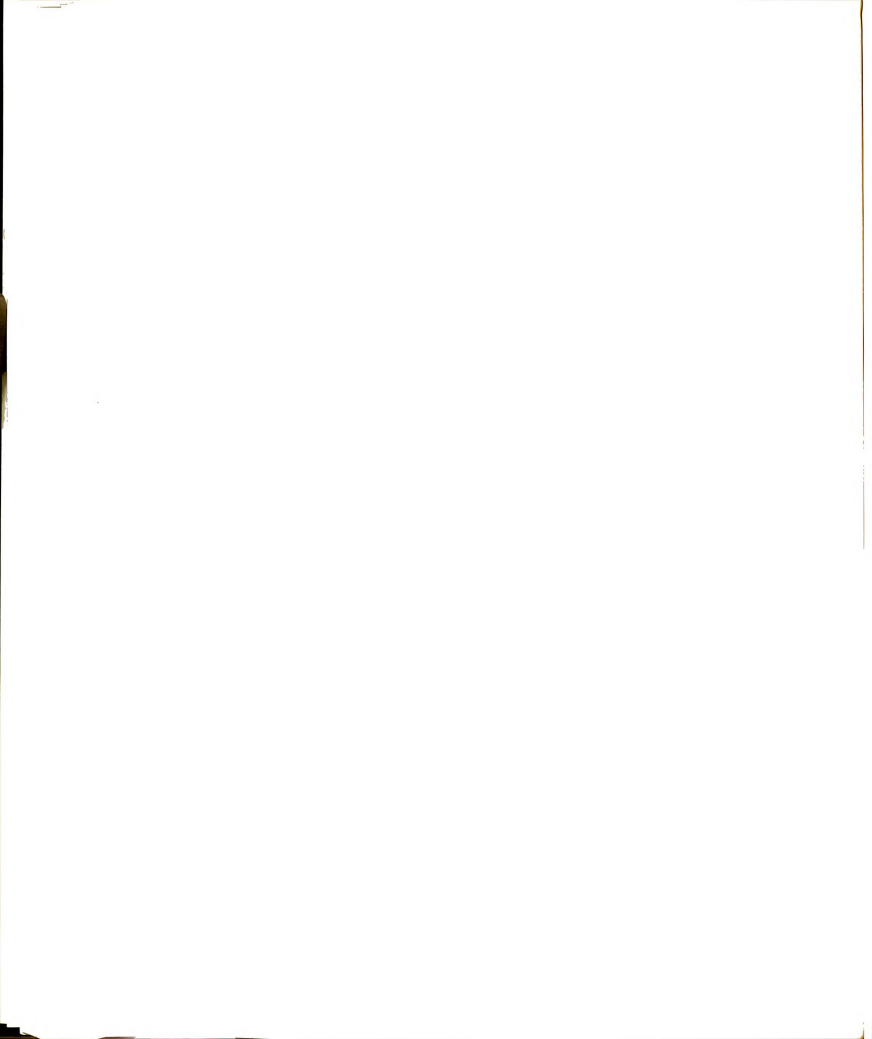


Fifth Data File

This data file consists of one data card with four variables defined on it. The first three variables, RLEP, SIG, and FMEG, are specified under El3.6 format. RLEP is the symbolic name for dielectric constant, and SIG is that for conductivity in S/m, while FMEG stands for frequency in terms of MHz. Finally, the last variable of this last data file is symbolically named MODE, which is read in under format A4 and may have one of the following values:

- "EXPZ"--is a four-letter code for plane wave which has complex exponential variation in z direction.
- "COSE"--is the code for incident field which has only the x-component of E field with cosine variation in the z direction.
- "COSH"--is the code for incident field which has only the y-component of H field with cosine variation in the z direction.
- Similarly, "SINE" ("SINH")--is the code for incident field which has only the x-component (the y-component) of E (H) field with sine variation in the z direction.

Obviously, the effect of EXPZ is equivalent to the combined results due to COSE, COSH, SINE, and SINH. As we have mentioned, the reason of dividing a plane wave into

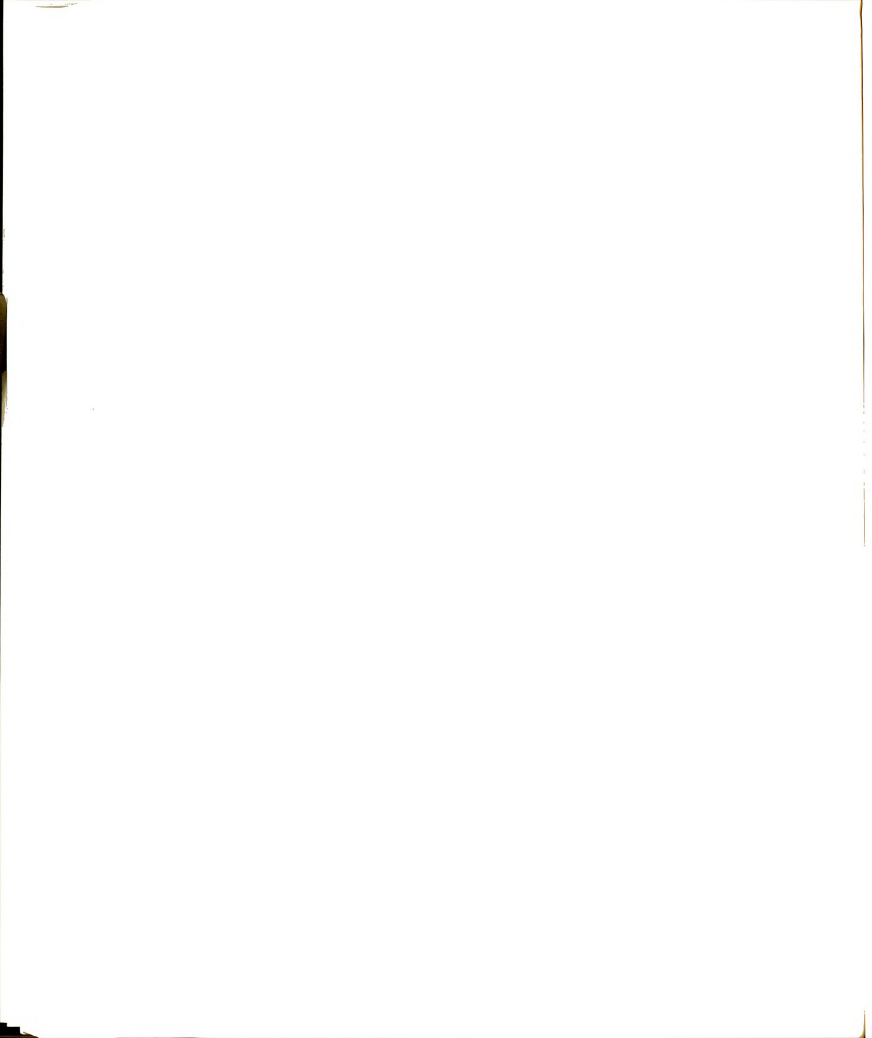


four different modes is for the purpose of applying symmetry conditions to a symmetrical body.

We have explained all the details about the input data files in this section. Now we are ready to use "SURFLDS" to solve for the EM field induced on the surface of an arbitrary body. An example is worked out in the next section.

4.10. An Example to Use the Program

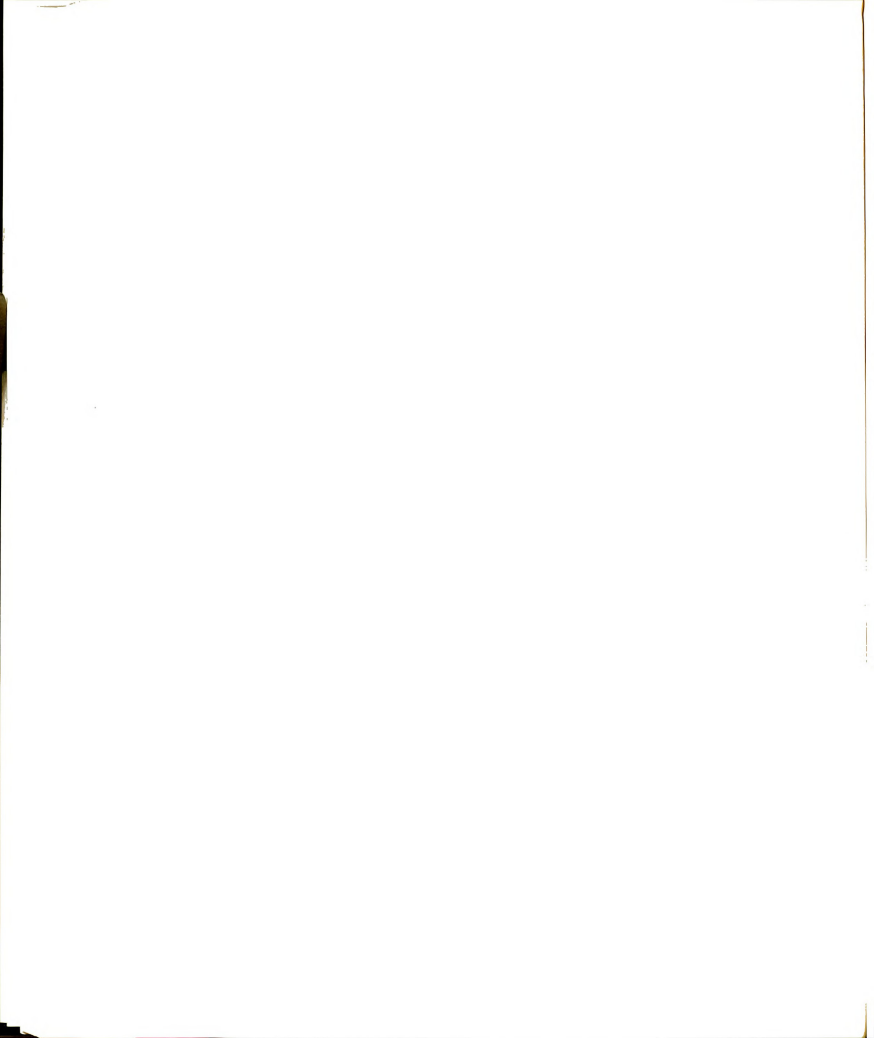
As an example about the usage of the program "SURFLDS," let us again consider the case of a cube illuminated by a plane wave as shown in Figure 4.3. We assume that the cube has dimensions 2 cm x 2 cm x 2 cm. and is constructed with a material with the following electrical parameters at the frequency of 2.45 GHz: $\sigma = 2.21$ S/m, ε_{m} = 47. The cube has eight-fold symmetry, such that it can be divided into eight different quadrants. Although the same problem can be solved by dividing the body into four quadrants, for the purpose of demonstrating the logic of decomposing the plane wave into four separate modes, we apply eight-quadrant symmetry conditions to this body. We further divide each surface of the first quadrant into four surface cells, such that there are totally 12 surface cells (or totally 48 surface unknowns) to be considered, where each of these surface cells has dimensions of 0.5 cm x 0.5 cm.



As mentioned previously, since the incident plane wave is decomposed into COSE, COSH, SINE, and SINH modes, we have to run the program in four parts—one for each constituting mode of the incident wave. The results due to each incident mode will be buffered into a logical unit with one of the following logical names, "TAPE1," "TAPE2," "TAPE3," and "TAPE4." And then the results contained within these units will be appropriately combined in order to obtain the true EM fields induced on the surfaces of the first and the fifth quadrants.

With the help of Section 4.9 and Table 4.3, we can easily list the input data files for the case of COSE incident mode as follows:

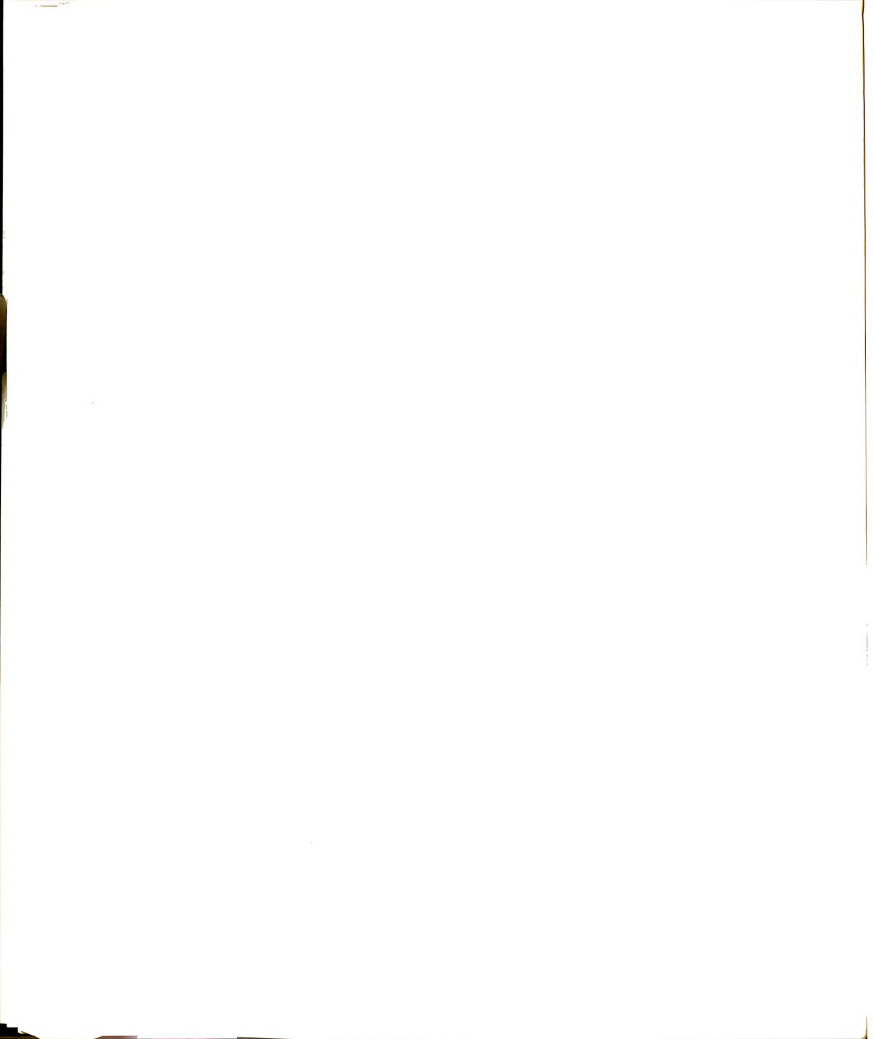
File No.	Infor	rmatio	n on t	he File		
1	03					
2	8000					
3	004	004	004	000	000	000
4.1	1.0	0.	.75	0.75	0.	5
4.2	1.0	0.	.75	0.25	0.	5
4.3	1.0	0.	.25	0.75	0.	5
4.4	1.0	0.	25	0.25	0.	5
4.5	0.75	1.	0	0.75	0.	5
4.6	0.25	1.	0	0.75	0.	5
4.7	0.75	1.	0	0.25	0.	5
4.8	0.25	1.	0	0.25	0.	5



5	47.0000	000E+00	2.210000E	+00	2.450000E+03	COSE
4.12	0.25	0.25	1.0	0	.5	
4.11	0.75	0.25	1.0	0	.5	
4.10	0.25	0.75	1.0	0	.5	
4.9	0.75	0.75	1.0	0	.5	

Now we assume that both the program "SURLDS" and the input data files are already stored in different permanent files with "SURFACEEW" and "SURFACEDATACOSE" as permanent file names, respectively. In this case, the commands needed in order to submit the job through the interactive terminals should be as follows:

Statement No.	Information in the Statement
1.	*JOBCARD*,RG1,JC1000,T600,CM170000.
2.	DISPOSE, **, V.
3.	HAL, BANNER, LEE, SURFLDS, 8SYMM, COSE.
4.	ATTACH, EWFILE, SURFACEEW.
5.	EDITOR.
6.	ATTACH, A, SURFACEB.
7.	FTN, I=Z,R,T.
8.	COPYL, A, LGO, B.
9.	PURGE, A.
10.	CATALOG, B, SURFACEB, RP=999.
11.	RETURN, EWFILE.
12.	ATTACH, EWFILE, SURFACEDATACOSE.
13.	EDITOR.



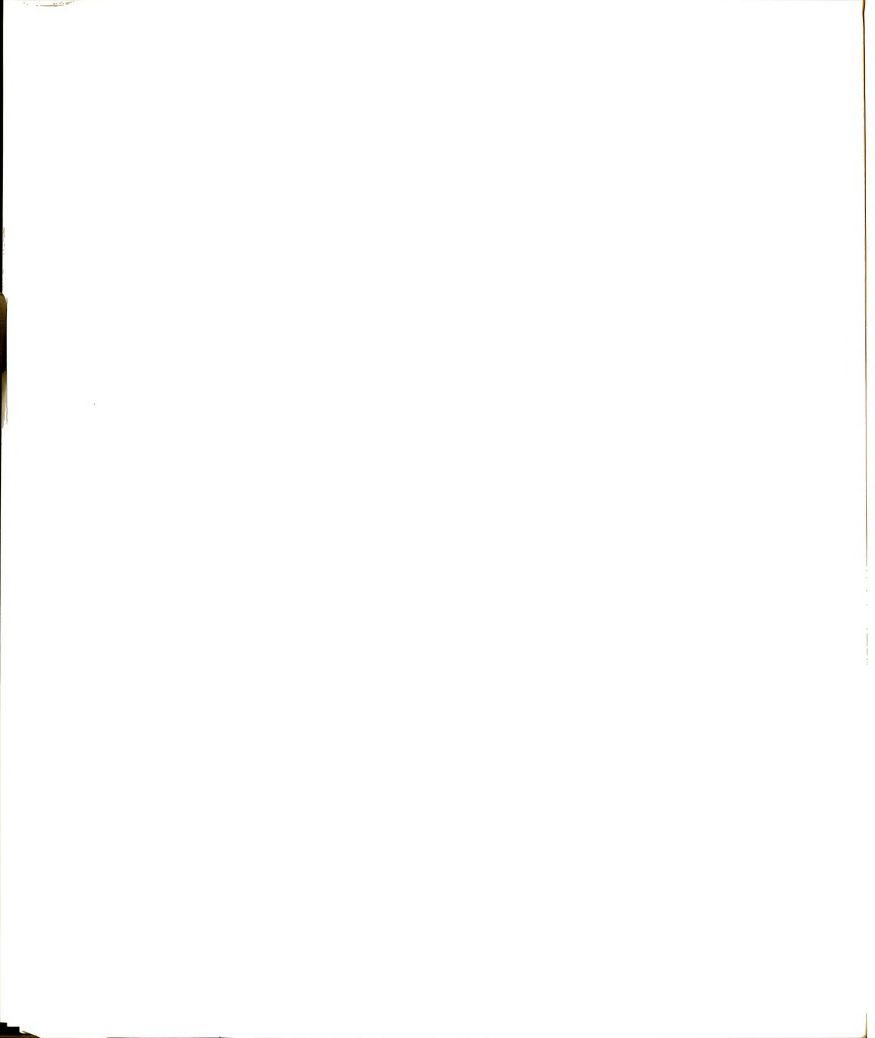
14.		
14.	B.1	iJ.

- 15. CATALOG, TAPE1, SURFACEDUETOCOSE.
- 16. *EOR
- 17. SAVE, Z, 100-780.
- 18. *EOR
- 19. SAVE, W, NS.
- 20. *EOF

There are several points we like to mention about the above job:

- 1) We assume that the program "SURFLDS" has been compiled, and the compiled binary codes are already stored in a file with permanent file name "SURFACEB."
- We don't have to recompile the whole program each time we use it. If the array dimensions have been changed, the only section that needs to be recompiled is the main program.
- 3) The computed induced surface fields are buffered out to TAPE1, and then cataloged as a permanent file named "SURFACEDUETOCOSE."

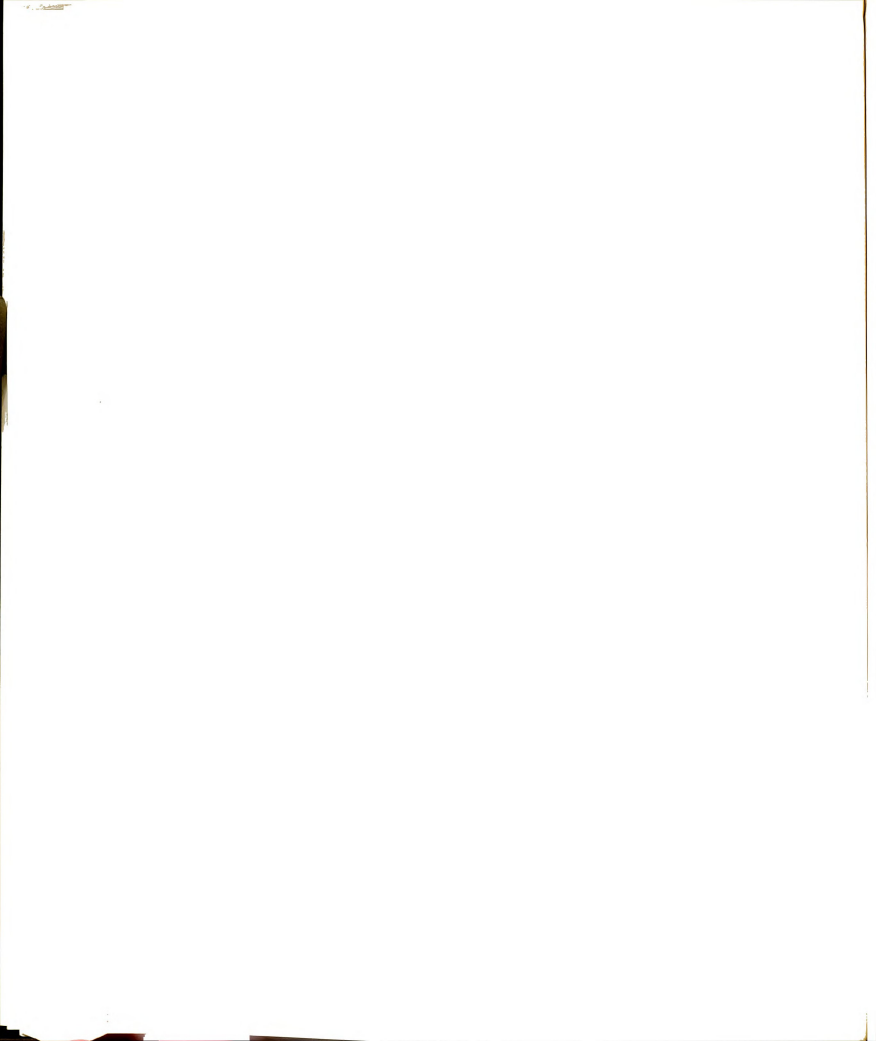
So the results due to COSE mode of incident field have been obtained and stored into "SURFACEDUETOCOSE." To obtain the results due to the other three incident modes, the same program has to be rerun three more times with the only change in the last data file where the correct code



for the incident mode must be used. For example, when COSH mode is considered, the program can be executed without any recompilation by the use of the following commands:

Statement No.	Information in the Statement
1.	*JOBCARD*,RG1,JC1000,T600,CM170000.
2.	DIPOSE,**,V.
3.	HAL, BANNER, LEE, SURFLDS, 8SYMM, COSH.
4.	ATTACH, A, SURFACEB.
5.	ATTACH, EWFILE, SURFACEDATACOSH.
6.	EDITOR.
7.	A,W.
8.	CATALOG, TAPE2, SURFACEDUETOCOSH.
9.	*EOR
10.	SAVE, W, NS.
11.	*EOF

After obtaining results for all four different modes and creating four different permanent files for them separately, we are now in a position to combine these results in such a way so as to yield the total induced surface fields on the body surfaces. Another program called "COMBINE" has been written for this purpose. Program "COMBINE" has output including the magnitude and phase information of the total surface fields in quadrants 1 and 5. The surface fields on the rest of the body, either

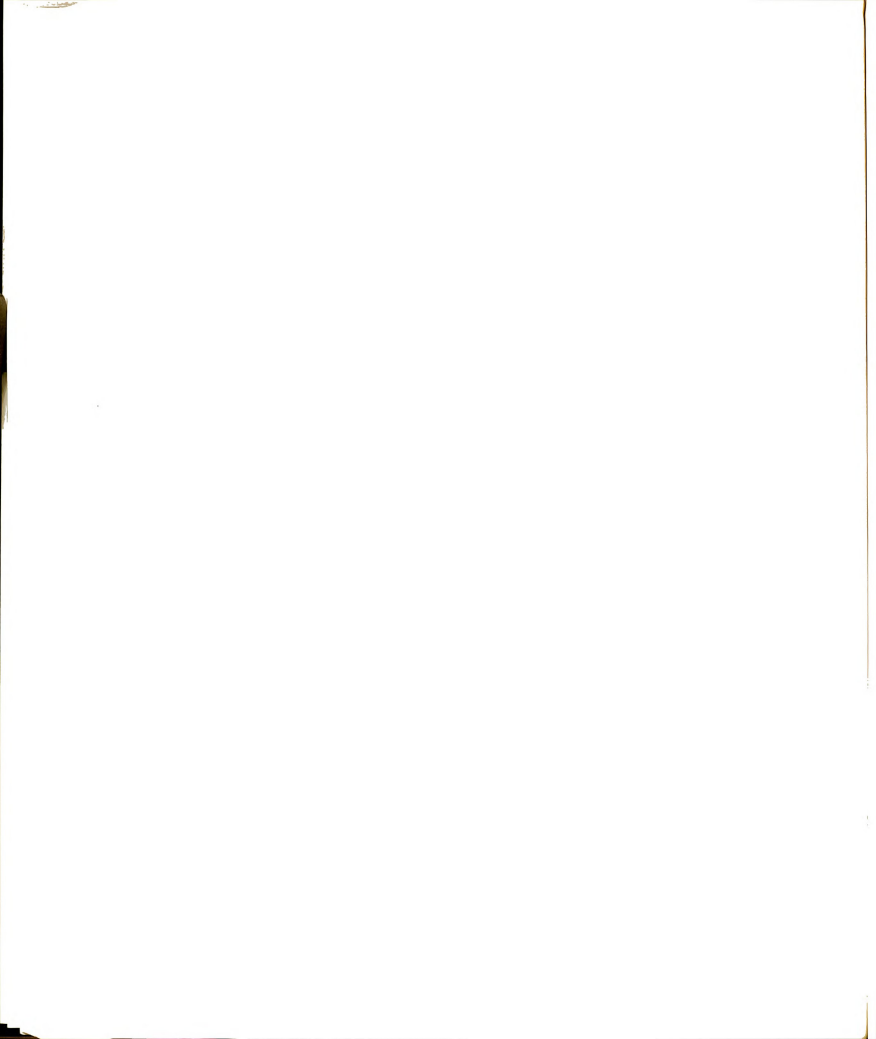


magnitude or phase, can be deduced from the information of the first or the fifth quadrant by intuition.

The data files for "COMBINE" are the same as those for program "SURFLDS," except that the variable MODE of the last data file for "SURFLDS" is redundant here. Hence the input data files for "SURFLDS" can be used for "COMBINE" without any modifications.

The commands needed in order to submit the program "COMBINE" interactively, assuming that both the program and the data files have been cataloged into permanent files, will be as follows:

Statement No.	Information in the Statement
1.	*JOBCARD*,RG1,JC500,T100.
2.	DISPOSE, **, V.
3.	HAL, BANNER, LEE, SURFLDS, 8SYMM, COMBINE.
4.	ATTACH, EWFILE, COMBINEEW.
5.	EDITOR.
6.	ATTACH, A, COMBINEB.
7.	FTN, I=Z,R,T.
8.	COPYL, A, LGO, B.
9.	PURGE, A.
10.	CATALOG, B, COMBINEB, RP=999.
11.	RETURN, EWFILE.
12.	ATTACH, TAPE1, SURFACEDUETOCOSE.
13.	ATTACH, TAPE2, SURFACEDUETOCOSH.

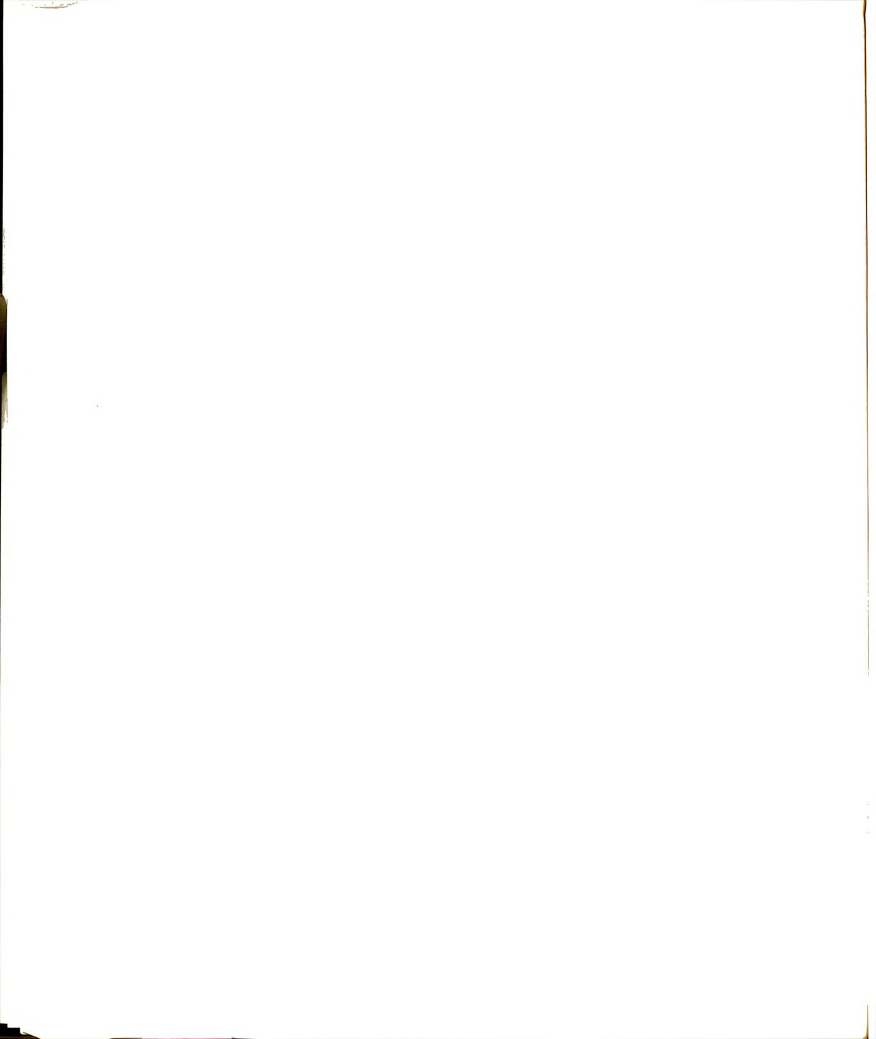


14.	ATTACH, TAPE3, SURFACEDUETOSINE.
15.	ATTACH, TAPE4, SURFACEDUETOSINH.
16.	ATTACH, EWFILE, SURFACEDATACOSE.
17.	EDITOR.
18.	B,W.
19.	RETURN, EWFILE.
20.	PURGE, TAPE1.
21.	PURGE, TAPE2.
22.	PURGE, TAPE 3.
23.	PURGE, TAPE4.
24.	*EOR
25.	SAVE, Z, 100-1820.
26.	*EOR
27.	SAVE, W, NS.
28.	*EOF

Note that in the above job, we has assumed that program "COMBINE" has been cataloged as permanent file "COMBINEEW," and that the compiled program has been stored in permanent file named "COMBINEB." Furthermore, instead of creating a new input data file, the file "SURFACEDATACOSE" has been used.

4.11. Printed Output

The first output file of program "SURFLDS" mainly performs the echo checking of the input data. The location and dimension of each surface cell are listed first, then



the number of surface cells on surfaces of the first quadrant, the electrical parameters of the body, as well as the frequency and the type of mode of the incident field are all printed out as shown in Table 4.4.

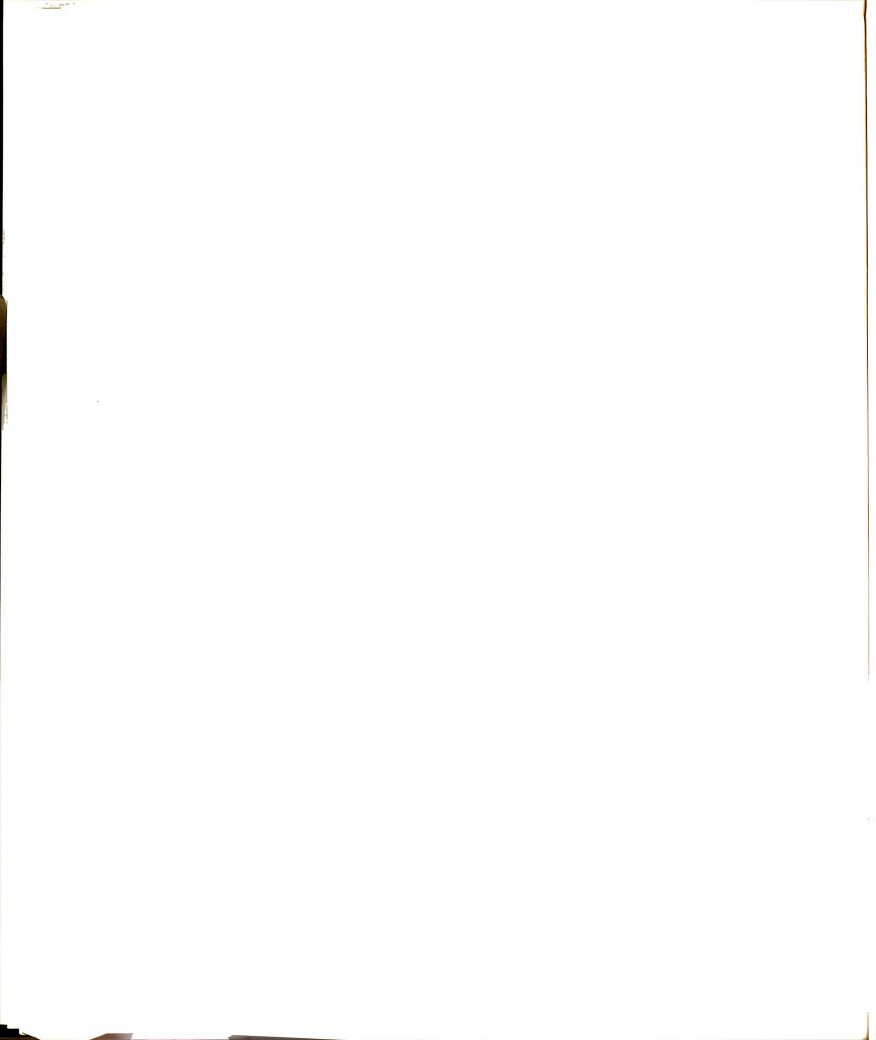
The second output file is the listing of the real and imaginary parts of the incident equivalent surface currents which are internally determined for each surface cell.

This file is shown in Table 4.5.

Then the computed induced surface currents at various surface locations are listed in the third output file where all the surface currents are expressed in terms of Amp/meter, as shown in Table 4.6.

The last output file consists of the information of the induced surface fields at various locations on the body surface as shown in Table 4.7. It is this file which will be buffered out to a magnetic tape with one of the following local file names, TAPE1, TAPE2, TAPE3, and TAPE4. Then this magnetic tape will be cataloged as a permanent file which has one of the following PFN's, "SURFACEDUETOCOSE," "SURFACEDUETOCOSH," "SURFACEDUETOSINE," and "SURFACEDUETOSINE,"

Now we briefly discuss the output files of the program "COMBINE." The first file is the echo messages of the input variables. The next four files contain the values of the induced surface fields which are buffered in from TAPE1, TAPE2, TAPE3, TAPE4, respectively.



First output file of program "SURFLDS." Table 4.4.

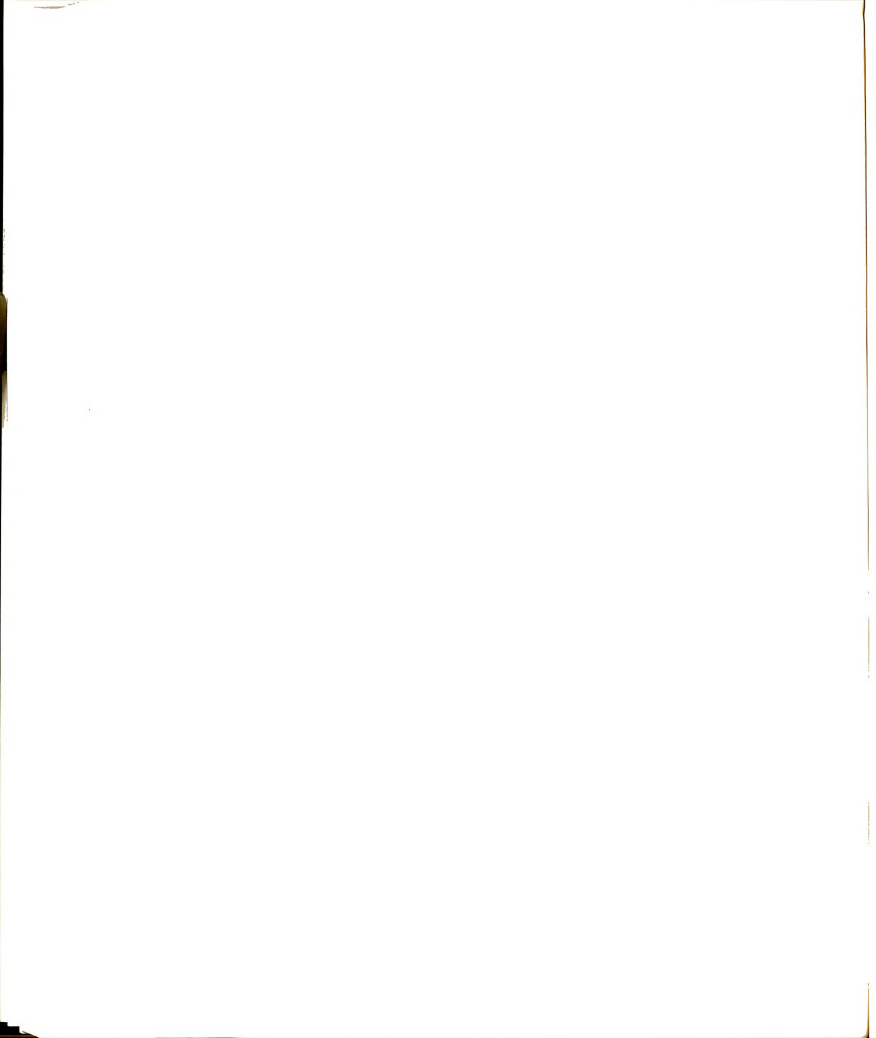
A DES STERET RODY WITH ARBITRARY FLECT PROSTRIES	8	.50.0	*01.65*	94.05	**************************************		20105.		.5000.	20005.	. 54096	96901.	
S STERFT	0 617 68												
HET ACT S OF A" 9 O	7 CN CO	2.750.€	P-250+0	.75000	4.250.0	. 75.00	4.45.7.	2-386.	*250.0	1.000.1	1.000-1	1.0000	
THIS IS SOLUTION OF THUBECTO FILLES ON THE CHEEKEN SOF AN A GOOD	4 614 510	39051.		.25.00	*250(b	1.00-1	1.09786	1.070.	1.00000	19.67.	.75-(1)	.24.50	
S SOLUTION OF LABE	x (1) (4)	1.00000	1.20063	1.101.1	1.0000.1	.7.199	20986.	0.054.	.25010	.75909	.25 11 6	C 487.	
THIS I	2	-	14	-			-		z	e	_	=	:

THERE ARE TISE A AVEC 4 A WAX. B ANNTE II AND WAZE " CELLS ON SUBTAFFS OF THE FIRST QUADRAVE FACH SURFACE CFLE IS DIVIDED 1 NY 3 SUM-SURFACE CFLES DIFLECTATE CONST. = .47830FF.482

.8978.

CONDUCTIVITY: .2211/CCT+31HUFANTER FREGUENCY= .2450111+14NTG. 12

TYPT OF INTRESSED FIFEDROSS



Second output file of program "SURFLDS." Table 4.5.

=	, REAL INAG		R' A1			REAL IMAG REAL IMAG REAL IMAG	INAG		9E AL		153
	ON THE TOP S	SUPFACE	ON THE TOP SUBFACE LE HAVE THE FULLOUS	FULLOWS							
	J- 10 1-12		•	J 2 04 HY		THI.	JAY OR 12/MD		š		-773- 20 ZMC
•	***************************************	:			:			:		:	
:	•	•	. 0.	:	•		÷	-	٠		٠
:	:	•		•	-	• • •		-			
:	:	•	•		-			-			
:	ċ	•	:		-	:	·	-			
:		:			:			:			
	ON THE RIGHS	UNFACE	IN THE RIGH SUPERCY WE HAVE THE FOLLOWS	Fritais							
	J' X OR HZ		31.2	Jr. 50 -HX		Ĕ	JHX 148 -(77Un		5	80 2	UF772 NO 245
•	***************************************	:			:			:			
:	:	•		÷	-			-		2	
·	ċ	-			-		ċ	-	. 2458245-02	20-	
ċ	ė	•	·	•	-			-	1 .243m49E-32 r.		
	:	•	÷		-	•	:	-	1 .2637695-19 6.	3	
:	***************************************	•			:			:		:	:
	ON THE REAR S	URFACE	ON THE REAR SURFACE UF HAVE THE FOLLOWS	FOI LAWS							
	J' X OR -HY			JIT OR HX		1	SULT OR CYLUS		ł,	TUL 00 - 54 741	14.73
:	***************************************				:			:		:	
:	:	•		:	•			-	(231*6F-95 B.	- 22	
	•	•	:		-	:		•	(23 traster 2 6.	~	
:		•	:	:	-		•	-	51 - 4 hE - 12 0.	- 22	
. 0.	9.	•	:		-					:	

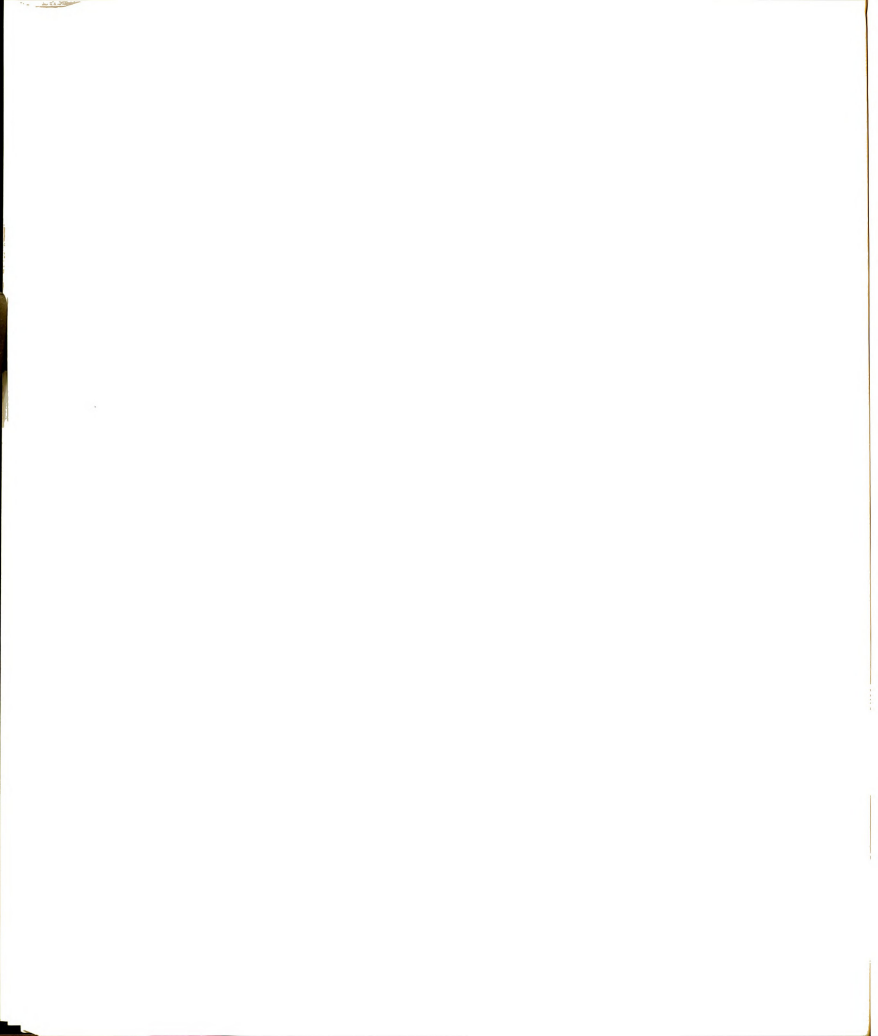


Table 4.6. Third output file of program "SURFLDS."

	THE PART CHAIR AND LIVERS AND MACAN	THE PURI CHAIR AND CHAIR STATE TWEE REAL THAC	REAL IMAG	R'AL 146
	OU THE TOT	SURFACE WE HAVE THE FOLLINS		
	JET OR -H7	JEZ OR III	JMY 08 F7/WS	CF/AL- 80 ZMP
	(4)-7053864- 63-746848-		111258451435845511	f .5342715-04 .164727-031
		(11 M 13 ME-43 . 1 M 19 M 1 10 7 M 6 M 1 5 3 6 9 M 4 M 19 M 1 1	(107h68F-15 6956461-34)	1.129545-35 .1/16345-01
	5 - 104 712F - 95	(2114061-1 - 1410426-03) (1317226-14 1471206-13)	(131/22f 1 16712nf 5)	1 .11-7195-03 .7303525-043
		(1451716-03 .1506776-3)	.150K77E37 (160199E-'3494815E- 4) (.143K77E-93	(.1934775-91 .737526-04)

	DN TH! RIGH SURFAC	ON THE RICH SURFACE OF HEVE THE FOLLOWS		
	JEX OR 112	JE7 OR -HX	JMX UR -F7/UA	17735 BG 2MP

	4 .101563E-42 .6688881-53	1 .2455621-7 -,2726725-151	(.543196F-B4 .11544R1-33)	(.539544E-95 .124749E-039
	6 (.1341n3'-(2 .87n968E-n5)	1 .3176975-441282135-631 ((.3573805-24 .2954565-14) ((.6-3780005. 20-3252878.)
	7 (.1309.982 91376-1-11	4 .710134E 4288342F-637 4	.713858E-74 .467252F-743	(.2184456-83 .5744495-44)
•	-	1 .1554115-141294456-031	(.289433F-F4 .114924F-04)	t .373269F-93 .9794245-443
	:		***************************************	
	ON THE REAR SURFACE	ON THE REAR SURFACE WE HAVE THE FOLLOWS.		
	J. X CE117	J. Y . R HK	JAX 114 17/UN	CPART OF THE
			***************************************	***************************************
•	(Tr-1395544. 84-1023PPP. ,	-	.231647r- 5 -,2072936-03) (-,646368E-04 -,1179991-13)	11 360 11 \$1 30 Hb. C 1
2	1 .13112F1-62 .A7619:4- 17	-	.co.71.f. t135714E-131 (15983E-1415083E-14	160-1611222- \$1-3.69235- 1
Ξ	(.136592F-12 143547E-13)	1 . HSATAIL - 4 2972434-159	(7256.95-"4 4988271-24)	(2753FFF - 115597404)
2	(-10.1257-52 -561751-51-50	1 -2075775- *154584F- 13	141-1415161- 42751616-141	140-15-1662*- 1-56cat 65*- 1

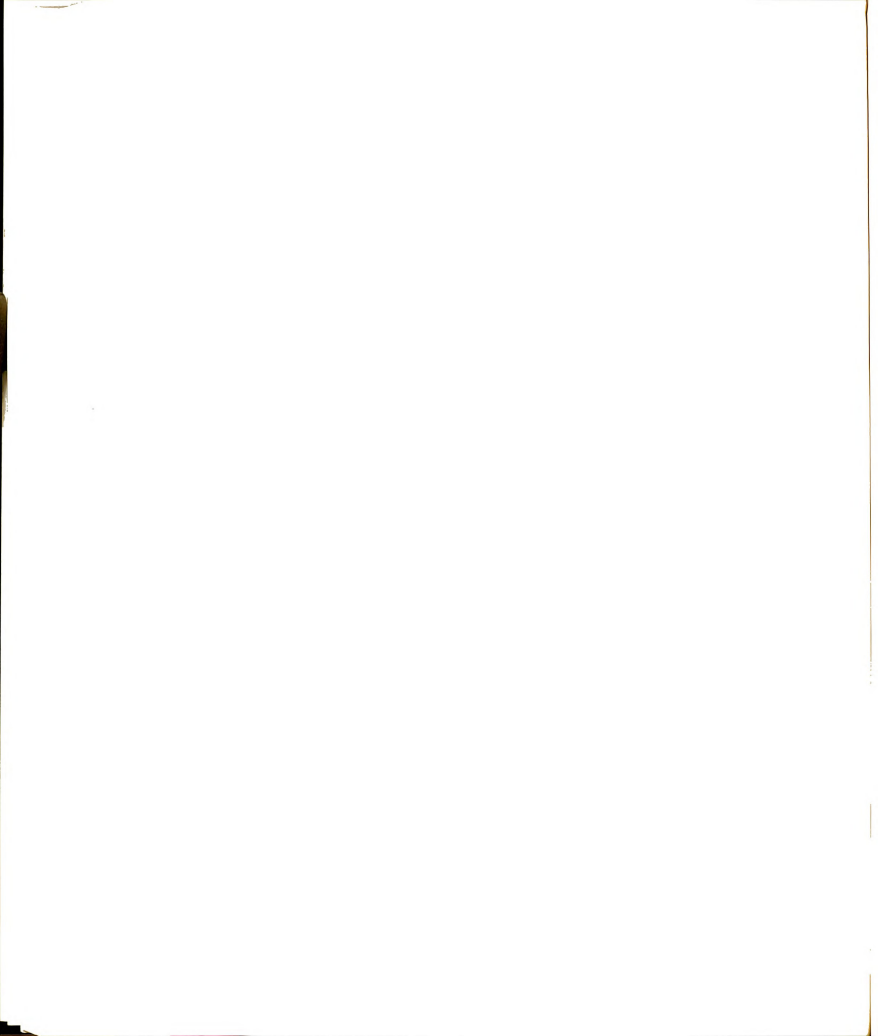
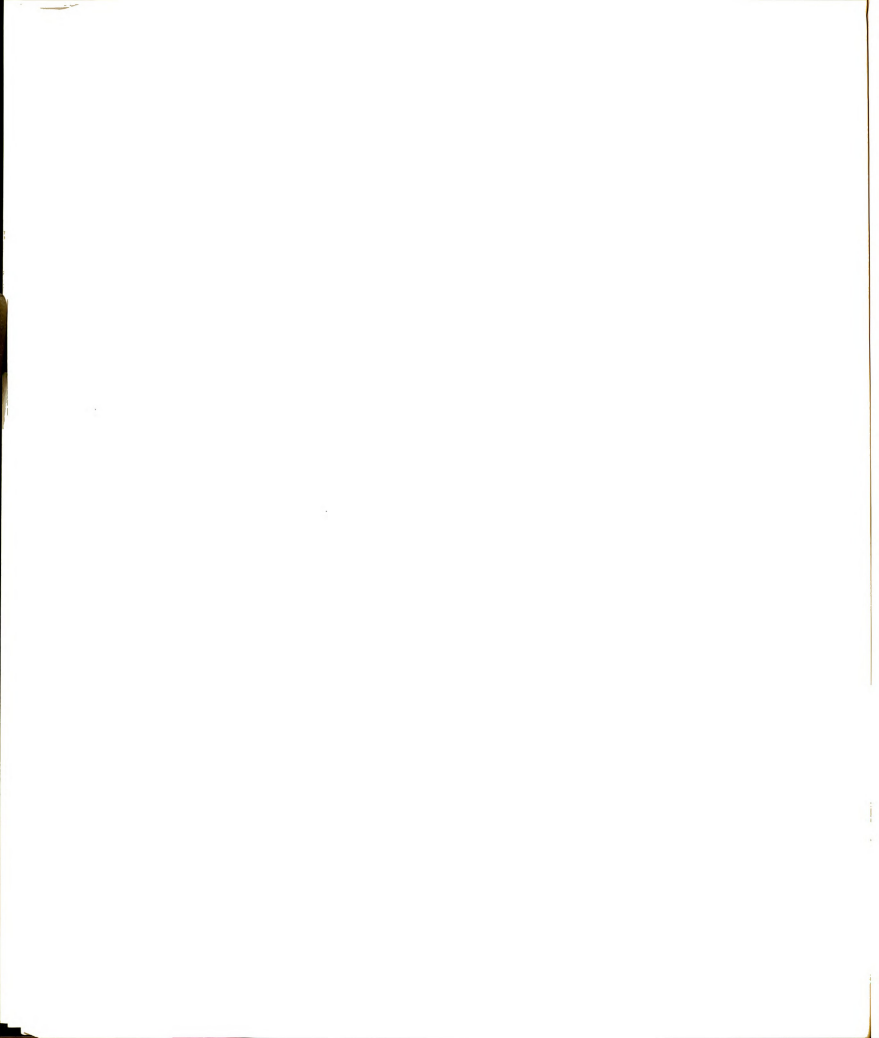


Table 4.7. Fourth output file of program "SURFLDS."

	THE PROPERTY OF ARE LESTED AS FOLLOWS CANDAM CONTINUES ON ILLEGUAL VILLAGOR TO THE CONTINUES OF ILLEGUAL	OLLOJE LAMP/PETER F	THE CREATS A	a littera			
	Atat lave	47.0	CWAI	STAL	Luve	Brat	6 44.5
	ON THE FOR SHREACE OF HAVE THE FOLLING	OF HAVE THE FOLLOW	2				
	211	ł.				12	
				***************************************	:		
	14)-1629845-14)		(+2866E	(351913: - 1539982r-'4) (1985f4r-n)598879r-n1) (202167g-n152 4546-91)	48755-413	10-3291202*- 1	16-3464 25*
		1 10413AF-03	(+ Jellee.	(406662C-*1252549F-*1)		(4084265-7] 4734745-01)	10-36Check*
		(S114881-05	1810536-031		11 11 +0.	10-3118110 1	
•		1 1451776 1	158477E- 33	*!\$#477E- 3) (642915E-c10581757- 1) (6177626-c1076559E-0))	11 12118		16-3455346-01
•	. :		:			***************************************	
	OR THE RIGH SURFACE OF HAVE THE FOLLOWS	UF HAVE THE FOLLOW	8				
	24	ř		2.1		ť	
			:		:		
•		1 2055626-1	121-121-01	.27072E-131 (24248F-n14555501-11) (1114529	1246251+81	111-385-350
		40-1165115*- J	12n213r-23	.128213F-53) (134732F-711117761-01) (11241-113	1 .2161925.00	**********
-		4 7101561 4	.ZARS42FS3	(268915F-F11761971-611	(142) -(1)	1 -1242424. 1	(14-26-1)
	-	f155411F- 4	.12"n45F-731	1210-1106-01	32711-123	11-70-12-90	.3509867-011
	:				:		
	ON THE RIVE SURFACE OF HAVE THE FOLLOWS	VE HAVE THE FOLLOW	٤				
	All	Ĭ		t		Ē	
					:	***************************************	
٠	(2-1246543 63-18524415	(.2514471-15283295E-05)	(Su-3564)	(2435.81E-81 444871- 1)		1-1228561.	114-30-1100
•	(1311201-62 876 1761-651	(6 -7857781 A1-237785- 5)	357347- 33	1 -1326781-1 -1145781-1	11 8.00		11
Ξ	1435-77-031	(.4343611-'4 -,2"72431,-633	112431-633	1 -,273912r-/1 -,1042RHI- 13	*2881 - 13	121-21-21- 1	(16-30/2291)
12	0 -1041255 - 20-1201491- 0	1 .2572771 - 415457145 . 31	18 3011265	1 11076051 4550701- 21	14 - 10161	Catalleten 5	1112965-111
			:				



The sixth and the eighth output files list the total surface fields induced by plane wave on the surfaces of the first quadrant in real-imaginary and magnitude-phase forms, respectively.

Finally, the seventh and the last output files list the total surface fields for the fifth quadrant in realimaginary and magnitude-phase forms, respectively. The above output files of the program "COMBINE" are shown in Table 4.8.

4.12. Listing of the Program

For the purpose of reference, the programs "SURFLDS" and "COMBINE" are listed on pages183 -229. For about 150 surface unknowns, "SURFLDS" requires approximately 170000B words memory, while "COMBINE" requires about 30000B words. When the number of unknowns is more than 150, the memory required for "SURFLDS" exceeds that obtainable from CDC 6500 at MSU. To overcome this difficulty, the job may be submitted through Merit Network System for execution at other computing facilities. In this case, due to different operating systems involved, apparently different control commands must be employed. Nevertheless, since the program itself has been coded in standard FORTRAN, there is no modification needed except a subroutine named "BLOCK DATA" must be added into program "SURFLDS." The function

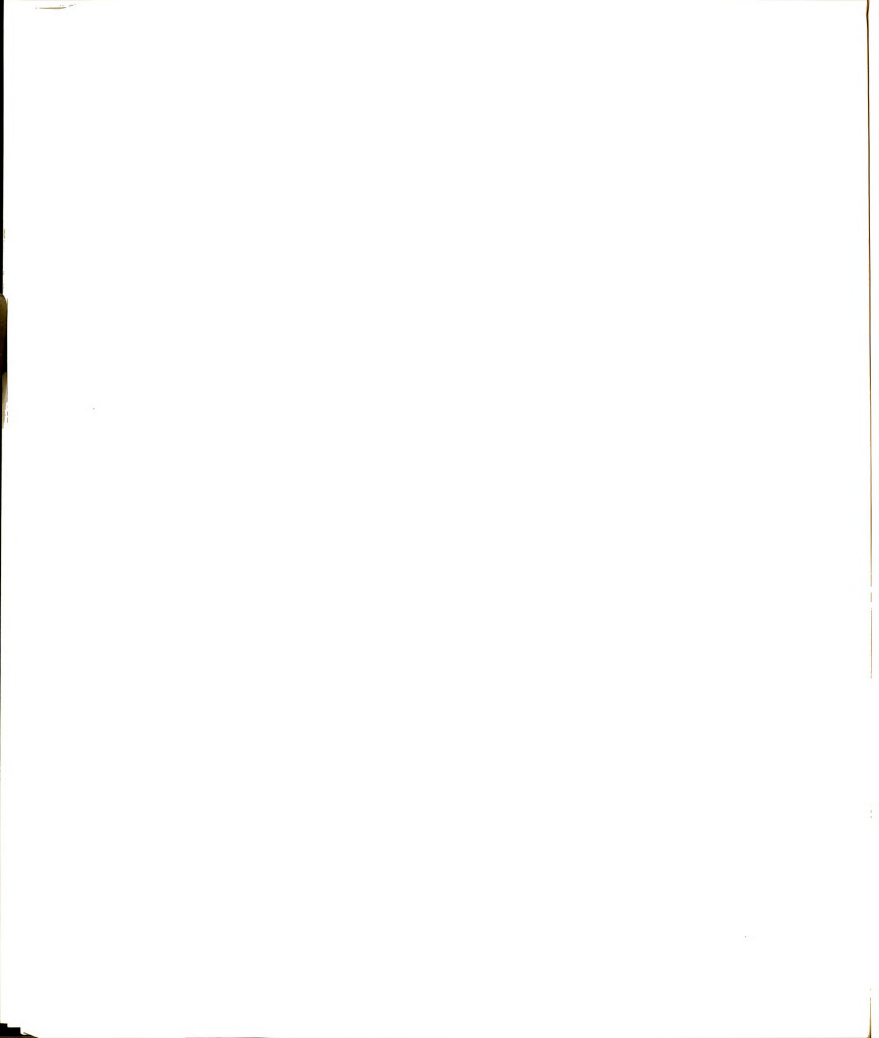


Table 4.8. Printed output of program "COMBINE."

		111 51	TOTAL	I Direct D	11.005.01	9		o disciplination of the same	out selling the	202 207 11		
STILL JORDINGS OF STANCE CONTROL OF STANCE CONTR	F SULTS AR	JAINI J.	Te di	1111111111	s RESULTS D		OR DIVERNAL					2
= 744	171	POLITON	i N	VOTEN INTO	OF FACE OU	WEACH-CELL	Arc LISIED BEI	20				
= 211			1 71	:	T C3N CP		CLN LA					
= 244		1.00	911.0		.75.01.0		11.051.	0.05				
- Z		1.00.1			0. 54.		9.452	0.45.				
= 211		1.30	906		forte.		75.00					
= 200		1.00	360		34 26.		.25010					
= 211		.151	100		1.0104		. 15067	**105				
7		.24	600		1.0 0.		. 15000					
= 211		.75	964		1.00000		6)052*					
ž		.54.	500		1.000.1			. 540				
ž		.15	000		. 75000		. 2000.	. 5678				
± 21 <u>.</u>	_	.55	13		.75.00		. 90 000	10000				
2	. =	.75	6.0		25.70		6.060.	. 2010				
= 711	2	.52.	2		.0			.51.18				
THE MENT CITL IS DEFINED FOR A COMPONENT OF THE CONTRACT OF TH	THEFE ARE	• "XII	W	=24.	* ***	U =4A 0	= 7111	CELLS 1913	PFACES OF THE FIF	ST DIRBOL	;	
THE CONTRACTOR OF THE CONTRACT	I ACH SURF	Act of the	13 5	141610 17		SUN-SURFAC	STILS.					
THE STATE OF THE S	CONDUCTIV	1175 .2	16.36.3	M/010114	17.8							
THE COLUMN TO SERVICE AND ADDRESS OF THE COLUMN	r R F CUETICY	245PL	.01.0	/H :: H/								

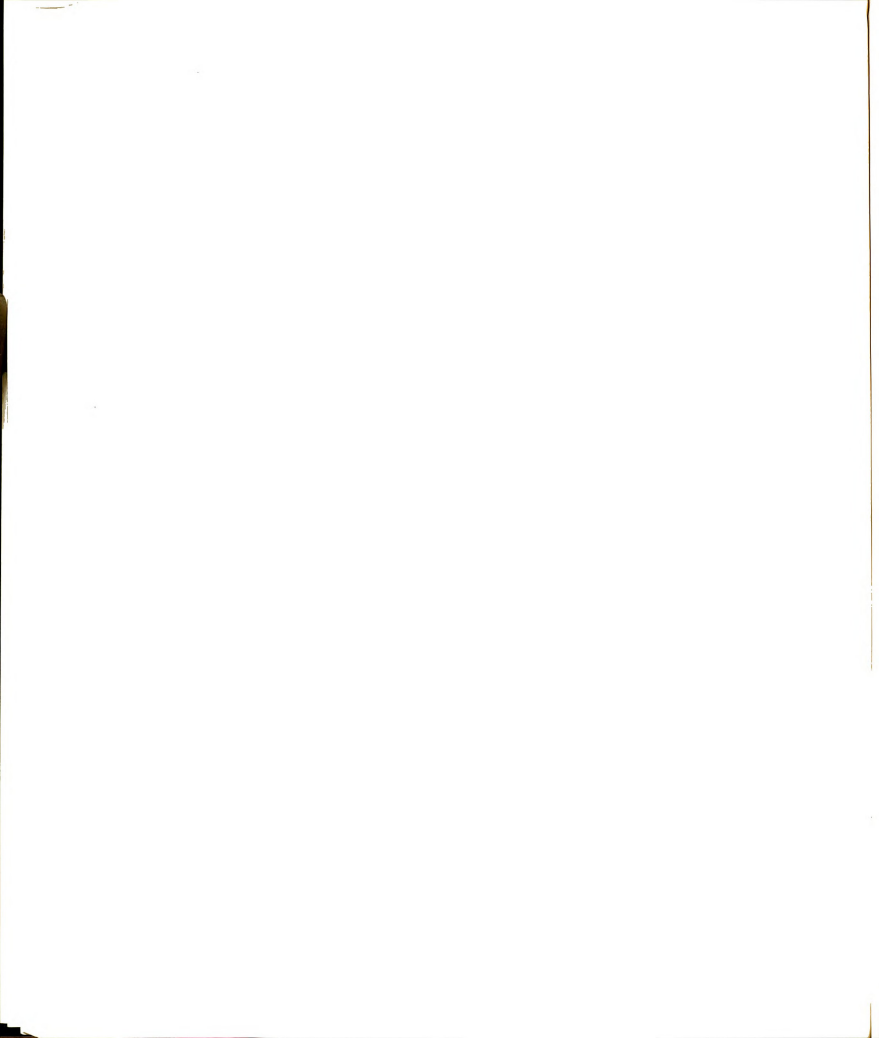


Table 4.8. (Cont'd.)

FILLIS IMMORE.				THE FILLS THOUGH DE CASE THE THE CASE THE PARTY STATE THE THE CASE THE THE CASE THE	Af AL	1 44 5
. 1444	1441	RC A1.				
Jot 14E 1of	TOF SHIFT ACE	SHELL OF HAVE THE ENELOUS				
1		Ť		22		
Ĭ						
	(+0-10-30004		10.00 BET 43	11198645-11-198646111	11-2751675-4152 3377-613	119-321 65
	1826116-633	(1681384 - 5.3	(+,-3641644		(1)-1606473*- 1,-1924844*-)	(lu-itetray*-
(4 1012131 - 11-12120F- 4)	(4 Just = 34)	(F114881-2*	(\$4-315.181.	(4959R5f-ul458041f-rl)	14133141	£13681.4c*-
1 - 1-980001-03 1458651 3	167-8-6-11	1 145177501	.15n677f-533	(198110501580158:1)	1	(11-)EXXXI
. :						
ott THE	RIGH SURFACE	ON THE RIGH SURFACE UE WAY! THE FOLLINGS	S.			
H,		*		**	13	
			:			
1015635-62	(E)-3888844.53	r205502F-13	.2720725-133	(2424R5f-"1475257r-01)	124621. 00	*****
	181-31-30-18,	************	.1242135-139	(1 14752E- 1 111776 01)	1 .2161825.1	111661798*
	41 1967 - 1983	************************************	.2893425-033	(268815F-911761471-415	1242434. 1	(14-36417174
-	. 5925431-039	115541111	120-3500661.	()		110-25546
NN THE	REAR SHAFACE	REAR SHIFACE ME HAVE THE FOLLOWS				
ţ		¥		:		
174-1246:344-63 -44453447-639	445346F-039	1 .2516477 - 1285293F-059	180-31625H2	(2436#1F-F1444#2"- 11	. 122959545	. 14-12-16-44
10 / 131120F-02 ATA 194L-14	W 1901 914.	1 .1.247711 41	113612-61		66+336421C*) (11.52122- 11
	W :- 11 15. VI *	(.E3+36](4297243F-633	2912435-633	t 273972F-(1 1842631: 1)	1 . 150.00 15-01	40-382-2010
4 1691r3r-r2	O 1061857*	(8 - 2642 68 1 ** 61 - 162 62 46 **)	1342047-133	(110747E-10587701- 51	theattly to a	111-34-11.

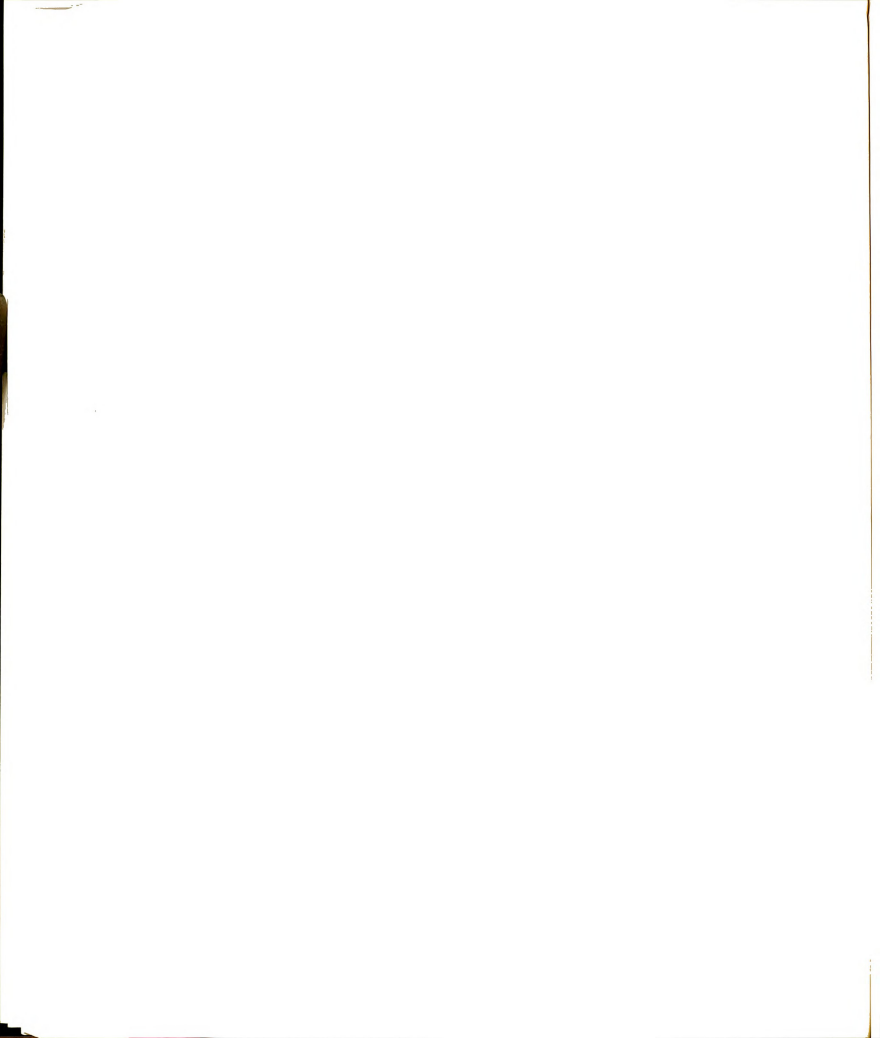


Table 4.8. (Cont'd.)

	BCAL	IMAG	1731	1146	REAL	24.4	RT AL	
	0M TH1 THE	in sineract	WE HAVE THE FOLLOWS	SAC				
	211		Att		2.5		ŧ	
		:			***************************************			
_	(559494[-113 -,794]46[-14)	141461-141	20-140745. 1	.567946F-033	-	. 7P2P61F-U1 . PA7F61F-U1) (1624245-07	164-15511-5
~	(2772426-036738706-05)	138701-05)	1 .2669715-02	.581152E3) (.1476675 + 11	. 1764767-913 (14-3226101.	.1114557-013
	11. 8 276 86 91 3 71	.7152346-443	20-1945 IE.)	15 3 \$ 1 5 6 6 7 5 7	t .702086E-01 .435500f-011		636.1158°)	.4271245-039
	t12R2RBI -03 .42	.4224795-043	(.3533R3E-"2	.1321-1631	(-150594E+**419457E+*1)		((č31 lbub;*
				:				
	0" THF RI	IGH SURFACE	OF THE RIGH SURFACE OF HAVE THE FOLLOWS	SAUT				
	211		ľ		٤		ž.	
	***************************************			:				
	(5392181-43 682671E-65)	170711-01	(795732F-93 413765F-93)	4137e5f-039	(10-11-6/10, 11-78/18/103,)	(14-11-6110.	(57*728E-31443*513F-013	110-1615-161
4	(154627E-n2 Pn.3832F-n3) (612170f-13244649E-13) (0.3832F-0.13	1 6121795-11	24649533		.236376F-'1994U16F-821	(118682F+ 9	.27.3049F-12)
-	(508291f3150111F-03)	501111-033	(1699611-12 11/71' 15-02)	11/1/15-02)	-	.1185725. 0 .121953t-913	1 1 1 3 3 4 7 5 - 9 1	(2-3.51 14.
60	C113294E-02144651E-150	05-215944	(117782F-'2 27/11/4F-03)		_	** ** *** ****************************	1	. 557.27.27.
		:						
	ON THE RE	EAR SUR ACE	THE REAR SUR ACE WE HAVE THE FOLLOWS	SAUT				
	Ē		•		1		ž.	
		:			***************************************			
	1 .2234H2F-#2	. 382 1771 - 1153	1 5155131-01 8754281-041 (8754281-041	(1c-352238c*- 1u-3618461*)		(10-30101.0°- 10-3000009°-)	flu-Jetot. b*
	19 1 .21KRRBF-"2 .23	.2320201-533	(26.849"1 - 3 171243F-84) (1712435-441	(.7249976- 2174614"- 11		(lu-161 - () -)	(In-161 - 111+
-	11 ' .2824"25-42 .41	A755'11-041	**************************************	.750 1285 -643	(-215515E-0213-6120- 1)		(5274 VF-C1 1774 NF-C1)	
-	05-11-222-1-2-1825-11-230	000-11-622	t 11+1936- 3	** 144.65 *1	** A G. CF * 9 121 CF 1 9 4 7 10 10 10 10			(fu-355; fac*

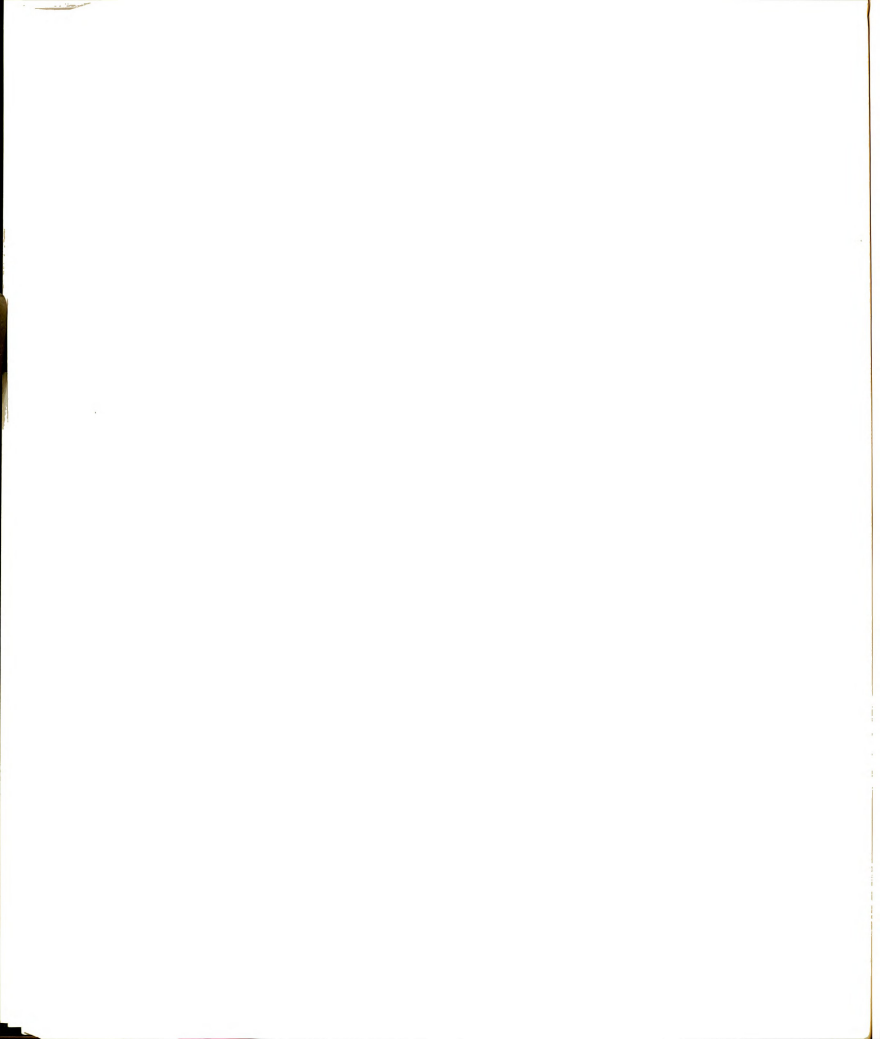


Table 4.8. (Cont'd.)

_	REAL		to Charles State of the Control of t	W SEAL HARA COLD STATE
		NE AL. THAS	REAL 1940	47.01
	ON THE THE SUBFAC	ON THE TOP SURFACE OF HAVE THE FOLLOWS		
	211	***		
_	(.242949F-05 .332484F-15)			
~	(.622075-051'7250E4)	-	22917652	110-210-111- 1-1211-1-
•	(151848f-: 4194431-151	-		(-3-3486112311248)
	(411918L-95 .103789L-55)		1 6817515-92	160-3110.12*- 21-3075210*- 1
		142-143 (444-145) (143-145) (143-145) (143-145)	1 . 3 . 2	
	ON THE RICH SUPEAC	ON THE RIGH SUPEACE OF HAVE THE FOLLOWS		
	11.7	E		
	1 .2617735-03156206F-159			: .
9	1 .2876901-032488735-253	(72255APE-14 .3254FPE-94)		
	* .10716A1-r3108n36F-:51	(590213F-04 ,207436F-141		
	1 -1234251-03 185552133	13454441-74 .2257491-043 (-16742A1 -412	
	ON THE REAR SHREECE	T WE HAVE THE FOLLOWS		
	Ī	ř		i
	(2273#1L-35 .1246##E-#43		. 44571-L- 7 -4491746-741 (1524677-111647795- 1)	
2	(27103Pf-c3 .214546g-133	÷	(20-186/16/*- 20-1805/16*-) (4)-1895/56*- 1159fing.*-)	
=	C 1858F3L-F3 .264823L-F3		(
2	' Plica2'-15 .478554- 53		(173671 273267E-00) (263267E-0 27567-13)	٠

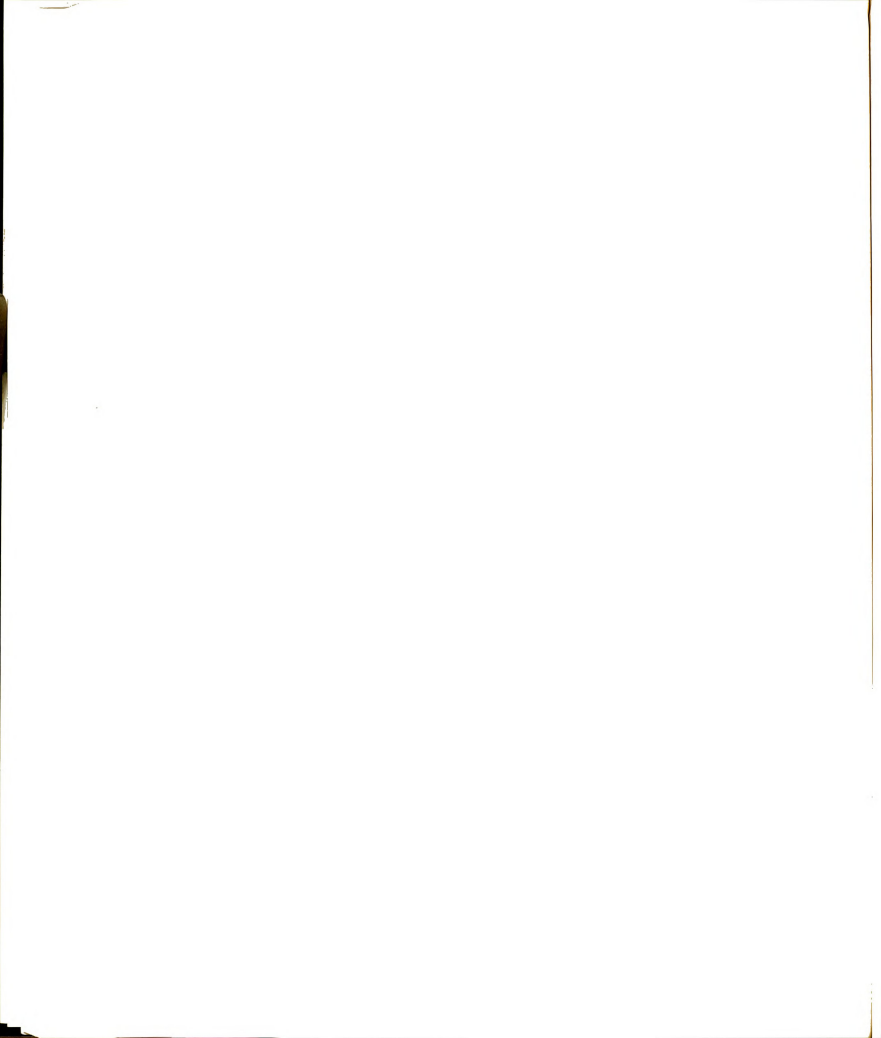


Table 4.8. (Cont'd.)

,				AND THE PROPERTY OF THE PARTY O	Could be a secretable south the secretable south to the secretable south the secretable south to the s
-	REAL .	5761	RFAL 1"AG	REAL 1746	1418
	to 1 : 11 110	P SURFACE	OR THE TOP SURFACE WE HAVE THE FOLLING		
	2		ŧ	1.7	:
-	1 1597251-43 25	***25634L=+ 33			
~	1 .36F 57RF - P.	. 78775661-			(18-510-4
-				5980075-01 6847075- 11 ((1-14/25/2-1-15/24/10-11)
•	Sa- Panana.			(.1264'3E+n312839Br+4.31 ((14-349541414-3183815)
		• 216.8 A 2 E - 7 X 3	1 1032651 3 2005651-03) ((.5494n3F-011251m1t+n/) (* 112-513040-1- 12-3535611- 1

	UN THE RTG	GH SURFACE	ON THE RIGH SHREACE VE HAVE THE FOLLOWS		
	211		¥	2	:

0	f669512F-63 .143164F-f23	31645-123	(900432F-**335237F-03) (110-1424713 10-1410951- 1	
9	t 119081f-02	.101257623	(3827765-"3 387478E-ne)		
-	. 9369531-63	.170019F-123	(72704Af39Af736F4)		
•	1 .1854-4E-n2	.225075E-123			10-25-9505
				611686-12*- /	116-31NH(3c*

	ON THE READ SURFACE	IR SIMPACF	WE HAVE THE BLEGUS		
	ì		**	£	ŧ
		:			
r		121-129		11 1121114- 1 12112811-111	1.0.700.32 15.01 . 10.19 55.007.
5	1 .7157781-13 3155121-121	121-121	(.5347ê 5' -" . 15"278F-04)	1 -1916615 50-381-082- 1	(127862° + n
=	1 1954711-63 5427791- 21	17795- 23	1 .2438834 -2.3 .3882737 -1493 -	(1-3316-31 16-3146-11)	150,000,000
~		1641-123	(8679201-93327164(-12) (.1172816-134454165-01)	(.) 0775F-72 -, 40170F-1	* 0-3x102220 10-38252000-)
		:	***************************************		

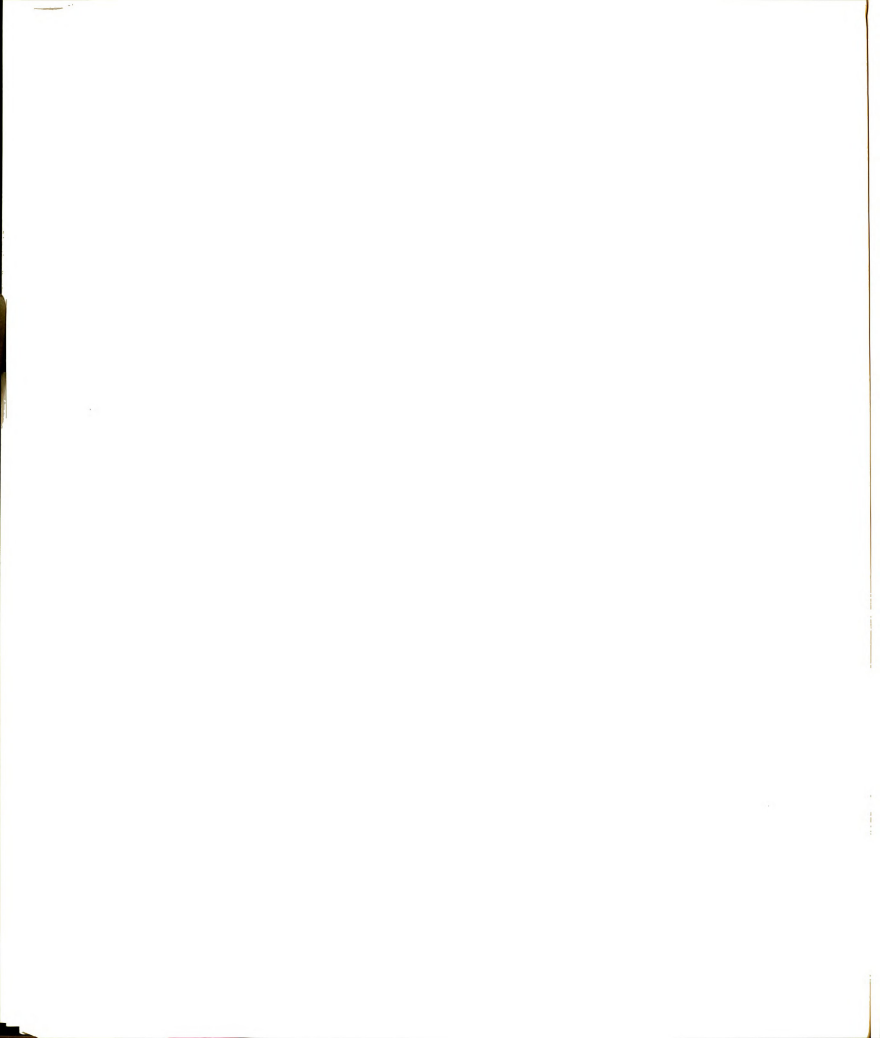


Table 4.8. (Cont'd.)

		RIAL	1440	RCAL IMAG	STAL IMAG	Stat. 1
		HI NO		. VE HAVE THE FALLING		
		1		i.	23	t
			:			
		36:2761-03		-	-	11-3/25883- 1
		1 .4.107161-113		-	-	10-jene211.)
		1 104591-01		-	-	**************************************
				-	-	
Committee of the first field of the field						
		1 10 11	L RIGH SURFACE	T WE HAVE THE FOLLOWS		
		211		¥		ž.

	•	1 313190E-04			-	-
ANATOR STRONG CONTROL		1 1106367-62			-	-
H-1860 (- - - - - - - - - - - - - - - -		1 .1845225-02				-
In the substance of the	_	C -25444715- 12			-	-
(1-1950) - 1-200(11-) (C-200(11-) (C-200(1						
		# IF	IC BLAP SURFACE	I WE HAVE THE FOLLOWS		
		E .		ř	٤	۲
CONTRACTOR OF CONTRACTOR OT CONTRACTOR OF CO						
H-MICHAEL H-MICHAEL L-MARKET H-MICHAEL H-MICHEL H-MICHEL H-MICHEL H-MICHEL H-MICHAEL H	6		(C3698866*-		-	
-			(2)-3+6+85;*-		-	
Desiration of the Instantant Learning of the Comment of the Commen	_	1157731 - 22	2571 775- 73	-		1 224 134- 1
		Set RPDF	246746- 23	-		

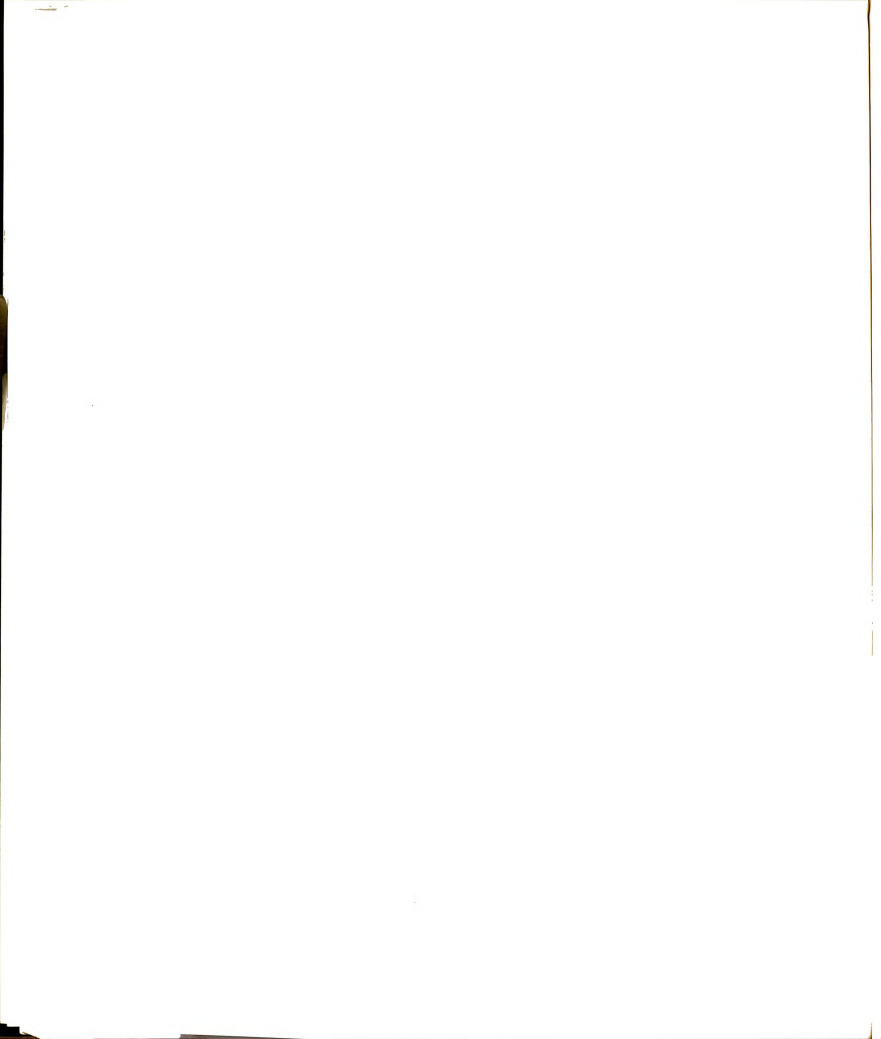


Table 4.8. (Cont'd.)

	KEAL	1146	PCA1.	1146	REAL	IMAG	Br AL	9
1 7 7	.H1 116	TOP SHR ACE	OF HAVE THE COLLINS	e.				
	/11		All I		22			

7	. 751854E-03	.7515871 13	(.769364F-w2 .2	185691-123	.218569r-923 (581612r- 1			
	.1146787-12	. (241 198-13)	t .2958874L 2 .9	.984291F- 11			-	
•	. 2016776-03	.7145555-143					10-3612146.)	(ub-206c, 61
•	***************************************					(44.3[6.41]		*11141444
:				100-112 11-0-	11403791408	.7587415-41)		(1286 Tr-of tutosacepay
						:		
	144 110	RIGH SURFACE	ON THE RIGH SURFACE OF HAVE THE FOLLOWS					
	211		ř		:		-	:
•								
7	.72355g-03	. 205878f623	1 .2514356-014798735-033 (190735-033	1 -102443E-01	.142549: + 141	1304687.00	
-	.140640F-U2	. 173534F-n21	1 1998715-03 3045476-533 (45475-753	11-1554-22- 1	11-101Resc.	2.03069966.	
	.2647477-02	121-14699116	.2466945-623 't9655781-531248415-'23			(10-1055/26*	C. SANGERE	
:	. 446374E-02	14 14 15 83 1E =/ 21	(M82573E-05 3915-1E-05)		. 13661936-11	***619361102792'- 13	-	
1		***************************************	***************************************	:				
	IN THI	FRUT SURFACE	ON THE FRUT SURFACE OF MAYE THE FOLLOWS					
	Ē		ľ		٥		5	
				:				
•	20-119824		1 912670F- 5 552675F-043 (20.728-043	(1.1597%ng-4)11502713		10-3611696*)	. 511724 15 + 911
	256320t-12	447819F-723	bb 1 36473E. *-)	(**-35.4964	1 11/2-12/2-22 12/1/14/ 11 1	115-1411121-	0.+10x551c* 1	6. 3+252150+*
:	. 20-1150010.	. 11-786E-023	1 41 1976 3 -29	11335.04	-24484(E1) (998185F-0210.7101-01)	(10-1015),01	13-1214-19. 1	(40.3501695.
ě.	.5152091-02	123-120-115.	1 26832997 3	12 146-31	-197975-51 (1093875-22654099- 21	12 - 1664623.	1.1570495.0	
i			***************************************					

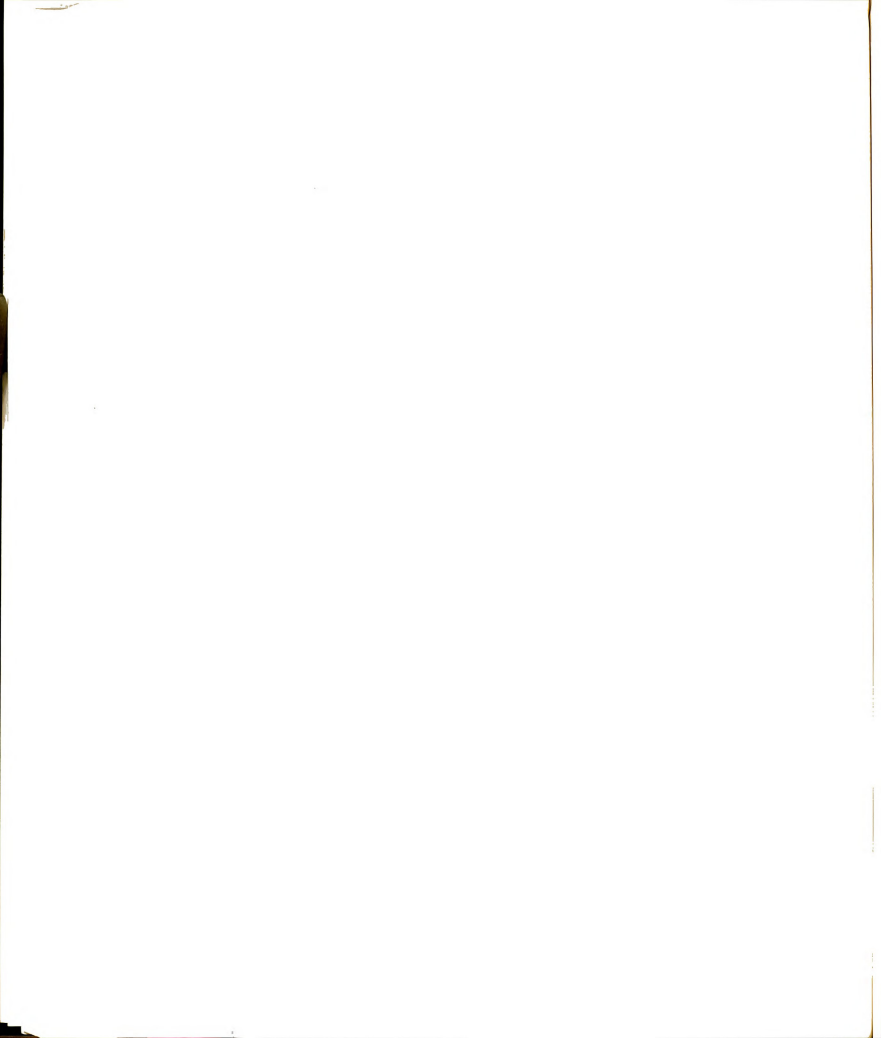


Table 4.8. (Cont'd.)

	ABSL	PHAS	W ABSL FHAS ARSL FIRS ARSL 111AS ARSL	ARSL LIAS	1504
	THE BIS	ON THE TOP SUPERCE	SUPERACE WE HAVE THE FOLLING		
	211		ŧ	t	ž
:					
-	.79838FE-03	.1711AAF SI	(.2685691-922485651-92)	1 -1918956+0017177-50+023	
-	En-1404148.		(.27371H -: 2 -, 38171951 - 31	-	-
	.3008361-63	.1292726+ 33	121-16-0226-4946-121	1 .2041095+101617341+123	-
-	.2213477-03	*253491(+-2)	(.3547ATF-42 -,774520F+21)	4 .26.056.00 60.00477 23	0-1037346-19
:					
	111. 40	RICH SURFACE	PH THE RIGH SURFACE OF HAVE THE FOLLOWS		
	211		ķ	73	
:		:			
-	.1342591-02	**135671. 21	(11925L- " 1276115.)	1 .130230E+*031**31F+223	(.11911ntonn734535. 23
•	-1969981-92	.124148147 53	(**************************************	(.501347r-n147039kr+r2)	.34589AF-U
-	-241076'-62		i .7697491216148FE+633	131728+"02267981+021	(.1234ppress . Stpaceters)
-	-2946111-52	.261452E+123	(.15*643E- 2176161E+03)	1124141-14851474421	(.2235'4F490 ,4 ***9854.93
:	***************************************				
	IN THE	RESP SURFACE	ON THE READ SUBTACE OF MAYE THE FOLLOWS		
	Ē		Ē	2	č
:					
-		**32378E-62 -**2*482[+62]		1 .1252255+1077294,27+121	120+366-1-u* 13640200*)
-	- 59-1771-02 -	.5818771-02 (**17*00***2)	f .0228495-55 154013E+65)	(.527477E-"1 347834[+12]	(
•	- 27- 121172 - L2 -	.281122 -L2451271F+P31	1 (600) 300 6989** \$ 5- 1682290* 1	the statement of the state of t	0 .1281 . 1. 1. 1. 1. 1. 1. 1. 1. 1. 1. 1. 1.
12 (-240272F-02 MY2046F+023	1 .1202-6	(50-14 1111 13)	the sand duty the said deter the
:					

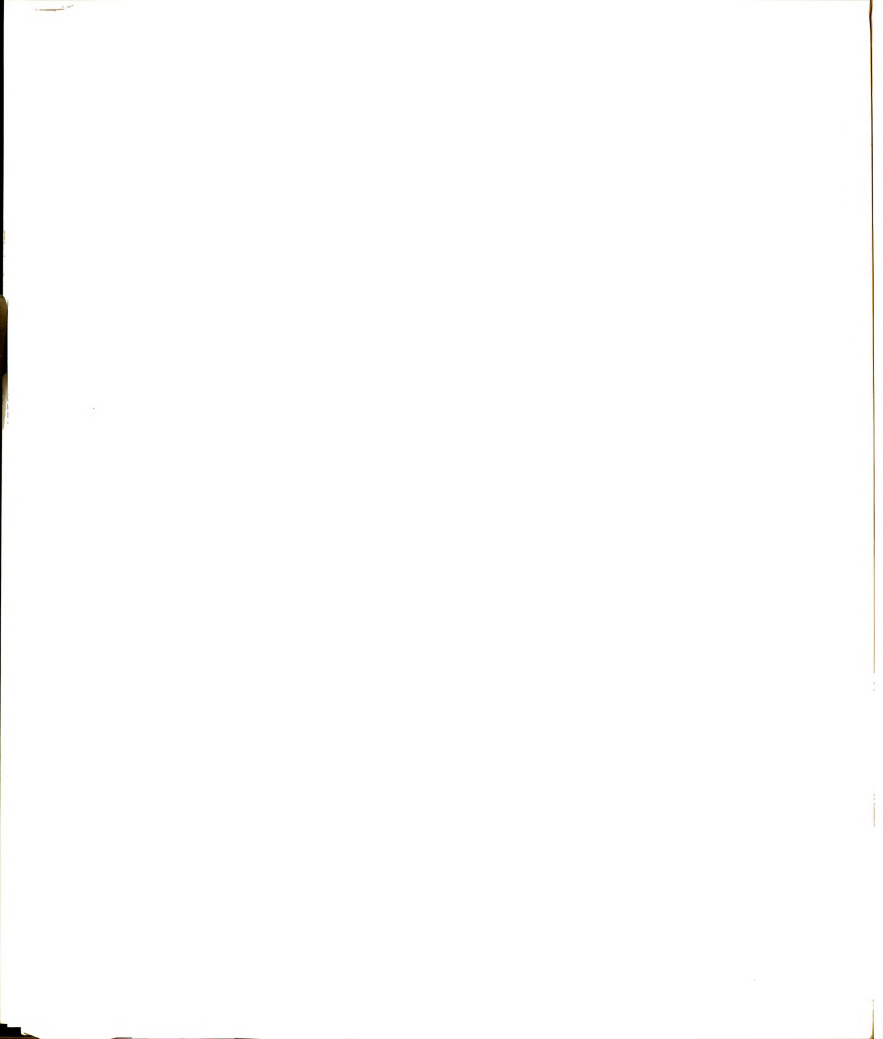
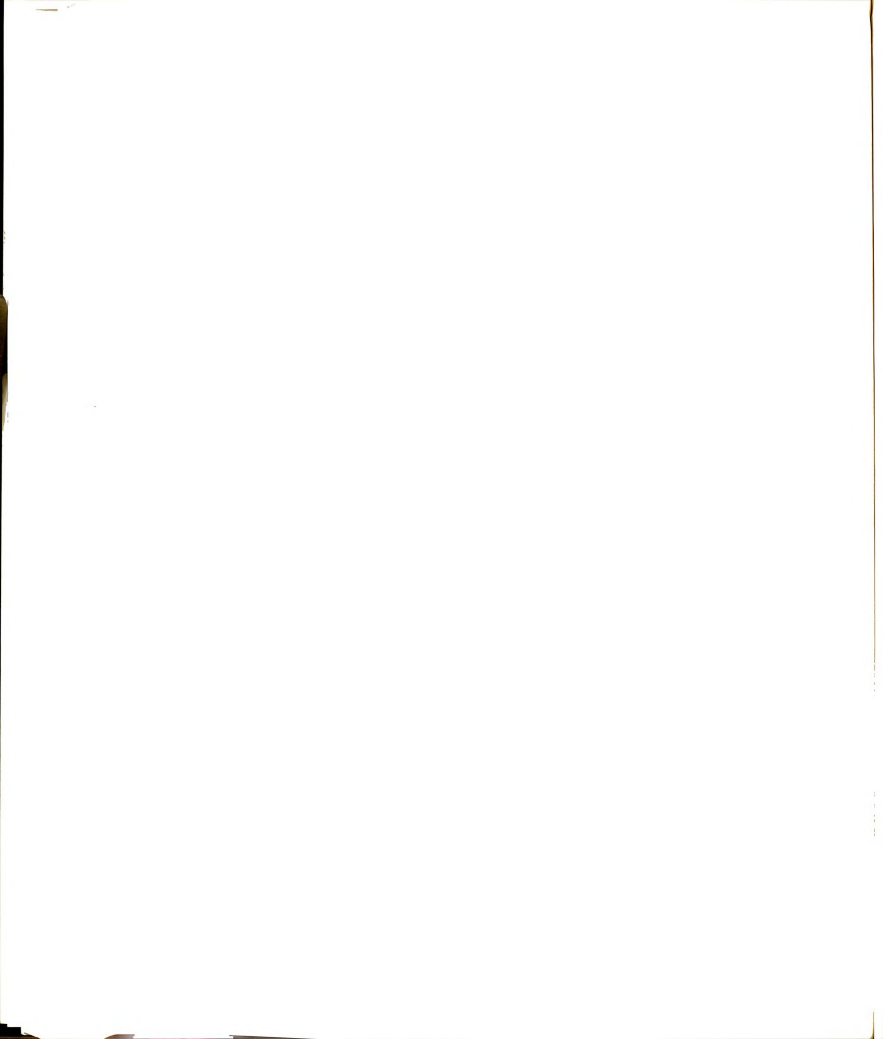
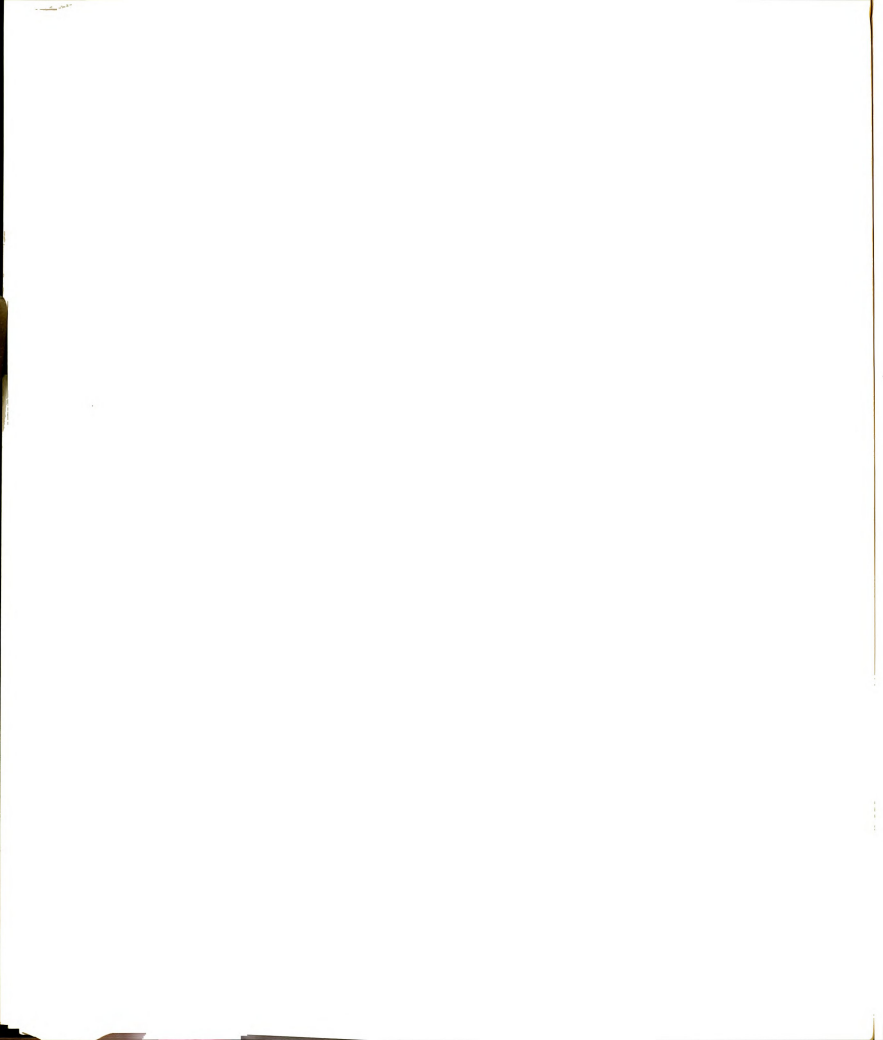


Table 4.8. (Cont'd.)

	ABCL.	CHAS	JSHV	LHAS	1004		A THE THE PROPERTY OF THE PROP	Design was a second
	1 10	H TOP SURFACE	ON THE THE SURFACE OF HAVE THE COLL SE	250		İ	1544	v #7.
			Ē					
•		***************************************						
-	1 .1963078-92	·1063076-92 .4478986+023		. See 11600 F.	20,7412,15.			
2	1375/11-02					(C 1922		1644316661
				. Industria	1 .2136921 9	.49724.7[+ 623	(c++30*+*+*- 6++384+*+**)	4-4-40623
		.132873E+F;3	1 .4174335-7	1 (2003)		. Partiblence	(1 6-20-21 1 11 12-20-10-10-10-10-10-10-10-10-10-10-10-10-10	11 1 150 1 1 1
	10-15:6094*	.4689:51-63 .luu131E+r1) (21-1622201-12	. 5564015.911		.2839091.923		
•								
	*	HE RIGH FURFACE	IN THE RIGH FURFACE OF HAVE THE FOLLPACE	JA.				
	112	~	47,					
•							•	
·		.2948921-62 . PF7967E++23	. 724196F 3	. 6966777. 20023	.7241967-13-6966777-003		:	
•	.3991475-02	. 6.9 \$6.26 Fed. 2.			Date Tonic Co. 1	.2 194624.	.28.54.135.40	.50.35.05.
				() - - - - - - -	10-3626555	.**(K77F.ng)	0 +32,0950.)	
		. 1798008-123	4 .154PB65-121277545-13) (-1277545-131	.1568348 . 0	.385.486.492	0. +544454.)	.27.757.751
	.4874415-62	.235R7RE - U.2)	-	.1540745. 31	.967327F-53154074E+ 31 (.477484F-61124231F++2)	.1242316.23	20031740750	
•					***************************************			
	11 110	I' FRNT SIRFACE	ON THE FRAT SHREAGE OF HAVE THE FOLLOWS	200				
	Ē		ř		-		:	
•		:						
	C .466A0B5-4.2	141.0028+121	1 .90537705-15 1764941 1	1764941 (2)	1 .6273411-01 1713541-21 (77155414.23	2002174174	
	-1150261-02	1211-151-661-7.	1 (8.4384-13 -11-1941+3) (17-7-46 +7 33		122231(+0.1)		
=	-523165' -n2	124.36.0711.	to earliette a contract to	13.11.61.41	1 .19775AF- 1 1"4414F+ 3) (1:**141. 31		.721 Coress
15 ,	4-585162F-12		1 . Sydian, - 3 . Laupogra 51 (14"F62" . 33	1 Garage LI - Jangarette)	I sacate ev.		.54.00000
٠								



of "BLOCK DATA" can be found in most of the computer user's manuals.



```
DD 101 T=1,N
ENTT 5, IXEND(I), ZEND(I), XAA(I), ZEB(I), AREA(I)
CONTINUE
PRINT 6
DO 102 I=1,N
                                                                                                                                                                                                                                                      0
                                                                                                                                                                                                   PRINT 6-

PRINT 6-

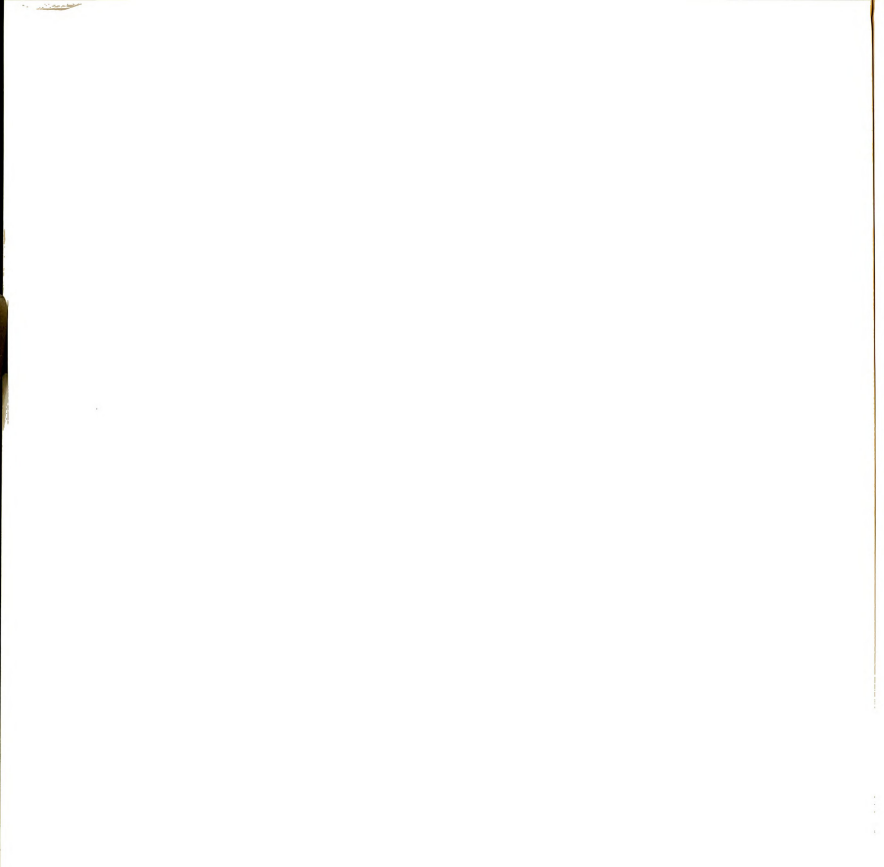
PRINT 6-

CONTINUE 1. XCEN(1), ZCEN(1), REP (1), SIG(1)

CONTINUE 1. XCEN(1), NPAR, AERR, RERR, LEE

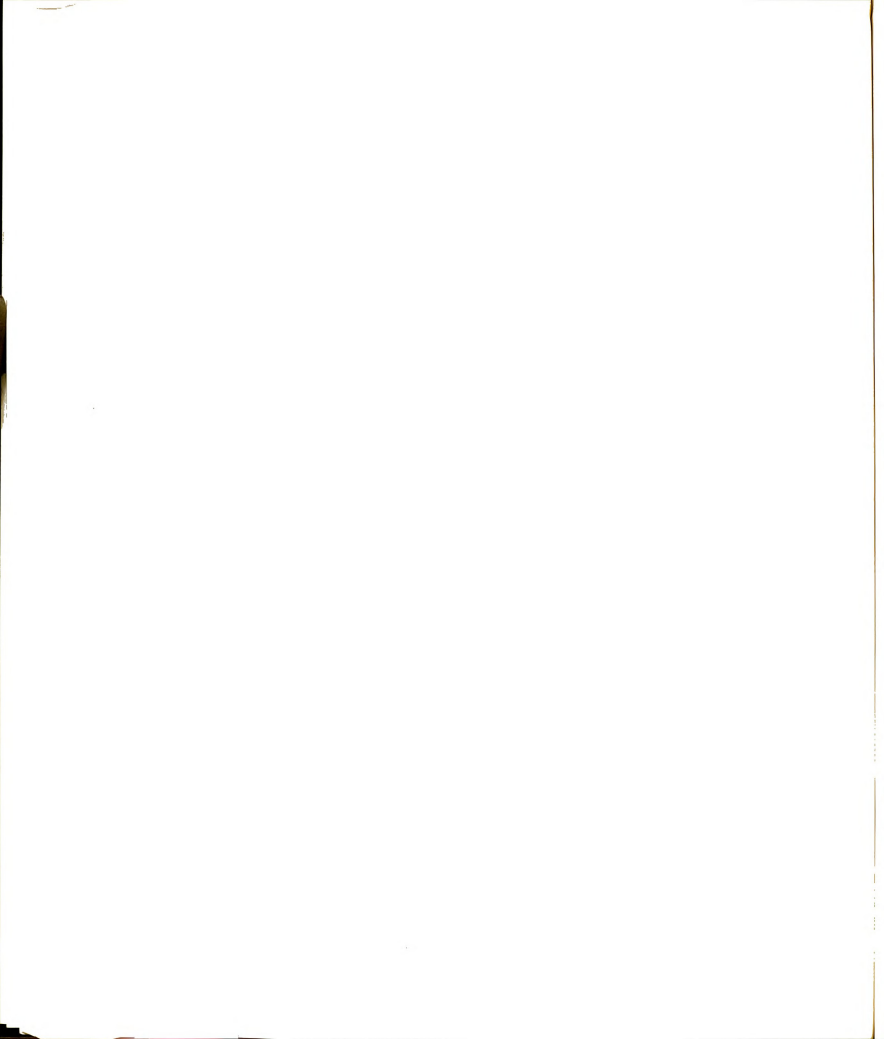
PRINT 6-

PRINT 1. XCEN 1. ....
                                                                                                                                                                                                                                         .LT, NX) GD TD 50
=1,N
=-1,0*CMPLX(0.0,1.0)*KO*XCEN(I)/2.
                                                                                                                                                                                                                           102
                                                                                                                                                                                                      101
```



```
LEE(I, NP1)=EINC(I)
CONTINUE
C
                                                                                                                                                                                                                                                                                                                                                                                                                                                                                                                                                                                                                                                                                                                                                                                                                                                                                                                                                                                                                                                                                                                                                                                                                                                                                                                                                                                                                                                                                                                                                                                                                                                                                                                                                                                                                                                                                                                                                                                                                                                                                                                                                                                                                                                                                                                                                                                                                                                                                                                                                                                                                                                                                                                CALL PUCKEKINC, N. NX. XCEN, MAG)

CALL PROMICTOR CONTROL OF A STATE OF A STA
                                                                                                                                                                                                                                                                                                                                                                                                                                                                                                                                                                                                                                                                                                                                                                                                                                                                                                                                                                                                                                                                                                                                                                                                                                                                                                                                                                                                                                                                                                                                                                                                                                                                                                                                                                                                                                              CALL CMATP(LEE, N, 1, DET, 1, OE, 50)
DRING 10, FRETING, NPAR, AERR, RERR
DO 104 1=1, N. DET, 1, MAG(1), PHA(1)
CONTINUE.
                                                                                                                                                                                                                                                                                                                                                                                                                                                                                                                                                                                                                                                                                                                                                                                                                                                                                                                                                                                                                                                                                                                                                                                                                                                                                                                                                                                                                                                                                     DO 109 I=1, N
LEE(I, NP1)=EINC(1)
PRINT 9, I, EINC(1)
CONTINUE
PRINT 14
                                                                                                                                                                                  103
                                                                                                                                                                                                                                                                                                                                                                                                                                                                                                                                                                   106
                                                                                                                                                                                                                                                                                                                                                                                                                                                                                                                                                                                                                                                                                                                                                                                                                                                                 107
                                                                                                                                                                                                                                                                                                                                                                                                                                                                                                                                                                                                                                                                                                                                                                                                                                                                                                                                                                                                                                                                                                                                                                                                                                                                                                                                                                                                  108
                                                                                                                                                                                                                                                                                                                                                                                                                                                                                                                                                                                                                                                                                                                                                                                                                                                                                                                                                                                                                                                                                                                                                                                                                                                                                                                                                                                                                                                                                                                                                                                                                                                                                                           109
                                                                                                                                                                                                                                                                                                                                                                                                                                                                                                                                                                                                                                                                                                                                                                                                                                                                                                                                                                                                                                                                                                                                                                                                                                                                                                                                                                                                                                                                                                                                                                                                                                                                                                                                                                                                                                                                                                                                                                                                                                                                                                                                                                                                                                104
                                                                                                                                                                                                                                                                                                                                                                                                                                                                                                                                                                                                                                                                                                                                                                                                                                                                                                                                                                                                                                                                                                                                                                                                                                                                                                                                                                                                                                                                                                                                                                                                                                                                                                                                                                                                                                                                                                                                                                                                                                                                                                                                                                                                                                                                                                                                                                                                                                                                                                                                                                                                                 105
                                                                                                                                                                                                                                                                                                                                                                                                                                                                                                                                                                                                                                                                                                                                                                                                                                                                                                                                                                                                                                                                                                                                                                                                                                                                                                                                                                                                                                                                                                                                                                                                                                                                                                                                                                                                                                                          51
```



```
***********
PERMAT(""0", 8X, 13.4(2X, E13.5))

SCHORMAT("1", 10M"1 UNIT INTOBERS ELECTRIC FIELD DUE TO INCIDENT MACNETS

3"N", 10D", 10M"1 UNIT UNIT UNITED THE CRIED ("UCTS/METER)", """, 24X, "REAL", 22X,

4" ITAGA", "IMPRESS ELECTRIC FIELD IS AS FOLLOW"/"", 10X,

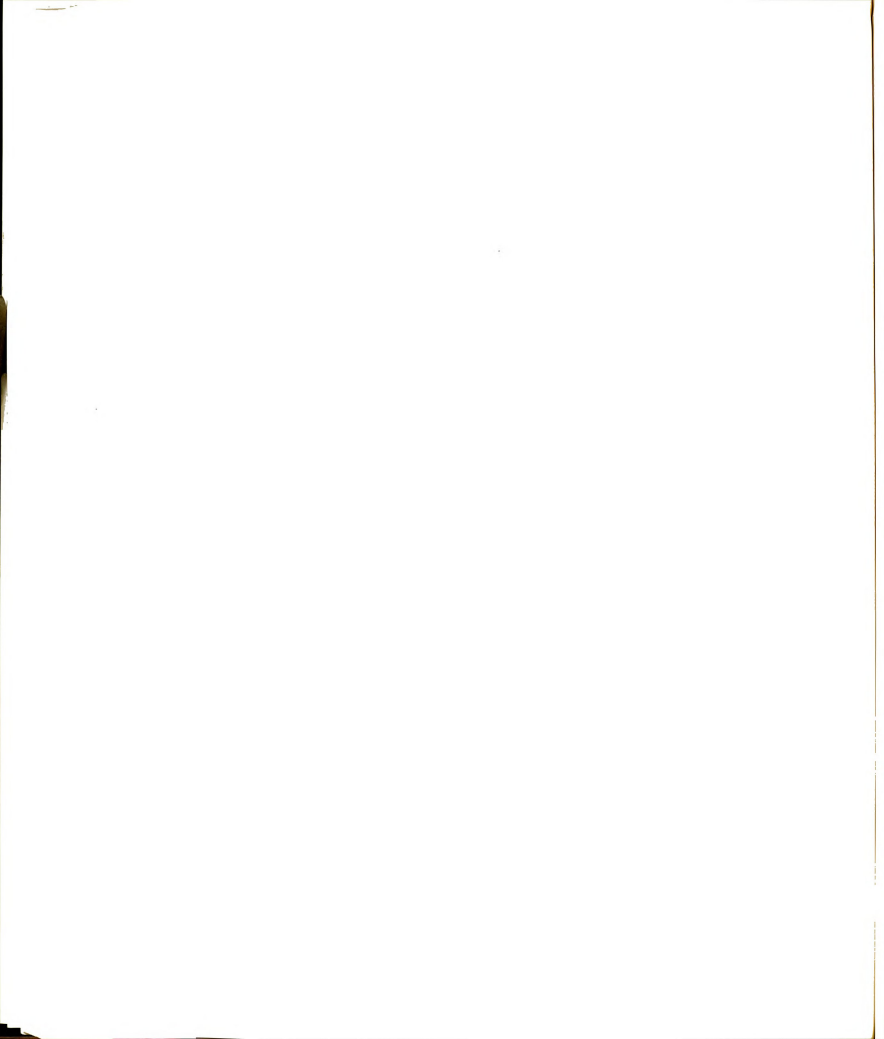
5" FORMAT("1", "THE "INDUCED ELECTRIC FIELD IS AS FOLLOW,

2" FORMAT("1", "THE "INDUCED ELECTRIC FIELD IS AS FOLLOW,

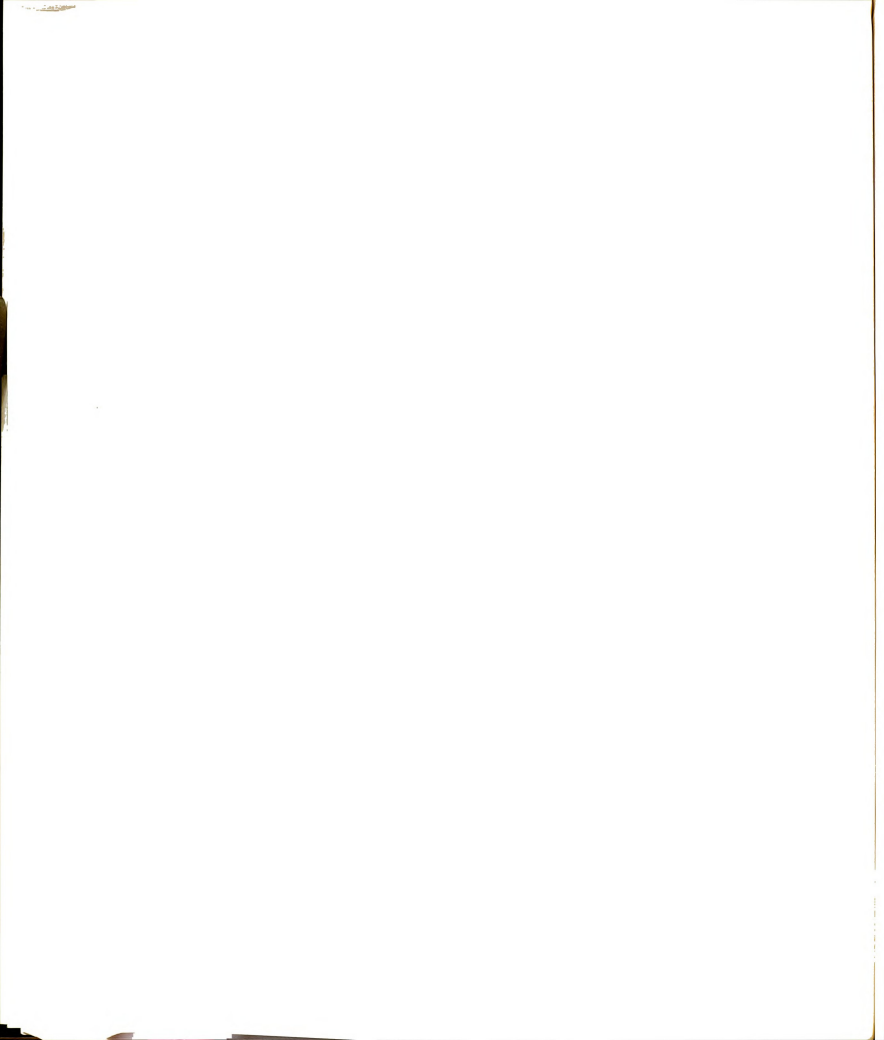
2" FORMAT("1", "THE "INDUCED ELECTRIC FIELD IS AS FOLLOW,

5" FORMAT("1", "THE "INDUCED ELECTRIC FIELD IS AS FOLLOW,

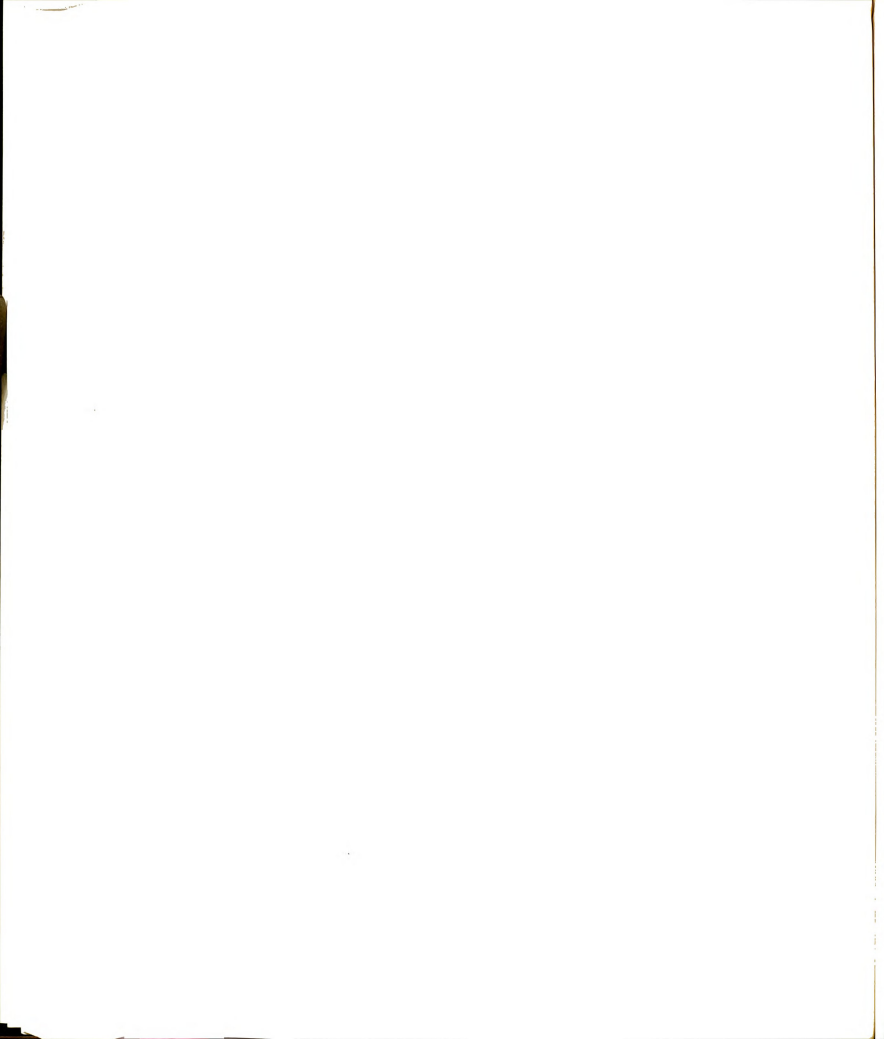
5" FORMAT("1", "THE "INDUCED IN "INDUCED EREAL ("OLLOW, "N", "INDUCED EREAL ("OLLOW, "N", "INDUCED "INDUCED EREAL ("OLLOW, "N", "INDUCED "INDUCE
                                                                                                                                                                                                                                                                                                                                                                                                                                                                                                                                                                                                                                                                                                                                                                                                                                                                                              C****
```



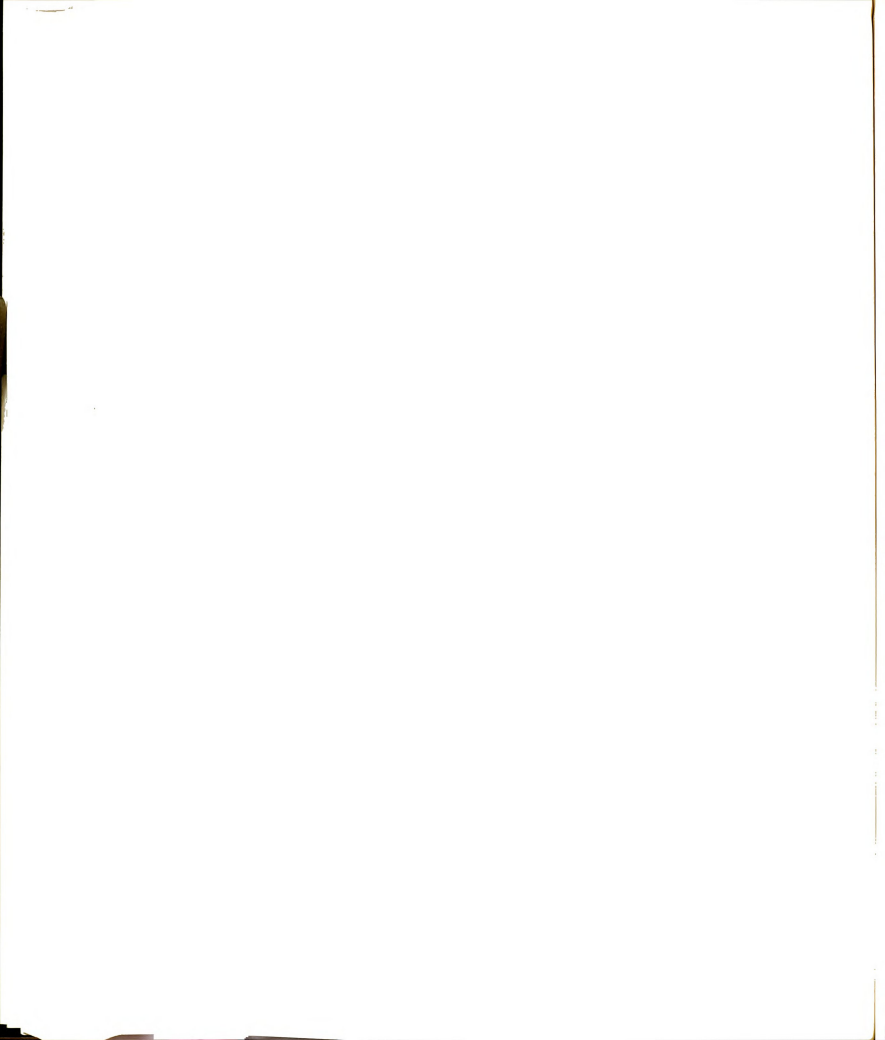
```
FUNCTION FMMC VALUE AND VA
                                                                                                                                                                                                                                                                                                                                                                                                                                                                                                                                                                                                                                                                                                                                                                                                                                                                                                                                                                                                                                                                                                                                                                                                                                                                                                                                                                                                                                                                                                                                                                                                                                                                                                                                                                                                                                                                                                                                                                               ALPA-BETA
BETA-BETA
BETA-B
                                                                                                                                                                                                                                                                                                                                                                                                                                                                                                                                                                                                                                                                                                                                                                                                                                                                                                                                                                                                                                                                                                                                                                                                                                                                                                                                                                                                                                                                                                                                                                                                                                                                                                                                                                                                                                                                                                                                                                                                                                                                                                                                                                                                                                                                                                                                                                                                                                                                                                                                                                                                                                                                                                                                                                           C****
                                                                                                                                                                                                                                                                                                                                                                                                                                                                                                                                                                                                                                                                                                                                                                                                                                                                                                                                                                                                                                                                                                                                                                                                                                                                                                                                                                                                                                                                                                                                                                                                                                                                                                                                                                       33
                                                                                                                                                                                                                                                                                                                                                  2
                                                                                                                                                                                                                                                                                                                                                                                                                                                                                                                                                                                                                                                                                                                                                                                                                                                                                                                                                                                                                                                                                                                                                                                                                                                                                                    52
```



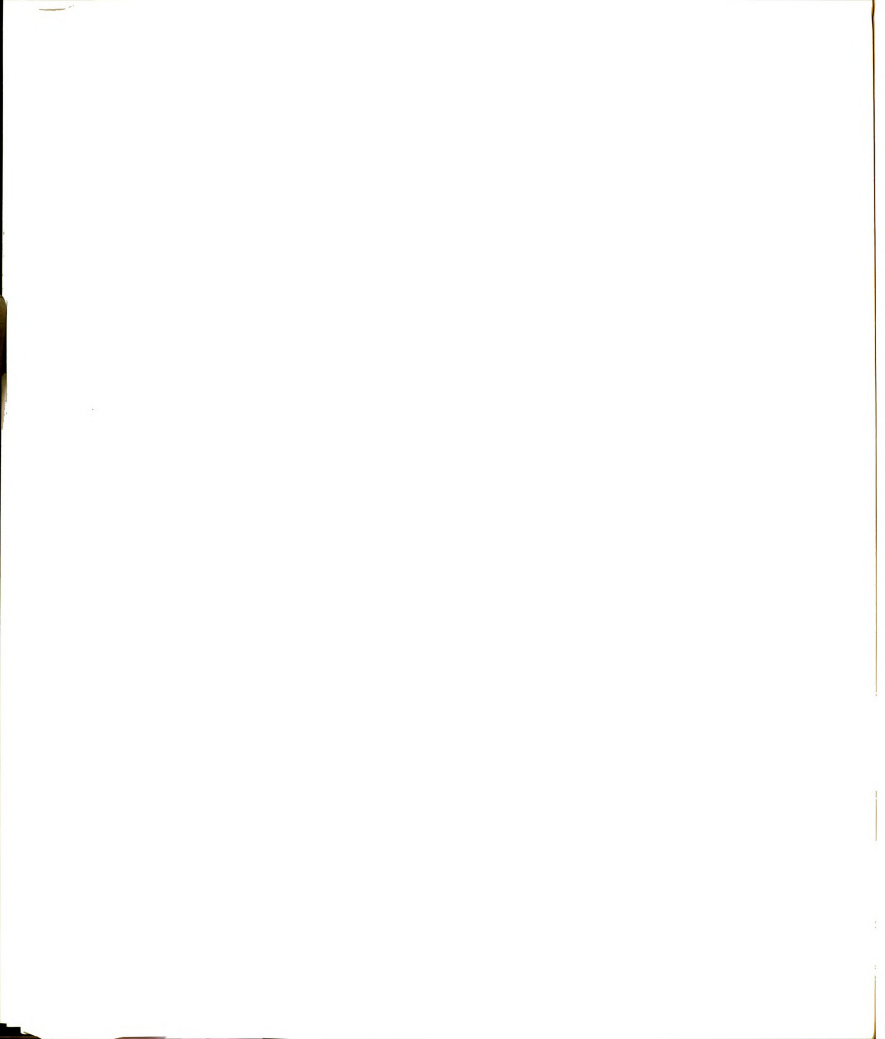
```
*******************
                                                 COMPLEX A, B, DET, CONST, S
DIMENSION A(12, 13)
                                                                                                                                                  CMPLX(1.0)
                                                                                                                                                                            CARS(ACL. J))
                                                                                                                                                 DET = CMPLX(
NPM = N + 1
NPM = N - 1
DO 4 0 = 1,N
C = CABS(AC, 1
DO 5 1 = JF1
                                                                                                                            C****
                                                                                                                                                                C
                                                                                                                                  O
```



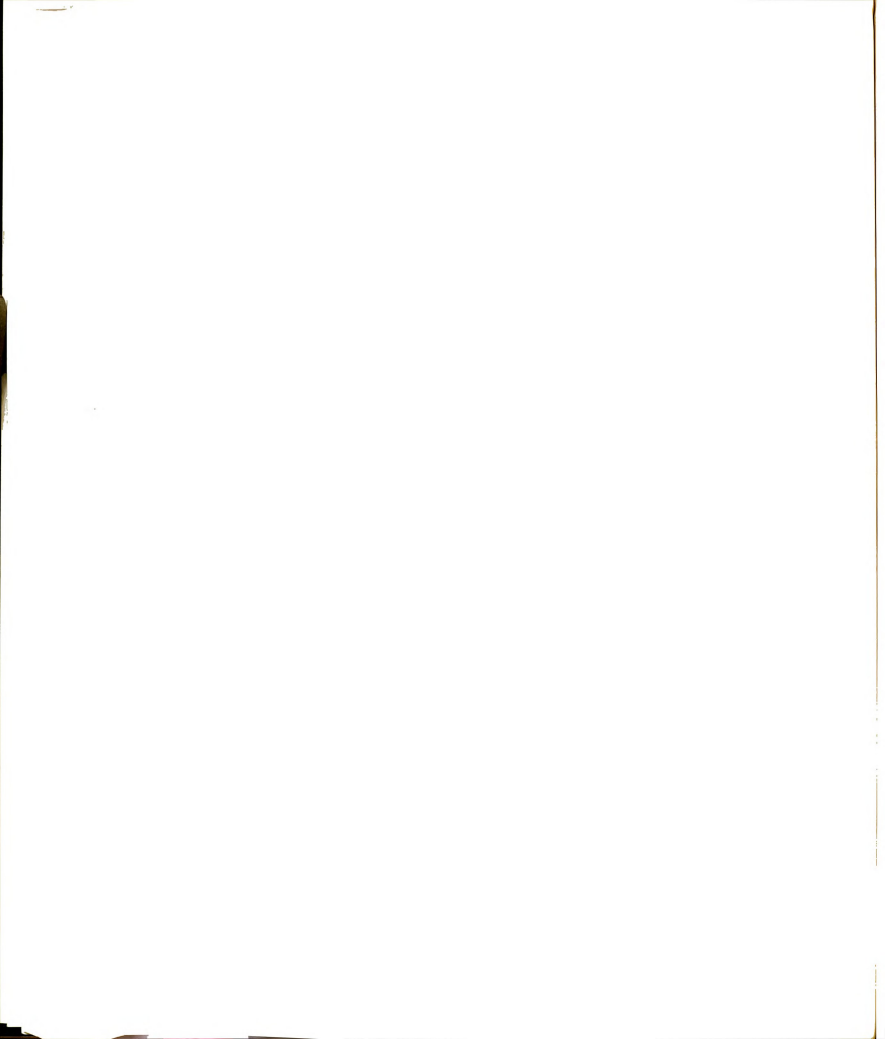
```
(3) * A(J,L)
(K,L) - S)/A(K,K)
2HTHE DETERMINANT OF THE SYSTEM EQUALS ZERO./
36HTHE PROGRAM CANNOT HANDLE THIS CASE.//)
                                                  J))-EP)14, 15, 15
                                                                                         IF(CABS(A(N,N))-EP)14,18,18
DET = CMPLX(0, , 0,)
REINT 30
CENTINUE
CONTINUE
DO 12 I = 1,N
                                                                                                                                                            12, 19, 19
                                                                CONST = A(I, J)/A(J, J)
DO 4 K = JP1, NPM
A(I,K) = A(I,K) - CON
        I. MPH
10
                                                                                                                                            SOD 1
                                                                                                                                                                                                                         C****
                                                                                                                                                                                                                                                                                                         9
                                                                                                 14
                                                                                                                                                                       5000
```



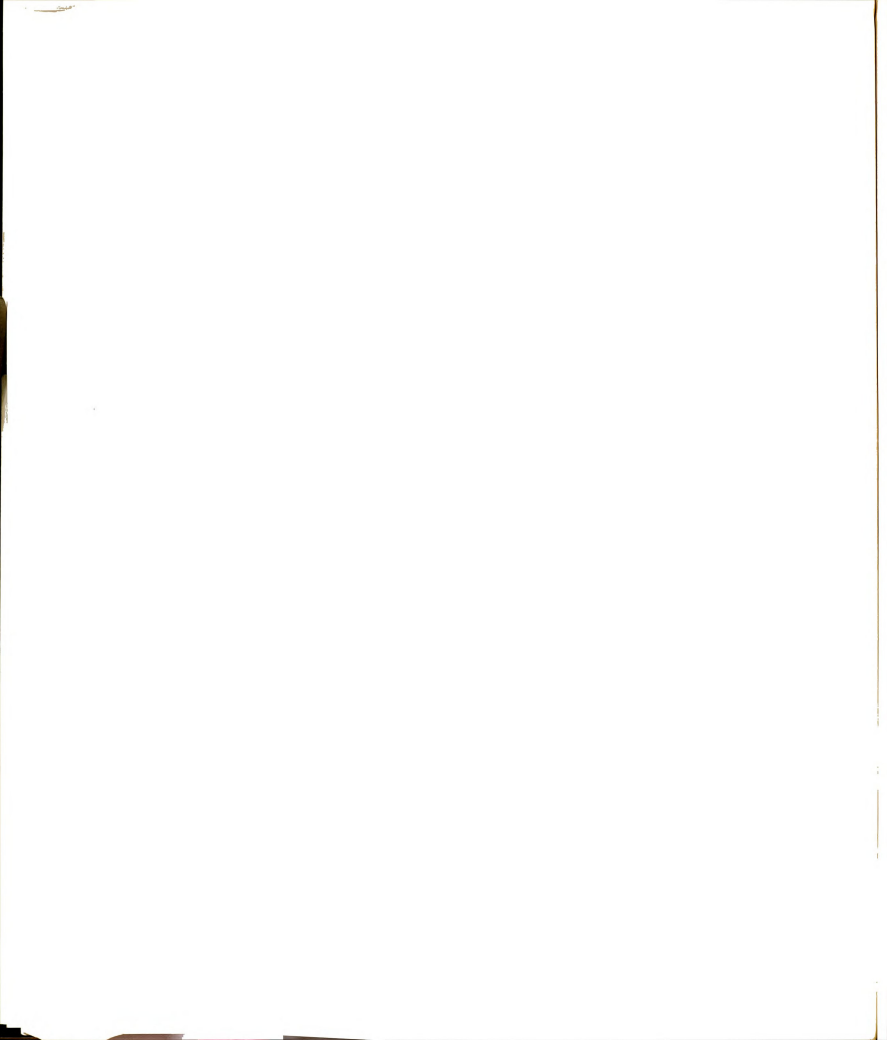
```
20
 9
    40
      9
```



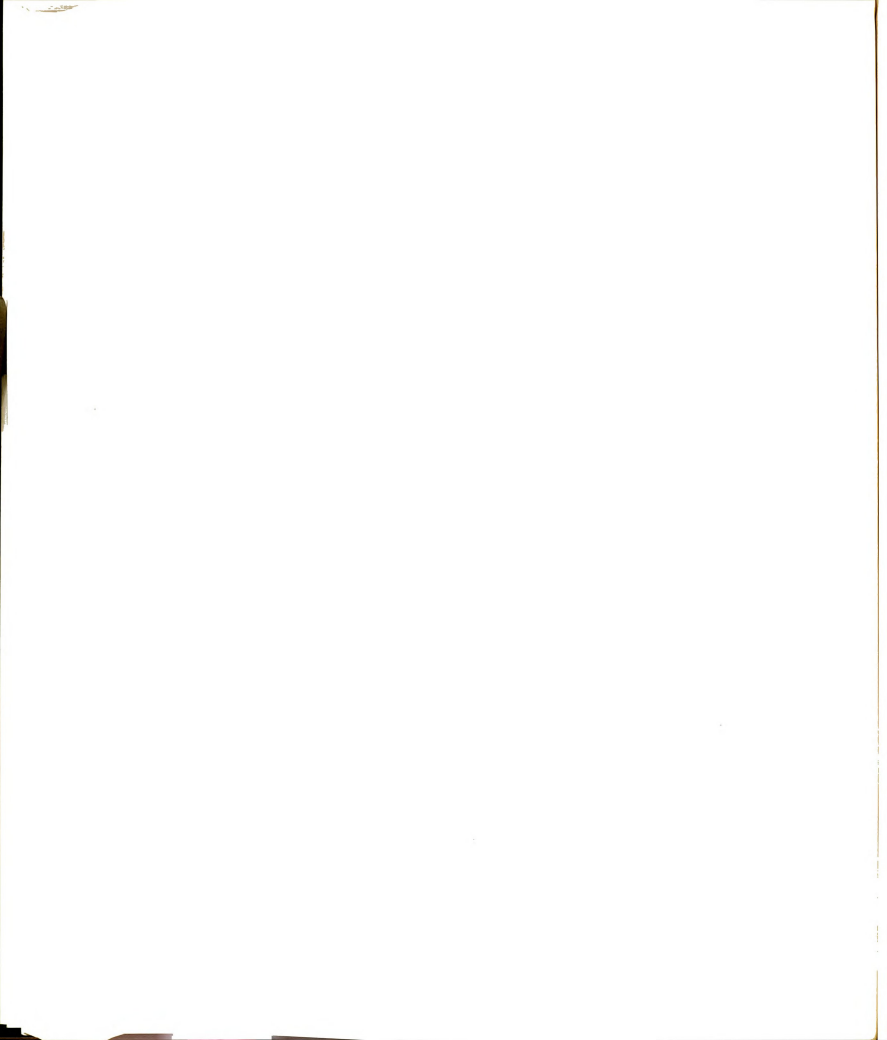
```
0, 0. 0, X(NX+1), X(NX+2))
INC. FIELD) IN DEG., 37, 6. 0,
       40
                                   550
                                            9
               88
```



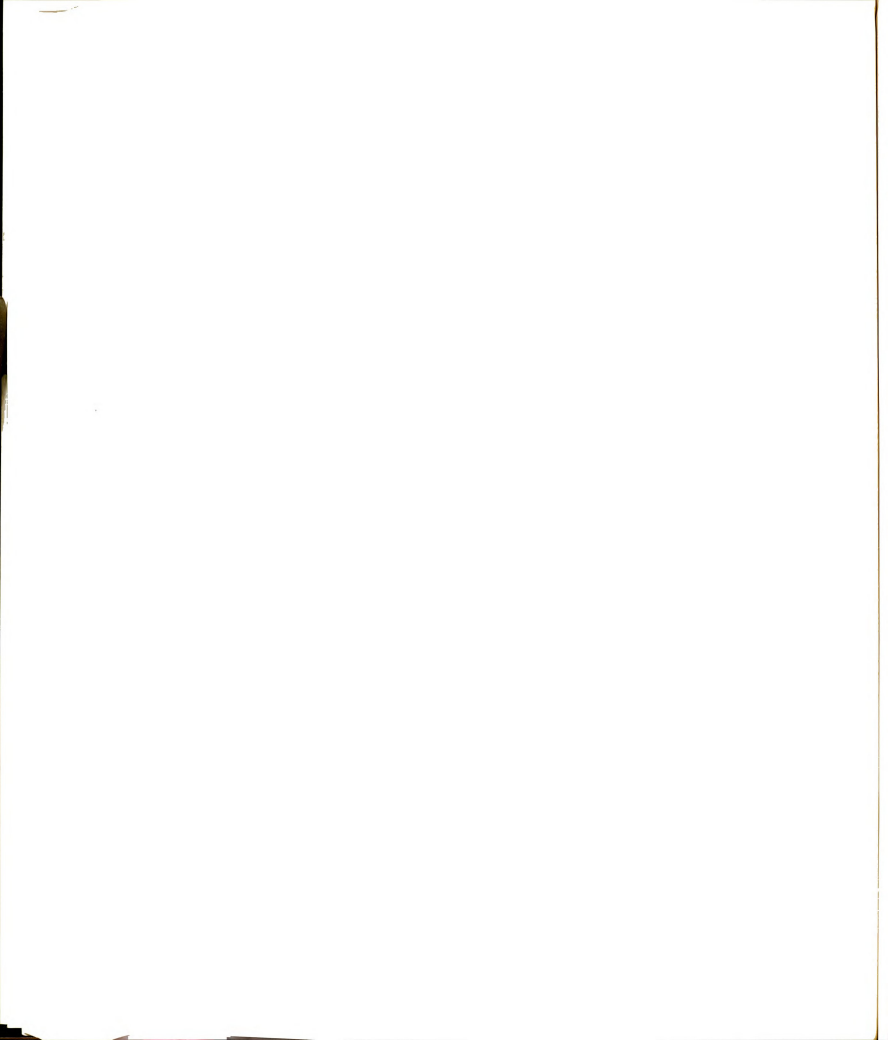
**************************************	120 130 140 150	170	190		0000	280	2000 2000 2100	8888 8888 8888 8888 8888 8888 8888 8888 8888	33000	00444 00000	0444 0008 0008 0008 0016
**************************************	REAL INDUSTRIES COPPLEX FW.L. DET. C.J. FHUN COPPRINT IN THE COPPRINT OF THE C	COMPON Y NXYZYXX, NY, NZ, NNX, NNY, NNZ COMPON V CENS/PI, MUO, EPO COMPON V CENS/VCJ	CONTROL MORAL FILING CONTROL MORAL FILING CONTROL MORAL CONTROL CONTRO	DATA INDU/ALES/AHFLDS/ CALL NOBLANDU/, FLDS/AHFLDS/ BIT-3 (ALEDS)	MU0=1, 19789333 MU0=1, 25663763 PO=8, 846F-12, 12 C. I=78PI V (n. 0.)	1 READ 11, VIV. 11 PORMAT(12)	FEAD 3, 146 5 FORMAT (14) 1 NX, NY, NZ, NNX, NNY, NNZ 1 FORMAT (17, 12)	NOELL-NX-NY-NZ-HNIX-NNY-NNZ DD 21 = 1, NGELL READ 30, FL), V(1), Z(1), DCELL(1)	3 FORMAT (4F10.5) A FORMAT (4FP, S.16, FNEG, MODE A FORMAT (3F12)	IF((10 Eq. 050-8) 40	FORMY (1414 LOX AZAHILLEGAL SYMM CONDITION, 144.1X AHARAS FEEN APPLIED. PROBLEM CAN NOT BE HANDLED) 1F (KNDE FOR EGE COSH) (RC. (MODE: FO. GOSE) + OR. (MODE: FO. GOSH) (RC. (MODE: FO. SINE)



00000000 00000000	570 580 580 ******	**************************************
PRINT 999, MUNE. 999 FORMAT (HILL CA. LIMPRESSED NUDE, IX, A4, IX.) 9 CONTINE CONTIN	STO C****EDD C****BLOCK DATA***********************************	C*****SUBROUTINE MNSB************************************



```
920
                                                                                                                                             670
                                                                                                                                                                                                                             9
                                                                                                                                                                                                                                                                                                                                                                                                            760
                                                                                                                                                                                                                                                                                                                                                                                                                                                                                                                                                                                                                                                                                                                                                              | The control of the 
                                                                                                                                                                                                                                                                                                                                                                                                                                                                                                                                                              106
                                                                                                                                                                                                                                                                                                                                                                                                            103
                                                                                                                                                                                                                                                                                                                                                                                                                                                                                   104
                                                                                                                                                                                                                                                                                                                                                                                                                                                                                                                                                                                                                                                                       100
                                                                                                                                                                                                                                                                                                                                                                                                                                                                                                                                                                                                                                                                                                                                                  107
                                                                                                                                                                                                                                                                                                                                                                                                                                                                                                                                                                                                                                                                                                                                                                                                                                                                                                                                                                                                                                                          S
```

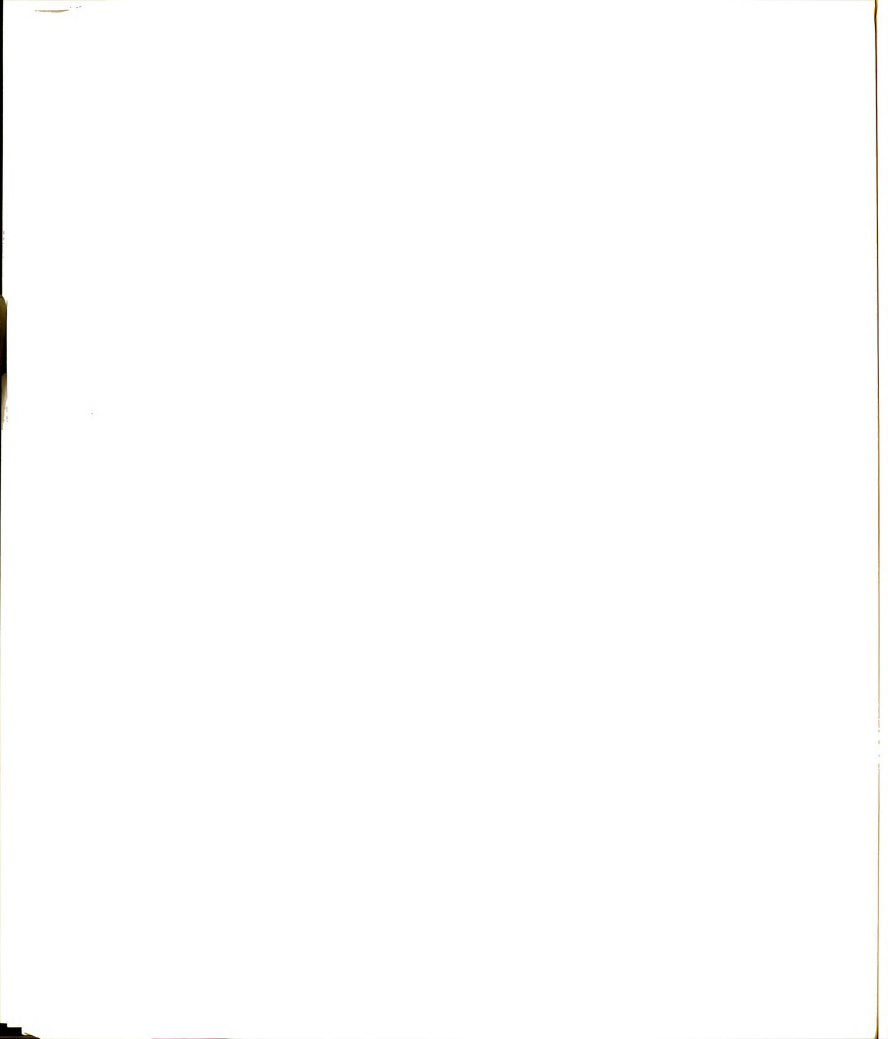


```
070
080
090
100
120
                                                                                                                                                                                                                                                                                                                                                                                                                                                                                                                                                                                                                                         1140
                                                                                                                                                                                                                                                                                                                                                                                                                                                                                                                                                                                                                                                                                                                                                                                                                                 )+NV(2);

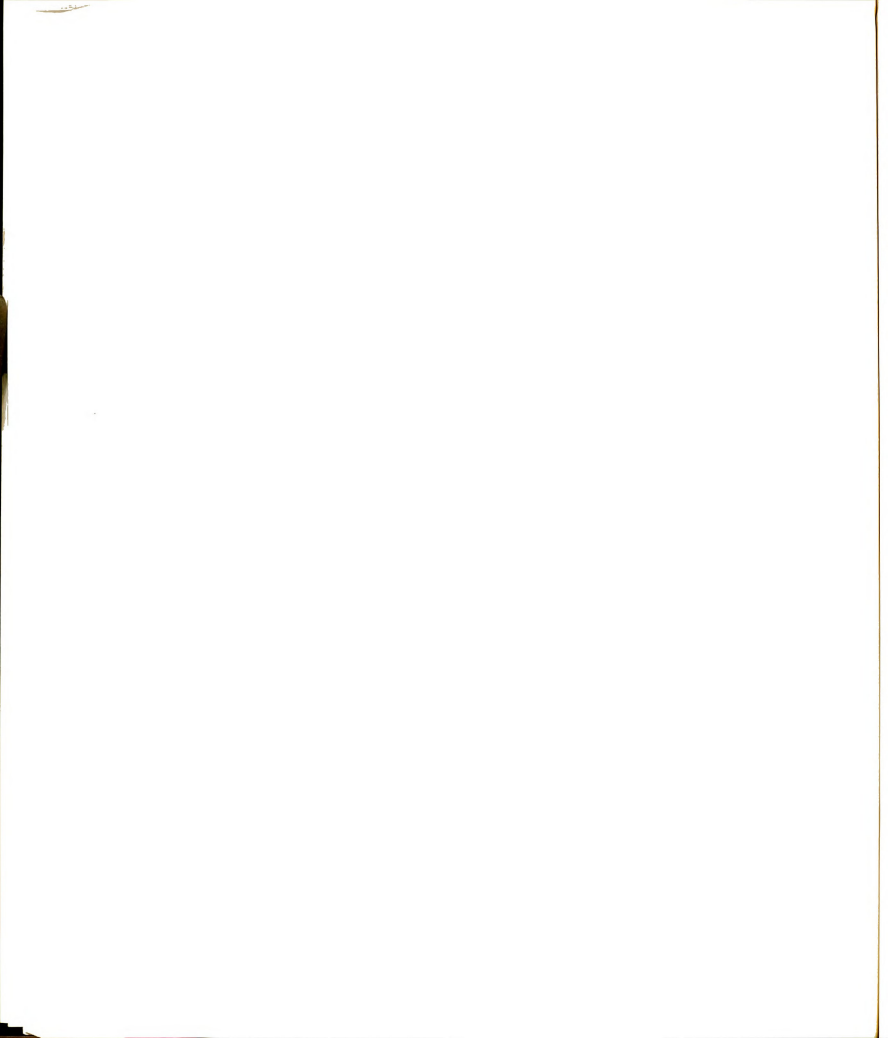
+NV(2)+NV(3);

+NV(2)+NV(3)+NV(4);

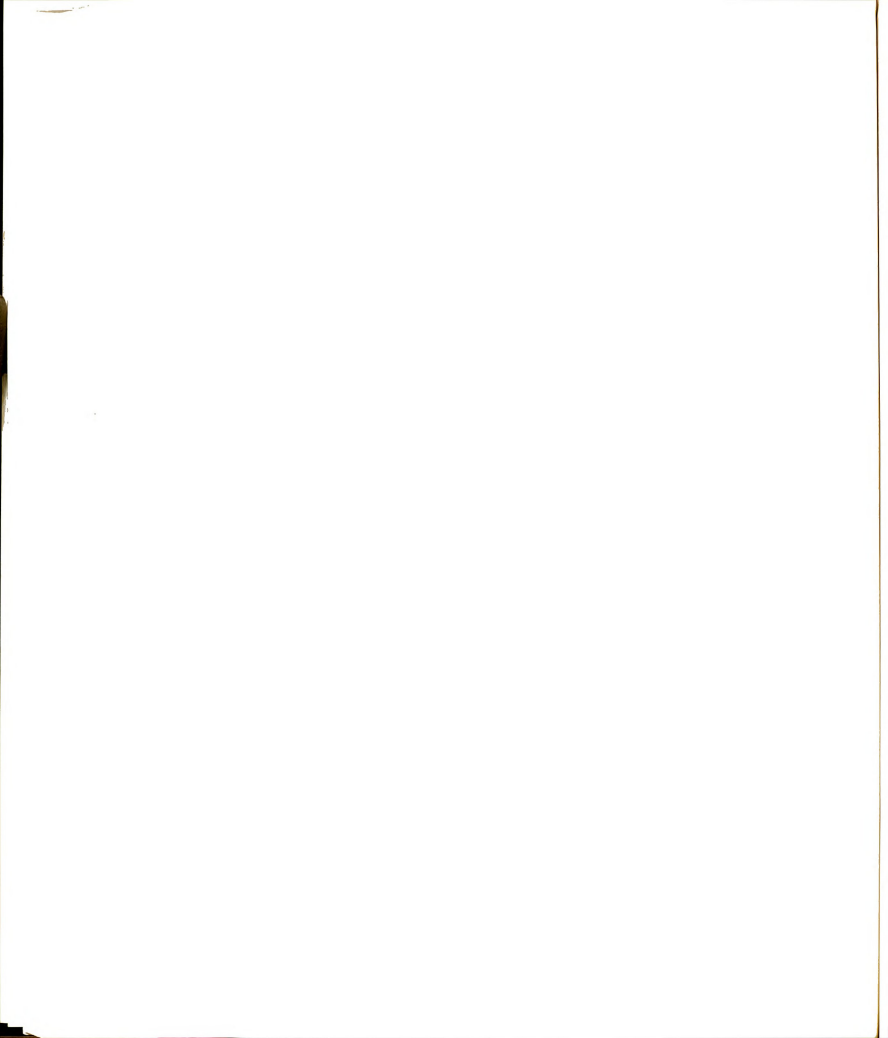
)+NV(2)+NV(3)+NV(4);
                                                                                                                                                                                                                              Z (MCELL), ARE (MCELL), MUO, MDDE
6), CJ, FK, FHUN
                                                                                                                                                                                                                                                                                                                                                                                                                                                                                                                                                                                                                                                                                                                                                                                                                                                                                                                                                                                                                                                                                                                                                                                                                                                                                                                                                                                                                                                                                                                                                                                                                                                                                                                                                                                                                                                                                                                                                                                                                                                                                                                                                                                                                                                                                                                                                                                                                                                                                                                                                                                                                                                                                          )+NV(2) +V(3) +V(3) +V(4) +V(2) +V(2) +V(3) +V(4) +V(5) +V(4) +V(4) +V(5) +V(4) +V(4) +V(5) +V(4) +V(4) +V(5) +V(4) +V(4
                                                         RAPRETER CORPERATOR CONTRACT NOT CONTRACT NO
| Harring | Harring | Harring | Harring | Harring | Harring | Harring | Harring | Harring | Harring | Harring | Harring | Harring | Harring | Harring | Harring | Harring | Harring | Harring | Harring | Harring | Harring | Harring | Harring | Harring | Harring | Harring | Harring | Harring | Harring | Harring | Harring | Harring | Harring | Harring | Harring | Harring | Harring | Harring | Harring | Harring | Harring | Harring | Harring | Harring | Harring | Harring | Harring | Harring | Harring | Harring | Harring | Harring | Harring | Harring | Harring | Harring | Harring | Harring | Harring | Harring | Harring | Harring | Harring | Harring | Harring | Harring | Harring | Harring | Harring | Harring | Harring | Harring | Harring | Harring | Harring | Harring | Harring | Harring | Harring | Harring | Harring | Harring | Harring | Harring | Harring | Harring | Harring | Harring | Harring | Harring | Harring | Harring | Harring | Harring | Harring | Harring | Harring | Harring | Harring | Harring | Harring | Harring | Harring | Harring | Harring | Harring | Harring | Harring | Harring | Harring | Harring | Harring | Harring | Harring | Harring | Harring | Harring | Harring | Harring | Harring | Harring | Harring | Harring | Harring | Harring | Harring | Harring | Harring | Harring | Harring | Harring | Harring | Harring | Harring | Harring | Harring | Harring | Harring | Harring | Harring | Harring | Harring | Harring | Harring | Harring | Harring | Harring | Harring | Harring | Harring | Harring | Harring | Harring | Harring | Harring | Harring | Harring | Harring | Harring | Harring | Harring | Harring | Harring | Harring | Harring | Harring | Harring | Harring | Harring | Harring | Harring | Harring | Harring | Harring | Harring | Harring | Harring | Harring | Harring | Harring | Harring | Harring | Harring | Harring | Harring | Harring | Harring | Harring | Harring | Harring | Harring | Harring | Harring | Harring | Harring | Harring | Harring | Harring | Harring | Harring | Harring | Harring | Harring | Harr
```

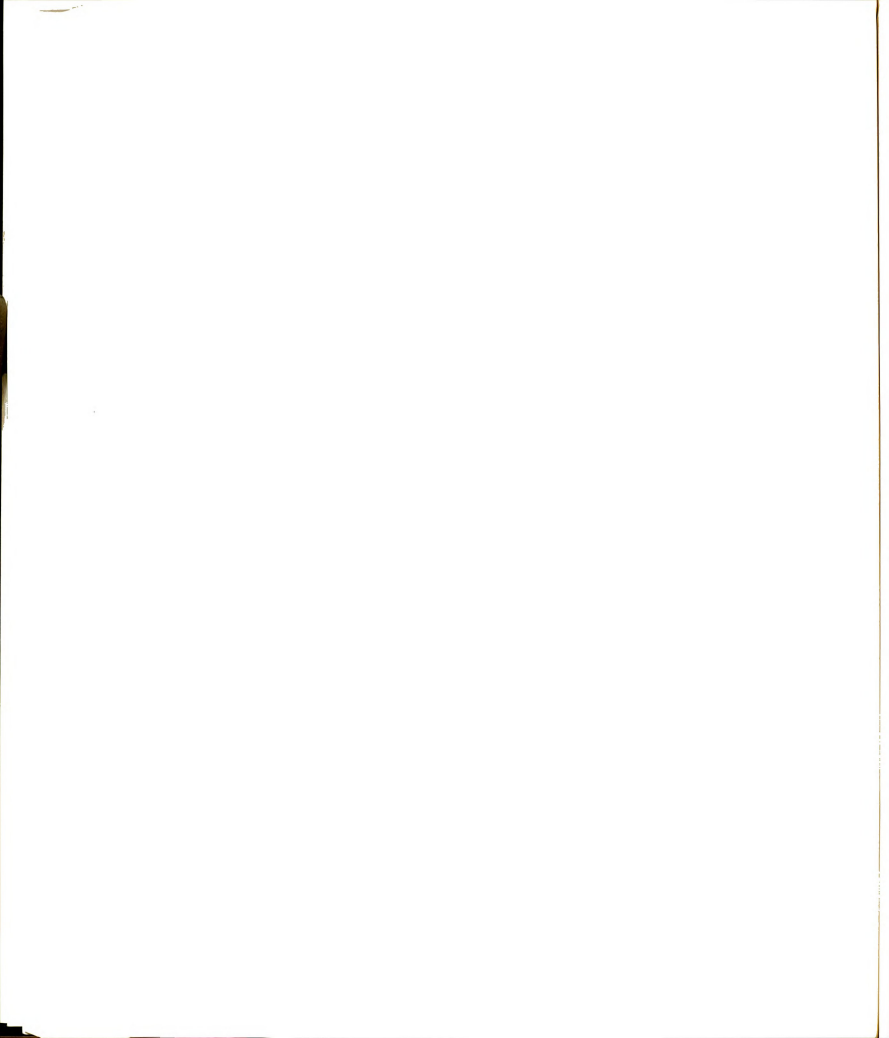


11510 1510 1510 1510 1510 1510 1510 151	1 1 2 0 0 0 0 0 0 0 0 0 0 0 0 0 0 0 0 0	11111111111111111111111111111111111111
1510 1520 ER. J. DR. NDIR . ER. 4) CALL ELEMX (MDIR, NDIR, M, N, X, Y, Z, ARE, NDIS, M, N, X, W, Z, ARE, NDIS, M, N, X, W, Z, ARE, NDIS, M, N, Z, ME, NDIS, M, N, X, W, Z, ME, NDIS, M, M, M, M, W, W, W, M, M, M, M, W, W, W, M, M, M, M, M, W, W, W, M,	NOELL J. VIVELL J. STEEL NOTE, IN J. Y. Y. Z. ARE, NOELL, E) NOELL J. VIVELL J. STOKELL J. ARE NOELL, E) NOELL J. VIVELL J. STOKEL J. ARE NOELL, FUNCELL J. STOKEL J. ARE NOEL J. VIVELL J. STOKEL J. ARE NOEL J. VIVELL J. STOKEL J. ARE NOEL J. MODE, MUO NO STOKE J. MUO, EPO J. STOKE J. STOKE J. STOKE J. MUO NOEL J. STOKE J. MUO, EPO J. STOKE J.	IF (ND IR EG. 4) NN=N IF (ND IR EG. 4) NN IR
NP=NT+NV(NDIP) NPP=NP+V(NDIP) NPP=NP+V(NDIP) +ELL, BT (NDIR EG. 1. OR NI +ELL, BT (NDIR EG. 2. OR NI +ELL, BT (NDIR EG. 3. OR NI NU +ELL, BT (AND THE ELEMAN OF THE PROPERTY	201 KNDIR EG. 1) NNIR LIFT (NDIR EG. 1) NNIR

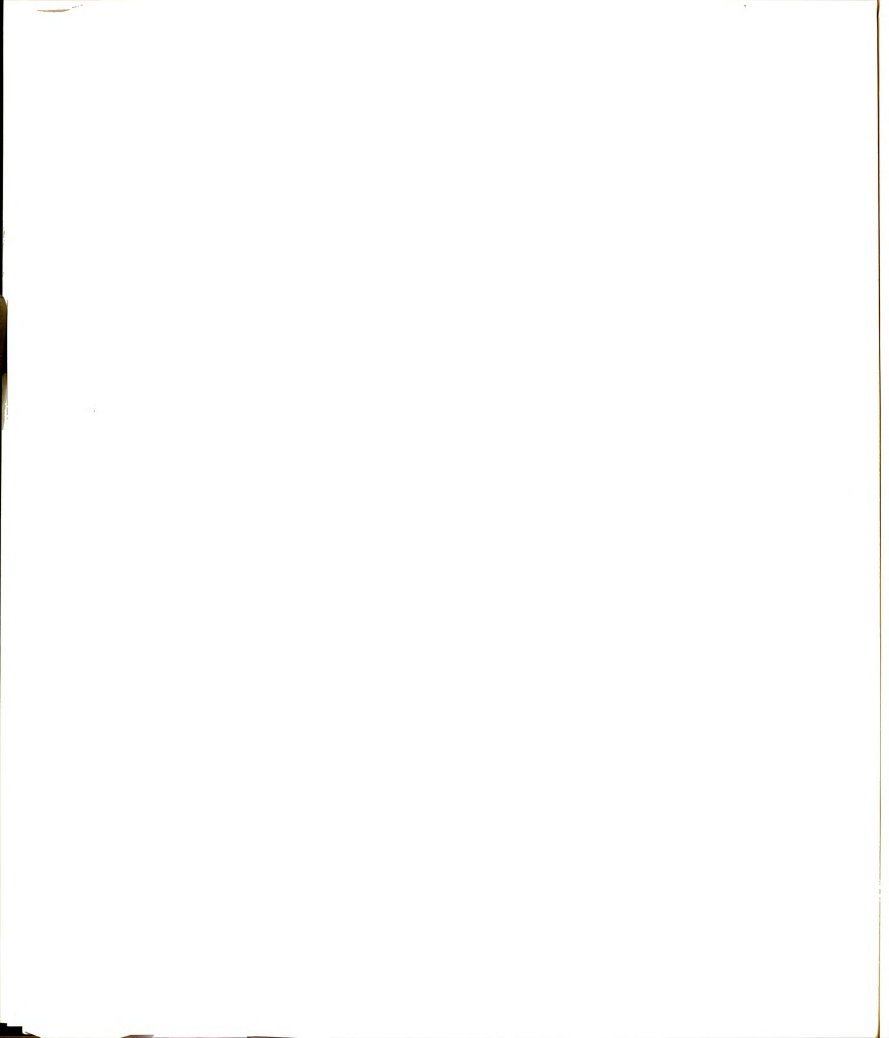


9 CONTINUE
3 CONTINUE
3 CONTINUE
3 CONTINUE
3 CONTINUE
3 CONTINUE
4 CONTINUE
4 CONTINUE
5 CONTINUE
5 CONTINUE
5 CONTINUE
6 CONTINUE





```
82
IF(10, Eq. 1234) YN=-1, O9YN
IF(10, Eq. 1234) GO TO 103
CALL COEFX (MDIR, AREA, MY, YN, ZM, XN, YN, ZN, C)
IF(MDDE, Eq. COBH OR, MODE, Eq. SINE) GO TO 66
                                                                                                                                                                                                                     82
                                                                                                                                                                                                                                                                8
                                                                                                                                                                                                                                                                                    84
                                                                                                                                                                                                                                                                                                85
                                                                                                                                                                                                                                                                                                                    88
                                                                                                                                                                   89
                                                                                                                                                                                        69
                                                                                                              65
                                                                                                                           99
                                                                                                                                                67
                                                   62
                                                                       63
                                                                                            64
```



```
3580
3590
3610
3620
                                                                                                                                                                                                                                                                                                                                                                                                                                                                                                                                                                                                                                                                               3640
                                                                                                                                                                                                                                                                                                                                                                                                                                                                                                                                                                                                                                                                                                                                                3260
33770
33770
33770
33770
33770
33770
33770
33770
33770
                                                                                                                                                                                                                                                                                                                                                                                                                                                                             DO BY 1=9,16

E(1)=E(1)+C(1)

4 CONTINUE

CONTINUE

DO 94 = 11,4

DO 97 = 15,4

DO 71=C(1)+C(1)

DO 97 = 15,4

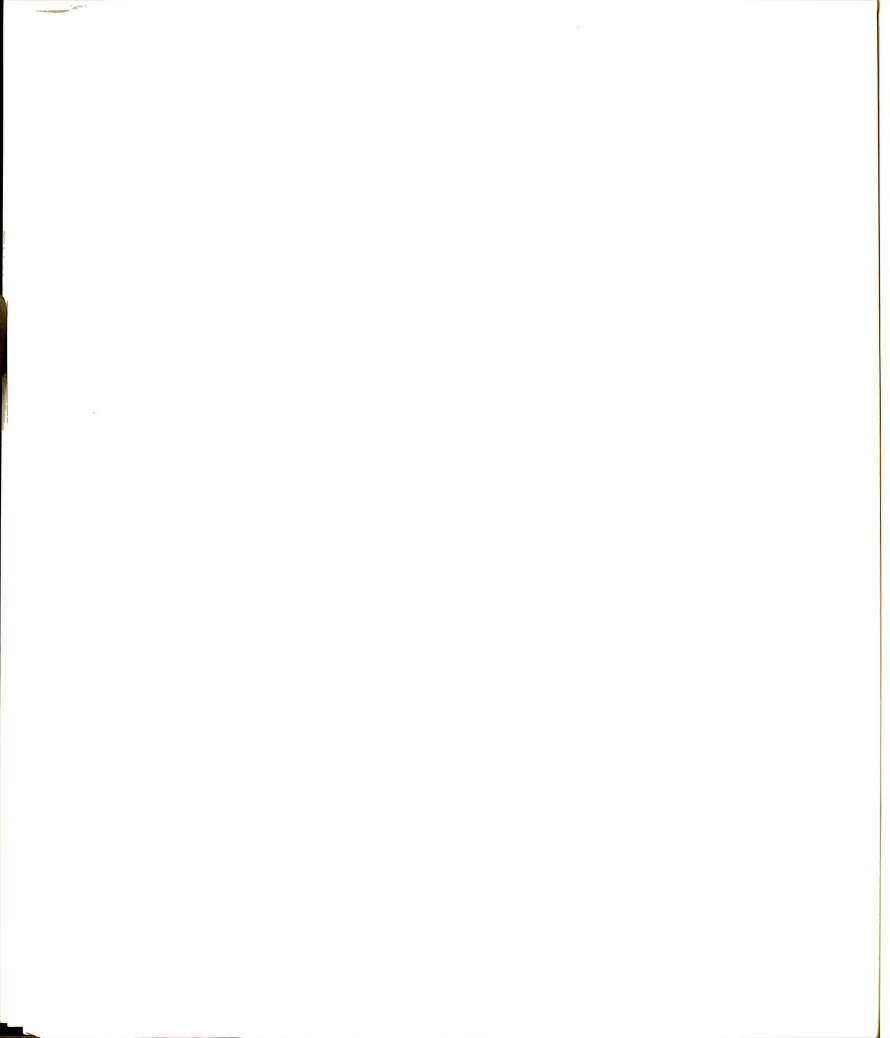
DO 97 = 13,16

E(1)=E(1)+C(1)

DO 97 = 12,16

E(1)=E(1)+C(1)

E(1)
                                                                                                                                                                                                                                                                                                                                                                                                                                                                                                                                                                                                                                                                                                                                                                                                                                                                                                                                                              XM=X
YM=X
XM=X
XN=X
XN=X
XN=X
XN=X
XN=X
                                                                                                                                                                                                                                                                                                                                                                                                                                                                                    C****
                                                                                                               103
                                                                                                                                                                                                                                                        4
                                                                                                                                                                                                                                                                                                                                                                                             100
                                                                                                                                                                                                                                                                                                                                                                                                                                                                                                                                                                                                                                                                                                                                                                                                                                                                                                                                                                 201
```



```
EQ. 1458) ZN=-1. 0*ZN
EQ. 1458) GO TO 300
0*XN
COEFY (MDIR, AREA, XM, YM, ZM, XN, YN, ZN, C)
                                                                                                                           COEFY (MDIR, AREA, XM, YM, ZM, XN, YN, ZN, C)
                                                                                                                                                                                                                                                                                                                                                                                                                                                                                                              YN=Y(V<sub>1</sub>,

YN=Y(V<sub>1</sub>,

XN=XM

N=Z(NN)

AREA=ARE(NN)

CALL COEFY(MD)

DO 2 1=1,16

CONTINUE

GONTINUE
                                                                                                                                                                                                                                                                                                                                                                                                                                                                                                                                                                                                                                                                                                                                                                                                                                                                                                                                                                                                                                                                                                                                                                                                                                                                                                                                                                                                                                                                                                                                                                                                                                                                                                                                                                                                                                                                                                                                                                                                                                                                                                                                                                                                                                                                                                                                                                                                           203
                                                                                                                                                                                                                                                                                                                               C
                                                                                                                                                                                                                                                                                                                                                                                                                                                          202
```

```
6 CONTINUE (17-67)

6 CONTINUE (17-67)

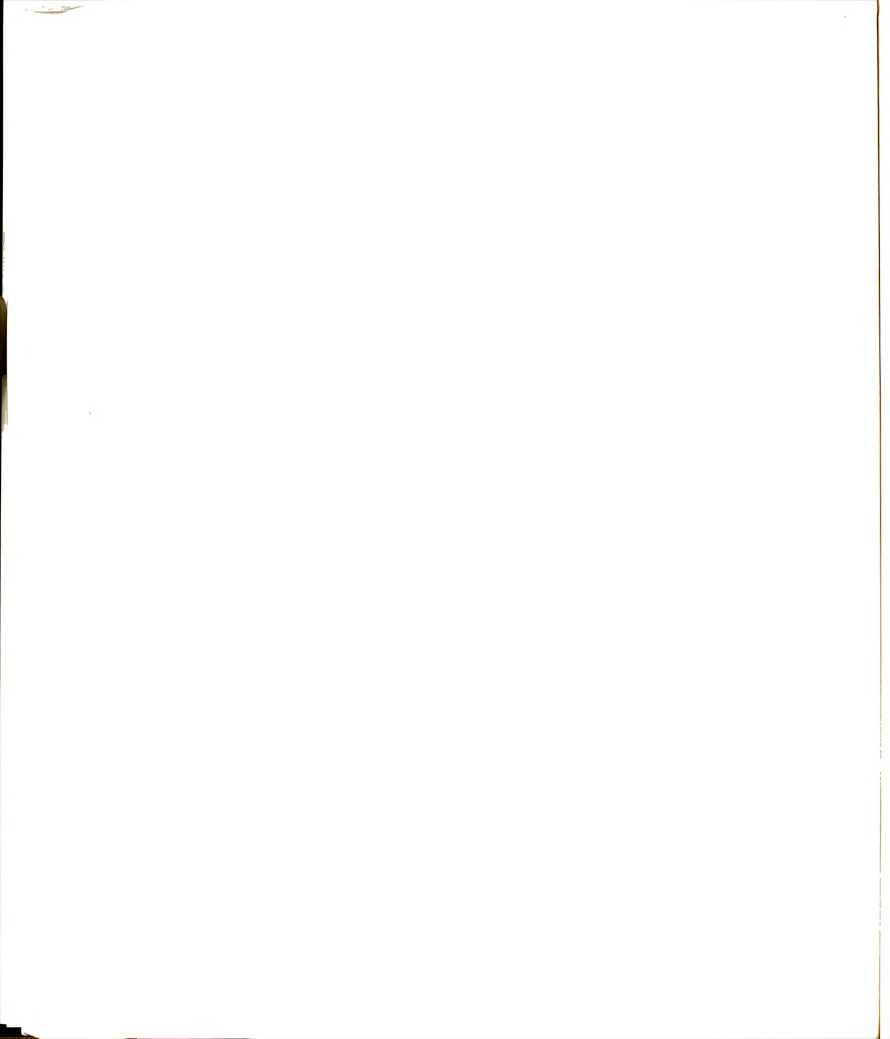
1 F (13 E G 12-7)

2 F (13 E G 12-7)

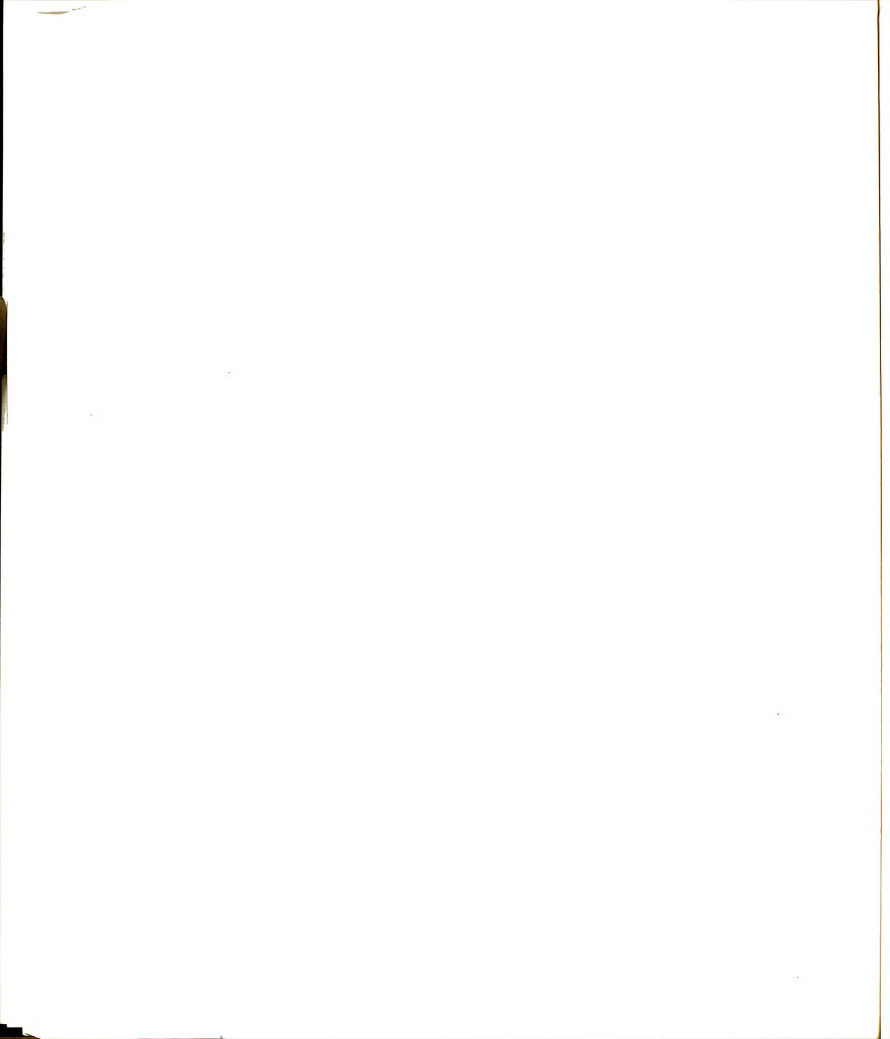
3 F (13 E G 12-7)

4 F (13 E G 12-7)

5 F (13 E G
```



```
47 CONTINUE
60 48 E-9, 16
61 J=6 (1) = 6 (1) = 6 (1) = 6 (1) = 6 (1) = 6 (1) = 6 (1) = 6 (1) = 6 (1) = 6 (1) = 6 (1) = 6 (1) = 6 (1) = 6 (1) = 6 (1) = 6 (1) = 6 (1) = 6 (1) = 6 (1) = 6 (1) = 6 (1) = 6 (1) = 6 (1) = 6 (1) = 6 (1) = 6 (1) = 6 (1) = 6 (1) = 6 (1) = 6 (1) = 6 (1) = 6 (1) = 6 (1) = 6 (1) = 6 (1) = 6 (1) = 6 (1) = 6 (1) = 6 (1) = 6 (1) = 6 (1) = 6 (1) = 6 (1) = 6 (1) = 6 (1) = 6 (1) = 6 (1) = 6 (1) = 6 (1) = 6 (1) = 6 (1) = 6 (1) = 6 (1) = 6 (1) = 6 (1) = 6 (1) = 6 (1) = 6 (1) = 6 (1) = 6 (1) = 6 (1) = 6 (1) = 6 (1) = 6 (1) = 6 (1) = 6 (1) = 6 (1) = 6 (1) = 6 (1) = 6 (1) = 6 (1) = 6 (1) = 6 (1) = 6 (1) = 6 (1) = 6 (1) = 6 (1) = 6 (1) = 6 (1) = 6 (1) = 6 (1) = 6 (1) = 6 (1) = 6 (1) = 6 (1) = 6 (1) = 6 (1) = 6 (1) = 6 (1) = 6 (1) = 6 (1) = 6 (1) = 6 (1) = 6 (1) = 6 (1) = 6 (1) = 6 (1) = 6 (1) = 6 (1) = 6 (1) = 6 (1) = 6 (1) = 6 (1) = 6 (1) = 6 (1) = 6 (1) = 6 (1) = 6 (1) = 6 (1) = 6 (1) = 6 (1) = 6 (1) = 6 (1) = 6 (1) = 6 (1) = 6 (1) = 6 (1) = 6 (1) = 6 (1) = 6 (1) = 6 (1) = 6 (1) = 6 (1) = 6 (1) = 6 (1) = 6 (1) = 6 (1) = 6 (1) = 6 (1) = 6 (1) = 6 (1) = 6 (1) = 6 (1) = 6 (1) = 6 (1) = 6 (1) = 6 (1) = 6 (1) = 6 (1) = 6 (1) = 6 (1) = 6 (1) = 6 (1) = 6 (1) = 6 (1) = 6 (1) = 6 (1) = 6 (1) = 6 (1) = 6 (1) = 6 (1) = 6 (1) = 6 (1) = 6 (1) = 6 (1) = 6 (1) = 6 (1) = 6 (1) = 6 (1) = 6 (1) = 6 (1) = 6 (1) = 6 (1) = 6 (1) = 6 (1) = 6 (1) = 6 (1) = 6 (1) = 6 (1) = 6 (1) = 6 (1) = 6 (1) = 6 (1) = 6 (1) = 6 (1) = 6 (1) = 6 (1) = 6 (1) = 6 (1) = 6 (1) = 6 (1) = 6 (1) = 6 (1) = 6 (1) = 6 (1) = 6 (1) = 6 (1) = 6 (1) = 6 (1) = 6 (1) = 6 (1) = 6 (1) = 6 (1) = 6 (1) = 6 (1) = 6 (1) = 6 (1) = 6 (1) = 6 (1) = 6 (1) = 6 (1) = 6 (1) = 6 (1) = 6 (1) = 6 (1) = 6 (1) = 6 (1) = 6 (1) = 6 (1) = 6 (1) = 6 (1) = 6 (1) = 6 (1) = 6 (1) = 6 (1) = 6 (1) = 6 (1) = 6 (1) = 6 (1) = 6 (1) = 6 (1) = 6 (1) = 6 (1) = 6 (1) = 6 (1) = 6 (1) = 6 (1) = 6 (1) = 6 (1) = 6 (1) = 6 (1) = 6 (1) = 6 (1) = 6 (1) = 6 (1) = 6 (1) = 6 (1) = 6 (1) = 6 (1) = 6 (1) = 6 (1) = 6 (1) = 6 (1) = 6 (1) = 6 (1) = 6 (1) = 6 (1) = 6 (1) = 6 (1) = 6 (1) = 6 (1) = 6 (1) =
```



```
5540
                                                                                       CONTINUE

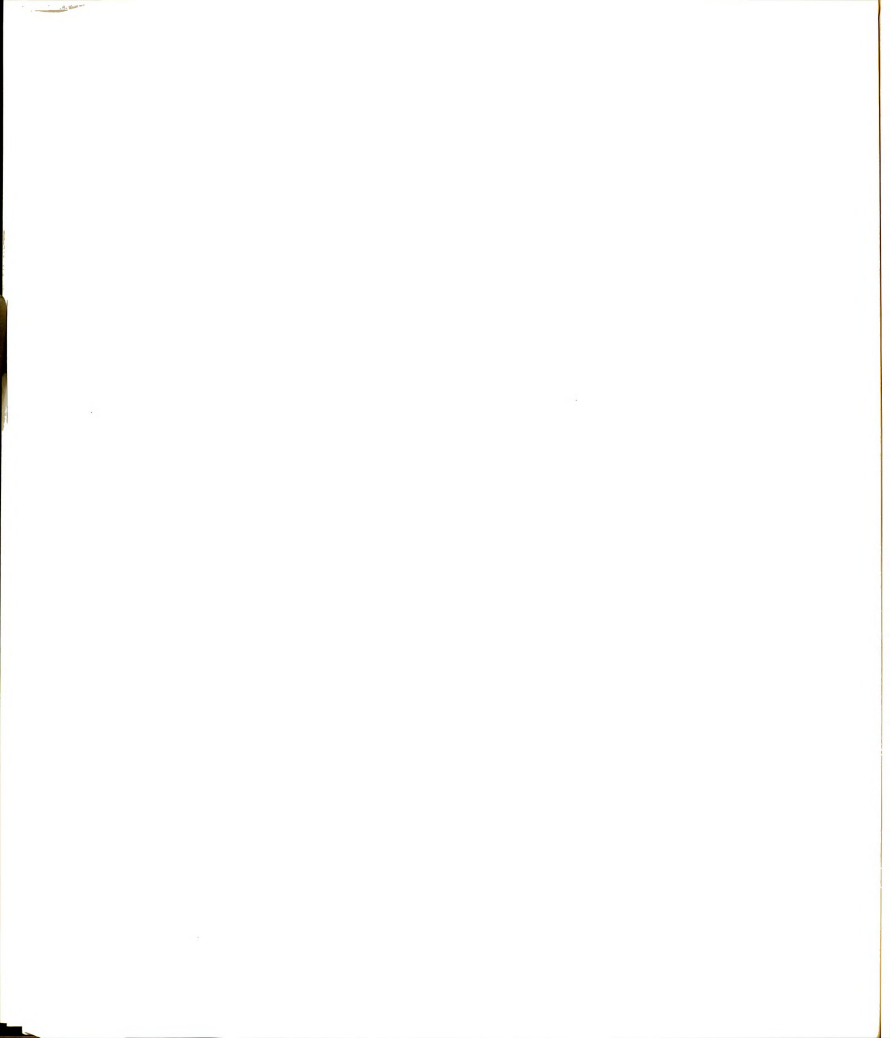
E(1) = E(1) + C(1)

E(1) = E(1) + C(1)

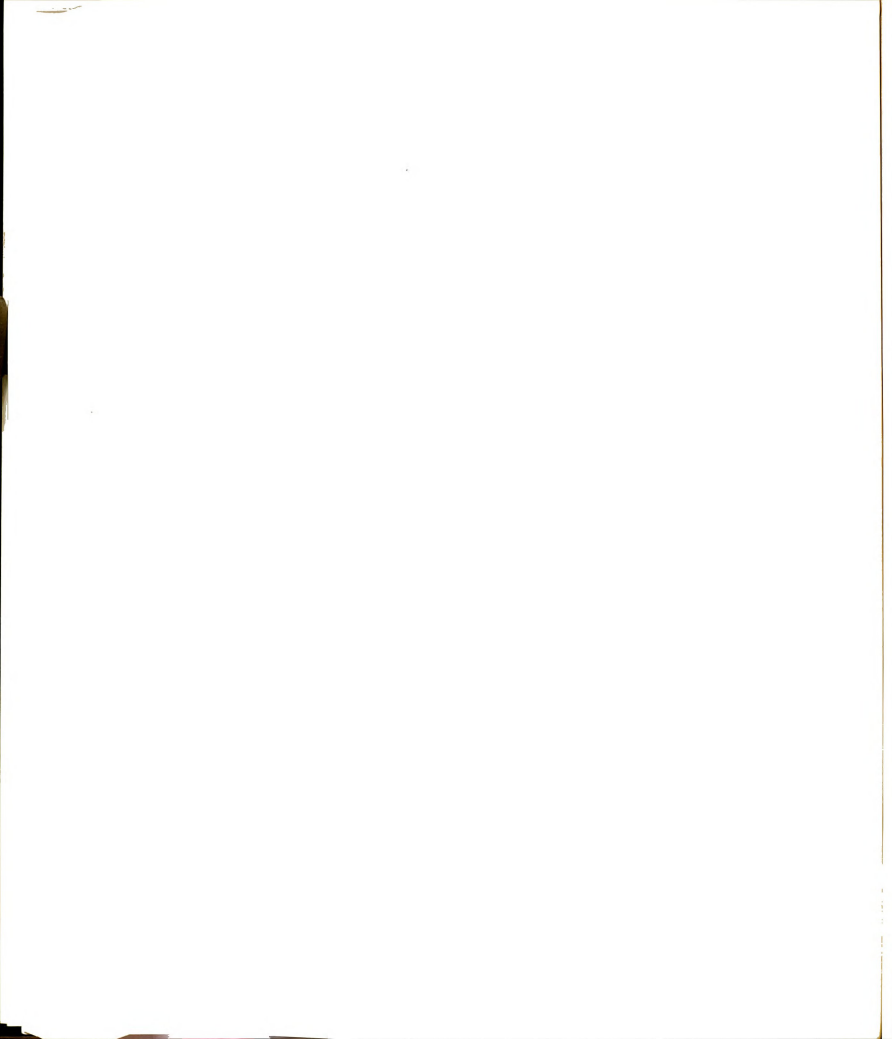
E(1) = E(1) + C(1)

E(1) = E(1) = E(1)

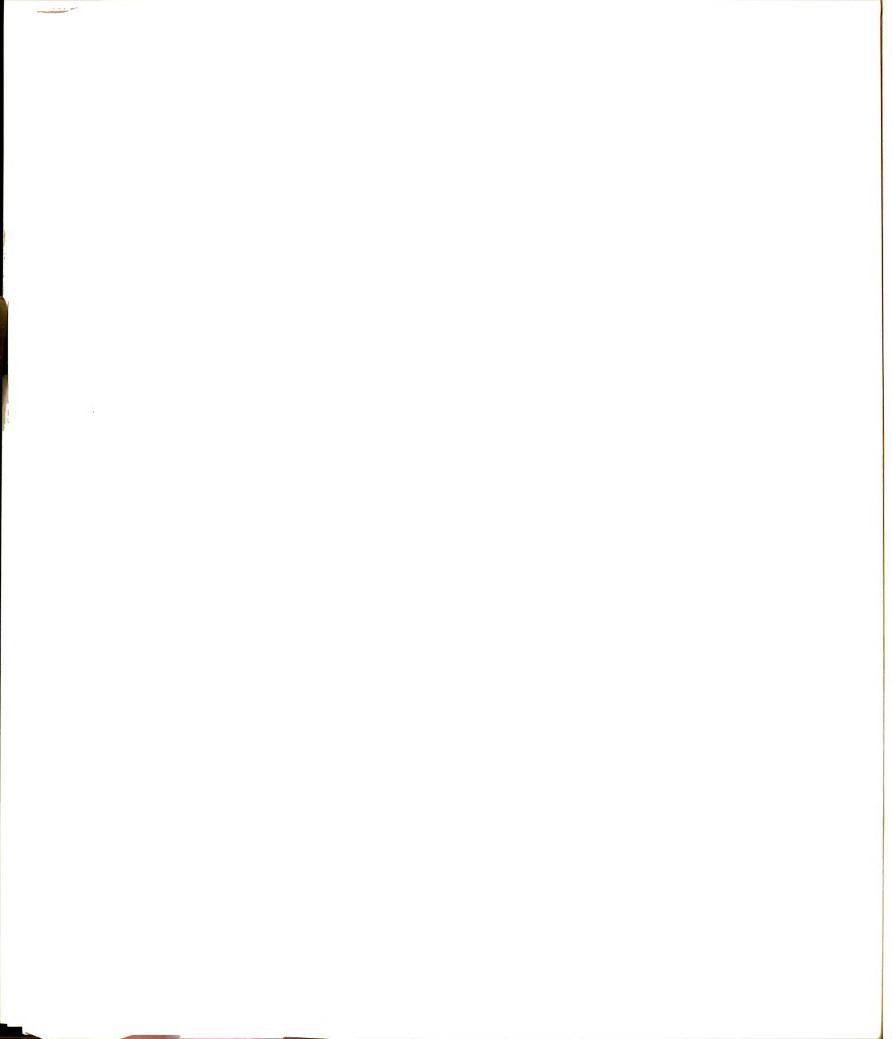
                                                                         CONTINUE
CONTINUE
RETURN
END
                                                                                         C****
95
           96
                                                   100
                                                              101
                                                                           102
                                                                                                                                                                    201
```



```
XI=X (YN)
XN=X (NN)
XN (
                                                                                                                                                                                                                                                                                                                                             N
                                                                                                                                                                                                                                                                                                                                                                                                                           202
                                                                                                                                                                                                                                                                                                                                                                                                                                                                                                                                                                                                                                                                                                                                                                                                                                                                                                                                                                                                                                                                                                                                                                                                                                                                                                                                                                                                                                                                                                                                                                                                                                                               203
```



```
E(1) = ((1) - (1) - (1) - (1) - (1) - (1) - (1) - (1) - (1) - (1) - (1) - (1) - (1) - (1) - (1) - (1) - (1) - (1) - (1) - (1) - (1) - (1) - (1) - (1) - (1) - (1) - (1) - (1) - (1) - (1) - (1) - (1) - (1) - (1) - (1) - (1) - (1) - (1) - (1) - (1) - (1) - (1) - (1) - (1) - (1) - (1) - (1) - (1) - (1) - (1) - (1) - (1) - (1) - (1) - (1) - (1) - (1) - (1) - (1) - (1) - (1) - (1) - (1) - (1) - (1) - (1) - (1) - (1) - (1) - (1) - (1) - (1) - (1) - (1) - (1) - (1) - (1) - (1) - (1) - (1) - (1) - (1) - (1) - (1) - (1) - (1) - (1) - (1) - (1) - (1) - (1) - (1) - (1) - (1) - (1) - (1) - (1) - (1) - (1) - (1) - (1) - (1) - (1) - (1) - (1) - (1) - (1) - (1) - (1) - (1) - (1) - (1) - (1) - (1) - (1) - (1) - (1) - (1) - (1) - (1) - (1) - (1) - (1) - (1) - (1) - (1) - (1) - (1) - (1) - (1) - (1) - (1) - (1) - (1) - (1) - (1) - (1) - (1) - (1) - (1) - (1) - (1) - (1) - (1) - (1) - (1) - (1) - (1) - (1) - (1) - (1) - (1) - (1) - (1) - (1) - (1) - (1) - (1) - (1) - (1) - (1) - (1) - (1) - (1) - (1) - (1) - (1) - (1) - (1) - (1) - (1) - (1) - (1) - (1) - (1) - (1) - (1) - (1) - (1) - (1) - (1) - (1) - (1) - (1) - (1) - (1) - (1) - (1) - (1) - (1) - (1) - (1) - (1) - (1) - (1) - (1) - (1) - (1) - (1) - (1) - (1) - (1) - (1) - (1) - (1) - (1) - (1) - (1) - (1) - (1) - (1) - (1) - (1) - (1) - (1) - (1) - (1) - (1) - (1) - (1) - (1) - (1) - (1) - (1) - (1) - (1) - (1) - (1) - (1) - (1) - (1) - (1) - (1) - (1) - (1) - (1) - (1) - (1) - (1) - (1) - (1) - (1) - (1) - (1) - (1) - (1) - (1) - (1) - (1) - (1) - (1) - (1) - (1) - (1) - (1) - (1) - (1) - (1) - (1) - (1) - (1) - (1) - (1) - (1) - (1) - (1) - (1) - (1) - (1) - (1) - (1) - (1) - (1) - (1) - (1) - (1) - (1) - (1) - (1) - (1) - (1) - (1) - (1) - (1) - (1) - (1) - (1) - (1) - (1) - (1) - (1) - (1) - (1) - (1) - (1) - (1) - (1) - (1) - (1) - (1) - (1) - (1) - (1) - (1) - (1) - (1) - (1) - (1) - (1) - (1) - (1) - (1) - (1) - (1) - (1) - (1) - (1) - (1) - (1) - (1) - (1) - (1) - (1) - (1) - (1) - (1) - (1) - (1) - (1) - (1) - (1) - (1) - (1) - (1) - (1) - (1) - (1) - (1) - (1) - (1)
```



```
CONTINUE (1)-((1))
CONTINUE (1)-((1))
DO 68 113.16
E(1.1=E(1.)+((1))
CONTINUE
F(1.0=E(1.)+((1))
F(10.0=E(1.)+((1))
F(10.0=E(1.)+((1))
F(10.0=E(1.)+((1))
F(10.0=E(1.)+((1))
F(10.0=E(1.)+((1))
F(1.0=E(1.)+((1))
F
                                                                                                                                                                                                                                                                                                                                                                                                                                                                                                                                                                                                                                                                                                                                                                                                                                                                                                                                                                                                                                                                                                                                                                                                                                                        30
                                                                                                                                                                                                                                                                                                                                                                                                                                                                                                                                                                                                                                     DO 65 1=1,4

E(1)=E(1)-C(1)

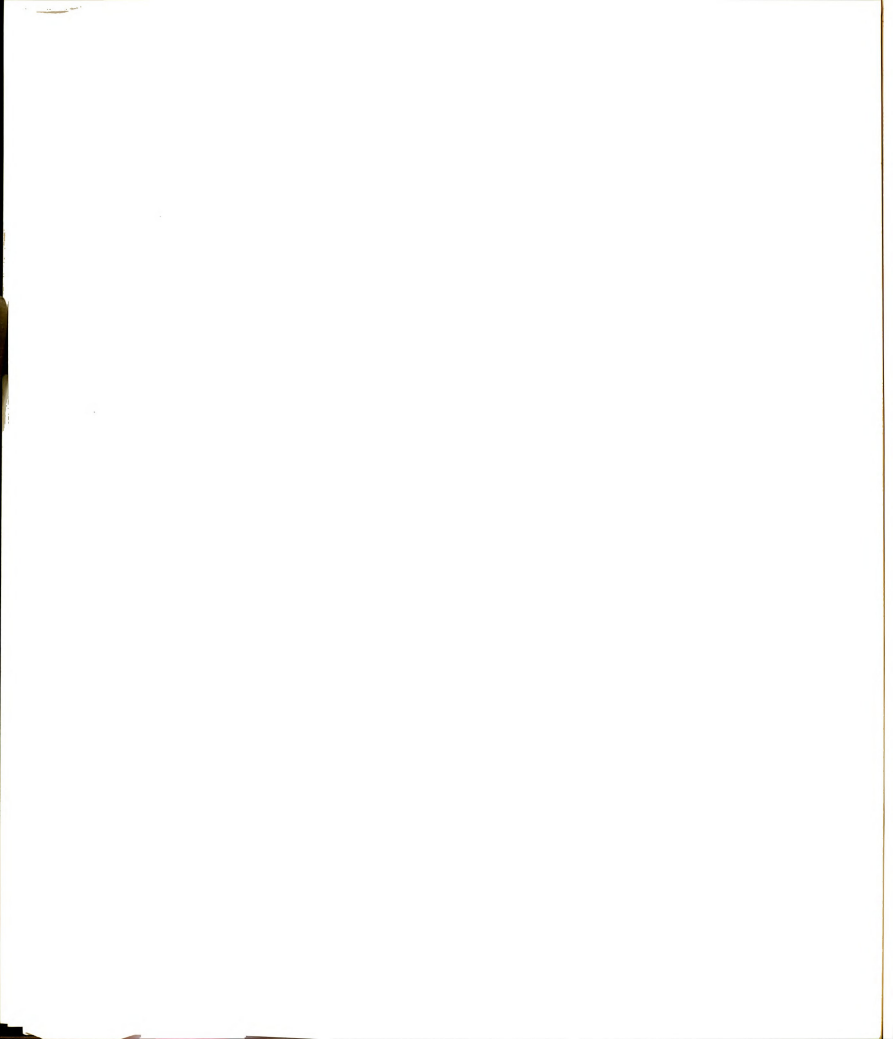
CONTINUE

DO 66 1=5,8

E(1)=E(1)+C(1)

CONTINUE

DO 67 1=9,12
                                                                                                                                                                 9
                                                                                                                                                                                                                                                                                                                                                                                                                                                                                                                                                                                                                                                                                                                                                                                                                                                                                                                                                                                                                                                                                                                                                                                                                                                                                                                                                                                                                                                                                                                                                                                    83
                                                                                                                                                                                                                                                                                                                                                                                                                                                                                                                                                                                                                                                                                                                                                                                                                                                                                                                                                                                                                                                                                                                                                                                                                                                                                                                                                                                                                                                                                                                                                                                                                                                                                                                                                                                                                   92
                                                                                                                                                                                                                                                                                                                                                                                                      62
                                                                                                                                                                                                                                                                                                                                                                                                                                                                                                                     63
                                                                                                                                                                                                                                                                                                                                                                                                                                                                                                                                                                                                49
                                                                                                                                                                                                                                                                                                                                                                                                                                                                                                                                                                                                                                                                                                               65
                                                                                                                                                                                                                                                                                                                                                                                                                                                                                                                                                                                                                                                                                                                                                                                                                                     99
                                                                                                                                                                                                                                                                                                                                                                                                                                                                                                                                                                                                                                                                                                                                                                                                                                                                                                                                                                 67
                                                                                                                                                                                                                                                                                                                                                                                                                                                                                                                                                                                                                                                                                                                                                                                                                                                                                                                                                                                                                                                                                96
                                                                                                                                                                                                                                                                                                                                                                                                                                                                                                                                                                                                                                                                                                                                                                                                                                                                                                                                                                                                                                                                                                                                                                                                                                                                                                                                                                                          81
                                                                                                                                                                                                                                                                                                                                                                                                                                                                                                                                                                                                                                                                                                                                                                                                                                                                                                                                                                                                                                                                                                                                                                                                                                                                                                                                                                                                                                                                                                         85
                                                                                                                                                                                                                                                                                                                                                                                                                                                                                                                                                                                                                                                                                                                                                                                                                                                                                                                                                                                                                                                                                                                                                                                                                                                                                                                                                                                                                                                                                                                                                                                                                                                                                                   4
                                                                                                                                                                                                                                                                                      61
```



```
77740
77750
77780
7800
7810
 (MDIR, AREA, XM, YM, ZM, XN, YN, ZN, C)
. COSH. OR. MODE. EQ. SINE) GO TO 98
                                                                                                                                                                                                                                                                                                                                          ÎP=Î+4*NX+3*NY
L(IP, MATP)=CEXP(-1.0*CJ*Z(II))/377.0
                                                                                                                                                                                                                                                                                                              (ATP)=CEXP(-1.0*CJ*Z(I))/377.0
                                           E(1)=E(1)-C(1)

CONTINUE

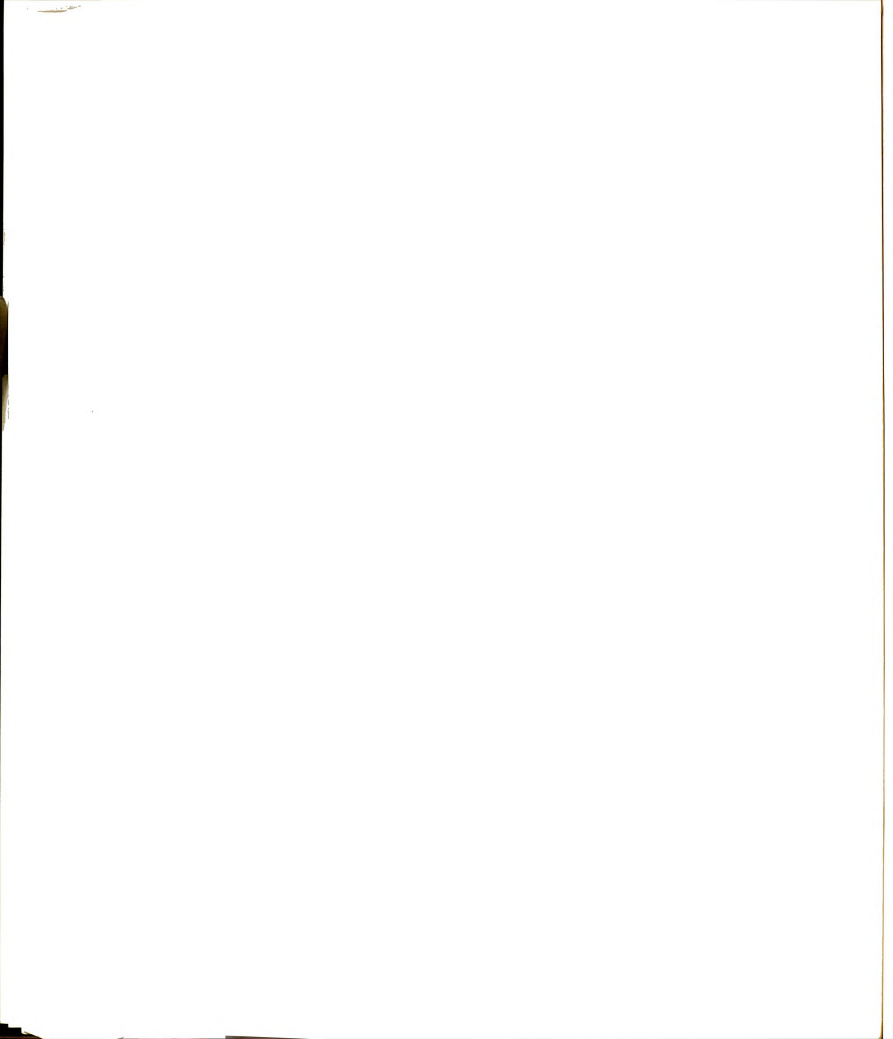
DO 96 1=9,12

E(1)=E(1)+C(1)

CONTINUE

DO 97 1=13,16

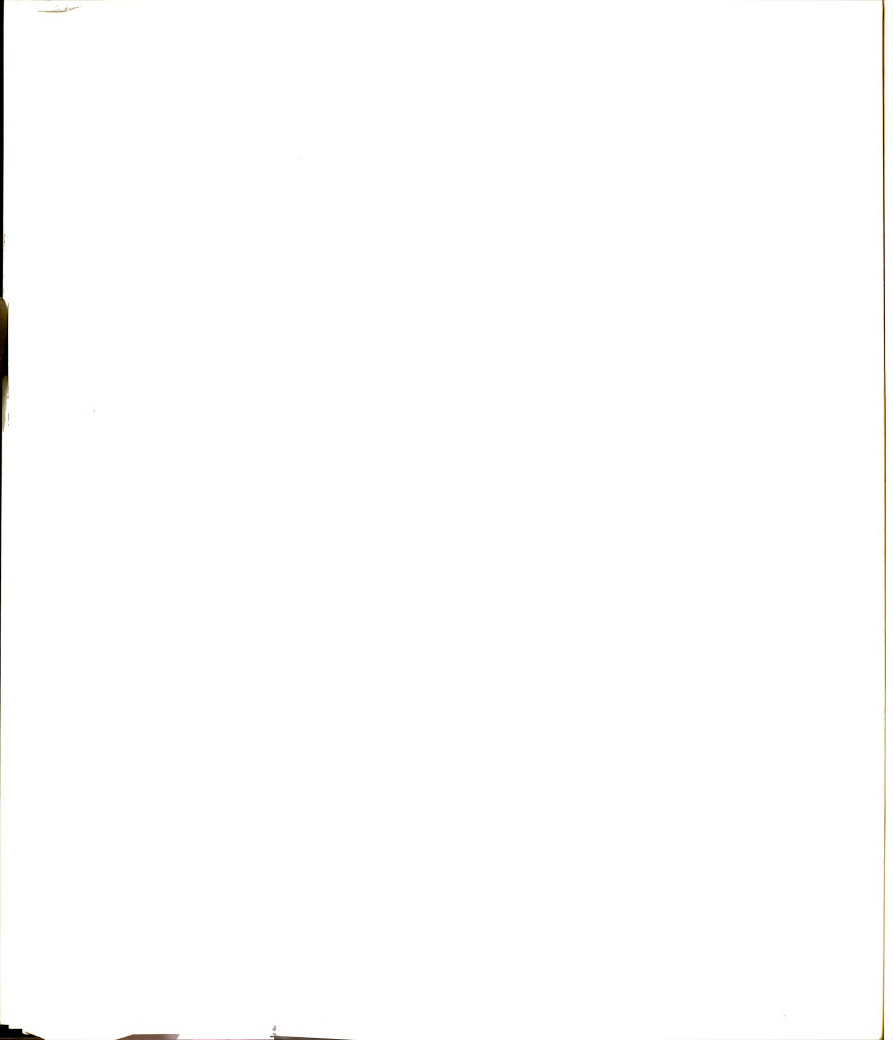
E(1)=E(1)=E(1)
                                                                                                                                                                                                                                                                                                                          1 I=1, NY
                                                                                                                                                                                                       301
                                                    95
                                                                          96
                                                                                                47
                                                                                                                                                          8
                                                                                                                                                                                 5
```



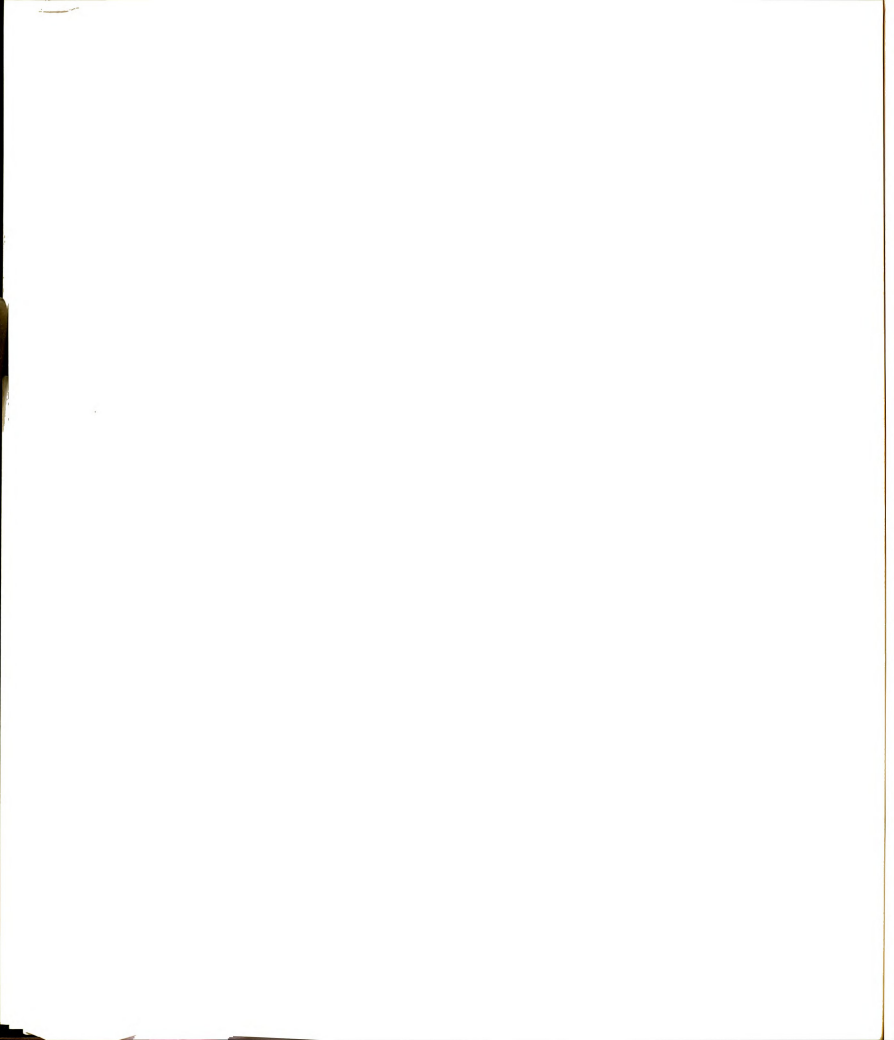
```
74430
74440
74460
74460
74460
7480
7480
7480
88040
88040
88040
88040
88140
88110
88110
88110
88110
88110
88110
88110
88110
88110
88110
88110
88110
88110
88110
88110
88110
88110
88110
88110
88110
88110
88110
88110
88110
88110
88110
88110
88110
88110
88110
88110
88110
88110
88110
88110
88110
88110
88110
88110
88110
88110
88110
88110
88110
88110
88110
88110
88110
88110
88110
88110
88110
88110
88110
88110
88110
88110
88110
88110
88110
88110
88110
88110
88110
88110
88110
88110
88110
88110
88110
88110
88110
88110
88110
88110
88110
88110
88110
88110
88110
88110
88110
88110
88110
88110
88110
88110
88110
88110
88110
88110
88110
88110
88110
88110
88110
88110
88110
88110
88110
88110
88110
88110
88110
88110
88110
88110
88110
88110
88110
88110
88110
88110
88110
88110
88110
88110
88110
88110
88110
88110
88110
88110
88110
88110
88110
88110
88110
88110
88110
88110
88110
88110
88110
88110
88110
88110
88110
88110
88110
88110
88110
88110
88110
88110
88110
88110
88110
88110
88110
88110
88110
88110
88110
88110
88110
88110
88110
88110
88110
88110
88110
88110
88110
88110
88110
88110
88110
88110
88110
88110
88110
88110
88110
88110
88110
88110
88110
88110
88110
88110
88110
88110
88110
88110
88110
88110
88110
88110
88110
88110
88110
88110
88110
88110
88110
88110
88110
88110
88110
88110
88110
88110
88110
88110
88110
88110
88110
88110
88110
88110
88110
88110
88110
88110
88110
88110
88110
88110
88110
88110
88110
88110
88110
88110
88110
88110
88110
88110
88110
88110
88110
88110
88110
88110
88110
88110
88110
88110
88110
88110
88110
88110
88110
88110
88110
88110
88110
88110
88110
88110
88110
88110
88110
88110
88110
88110
88110
88110
88110
88110
88110
88110
88110
88110
88110
88110
88110
88110
88110
88110
88110
88110
88110
88110
88110
88110
88110
88110
88110
88110
88110
88110
88110
88110
88110
88110
88110
88110
88110
88110
88110
88110
88110
88110
88110
88110
88110
88110
88110
88110
88110
88110
88110
88110
88110
88110
88110
88110
88110
88110
88110
88110
88110
88110
88110
88110
88110
88110
88110
88110
88110
88110
88110
88110
88110
88110
88110
881
7820
7830
7840
7850
7870
7870
7890
7920
                                                                                                                                                                                                                                                                                                                                                                                                                                                                                                                                                                                                                                                                                                                                                                                                                                                                                                                      149
                                                                                                                              a
                                                                                                                                                                                                                                                                              40
                                                                                                                                                                                                                                                                                                                                                                                                                                                                                                                                                                                                                       57
```



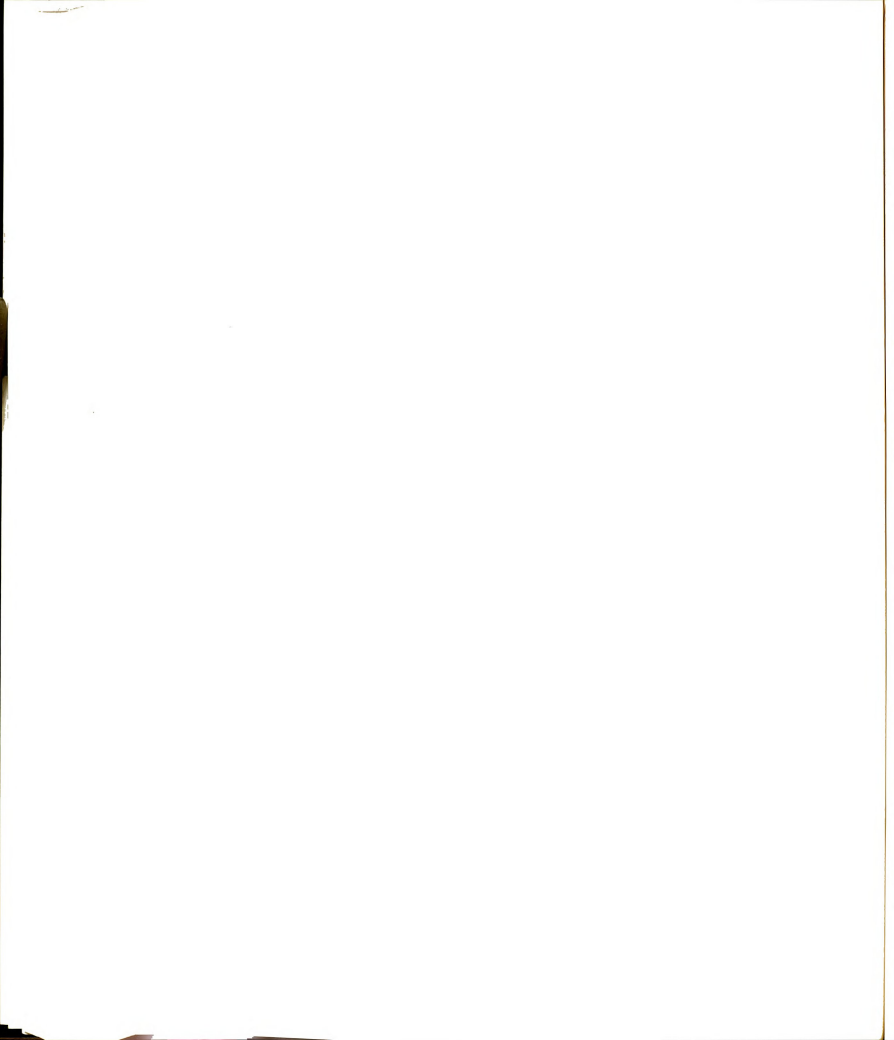
7470 7480	7500 7510 7520 7520	7550 7550 7580 7580 7580	7610 7630 7640 7640 7650	7680 7690 7710 7720 7730	7740 7780 7790	7800 7810 7820	7840 7850 7850 7870 7870 7870 7870 7890
COMMON / INCR/INFR. CRNT. COMMON / ACCESTIVE CRNT. COMMON / CONSTIT MUO. EPO COMMON / CONSTIT MUO. EPO COMMON / CONSTIT MUO. EPO	D0 1 =1.NY 1 I=1+44NX+0=NV IP=1+44NX+0=NV I CDN INHEP = CGS(Z(II))/377.0 1 D0 VI NA	I]=I=AKKANY IP=IA+KKANY+3=AKZ IP=IA+KANY+3=AKZ IP=IATY+3=(-1.0)*GDS(Z(II))/377.0 IFANY+G0.0			DO 3 T 1 1 MAT TO CONT L. MATP) 3 CANTINE -4. OAFTEL(I, MATP) 1 FICKINX EQ. 0), AND. (NNY. EQ. 0), AND. (NNZ. EQ. 0)) GO TO 9 MATT ==#CATT+1+AZ) MATT ==#CATT+1+AZ)	DO 8 1=1ATTP; MAT L(1, MATP) =-1.0+L(1, MATP) B(DATINUE) =-1.0+L(1, MATP) P(ETURN)	****SUBROUTINE CHIM************************************
	-	O	4-0	DI.	t)	wo	*



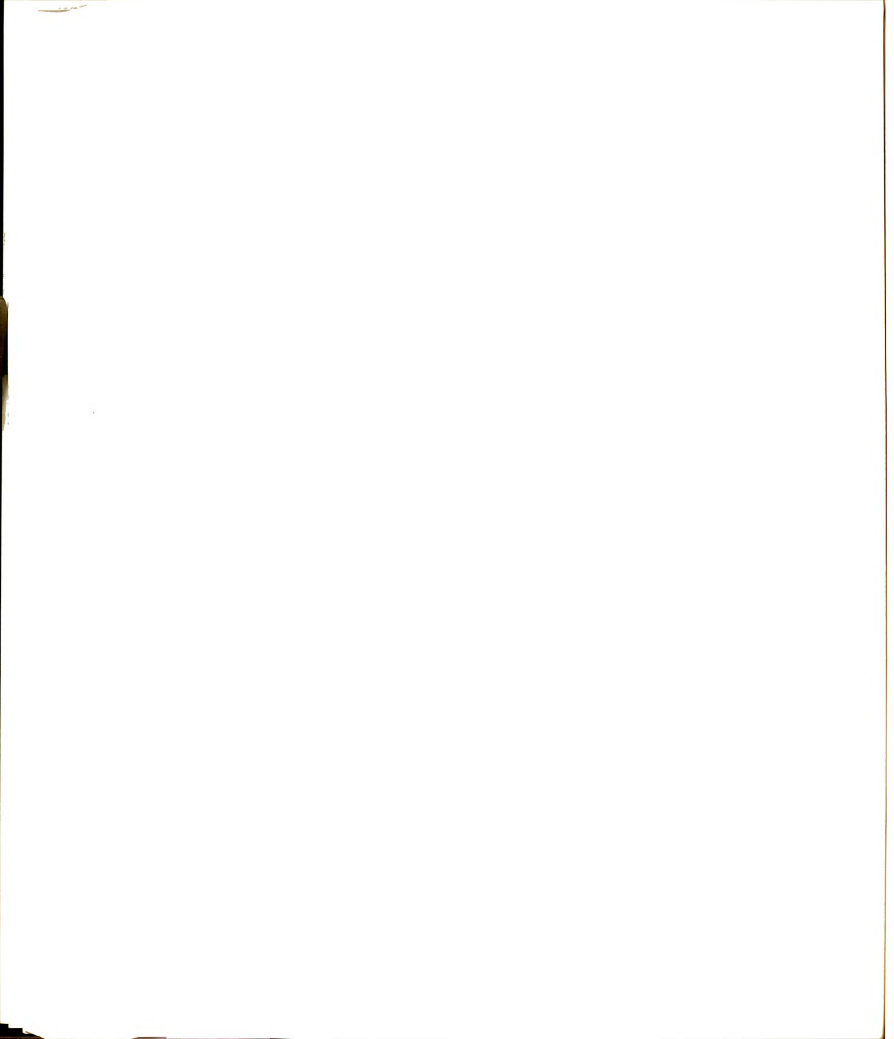
```
8200
8210
8220
                          88310
83310
83300
63400
                0
00
            らて
               n
                   80
     a
        40
```



```
8660
8670
8680
8690
8700
8610
8620
8630
                                                                                                                                                                                                                                                                                                                                                                                                                                                                                                                                                                                                                                                                                                                                                                                                                                                         8650
                                                                                                                                                                                                                                                                                                                                                                                                                                                                                                                                                                                                                                                                                                                                                                                                                                                                            0
                                                                                                                                                                                                                                                                                                                                                                                                                                                                                                                                                                                                                                                           09
                                                                                                                                                                                                                                                                                                                                                                                                                                                                                                                                                                                                                                E(IP, MATP)=(-1.0)*CJ*SIN(Z(I))/377.0
CONTINUE
                                                                                                                                                                                                                                                                                                                                                                                                                                                                                                                                                                                                                                                                                                                                                                                                                                                                                                                                                                                                                                      COMMON /NXYZ/NX, NY, NZ, NNX, NNY, NNZ
COMMON /CONS/PI, MUO, EPO
COMMON /CPLX/CJ
DO I I=1, NX
                                                                                                                                                                                                                                                                                                                                                                                                                                                                                                                                              CALL PRNT(IMPR, CRNT, L, MAT, MATP)
DO 3 1=1, MAT
L(I, MATP)=4. O*PI*L(I, MATP)
                                                                                                                                                                                                                                                                                                                                                                                                                                                                                                                                                                                                                                                                                                                                                                                                                                                                                                                                                                                                                                                                                                                                                                                                                                                                                                    +4*(NX+NY)
, MATP)=CJ*SIN(Z(II))/377.0
                           IIIINX + N.Y                                                                                                                                                                                                                                                                                                                                                                                                                                                                                                                                                                                                                                                                                                                                                                                                                                                                                                   C****
                                                                                                                                                                                                                                                                                                                                                                                                                                                                                                                                                                                                                                                                                                                                                                                                                                                                                                                                                                                                                                                                                                                                                                                                                                                                                                                                                           a
                                                                                                                                                                                                                                                                                                                                                                                                                                                                                                 5
                                                                                                                                                                                                                                                                                                                                                                                                                                                                                                                                                                                                                                         n
```

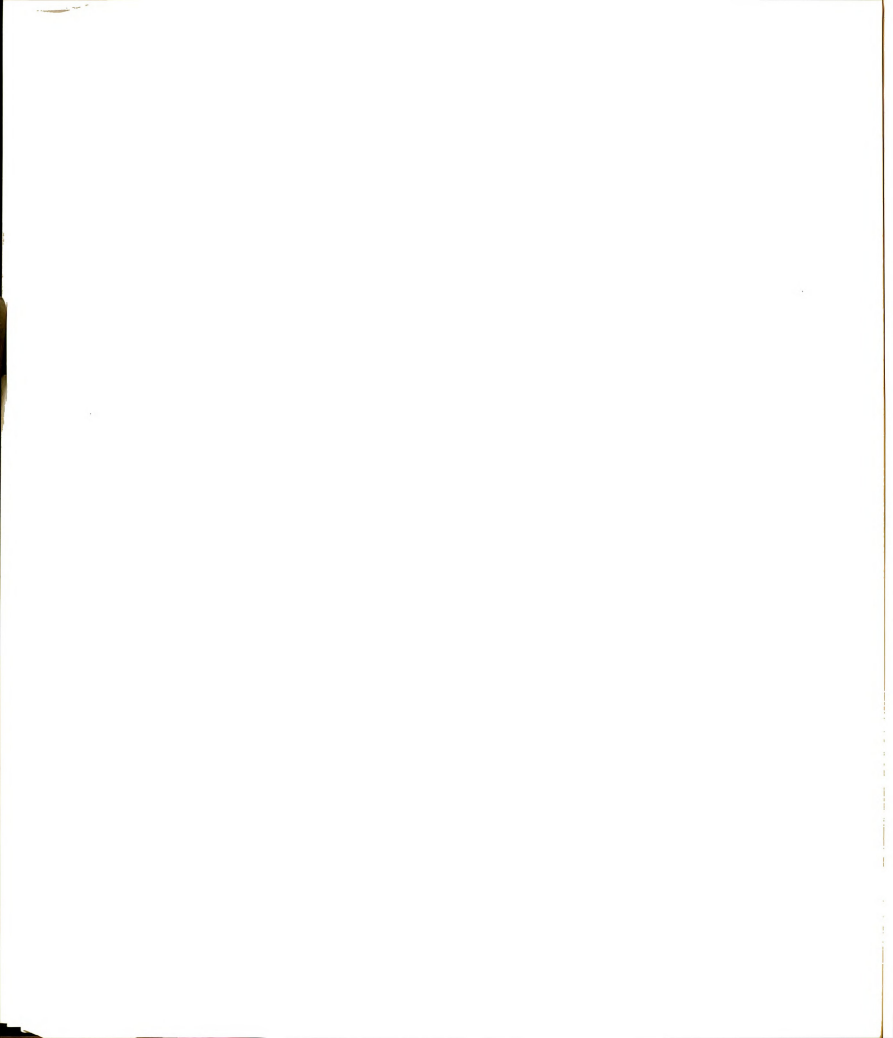


```
888100
888100
8881000
8881000
8881000
8881000
8881000
8881000
8881000
8881000
8881000
                                                                                                               9010
9020
9030
                                                                                                                                   9050
                                                                                                                                      ٥
                                            II=I+NY-NY-NY-NNY
IP=I+4* (NY-NY-NZ-NNY-NNY)
IP=I+4* (NY-NY-NZ-NNY-NNY)
IP=I+4* (NY-NY-NZ-NNY-NNY)
CDNIINUE
CDNIINUE
                                                                                                                                                     NXYZ/NX, NY, NZ, NNX, NNY, NNZ
=1, NX
              IP=I+4*(NX+NY+NZ)+NNX
L(IP,MATP)=CJ*SIN(Z(II))/377.(
CONTINUE
CONTINUE
                                                                                                                                     (=J+NX
(=J+NX)=-377.0*L(K,MATP)
20NTINUE
D0 131 I=1,NY
II=I+NY+4*NX
                                                                                                                                                                                                    I=I+NY+4*NX
(II, MATP)=-1.0*L(II, MATP)
=II+NY
                                                                                                                                                                                                                                                 O*L(II, MATP)
                                                                                                                                                                                                                   (J, MATP) =-377. 0*L(J, MATP)
                                                                                                                                                                                                                             ATP)=L(K, MATP)*377.0
                            ONTINUE
F(NNZ.EQ.O) GO TO 7
O S I=1, NNZ
60 10
           ZN+ AN+ XN+
                                                                                                                                      C****
                                                                                                                                                                                        130
                                                                                                                                                                                                                                 131
```

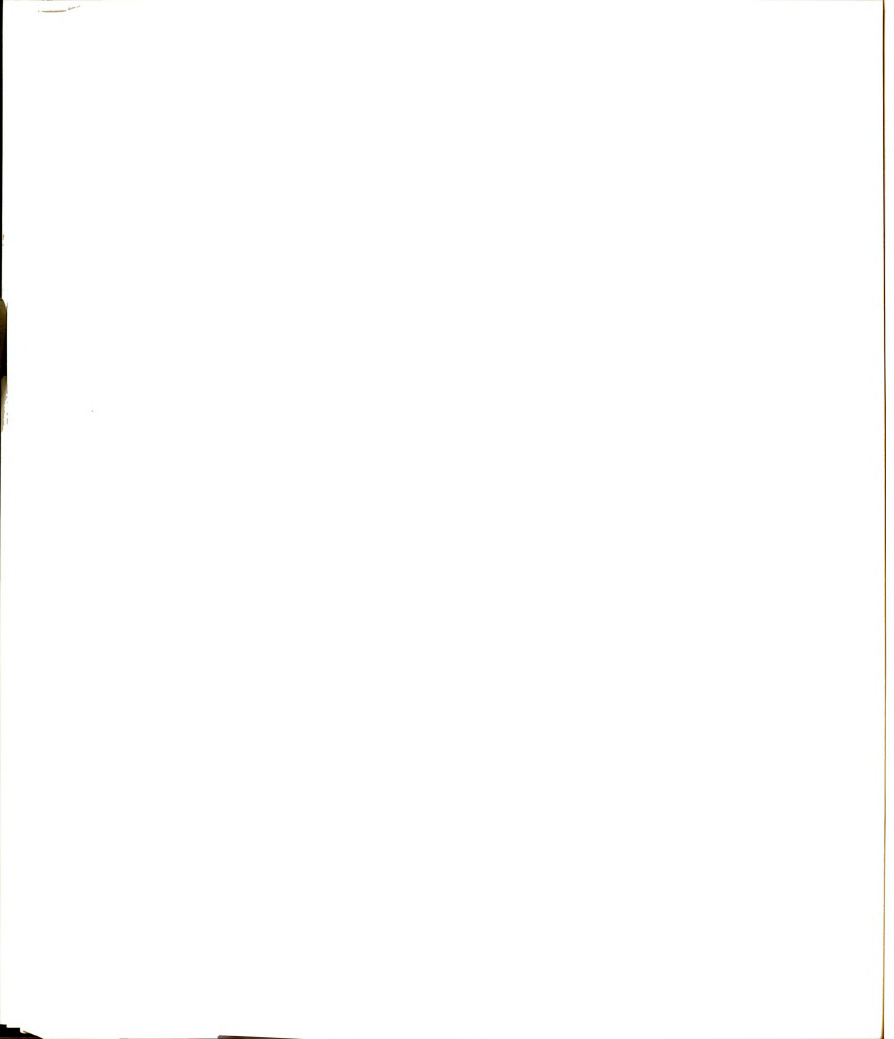


```
L(1) MATP)
L(1) MATP(X+N+VZ)+NNX
L(1) MATP(X+N+VZ)+NNX
L(1) MATP)
L(1) MATP)
L(2) MATP)
L(2) MATP)
L(3) MATP)
L(4) MATP)
L(5) MATP)
L(6) MATP)
L(7) MATP)

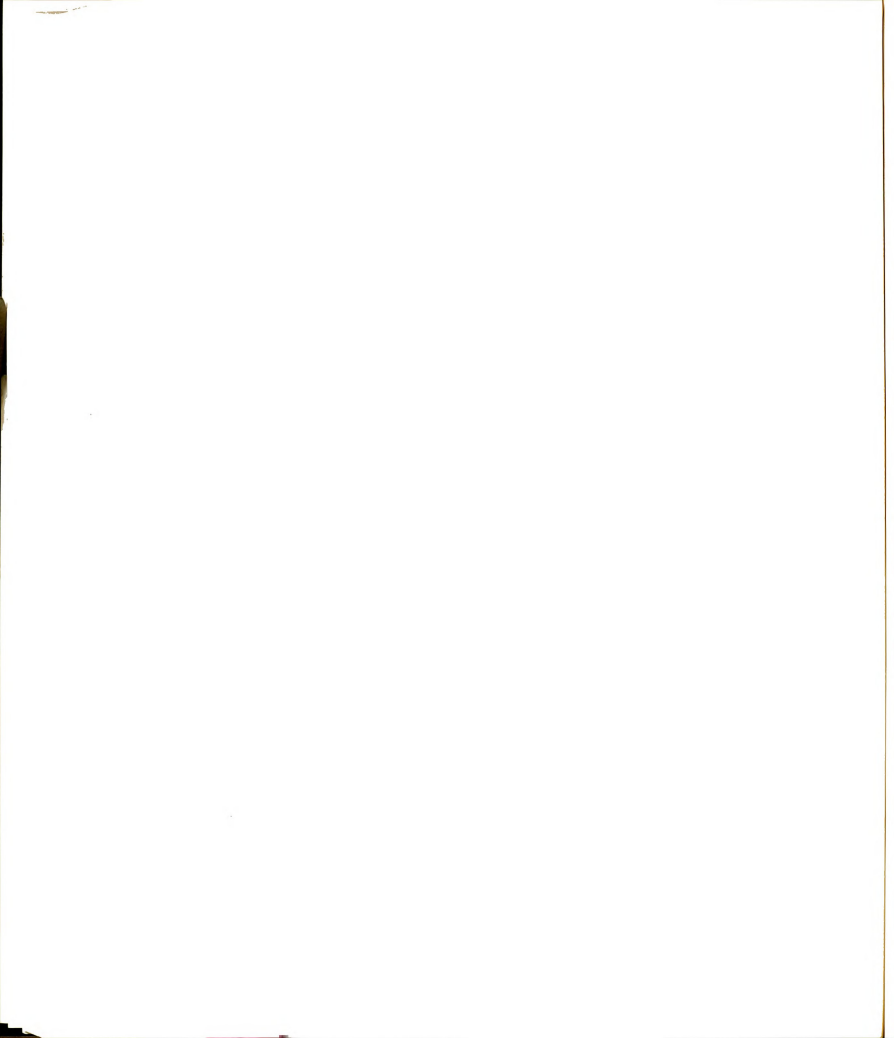
LGJ, MATP)=L(J, MATP)*377. 0
LGJ, MATP)=L(J, MATP)*377. 0
L(K, MATP)=-377. 0*L(K, MATP)
2 CONTINUE
CONTINUE
DQ 133 1=1, NNX
                                                                                                                                                                                                                                                                                                                                                                                                                                                                                                                                                                                                                                                                                                                                                                                                                                                                                                                                                   C****
                                                                                                                                                                                                                                                                                                                                 133
                                                                                                                                                                                                                                                                                                                                                                                                                                                                                                                                                                                  134
                                                                                                132
```



Ä	9750	9780	9810 9820 1	9850	94400 94400 94410 94410	9960		10010	100050 100050 100050 100050 100110 100110 101150 101150 101150	10190
1X, 4HIMAG, 11X, 4HRE	THE FOLLOWS)	HY, 20X, 12HJMY DR EZ/WO, 1	, 12H EZ , 1				7 -EZ/WO,	EZ ,) JR EY/WO.1	
11X, 4HREAL, 11X, 4HIMAG, 11X, 4HREAL, 11X, 4HIMAG, 11X, 4HRE	SURFACE WE HAVE	-HZ, 20X, 9HJEZ OR HY, 20X	20X, 9H HY , 20X, 12H	*************), L(IPP, MATP), L(IF	6, 1H), 1X))	10HJEZ OR -HX, 20X,	10н нх ,20х,13н),L(IPP,MATP),L(IP X,9HJEY OR HX,20X,	
), 11X, 4HREAL, 11X, 4H	X, 7HON THE , A4, 28H .DS) GO TO 136	-,14X,10HJEY OR -HZ,20	; 1-,14X,10H , HZ ,2C	-, 5X, 4 (2BH************************************), 1X, 4(1X, 1H(, 2E13. GHT .DS) GO TO 139	14x, 9HJEX OR HZ, 20X, OR EX/WO)	14X,9H , HZ ,2OX,1OH EX	122. 3X = 1. NY YY	
44	123 FORMAT(1H-, 15X, 7H IF(CRFL.EQ. FLDS)	71.5	PRINT 137 FORMAT (147 28X, 13H	25 11 11		13 FORMAT(1H-, I3 PRINT 123, RI IF(CRFL.EG. FL	113 FORMAT (1H-, 14 218X, 12HJMZ OR	GU TO 141 PRINT 140 FORMAT(1H-, 218X, 12H		142 PRINT 143

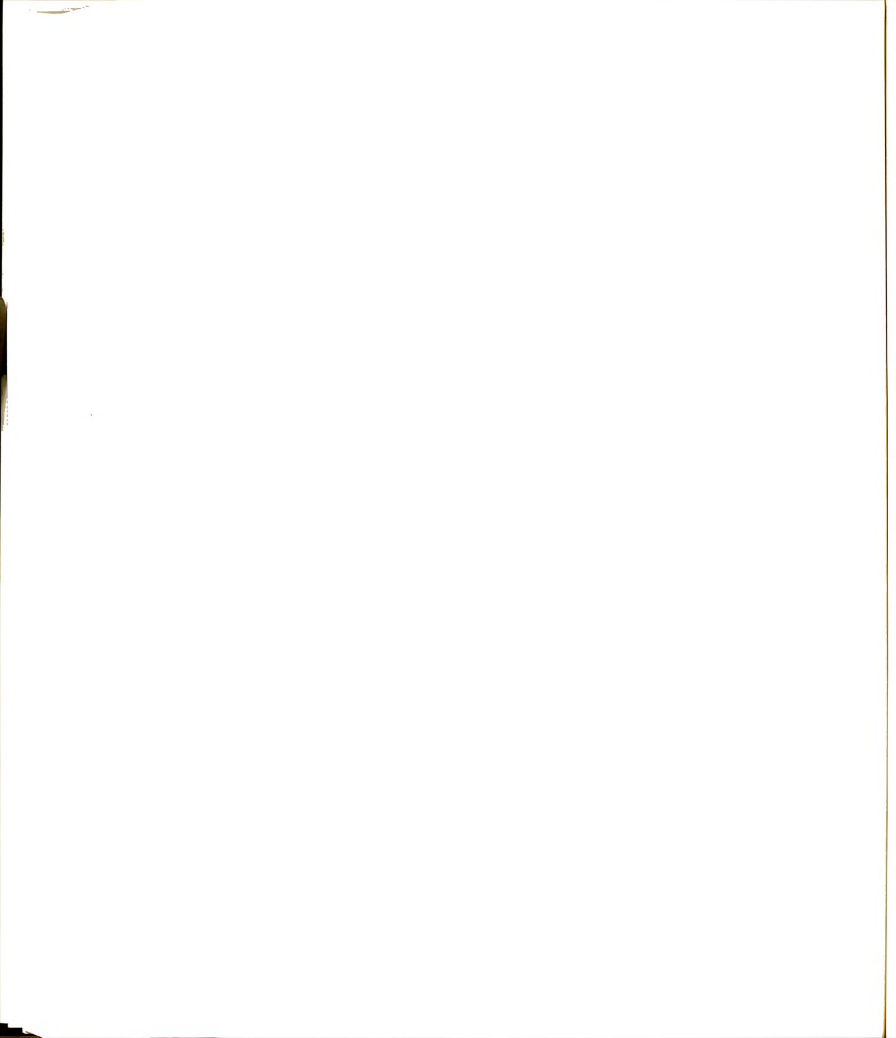


, 1 10230 10240 10250 10270 10280 10310 10310 10320 10320 10320 10340	00000000000000000000000000000000000000	10550 10550 10550 10550 10550 10650 10650 10650 10650
EV (TP)	Ĝ.	<u>ê</u>
20X, 12H	.(IPPP, MA	(IPPP, MA
(1H14X, 10H)	447 - L.Y.W.Y. LOLY LERION L. ON E.I.Y.W.Y. L.	UK EL/WO, 18X, 13HUML UK -EX/WO,) 10
20х, 9H ПР), L(IPI	TP), L(1PF	-EX/WO)
14X,10H , HY ,20X,9H ,2V ,2V ,9H ,2V ,2V ,9H ,2V	.L(IP, MA)	SHUMZ UK
14x, 10H) 2 Y) Y) , L(J, MATP), THG TO 19 FLDS) GO TO 26 FLDS) GO TO 27	NZ) NZ) (J, MATP) (G TG 20 T 20 T 20 T 20 T 32, 10HUEX	MO, 18X, 1 +NNX -NZ+NNX) -(J, MATP)
143 D C R M A L M	145 PRINT 145 PRINT 145 PRINT 10 14 10 14 11 14 14 PRINT 19 CONTAI 19 CONTAI 10 CONTAI 10 CONTAI 10 CONTAI	25 CONTINUE 125 125 125 125 125 125 125 125 125 125

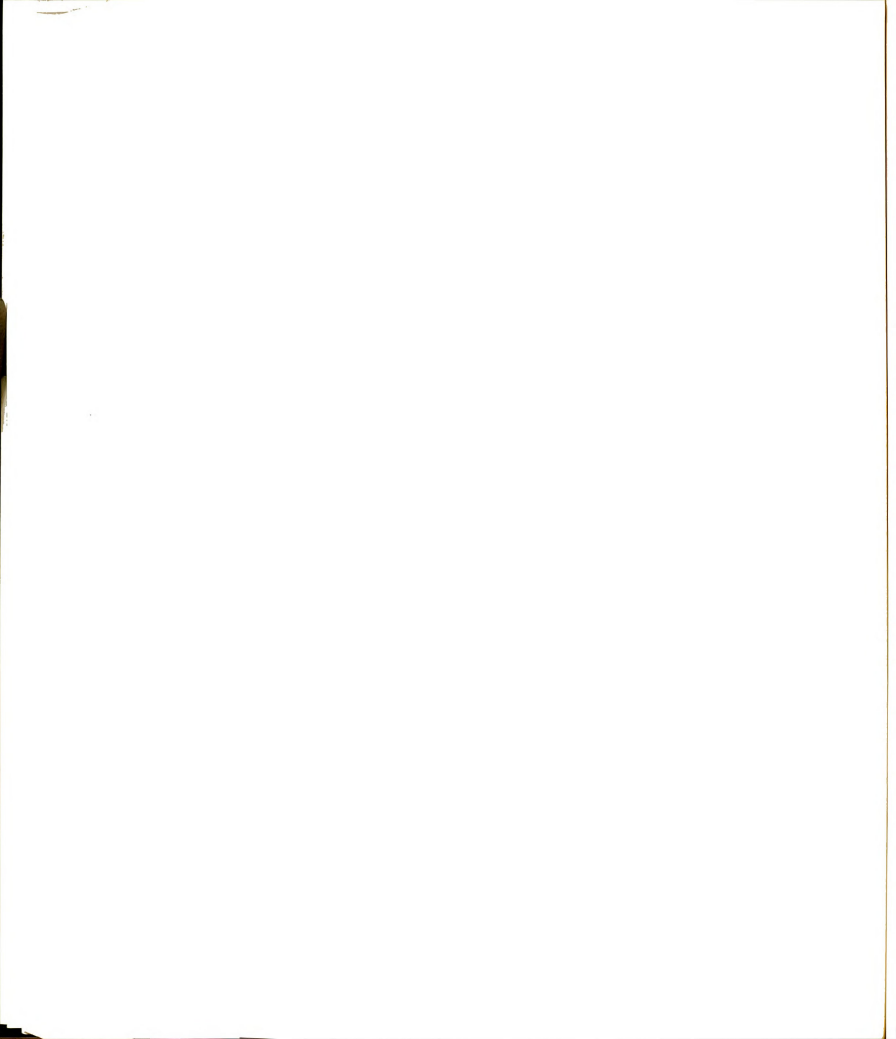


10680 10690 10700 10710	10740 10750 10750 10770 10780 10800 10810	10830 10840 10850 10850 10860 11730 11730	11750 11760 11790 11800 11810	11830 118840 118840 118850 118870 118880 11990	111920 111930 111940 111940 111940 111990 111990
		PPP, MATP) **********			
1JEY OR -HX, 20X,		.(IPP, MATP), L(I ************************************			
), GD TD 21 RNT FLDS) GD TD 153 14X, 9HJEX DR HY, 20X, 10HJEY EY/WO, 18X, 12HJMY OR EX.WO)	(ANN-	**************************************	EPO (10)	300 300	, YT, ZT, D, R, G) H)
NZ. EG. 0) GD TD 21 T. 123, FRNT TRL. ES FLDS) GD TD 153 T. 154 AT 11+-, 14X, 9H-JEX OR HY AT OR -EY/MO, 18X, 12H-JM	153 PRINT 143 155 PRINT 122 DO 18 1=1, NNZ 11=1-RX+RN+NZ+NNX+NNY J=1-A4* (NX+NY+NZ+NNX+NNY) IPP=1P+NNZ IPP=1P+NNZ IPP=1P+NNZ IPP=1P+NNZ	PRINT 12: 11.1.C.U.P.MATP). L(IPP.MATP). L(IPPP.MATP). L(IPPP.MATP). ECONTINUE END END END END END END END END END EN	1172 COMPIECE X (45), HT (5), FT (10) COMPIECE X (45), HT (5), FT (10) COMPIECE X (45), HT (5), FT (10) COMPIECE X (45), HT (45), FT (10) COMPIECE X (45), HT (45), FT (45) COMPIECE X (45), FT (45), FT (45), FT (45) COMPIECE X (45), FT (45),	DIR. GE. 4) MDIRM= DIRM-2) 100, 200, 1=0, 0 100 C N+(DLEN+DL)/2 N+(DLEN+DL)/2 N+(DLEN+DL)/2	Y = YY =
PATE 451	252 252 253 262 263 263 263 263 263 263 263 263 26	C****SUBROUT SUBROUT SUBROUT COMPLE		100 11 100 11 11 11 11 11 11 11 11 11 11	2 CONTINUE C

```
G(XM, YM, ZM, XN, YT, ZT, D, R, G) (R, G, Q)
                                                                                                                                                                                                              (XM, YM, ZM, XN, YT, ZT, D, R, G)
                                                                                                                                                                                                  (=1, NDIV
                                            K=1, NDIV
                                                                                           CONTINUE
CONTINUE
ZT=ZT+DLEN
                                                                                                                                                                                                                                                 200
                                                                                           102
                                                                                                                                                       300
                                                                                                                                                                    201
                                                                                                                                    105
200
                                                                                                               104
            101
```



```
ZT=ZT+DLEN
CONTINUE
DO 205 I=1, 10
FT(I)=FT(I)/NDIVD
CONTINUE
CALL CEFTX(FT, C)
RETURN
            子本本のおび
 204
     205
                                   100
                                                         S
```



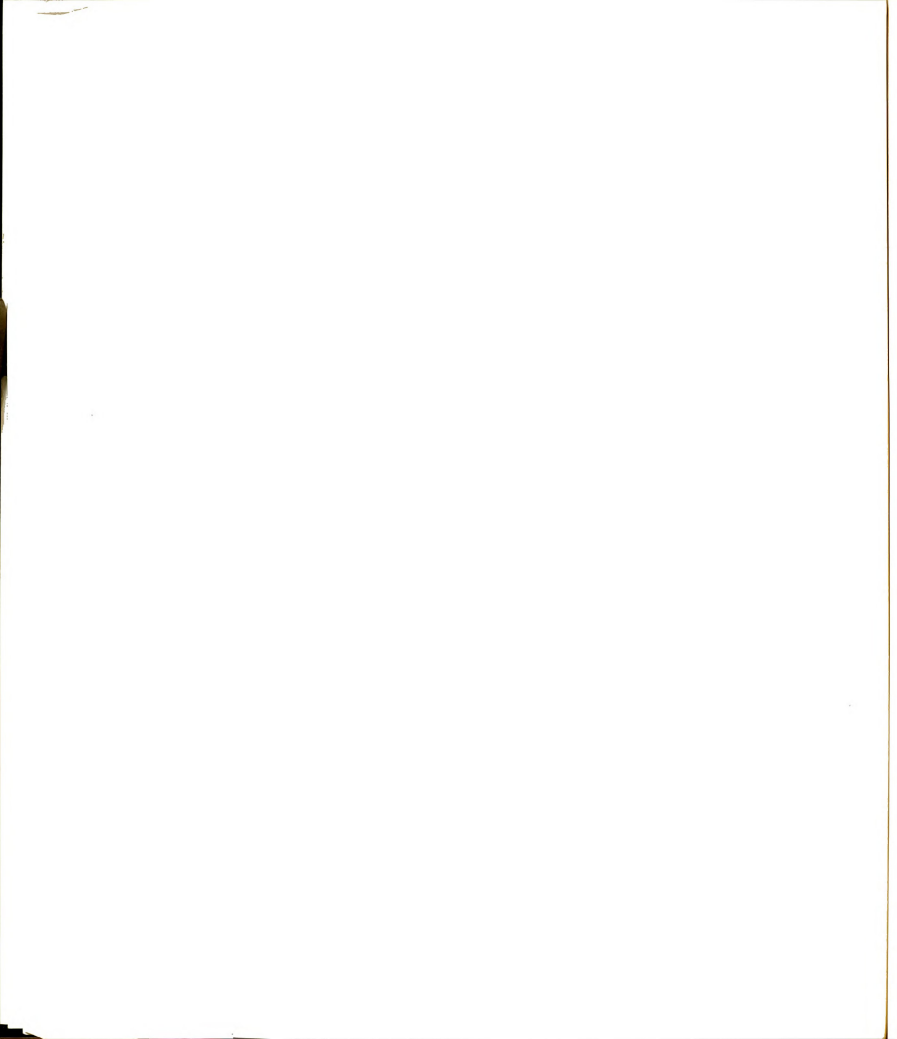
D, R, G)						D, R, G)			
5. Q. H)						, X I , YN, Z I , , Q, F)			
CONTINUE CT = 70 + (DE EN-DL)/2 XT = XN + (DE EN-DL)/2 XT = XN + (DE EN-DL)/2 DD 104 / = 1 N DD 107 XT = XT = XT = N DD 103 K = 1 N DD 1	LEN I=1,5 IT(1)/NDIV2	FYY(HT, C)	1=1, 10	JEN+DL)/2 DLEN+DL)/2 DLEN+DL)/2 J=1,NDIV	K=1, NDIV	(G(XM,YM,ZM A(R,G,Q) NZY(AREA,D I=1,10	T(1)+F(1) E E	I=1, 10	CONTINUE CONTINUE CALL CEFZV(FT, C) ERTURN
COD NO. COD NO	XT=XT+D CONTINU DO 105 HT(I)=H	CALL CE	DD 201 FT(I)=0	CONTINC ZT=ZN+ XT=XN+ DO 204	102 DQ	CALL CALL DO 202	CONTINUE CON	CONTINC	CALL CE
101				201			202	204	205

. 125

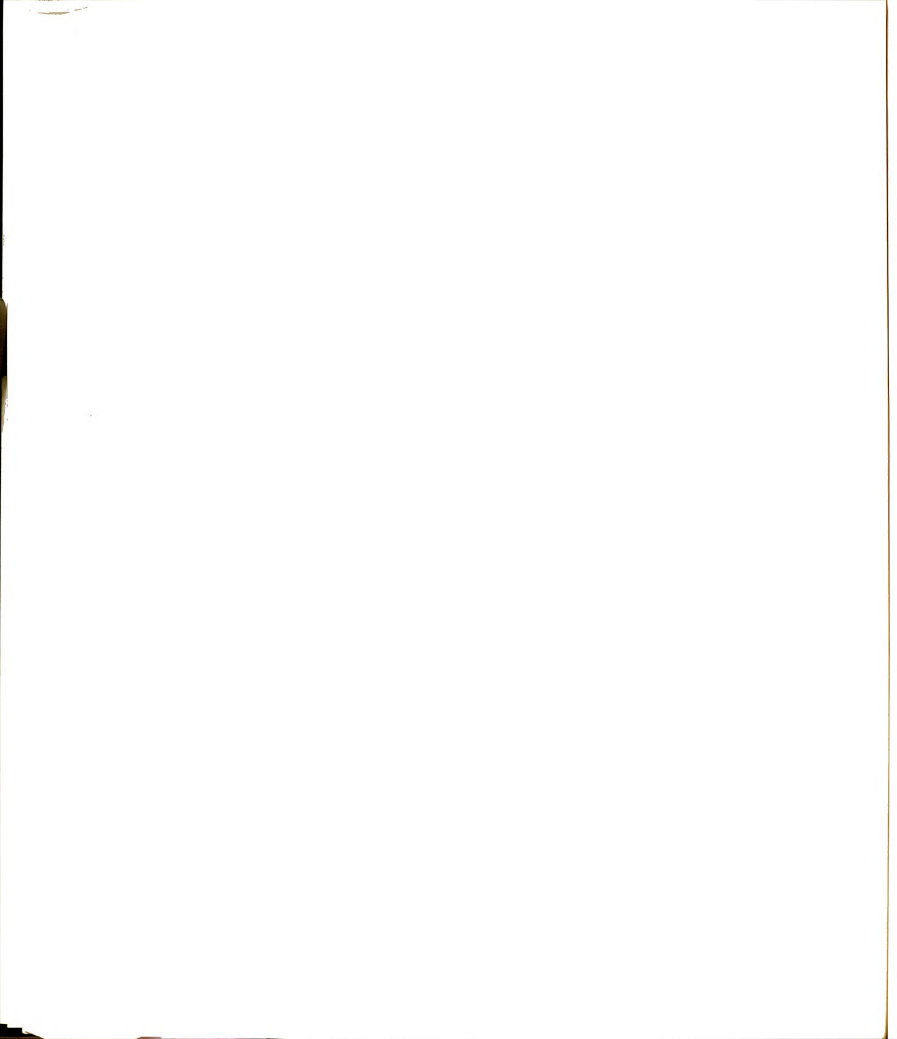
```
00010
00010
00010
            CONTINUE
YT=YN+(DLEN+DL)/2
XT=XN+(DLEN+DL)/2
DD 104 J=1,NDIV
YT=YT-DL
                                                                             K=1, NDIV
                                                                           YT=YT-DL
DD 103 K
XT=XT-DL
                                                                    101
```



```
3850
3880
3880
3880
                                                                                                                                                                                                                                                                                                                                                                                                                                                                                                                                                                                                                                                                                                                                                                                                                                                                                                                                                                                                                                                                                                                                                               )/R(3)
#G(2)/R(4) -3, 0*G(1)/R(5)
!)/R(3)
                                                                                                                                                                            CONTINUE
CONTINUE
CONTINUE
CONTINUE
CONTINUE
CONTINUE
CONTINUE
CONTINUE
CONTINUE
CONTINUE
CONTINUE
CONTINUE
CONTINUE
CONTINUE
CONTINUE
CONTINUE
CONTINUE
CONTINUE
CONTINUE
CONTINUE
CONTINUE
CONTINUE
CONTINUE
CONTINUE
CONTINUE
CONTINUE
CONTINUE
CONTINUE
CONTINUE
CONTINUE
CONTINUE
CONTINUE
CONTINUE
CONTINUE
CONTINUE
CONTINUE
CONTINUE
CONTINUE
CONTINUE
CONTINUE
CONTINUE
CONTINUE
CONTINUE
CONTINUE
CONTINUE
CONTINUE
CONTINUE
CONTINUE
CONTINUE
CONTINUE
CONTINUE
CONTINUE
CONTINUE
CONTINUE
CONTINUE
CONTINUE
CONTINUE
CONTINUE
CONTINUE
CONTINUE
CONTINUE
CONTINUE
CONTINUE
CONTINUE
CONTINUE
CONTINUE
CONTINUE
CONTINUE
CONTINUE
CONTINUE
CONTINUE
CONTINUE
CONTINUE
CONTINUE
CONTINUE
CONTINUE
CONTINUE
CONTINUE
CONTINUE
CONTINUE
CONTINUE
CONTINUE
CONTINUE
CONTINUE
CONTINUE
CONTINUE
CONTINUE
CONTINUE
CONTINUE
CONTINUE
CONTINUE
CONTINUE
CONTINUE
CONTINUE
CONTINUE
CONTINUE
CONTINUE
CONTINUE
CONTINUE
CONTINUE
CONTINUE
CONTINUE
CONTINUE
CONTINUE
CONTINUE
CONTINUE
CONTINUE
CONTINUE
CONTINUE
CONTINUE
CONTINUE
CONTINUE
CONTINUE
CONTINUE
CONTINUE
CONTINUE
CONTINUE
CONTINUE
CONTINUE
CONTINUE
CONTINUE
CONTINUE
CONTINUE
CONTINUE
CONTINUE
CONTINUE
CONTINUE
CONTINUE
CONTINUE
CONTINUE
CONTINUE
CONTINUE
CONTINUE
CONTINUE
CONTINUE
CONTINUE
CONTINUE
CONTINUE
CONTINUE
CONTINUE
CONTINUE
CONTINUE
CONTINUE
CONTINUE
CONTINUE
CONTINUE
CONTINUE
CONTINUE
CONTINUE
CONTINUE
CONTINUE
CONTINUE
CONTINUE
CONTINUE
CONTINUE
CONTINUE
CONTINUE
CONTINUE
CONTINUE
CONTINUE
CONTINUE
CONTINUE
CONTINUE
CONTINUE
CONTINUE
CONTINUE
CONTINUE
CONTINUE
CONTINUE
CONTINUE
CONTINUE
CONTINUE
CONTINUE
CONTINUE
CONTINUE
CONTINUE
CONTINUE
CONTINUE
CONTINUE
CONTINUE
CONTINUE
CONTINUE
CONTINUE
CONTINUE
CONTINUE
CONTINUE
CONTINUE
CONTINUE
CONTINUE
CONTINUE
CONTINUE
CONTINUE
CONTINUE
CONTINUE
CONTINUE
CONTINUE
CONTINUE
CONTINUE
CONTINUE
CONTINUE
CONTINUE
CONTINUE
CONTINUE
CONTINUE
CONTINUE
CONTINUE
CONTINUE
CONTINUE
CONTINUE
CONTINUE
CONTINUE
CONTINUE
CONTINUE
CONTINUE
CONTINUE
CONTINUE
CONTINUE
CONTINUE
CONTINUE
CONTINUE
CONTINUE
CONTINUE
CONTINUE
CONTINUE
CONTINUE
CONTINUE
CONTINUE
CON
CAL DBG(XM, XM, ZM, XN, YT, ZN, D, R, G)
CALL GORR, G, D, G, E)
DD 102 1=1,10
ET(1)=F(1)+F(1)
                                                                                                                                                                                                                                                                                                                                                                                                                                                                                                                                                                                                                                                                                                                                                                                                                                                                                                                                                                                                                                                                                                                                                               ***
                                                                                                                                                                                                                                                                                                                                                                                                                                                                                                                                                                                                                                                                                                                                                                                                                                                           202
                                                                                                                                                                                                                                                                                                                                                                                                                                                                                                                                                                                                                                                                                                                                                                                                                                                                                                                                                 204
                                                                                                                                                                                                                                                                                                                                                                                                                                                                                                                                                                                                                                                                                                                                                                                                                                                                                                                                                                                                                                       205
                                                                                                                                               102
                                                                                                                                                                                                                                                   104
                                                                                                                                                                                                                                                                                                                                          105
                                                                                                                                                                                                                                                                                                                                                                                                                                     300
                                                                                                                                                                                                                                                                                                                                                                                                                                                                                              201
```



```
11960
11980
11980
12000
12010
                                                                                                            COMPLEX E(16), L(MAT, MATP)
L(MT, NT)=E(1)
L(MP, NT)=E(2)
L(MPP, NT)=E(3)
L(MPP, NT)=E(4)
L(MT, NP)=E(5)
L(MT, NP)=E(5)
```

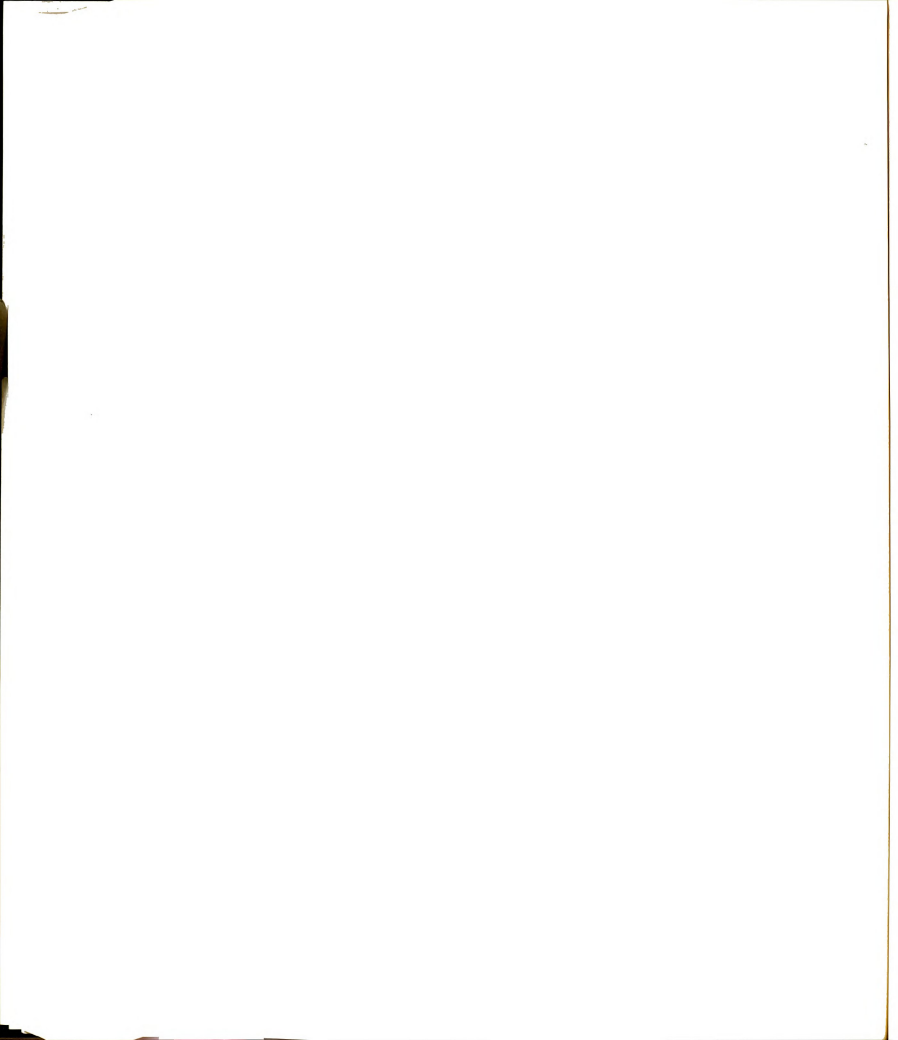


E(11) =E(13) =E(13) =(13) =(14) =(15) 1)=(15) 1)=(15) 1)=(113) =(114) 1)=(115) 1)=(1	

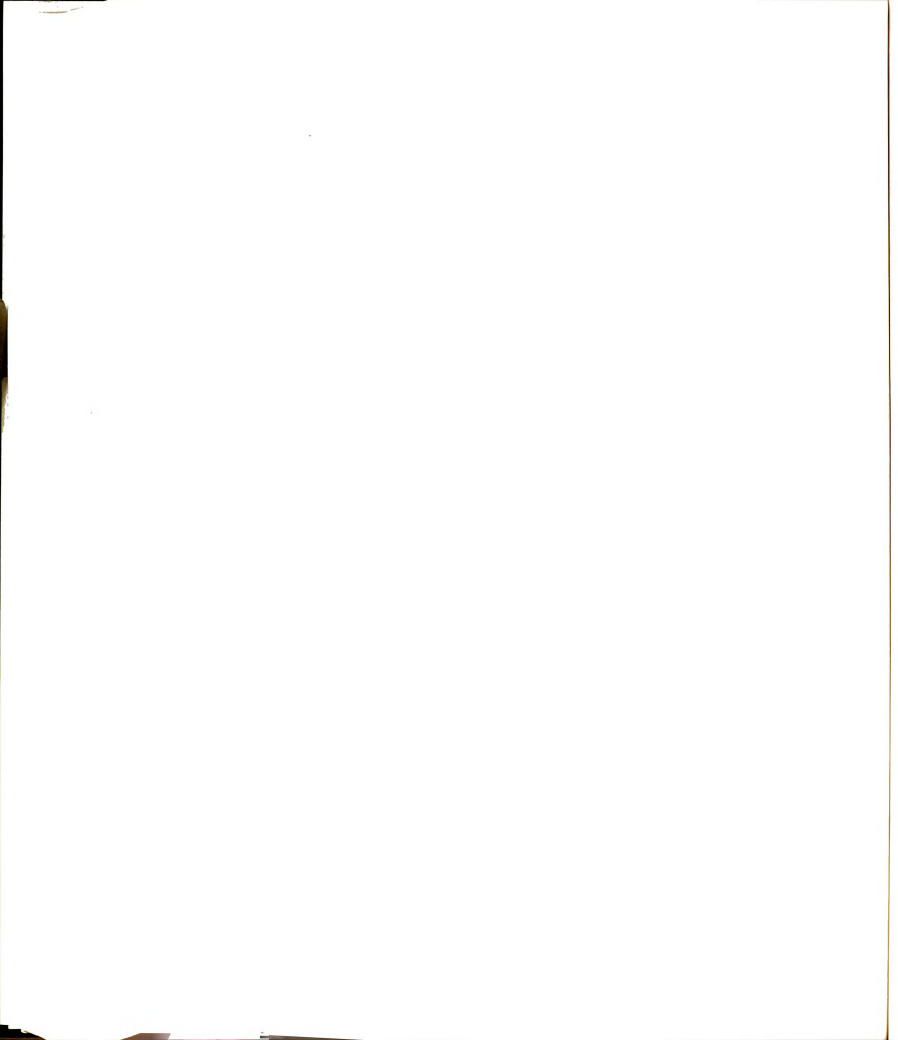
	COMMON ACPLANCE

A STATE OF THE STA	

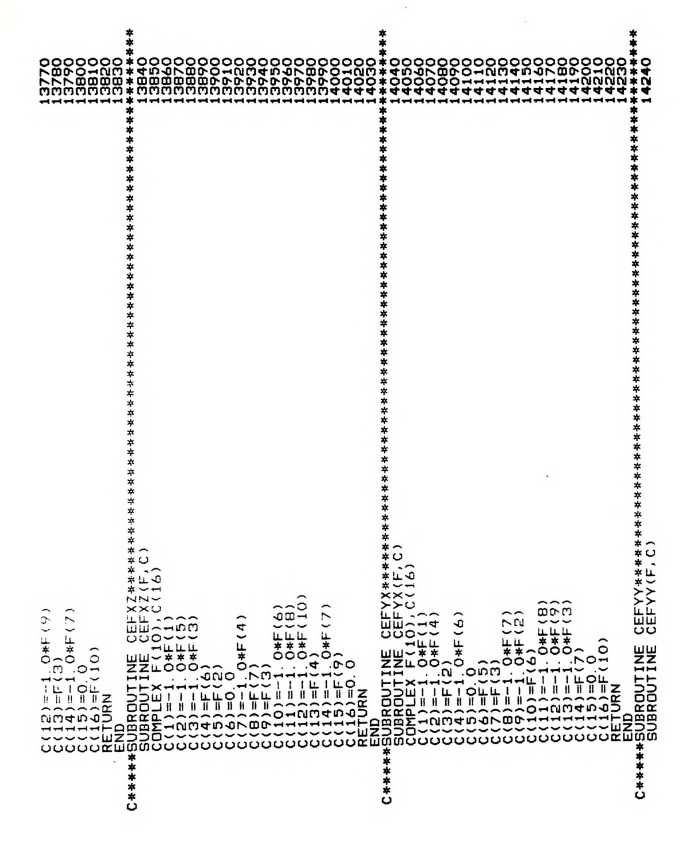
211 4201 4201 44001 644400 60000 60000 60000 60000 60000	เ÷ุยยย ข้อย ระเมณ	12650 12650 12650 1270 12710	**************************************	12790 12800 12810 12820 12820 12840 12840 12850 12860 12860
F(1)=AREA*D(2)*Q(1) F(2)=AREA*D(1)*Q(1) F(3)=CJ*AREA*D(1)*D(3)*Q(2) F(4)=CJ*AREA*D(2)*D(3)*Q(2) F(5)=AREA*D(3)*Q(1) F(5)=AREA*D(2)*D(1)*Q(2) F(5)=CJ*AREA*D(2)*D(1)*Q(2) F(7)=CJ*AREA*D(2)*Q(1) F(7)=CJ*AREA*D(2)*Q(3) F(9)=AREA*D(1)*Q(3) F(10)=AREA*D(1)*Q(3) RETURN	**************************************	(4) = AREA*D(3) *Q(1) (5) = AREA*D(2) *Q(1) (6) = CJ*AREA*D(1) *D(2) *Q(2) (7) = CJ*AREA*D(1) *D(3) *Q(2) (8) = AREA*D(1) *Q(3) (9) = AREA*D(3) *Q(3) (10) = AREA*D(2) *Q(3)	UBROUTINE FCNYY***********************************	SCOUNTY OF THE PARTY OF THE PAR

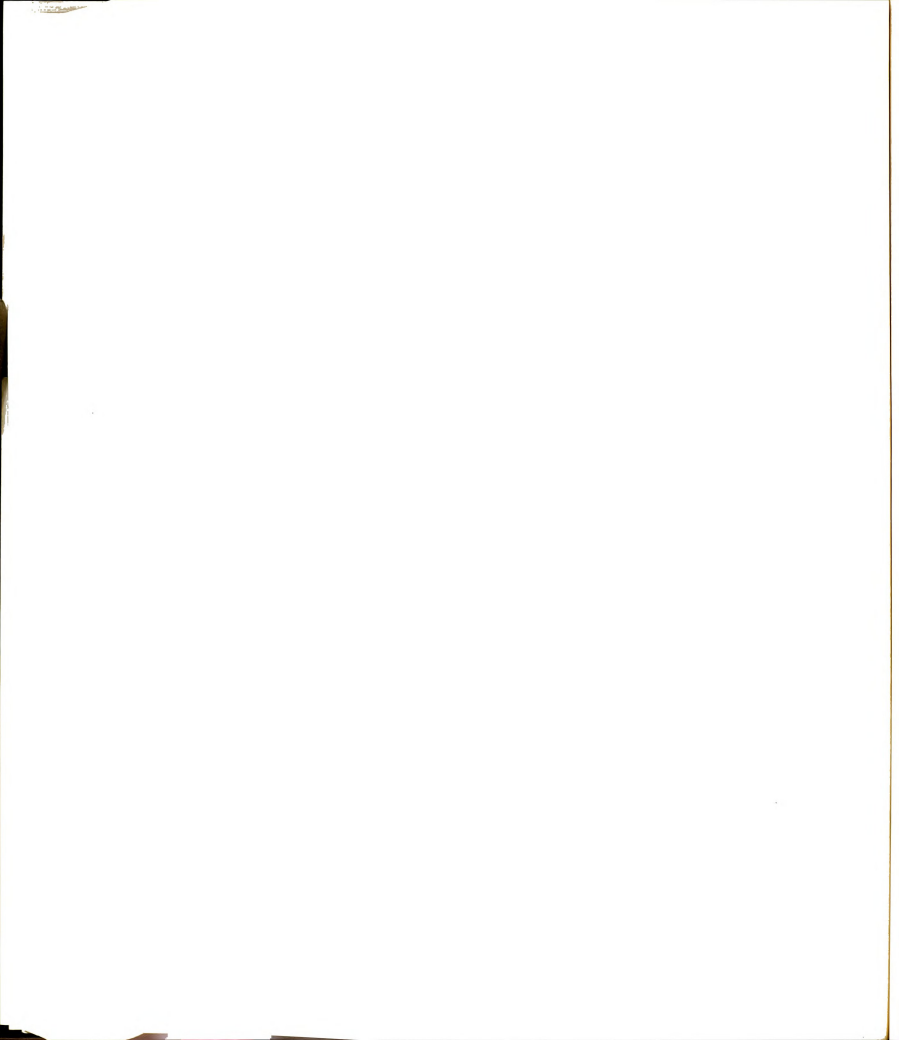


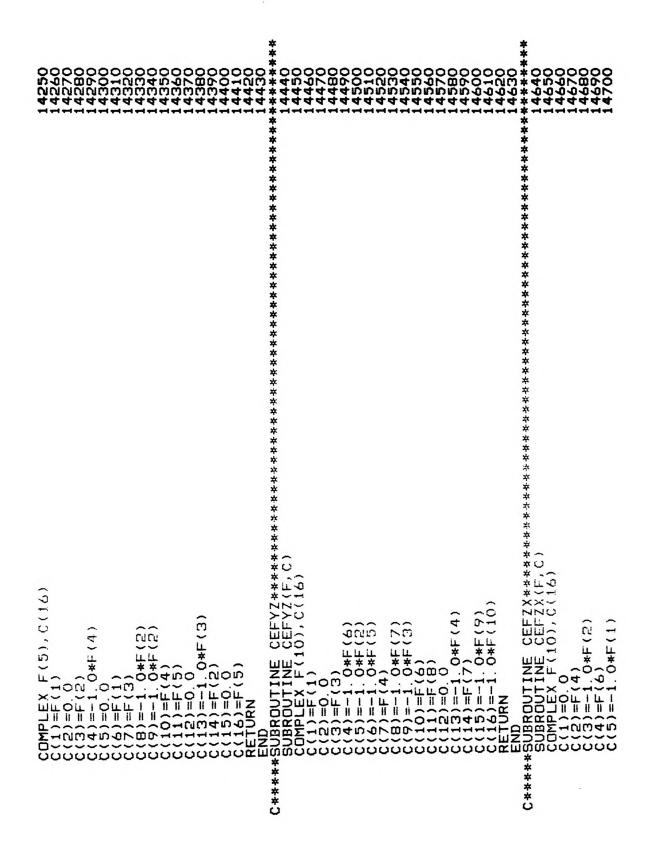
00000000000000000000000000000000000000		13050 130050 130050 130050 130150 130150 1500 150	13160 13170 13180 13190	11111111111111111111111111111111111111
	C****BIBOUTINE FCNIXX***********************************	F(1)=RF4ED1(1)*Q(1) F(2)=CV*AREAP(0(1)*Q(2)*Q(2)*Q(2))*Q(4)) F(3)=CV*AREAP(0(1)*Q(2)) F(3)=CV*AREAP(0(2)*Q(1)) F(3)=CV*AREAP(0(2)*Q(2)) F(3)=CV*AREAP(1)*Q(3) F(3)=AREAP(1)*Q(3) F(3)=AREAP(1)*Q(3) REIONAREAP(2)*Q(3)	C*****SUBOUTINE FCNZY************************************	F(2)=AREAP(3)*6(4) F(2)=AREAP(1)*6(1) F(3)=CAREAP(2)*6(1) F(4)=CAREAP(2)*(2)*(3)*(2) F(5)=REAP(2)*(1)*(1)*(2)*(2) F(5)=REAP(2)*(1)*(1)*(1)*(2)*(2) F(8)=AREAP(1)*(1)*(1)*(1)*(2)*(2) F(9)=AREAP(1)*(2)*(2)*(2) F(10)=AREAP(2)*(2)*(3) RETURN

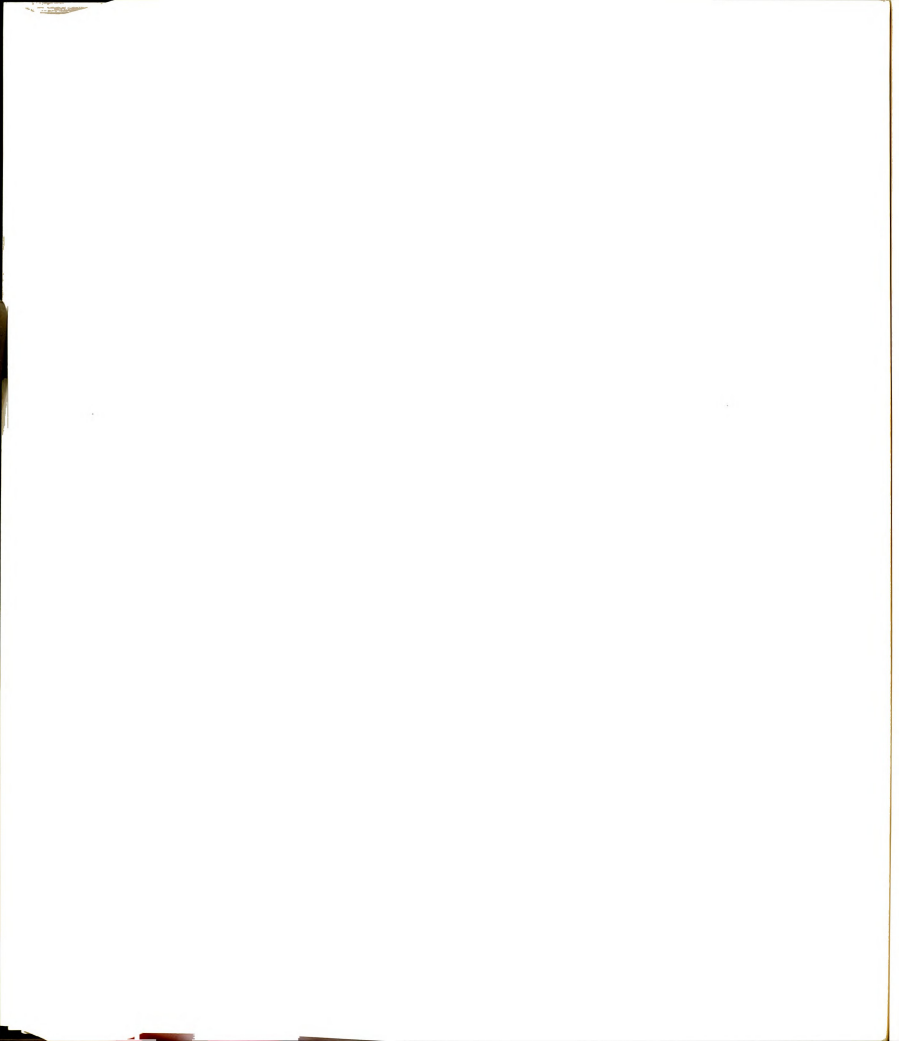


**************************************	133370 133390 13410 13410	*	11111111111111111111111111111111111111	136600 **13620 **13620 13620 13650 13660 13660 13660	13710 13720 13730 13750 13750
*****		****		****	
****		*****		** ** ** ** ** **	
FNIZ************************************	2)+Q(4)) 2)+Q(4))	CEFX(************************************		TELY/V************************************	
**************************************	1(2) 1D(2)*0(2)+ 1D(1)*Q(2)+	**		** ** ** ** ** **	
NE FCNZZ****** NE FCNZZ(AREA, D.), MUO O(1), F(3), CJ GCNZ/PI, NUO, EPO CCNS/PI, NUO, EPO	*&Q(1) (1)*D(2)*Q(2 (Q(1)+D(2)*D(1) (Q(1)+D(1)*D(1)*D(1)*D(1)*D(1)*D(1)*D(1)*D(1)*	:XX***** :XX(F,C)	4	XY************************************	
COUTINE FOR COUTINE FOR DUST, MUO PLEX Q(4), F 10N / CONS/F		SUBROUTINE CEFXX(F) SUBROUTINE CEFXX(F) COMPLEX F(5), C(16) C(1)=F(1) C(2)=-0.0)*F(3)*F(3)*F(3)	5)=0.0 JRN 100 JRN 100 ADUTINE C ACUTINE C ACU	5)=0.0 (6)=F(5) (7)=-1.0*F(3) (8)=F(7) (9)=F(2) (10)=-1.0*F(6) (11)=-1.0*F(8)
C***** SUBROU SUBROU REAL D COMPLE COMMON	ттттт	C**** SUBH SUBH COMP	240909090900000000000000000000000000000	**************************************	0000000

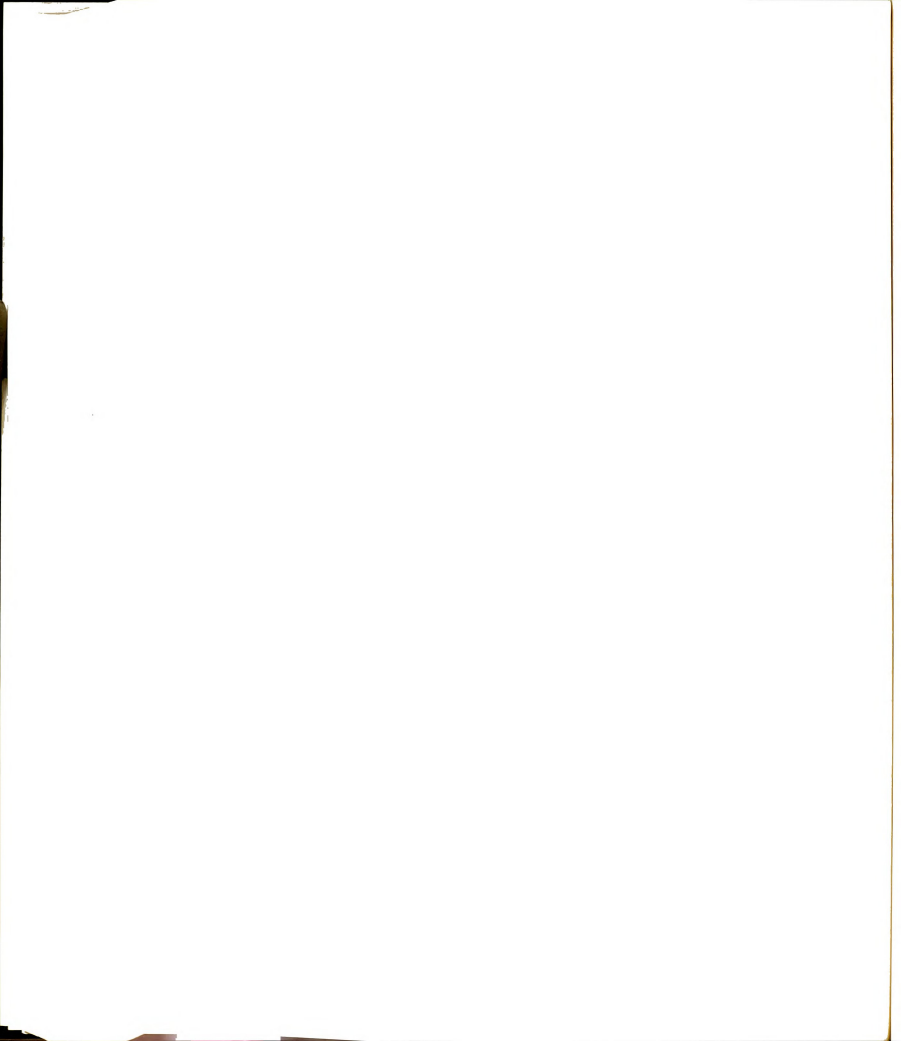








```
1144740
1144740
1144884
1144884
1144884
1144884
1144884
1144980
1144980
115000
115000
115000
116000
                                                                                                         COMPLEX F(5), C(16)
C(1) = F(1)
C(2) = 0.0
C(3) = -1.0*F(2)
C(4) = F(4)
C(5) = 0.0
C(5) = 0.0
C(7) = -1.0*F(3)
C(7) = F(2)
C(9) = F(2)
C(10) = -1.0*F(4)
```

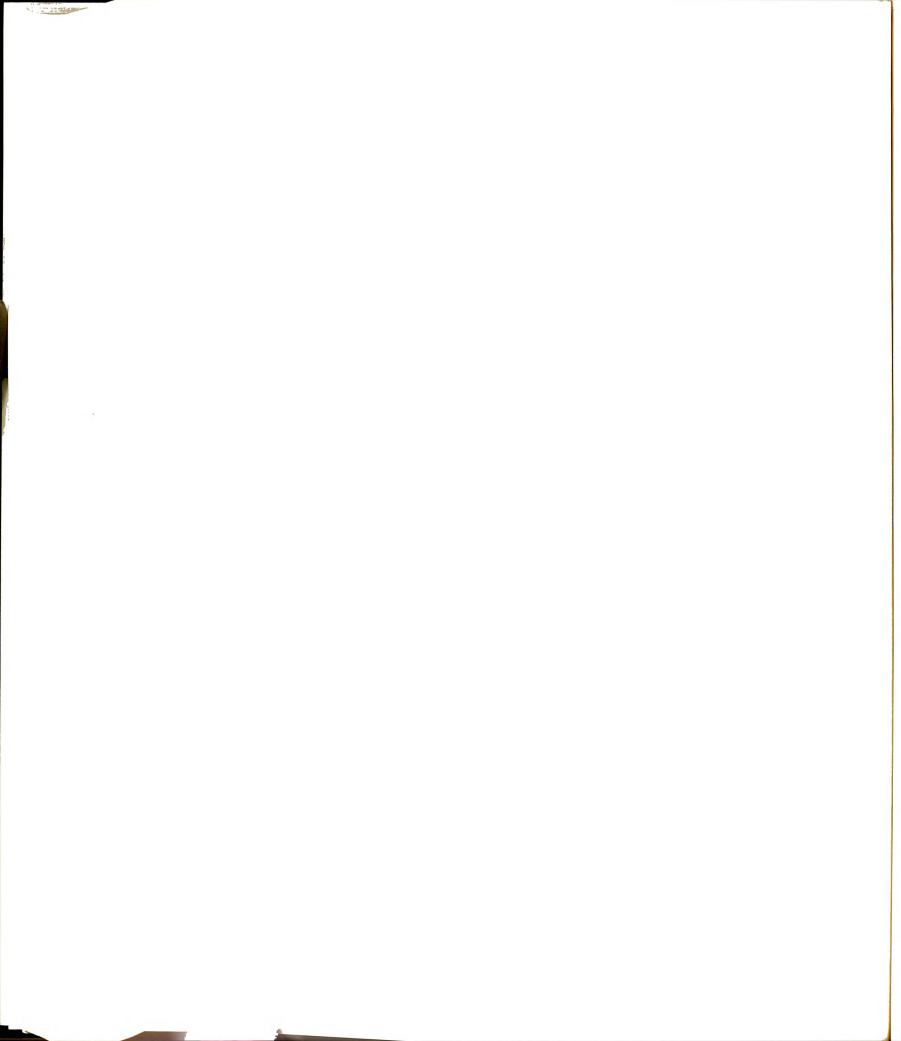


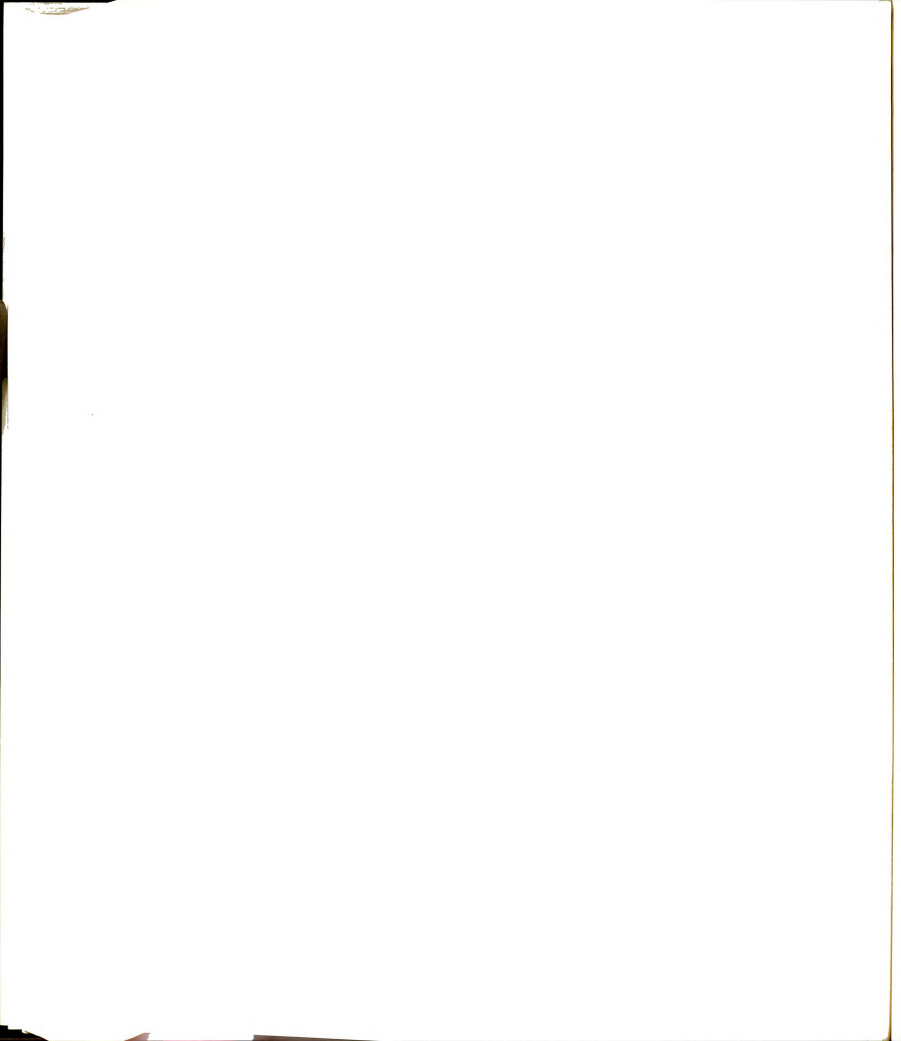
```
10170
115170
115170
115170
115170
115170
115170
115170
115170
115170
115170
115170
115170
115170
115170
115170
115170
115170
115170
115170
115170
115170
115170
115170
115170
115170
115170
115170
115170
115170
115170
115170
115170
115170
115170
115170
115170
115170
115170
115170
115170
115170
115170
115170
115170
115170
115170
115170
115170
115170
115170
115170
115170
115170
115170
115170
115170
115170
115170
115170
115170
115170
115170
115170
115170
115170
115170
115170
115170
115170
115170
115170
115170
115170
115170
115170
115170
115170
115170
115170
115170
115170
115170
115170
115170
115170
115170
115170
115170
115170
115170
115170
115170
115170
115170
115170
115170
115170
115170
115170
115170
115170
115170
115170
115170
115170
115170
115170
115170
115170
115170
115170
115170
115170
115170
115170
115170
115170
115170
115170
115170
115170
115170
115170
115170
115170
115170
115170
115170
115170
115170
115170
115170
115170
115170
115170
115170
115170
115170
115170
115170
115170
115170
115170
115170
115170
115170
115170
115170
115170
115170
115170
115170
115170
115170
115170
115170
115170
115170
115170
115170
115170
115170
115170
115170
115170
115170
115170
115170
115170
115170
115170
115170
115170
115170
115170
115170
115170
115170
115170
115170
115170
115170
115170
115170
115170
115170
115170
115170
115170
115170
115170
115170
115170
115170
115170
115170
115170
115170
115170
115170
115170
115170
115170
115170
115170
115170
115170
115170
115170
115170
115170
115170
115170
115170
115170
115170
115170
115170
115170
115170
115170
115170
115170
115170
115170
115170
115170
115170
115170
115170
115170
115170
115170
115170
115170
115170
115170
115170
115170
115170
115170
115170
115170
115170
115170
115170
115170
115170
115170
115170
115170
115170
115170
115170
115170
115170
115170
115170
115170
115170
115170
115170
115170
115170
115170
115170
115170
115170
115170
115170
115170
115170
115170
115170
115170
115170
115170
115170
115170
115170
115170
115170
115170
115170
115170
115170
115170
115170
115170
115170
115170
115
                                                                                                                                                                                                                                                                                                                                                                                                                                                                                                                                                                                                                                                                                                                                                                                                                                                                                                                                                                                                                                                                                                                                                                                                                                                                                                                                                                                                                                                                                                                                                                                                                                                                                                                                                                                                                                                                                                                                                                                                                                                                                                                                                                                                                                                                                                                                                                                                                                                                                                        THE SYSTEM EQUALS ZERO. THIS CASE. //)
                                                                                                                                                                                                                                                                                                                                                                                                  S=S+A(K, J)*A(J, L)
AKKAT (1.4 KL) = S)/A(K, K)
FORMAT (1.4 KL) = S)/A(K, L)
T. 364THE PROGRAM CANNOT HANDLE
REIURN
                                                                                                                                                                                                                                                                                                                                                                                                                                                                                                                                                                                                                                                                                                                                                                                                                                                                                                                                                                                                                                                                                                                                                                                                                                                                                                                                                                                                                                                                                                           TOWN (NEW YOR) (
                                                                                                                                                                                                                                                                                                                                                                                                                                                                                                                                                                                                                                                                                                                                                                                                                                                                                                                                                                                                                                                                                                                                                                                                                                                                                                                                                                                                                                                                                                                                                                                                                                                                                                                                                                                                                                                                                                                                                                                                                                                                                                                                                                                                           CMPLX(0.0,0)
=CMPLX(0.0,0.0)
F (N-KPI) 12,19,1'
                                 C(12)=0.0
C(13)=F(3)
C(14)=-F(3)
C(15)=0.0
C(15)=0.0
C(16)=F(5)
RETURN
                                                                                                                                                                                                                                                                                                                                                                                                                                                                                                                                                                                                                                                                                                                                                                                                                                                                                                                                                                                                                                                                                                                                                                                                                                                                                                                                                                                                                                                                          CONTINUE
IF (CABS
                                                                                                                                                                                                                                                                                                                                                                                                                                                                                                                                                                                                                                                                                                                                                                                                                                                                                                                                                                                                                                                                                                                                                                                                                                                                                                                                                                                                                                                                                                                                                                                                                                                                                                                                                                                                                                                                                                                                                                                                                                                                                                      X=N-11+1

XP 1=X+1

DO 12+1

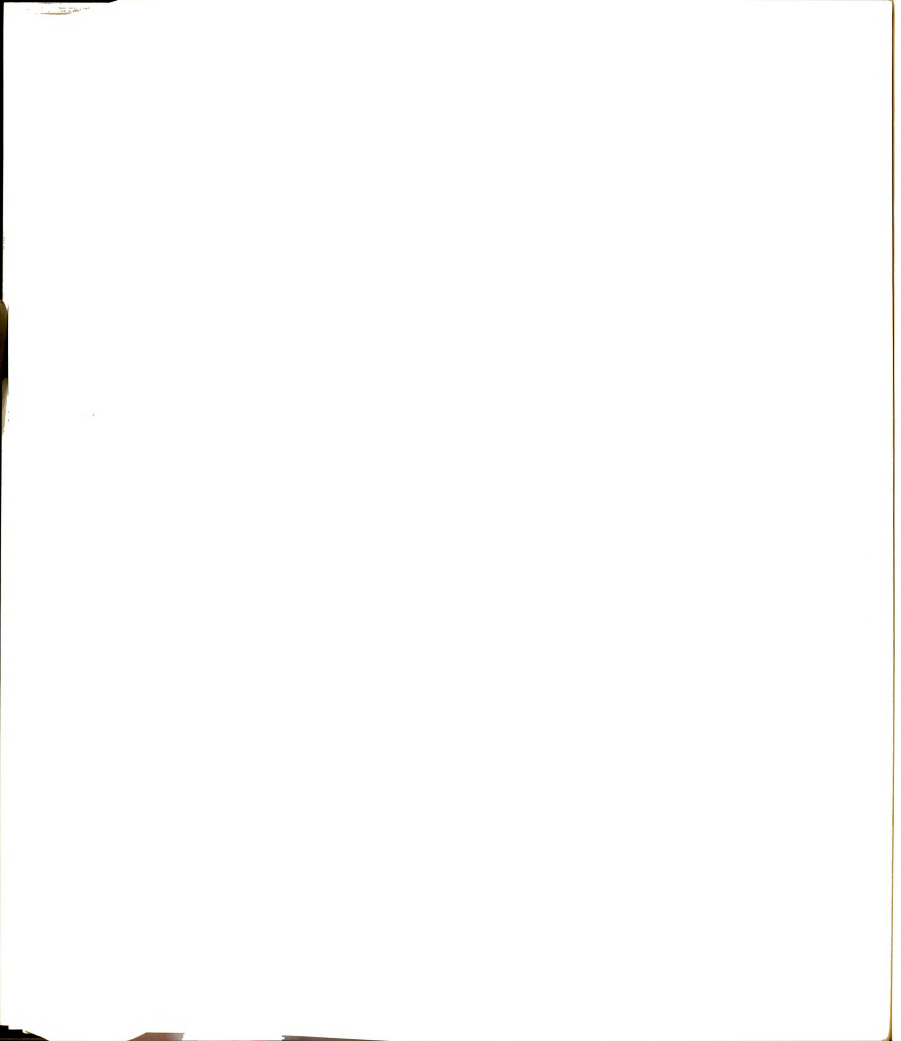
S=CMPL=
                                                                                                                                                                                                                                                                                                                                                                                                                                                                                                                                                                                                                                                                                                                                                                                                                                                                                                                                                                                                                                                                                                                                                                                                                                                                                                                                                                                                                                                                                                                                                                                                                                                                                                                                                                                                                                                                                                                                                                                                                                                                                                                                                                                                                                                                                                                                                                          5000
                                                                                                                                                                                                                                                                                                                                                                                                                                                                                                                                                                                                                                                                                                                                                                                                                                                                                                                                                                                                                                                                                                                                                                                                                                                                                                                                                                                                                                                                                                                                                                                                                                                                                                                                                                                                                                                                                                                                                                                                          18
```





```
7444vuvvvuvuvuvuvuvuvo
```

```
CALL PREL(FIRS, CPPL, COSE, ECRS, MAT)
CALL PREL(FIRS, CPPL, COSE, ECRS, MAT)
CALL PREL(FIRS, CPPL, SINH, HEIN, MAT)
CALL PREL(FIRS, CPPL, SINH, HEIN(I)
CALL PREL(FIRS, CPPL, SINH, SI
```



```
IF(NV(N) EQ. 0) 60 TO 38
DO 28 1=J.K
SUMP(1) == ECOS(1)+HCOS(1)+ESIN(1)-HSIN(1)
CONTINUE
-J-J-NV(N)
                                                                                                                                                                                                                                                                                                                                                                                                                                                                                                                                                                                                                                                                                                                                                                                                                                                                                                                                                                    K=K+NV(N)

DDD 29 I=J,K

SUNS(I)==ECDS(I)+HCDS(I)+ESIN(I)-HSIN(I)

CONTINUE
                                                                                                                                                                                                                                                                                                                                                                  12-14N(78)

KEK-HN(78)

EDMS(1) = ECDS(1)-HCDS(1)-ESIN(1)+HSIN(1)

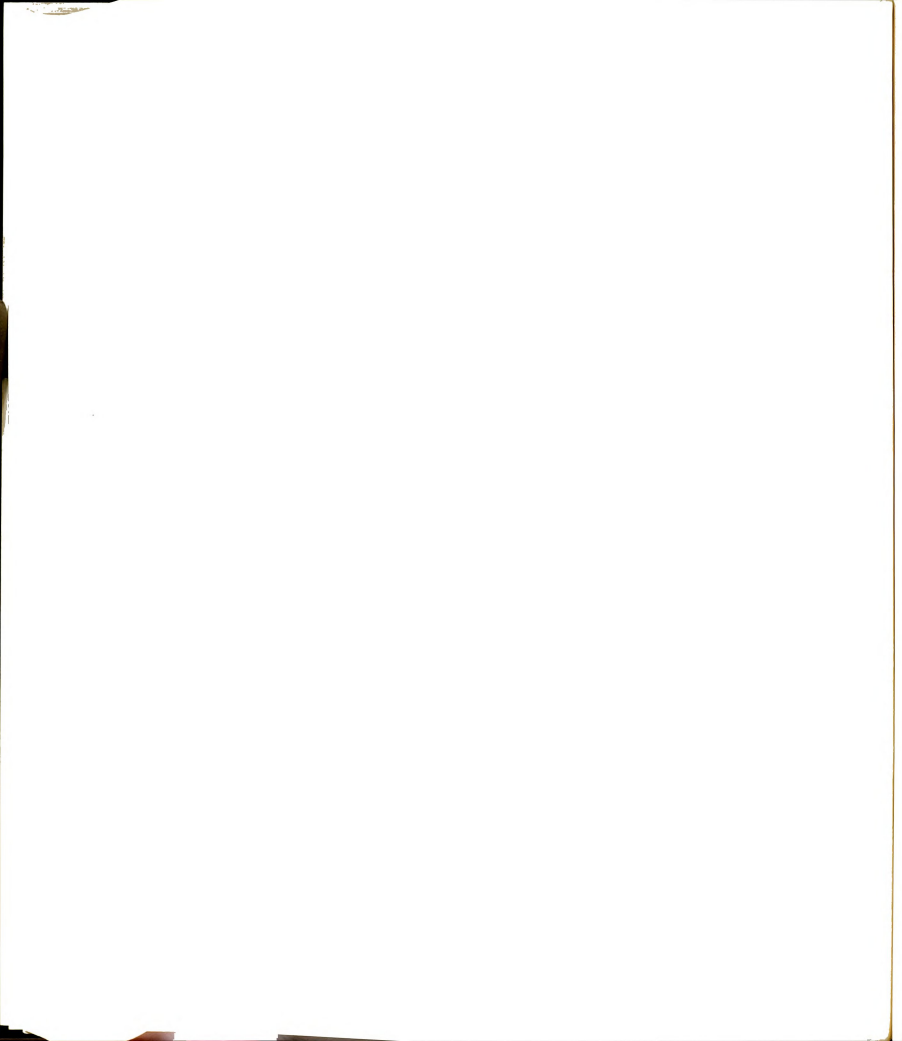
SDMS(1)=ECDS(1)-HCDS(1)-ESIN(1)+HSIN(1)

SDMS(1)=ECDS(1)-HCDS(1)-ESIN(1)+HSIN(1)

SDMS(1)=ECDS(1)-HCDS(1)-ESIN(1)+HSIN(1)

SDMS(1)=ESIN(1)+HSIN(1)

SDMS(1)=ESIN(1)+HSIN(1)+HSIN(1)+HSIN(1)+HSIN(1)+HSIN(1)+HSIN(1)+HSIN(1)+HSIN(1)+HSIN(1)+HSIN(1)+HSIN(1)+HSIN(1)+HSIN(1)+HSIN(1)+HSIN(1)+HSIN(1)+HSIN(1)+HSIN(1)+HSIN(1)+HSIN(1)+HSIN(1)+HSIN(1)+HSIN(1)+HSIN(1)+HSIN(1)+HSIN(1)+HSIN(1)+HSIN(1)+HSIN(1)+HSIN(1)+HSIN(1)+HSIN(1)+HSIN(1)+HSIN(1)+HSIN(1)+HSIN(1)+HSIN(1)+HSIN(1)+HSIN(1)+HSIN(1)+HSIN(1)+HSIN(1)+HSIN(1)+HSIN(1)+HSIN(1)+HSIN(1)+HSIN(1)+HSIN(1)+HSIN(1)+HSIN(1)+HSIN(1)+HSIN(1)+HSIN(1)+HSIN(1)+HSIN(1)+HSIN(1)+HSIN(1)+HSIN(1)+HSIN(1)+HSIN(1)+HSIN(1)+HSIN(1)+HSIN(1)+HSIN(1)+HSIN(1)+HSIN(1)+HSIN(1)+HSIN(1)+HSIN(1)+HSIN(1)+HSIN(1)+HSIN(1)+HSIN(1)+HSIN(1)+HSIN(1)+HSIN(1)+HSIN(1)+HSIN(1)+HSIN(1)+HSIN(1)+HSIN(1)+HSIN(1)+HSIN(1)+HSIN(1)+HSIN(1)+HSIN(1)+HSIN(1)+HSIN(1)+HSIN(1)+HSIN(1)+HSIN(1)+HSIN(1)+HSIN(1)+HSIN(1)+HSIN(1)+HSIN(1)+HSIN(1)+HSIN(1)+HSIN(1)+HSIN(1)+HSIN(1)+HSIN(1)+HSIN(1)+HSIN(1)+HSIN(1)+HSIN(1)+HSIN(1)+HSIN(1)+HSIN(1)+HSIN(1)+HSIN(1)+HSIN(1)+HSIN(1)+HSIN(1)+HSIN(1)+HSIN(1)+HSIN(1)+HSIN(1)+HSIN(1)+HSIN(1)+HSIN(1)+HSIN(1)+HSIN(1)+HSIN(1)+HSIN(1)+HSIN(1)+HSIN(1)+HSIN(1)+HSIN(1)+HSIN(1)+HSIN(1)+HSIN(1)+HSIN(1)+HSIN(1)+HSIN(1)+HSIN(1)+HSIN(1)+HSIN(1)+HSIN(1)+HSIN(1)+HSIN(1)+HSIN(1)+HSIN(1)+HSIN(1)+HSIN(1)+HSIN(1)+HSIN(1)+HSIN(1)+HSIN(1)+HSIN(1)+HSIN(1)+HSIN(1)+HSIN(1)+HSIN(1)+HSIN(1)+HSIN(1)+HSIN(1)+HSIN(1)+HSIN(1)+HSIN(1)+HSIN(1)+HSIN(1)+HSIN(1)+HSIN(1)+HSIN(1)+HSIN(1)+HSIN(1)+HSIN(1)+HSIN(1)+HSIN(1)+HSIN(1)+HSIN(1)+HSIN(1)+HSIN(1)+HSIN(1)+HSIN(1)+HSIN(1)+HSIN(1)+HSIN(1)+HSIN(1)+HSIN(1)+HSIN(1)+HSIN(1)+HSIN(1)+HSIN(1)+HSIN(1)+HSIN(1)+HSIN(1)+HSIN(1)+HSIN(1)+HSIN(1)+HSIN(1)+HSIN(1)+HSIN(1)+HSIN(1)+HSIN(1)+HSIN(1)+HSIN(1)+HSIN(1)+HSIN(1)+HSIN(1)+HSIN(1)+HSIN(1)+HSIN(1)+HSIN(1)+HSIN(1)+HSIN(1)+HSIN(1)+HSIN(1)+HSIN(1)+HSIN(1)+HSIN(1)+HSIN(1)+HSIN(1)+HSIN(1)+HSIN(1)+HSIN(1)+HSIN(1)+HSIN(1)+HSIN(1)+HSIN(1)+HSIN(1)+HSIN(1)+HSIN(1)+HSIN(1)+HSIN(1)+HSIN(1)
                                                                                                                                                                                                                                                                                                                                                                                                                                                                                                                                                                                                                                                                                                                                                                                                                                                                                                                                                                                                                                                                                                                                                                                                    K=K+NV(N)
DD 30 I=J,K
SUMS(I)=ECDS(I)-HCDS(I)-ESIN(I)+HSIN(I)
CONTINUE
                                                                                                                                                                                                                                                                                                                                                                                                                                                                                                                                                                                                                                                                                                                                                                                                                                                                                                                                                                                                                                                                                                                                                                                                                                                                                                                                                                                                                                                                                                            =ECOS(I)-HCOS(I)-ESIN(I)+HSIN(I)
                                                                                                                                                                                                                                                                                                                                                                                                                                                                                                                                                                                                                                                                                                                                                                                                                                                                                                                                                                                                                                                                                                                                                                                                                                                                                                                                                                                                                                                                                                                                                                                                                                                                                                                                                                                                                                                                                                            REL (FIRS, CMPL, EXPZ, SUM1, MAT)
12, FIRS
FL (FIFT, CMC)
                                                                                                                                                                                                                                                                                                                                                                                                                                                                                                                                                                                                                                                                                                                                                                                                                                                                                                                                                                                                                                                                                                                                                                                                                                                                                                                                                                                                                                                                                                                                                                                                                                                                                                                                                                                                                                           U=U+NV(3
K=K+NV(L
                                                                                                                                                                                                                                                                                                                                                                                                                                                                                                                                                                                                                                                                                                                                                                                                                                                                                                                                                                                                                                                                                                                                                                                                                                                                                                                                                                                                                                                                                                                                                                                                                                                                                                                                                                                                                                                                                                                          IF (NV (L)
GO TO 35
CALL PRE
PRINT 32
                                                                                                                                                                                                                                                                                                                                                                                                                                                                                                                                                                                                                                                                                                                                                                                                                                                                                                                                                                                                                                                                                                                                                                                                                                                                                                                                      8
                                                                                                                                                                                                                                                                                                                                                                                                                                                                                                                                                                                                                                                                                                                                                                                                                                                                                                                                                                                                                                                                                                                                                                                                                                                                                                                                                                                                                                                                                                                                                               333
                                                                                                                                                                                                                                                                                                                                                                                                                                                                                                                                                                                                                                                                                                                                                                                                                                                                                                                                                                                                                                                                                                                                                                                                                                                                                                                                                                                                                                                                                                                                                                                                                                                                                                                                                                                                                                                                                                                                                                                                                 34
                                                                                                                                                                                                                                                                                                                                                                                                                                                                                                                                                                                                                                                                                                                                                                                                                                                                             28
                                                                                                                                                                                                                                                                                                                                                                                                                                                                                                                                                                                                                                                                                                                                                                                                                                                                                                                                                                                                                                                                                                      53
                                                                                                                                                                                                                                                                                                                              56
                                                                                                                                                                                                                                                                                                                                                                                                                                                                                                                                                      37
                                                                                             52
```



```
***
          7760
7760
8820
8820
8820
8820
8820
8820
8820
ARS 111 - CAB (SUPIL(1))

ARS 111 - CAB (SUPIL(1))

CALL ANGLE (SUPIL(1) - ANG (1))

CALL ANGLE (SUPIL(1) - ANG (1))

SUMP (1) - COMPLY (ABS 5 (1) - ANG (1))

SUMP (1) - COMPLY (ABS 5 (1) - ANG (1))

SUMP (1) - COMPLY (ABS 5 (1) - ANG (1))

SUMP (1) - COMPLY (ABS 5 (1) - ANG (1))

SUMP (1) - COMPLY (ABS 5 (1) - ANG (1))

SUMP (1) - COMPLY (ABS 5 (1) - ANG (1))

SUMP (1) - COMPLY (ABS 5 (1) - ANG (1))

SUMP (1) - COMPLY (ABS 5 (1) - ANG (1))

SUMP (1) - COMPLY (ABS 5 (1) - ANG (1))

SUMP (1) - COMPLY (ABS 5 (1) - ANG (1))

SUMP (1) - COMPLY (ABS 5 (1) - ANG (1))

SUMP (1) - COMPLY (ABS 5 (1) - ANG (1))

SUMP (1) - COMPLY (ABS 5 (1) - ANG (1))

SUMP (1) - COMPLY (ABS 5 (1) - ANG (1))

SUMP (1) - COMPLY (ABS 5 (1) - ANG (1))

SUMP (1) - COMPLY (ABS 5 (1) - ANG (1))

SUMP (1) - COMPLY (ABS 5 (1) - ANG (1))

SUMP (1) - COMPLY (ABS 5 (1) - ANG (1))

SUMP (1) - COMPLY (ABS 5 (1) - ANG (1))

SUMP (1) - COMPLY (ABS 5 (1) - ANG (1))

SUMP (1) - COMPLY (ABS 5 (1) - ANG (1))

SUMP (1) - COMPLY (ABS 5 (1) - ANG (1))

SUMP (1) - COMPLY (ABS 5 (1) - ANG (1))

SUMP (1) - COMPLY (ABS 5 (1) - ANG (1)

SUMP (1) - COMPLY (ABS 5 (1) - ANG (1)

SUMP (1) - COMPLY (ABS 5 (1) - ANG (1)

SUMP (1) - COMPLY (ABS 5 (1) - ANG (1)

SUMP (1) - COMPLY (ABS 5 (1) - ANG (1)

SUMP (1) - COMPLY (ABS 5 (1) - ANG (1)

SUMP (1) - COMPLY (ABS 5 (1) - ANG (1)

SUMP (1) - COMPLY (ABS 5 (1) - ANG (1)

SUMP (1) - COMPLY (ABS 5 (1) - ANG (1)

SUMP (1) - COMPLY (ABS 5 (1) - ANG (1)

SUMP (1) - COMPLY (ABS 5 (1) - ANG (1)

SUMP (1) - COMPLY (ABS 5 (1) - ANG (1)

SUMP (1) - COMPLY (ABS 5 (1) - ANG (1)

SUMP (1) - COMPLY (ABS 5 (1) - ANG (1)

SUMP (1) - COMPLY (ABS 5 (1) - ANG (1)

SUMP (1) - COMPLY (ABS 5 (1) - ANG (1)

SUMP (1) - COMPLY (ABS 5 (1) - ANG (1)

SUMP (1) - COMPLY (ABS 5 (1) - ANG (1)

SUMP (1) - COMPLY (ABS 5 (1) - ANG (1)

SUMP (1) - COMPLY (ABS 5 (1) - ANG (1)

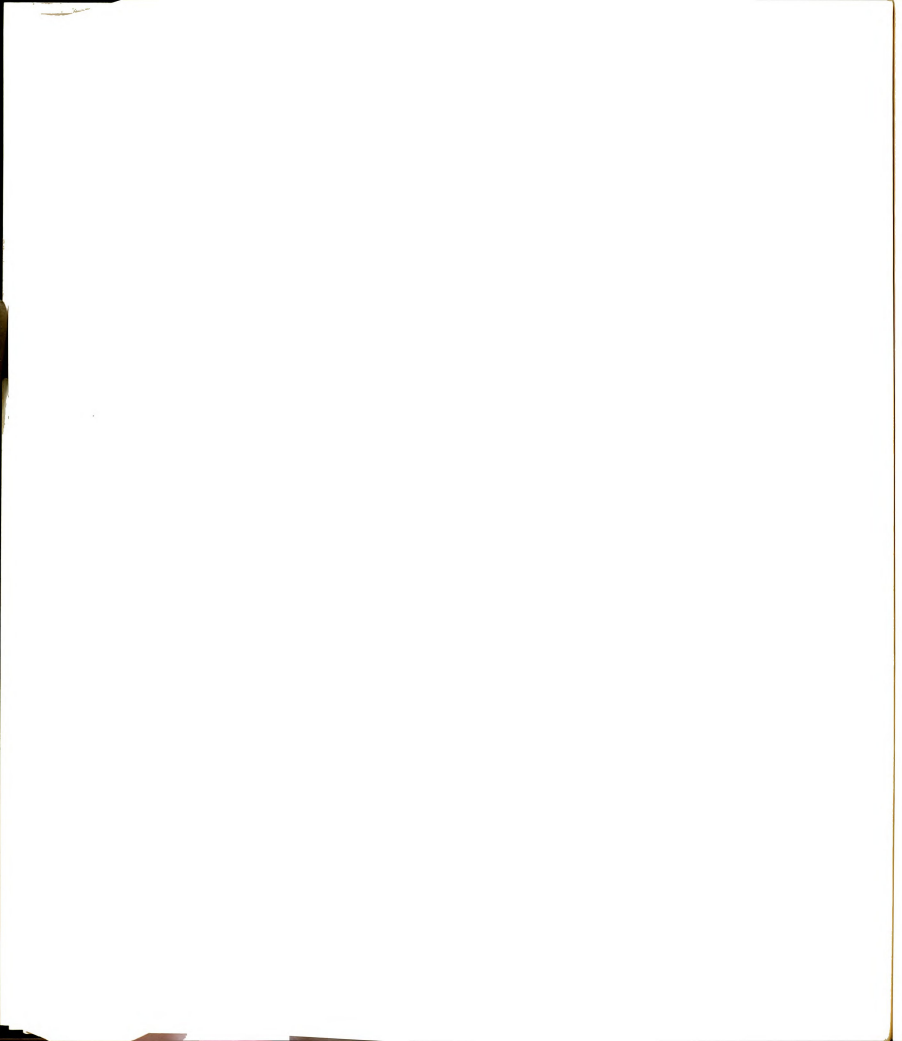
SUMP (1) - COMPLY (ABS 5 (1) - ANG (1)

SUMP (1) - COMPLY (ABS 5 (1) - ANG (1)

SUMP (1) - COMPLY (ABS 5 (1) - ANG 10

SUMP (1) - COMPLY (ABS 5 (1) - ANG 10

SUMP (1) - COMPLY (ABS 5 (1
                                                                                                                                                                                                                                                                                                                                                                                                                                                                                                                                                                                                                                                                                                                                                                                  C****
```



```
ppp=jpp+NX
RINT 13.11. INFL(J), INFL(IP), INFL(IPP), INFL(IPPP)
RINT 123, RIGHT
RINT 124. RINT 125. RIGHT
RINT 125. RIGHT 127. RIGHT
                                                                                                                                                                                                                                                                                                                                                                                                                                                                                                                                                                                                                                                                                                                                                                                                                                                                                                            ipp=ipp+NZ

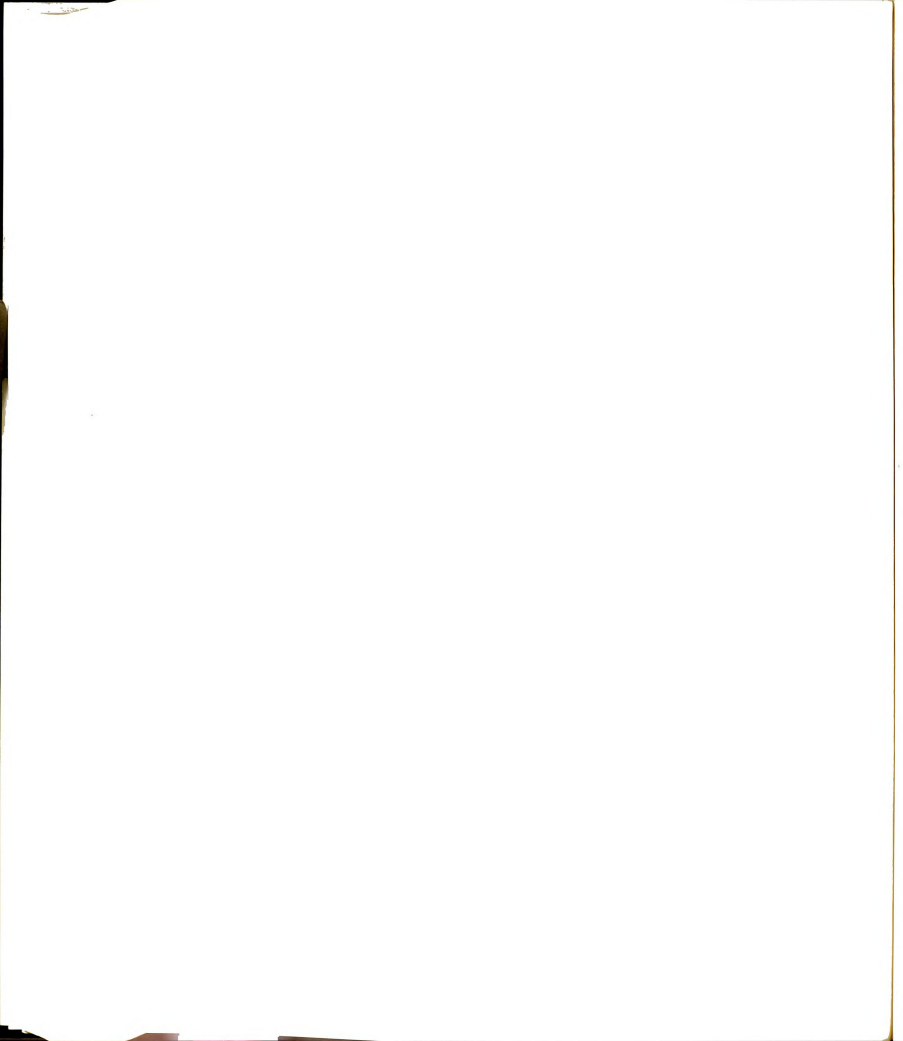
PRINT 13.11.INFL(J), INFL(IP), INFL(IPP),

PRINT 13.11.INFL(J), INFL(IP), INFL(IPP)

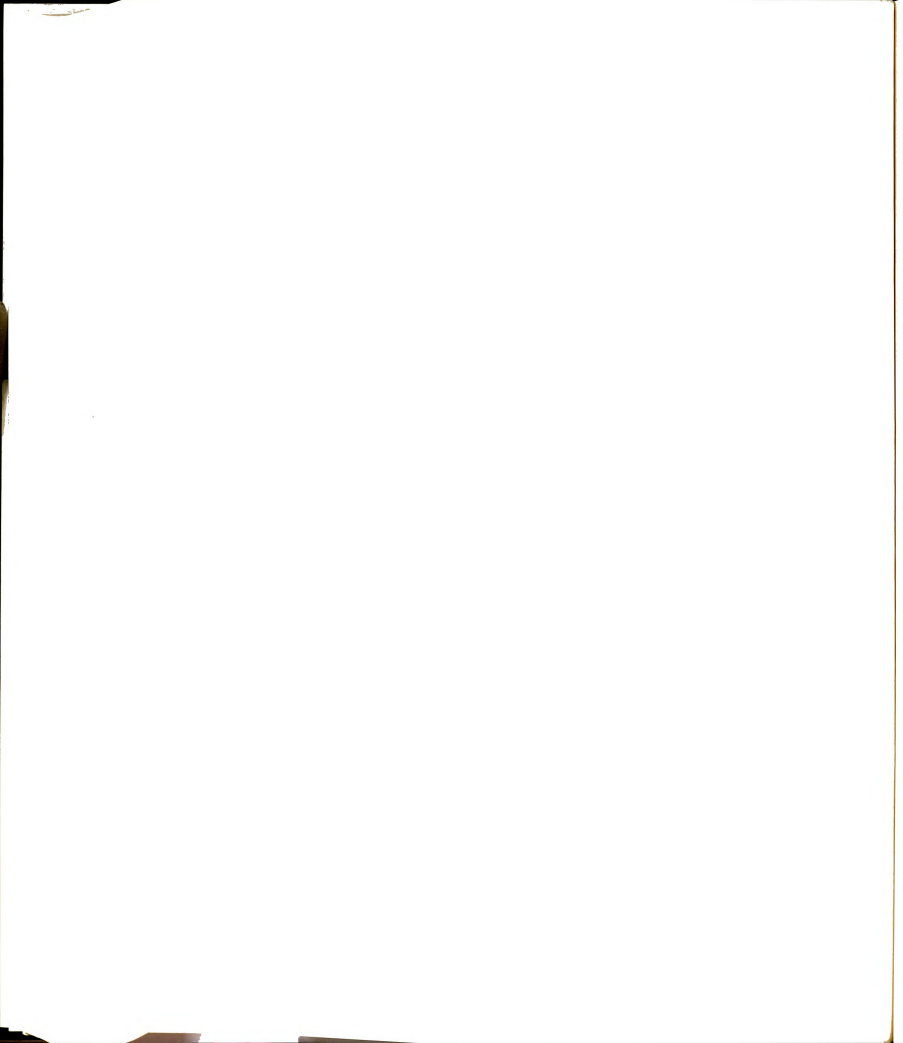
PRINT 13.11.INFL(J)

PRINT 137.

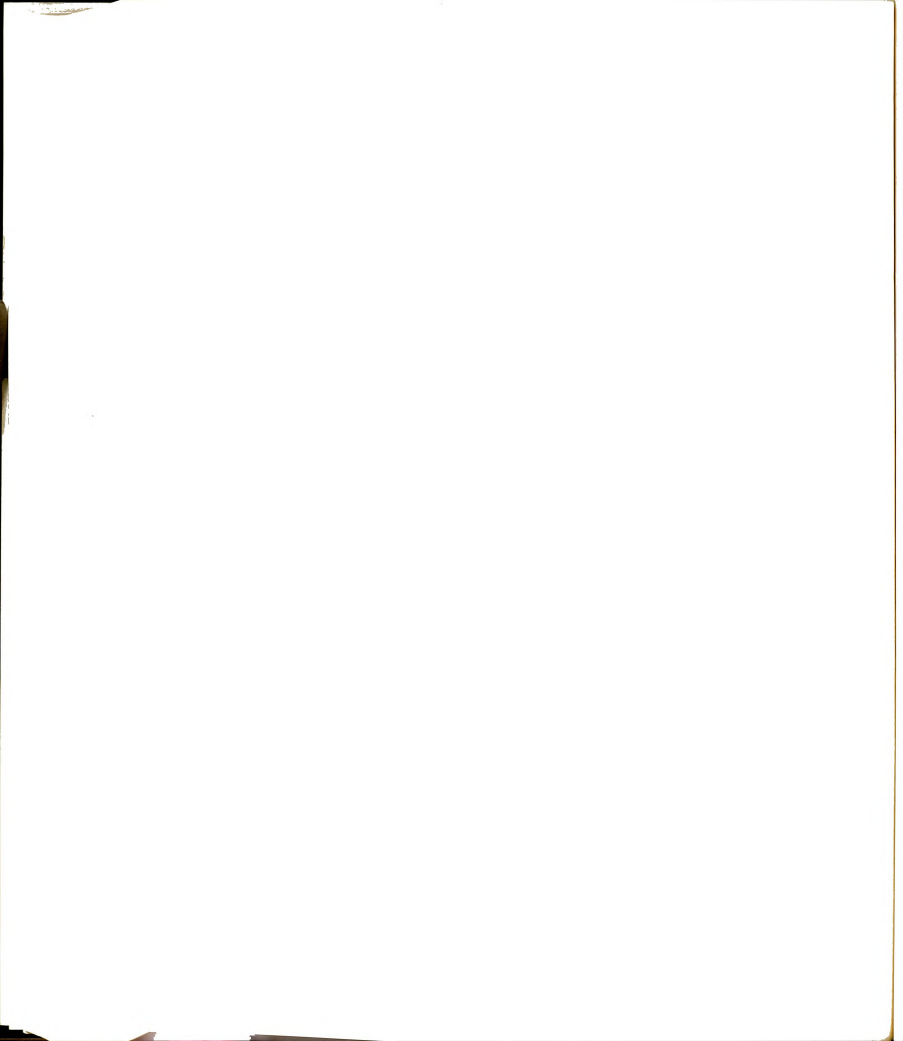
PRINT 137.
                                                                                                                                                                                                                                                                                                                                                                                                                                                                                                                                                                                                                                                                                                                                                                                                                                                                                                                                                                                                                                                                                                                                                                                                                                                                                                                                                                                                                                                                                                                                                                                                                                                                                                                                                                                                                                                                                                                                                                                                                                                PATHWIN
PETTHWIN
IPPETTHWIN
IPPETTI 13-11 INFL(J), INFL(IPP), INFL(IPPP)
PRINT 122
D0 12 I=1, NX
II=I
U=I
IP=U+NX
IPP=IP+NX
                                                                                                                                                                                                                                                                                                                                                                                                                                                                                                                                                                                                                                                                                                                                                                                                                                                                                                                                                                                                                                                                                                                                                                                                                                                                                                                                                                                                                                                                                                                                                                                                                                                                                                                                                                                                                                                                                                                                                                                                                                                                                                                                                                                                                                     16
                                                                                                                                                                                                                                                                                                                                                                                                                                                                                                                                                                                                                                                                                                                                                                                                                                                                                                                                                                                                                                                                                                                                                                                                                                                                                                                                                                                                                                                                                                                                                                                                                                                                                                                                                                                                                                                                                                                                                                                                                                                                                                                                                                                                                                                                                                                                   19
                                                                                                                                                                                                                                                                                                                              12
```



```
DO 17 1=1.NNY
15 FARINX THANKANNY
16 FARINX THANKANNY
17 FARINX THANKANNY
18 FARINX THANKANNY
18 FARINX THANKANNY
19 FARINX THANKANNY
19 FARINX THANKANNY
10 FARINX THANKANNY
11 FORMAN TH
       C****
                                                                                                                                                                                                                                                                                                                                                                                                                                                                                                                                                                                                                                                                                                                                                                                                                                                                                                                                                                                                                                                                        9
```



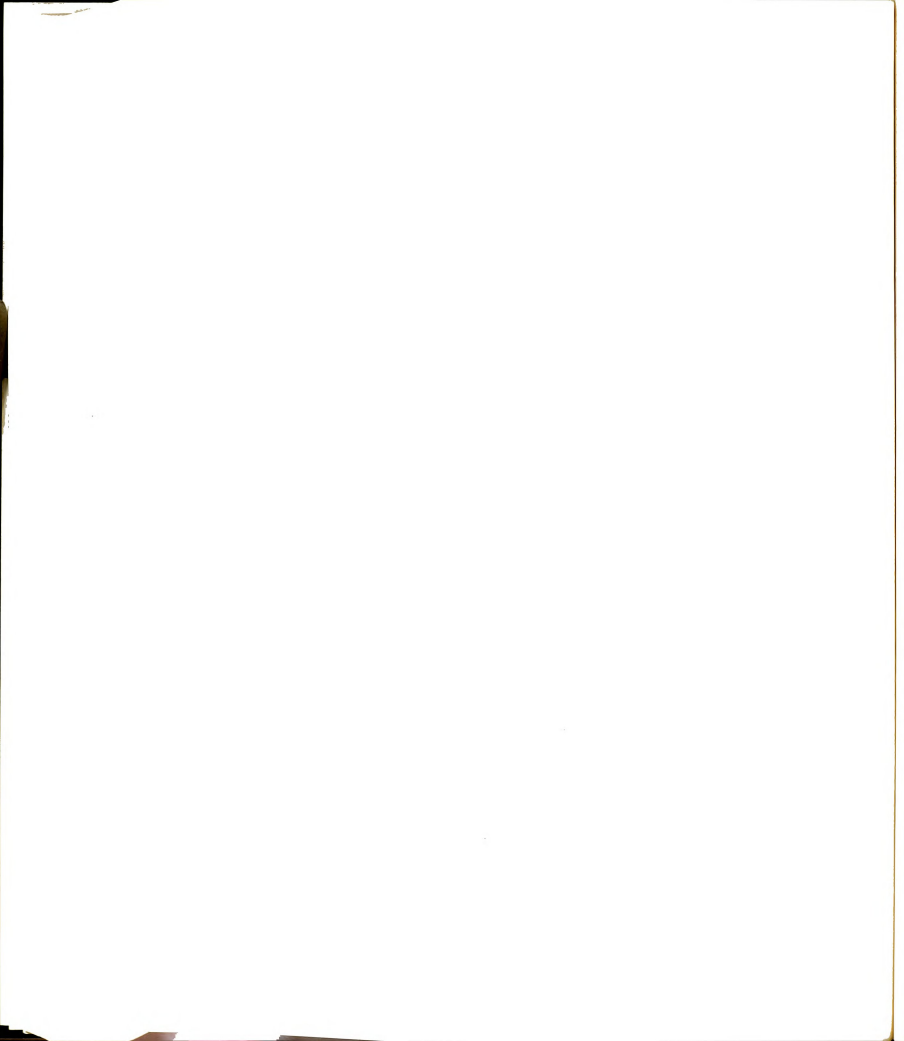
```
40 EF=F*ATAN2(AIMAG(G), REAL(G))
50 GT 100
50
```



CHAPTER V

SUMMARY

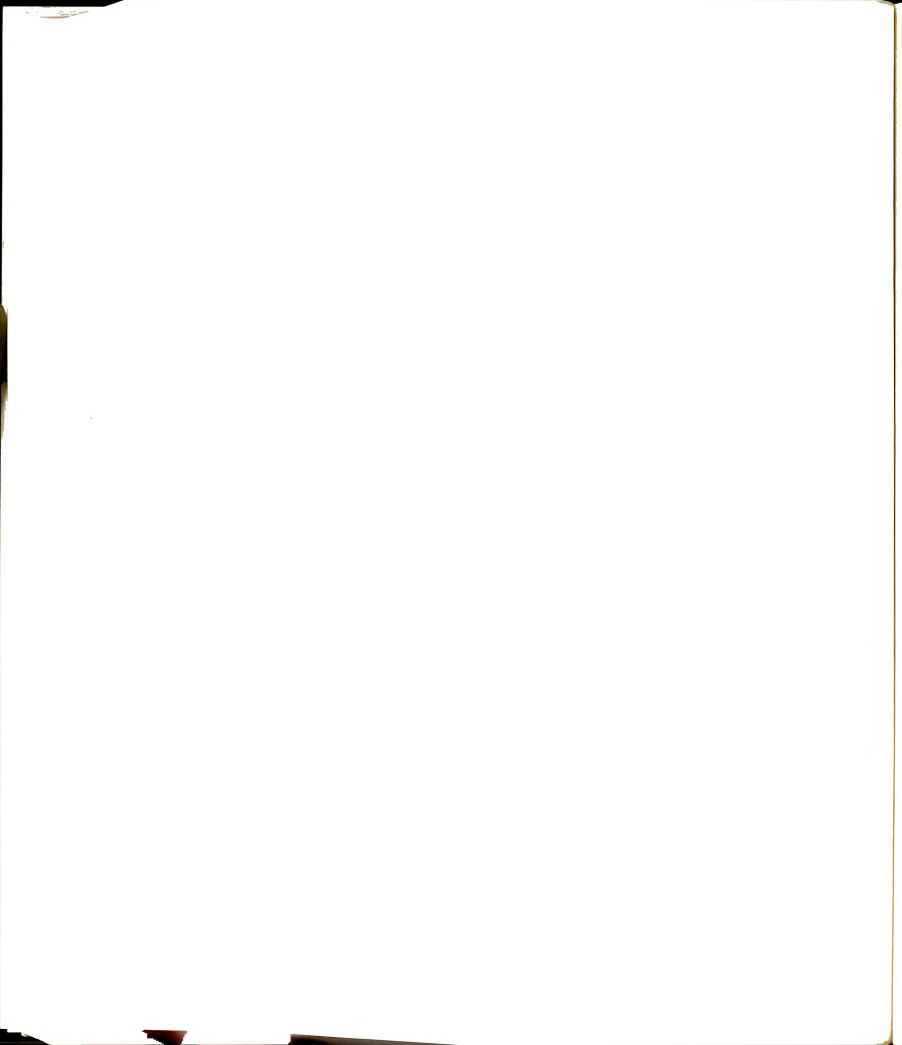
A new theoretical method for determining the eddy current induced by an oscillating magnetic field in a finite conducting body with rotational symmetry was presented in Chapter II. This study was motivated mainly by two reasons: (1) More biological research and medical applications utilize the irradiation of RF magnetic fields. (2) When a thick biological body is irradiated by a HF-VHF EM wave, the induced current can be divided into the electric and magnetic modes. The magnetic mode of induced current, also called the eddy current, is predominant and is difficult to determine with a numerical method. The new theoretical method was derived by utilizing the theory of vector potential, and the numerical results were obtained by using the point-matching and matrix inversion techniques. Two different forms of magnetic fields were considered in Chapter II, namely, a uniformly impressed magnetic field and a beam of uniform magnetic field. For both cases, the results obtained by the new method were found to deviate significantly from the conventionally used, quasi-static solution. An experiment for measuring the magnitudes of the induced



electric fields inside rotationally symmetrical bodies was conducted, and some experimental results were presented. Also, a closed form solution for the induced electric field inside a finite conducting sphere was given in that chapter. The accuracy of the new method was verified by comparing the present solution with the experimental measurements as well as the closed form solution for a finite conducting sphere.

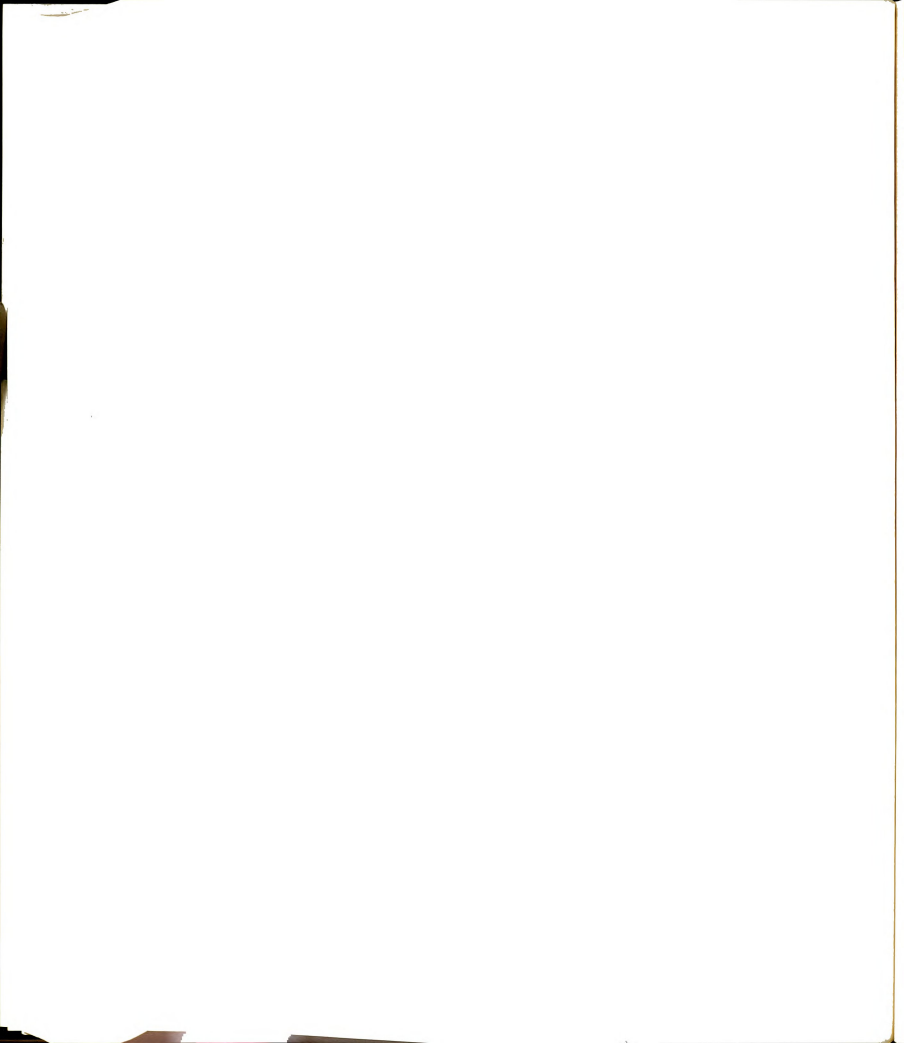
In the quantification of the magnetic mode of the induced current in an irradiated biological body, one often encounters the difficulty of numerical convergence. The new method presented in Chapter II shows an excellent numerical convergence and accuracy, and should help solve this problem. It is noted that the applicability of this new method is restricted to the cases of rotationally symmetrical bodies which are constructed with nonmagnetic materials. For the cases of magnetic materials without rotational symmetry, a different technique should be developed.

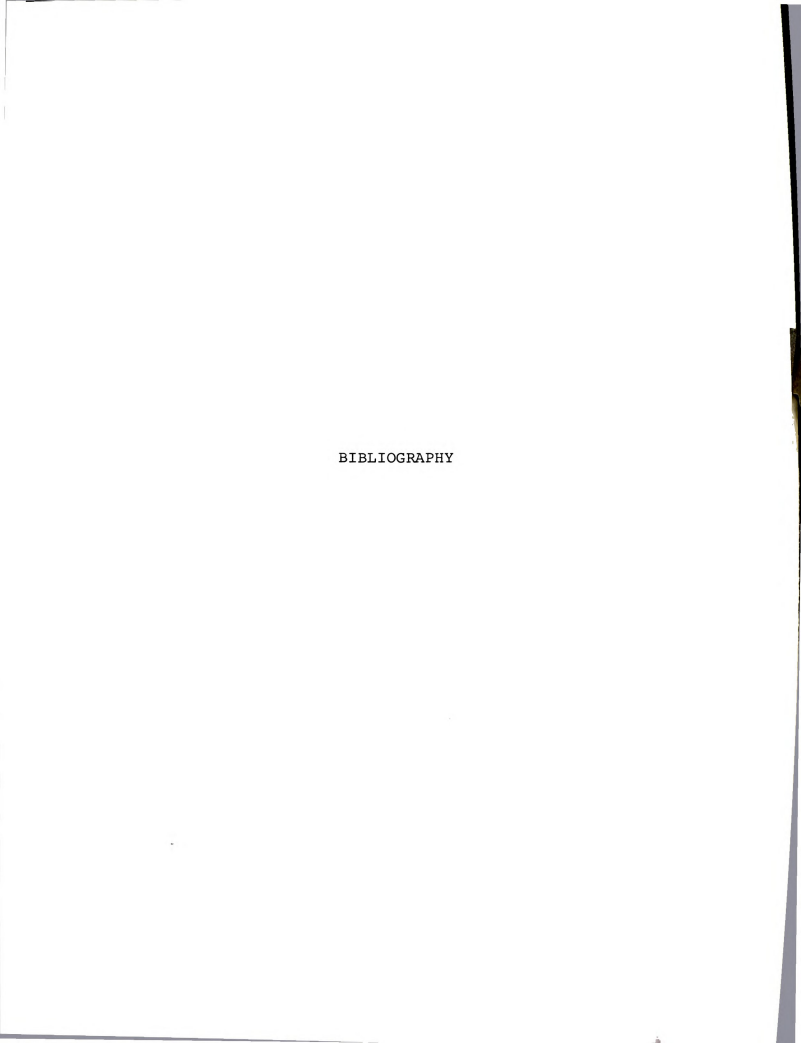
In Chapter III, the microwave interactions with finite conducting, biological bodies were studied. As the first step, we derived two coupled, surface integral equations which relate the induced fields to the incident fields. The validity of these equations was then verified by considering the special case of a two-dimensional, infinite interface between free space and a finite conducting medium.

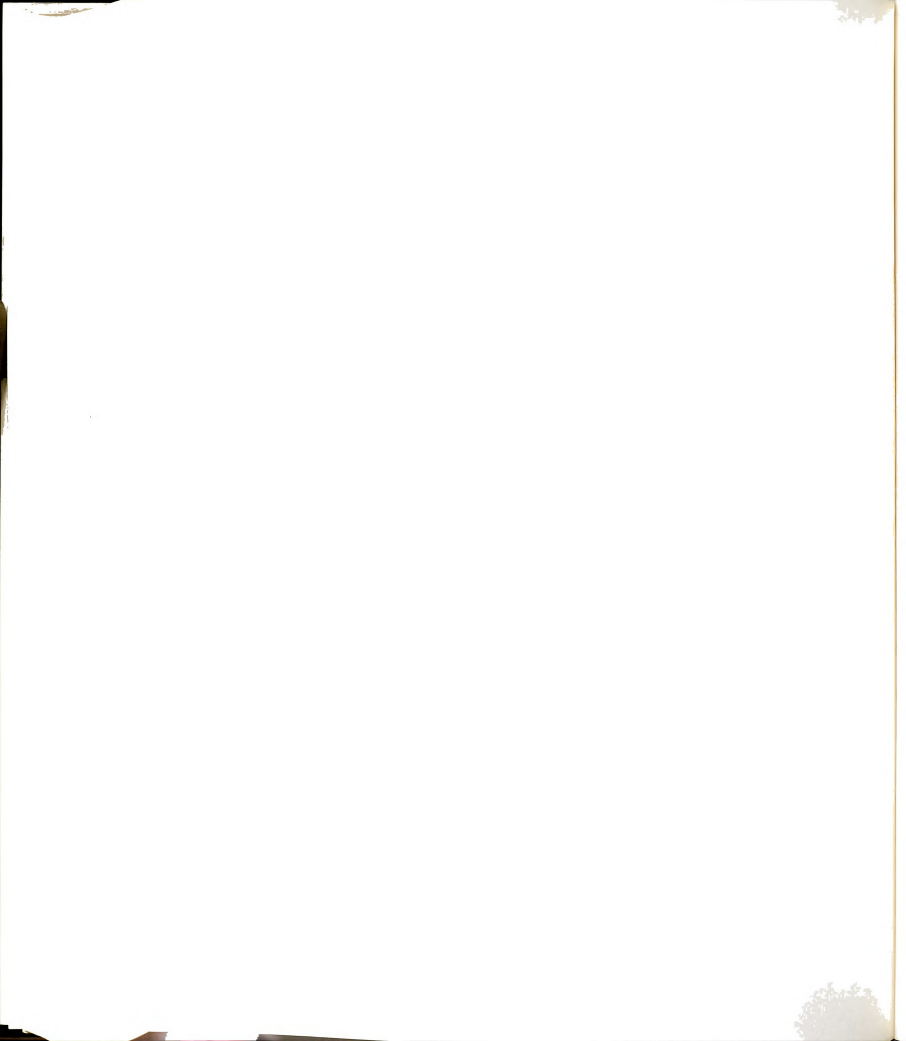


These two surface integral equations were solved numerically by use of moment-method. The results so obtained agree quite well with the solutions obtained by a volume integral equation method.—Tensor Integral Equation Method. For the purpose of reducing the number of unknowns, only the cases involved with electrically small bodies were demonstrated in Chapter III. It is believed that this surface integral equation method is potentially more efficient than the volume integral equation method since when an electrically large body is irradiated by EM waves, the fields induced inside the body mainly concentrate in the region near the body surface. Under this condition, solving the internal fields through the volume integral equation becomes impractical.

Moreover, with a finer subdivision of the body for the method of moment, the number of unknowns encountered in solving the surface integral equations is usually less than that encountered for the volume integral equation, if the number of unknowns exceeds a certain number as in an electrically large body. It is pointed out that the validity of the surface integral equation method is limited to the cases of homogeneous bodies due to the nature of deriving the equations.

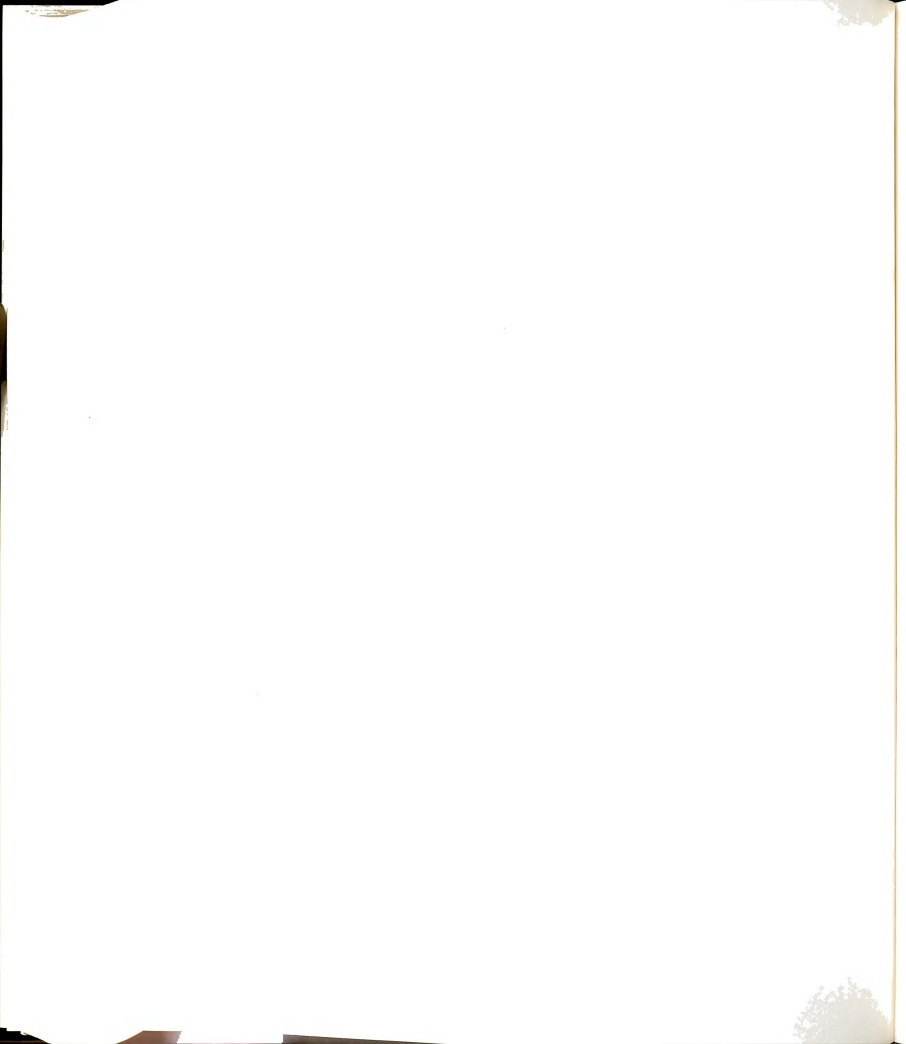




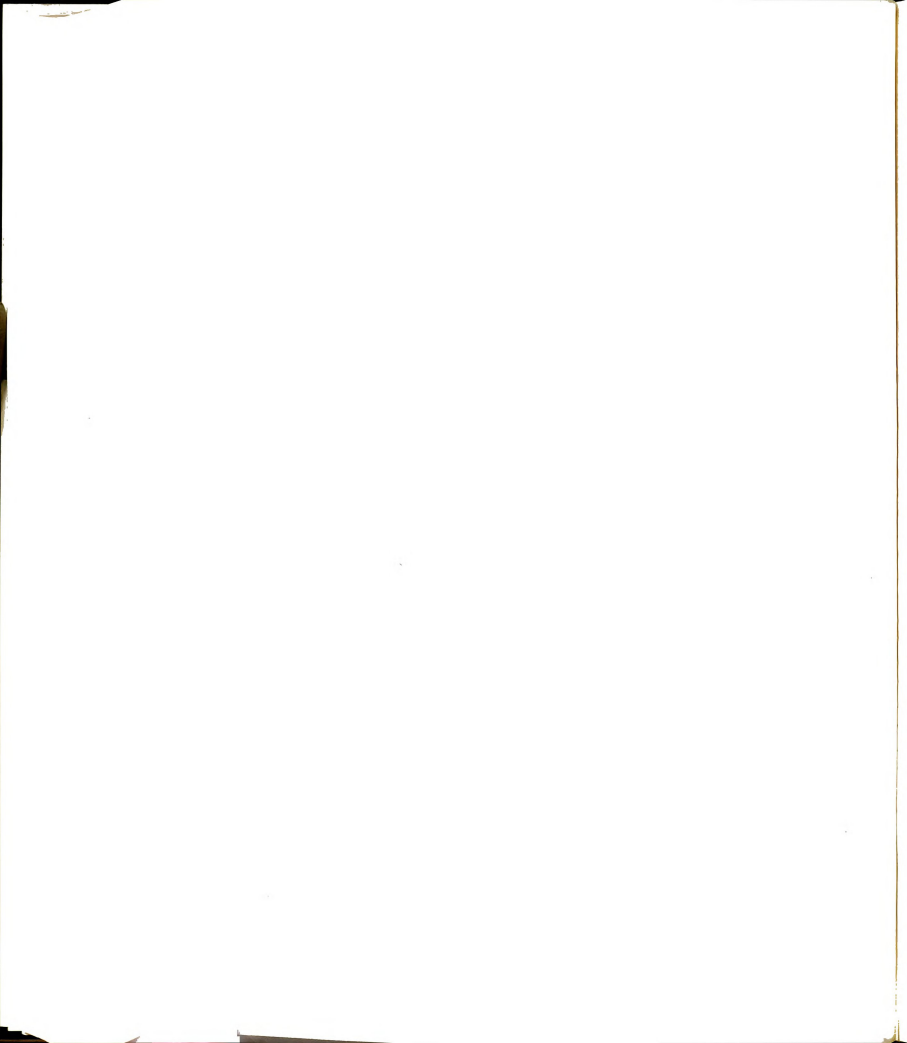


BIBLIOGRAPHY

- Lin, J. C., A. W. Guy and C. C. Johnson, "Power deposition in a spherical model of man exposed to 1-20 MHz electromagnetic fields," IEEE Transactions on Microwave Theory and Techniques, vol. MTT-21, No. 12, December 1973, pp. 791-797.
- Spiegel, R. J., "High-voltage electric field coupling to humans using moment method techniques," IEEE Transactions on Biomedical Engineering, vol. BME-24, No. 5, May 1977, pp. 466-472.
- Van Bladel, J., <u>Electromagnetic Fields</u>, McGraw-Hill Co., New York, 1964, pp. 274-279.
- Chen, K. M., S. Rukspollmuang and D. P. Nyquist, "Measurement of induced electric fields in a phantom model of man," presented in Symposium on Biological Effects of Electromagnetic Waves, Helsinki, Finland, August 1-8, 1978.
- Mousavinezhad, S. H., K. M. Chen and D. P. Nyquist, "Response of insulated electric field probes in finite heterogeneous biological bodies," IEEE Transactions on Microwave Theory and Techniques, vol. MTT-26, No. 8, August 1978, pp. 599-607.
- Johnson, C. C., C. H. Durney and H. Massoudi, "Long-wavelength electromagnetic power absorption in prolate spheroidal models of man and animals," IEEE Transactions on Microwave Theory and Techniques, vol. MTT-23, No. 9, September 1975, pp. 739-747.
- Van Bladel, J., <u>Electromagnetic Fields</u>, McGraw-Hill Co., New York, 1964, pp. 45-48.
- Massoudi, H., C. H. Durney and C. C. Johnson, "Long-wavelength electromagnetic power absorption in ellipsoidal models of man and animals," IEEE Transactions on Microwave Theory and Techniques, vol. MTT-25, No. 1, January 1977, pp. 47-52.



- Livesay, D., and K. M. Chen, "Electromagnetic field induced inside arbitrarily shaped biological bodies," IEEE Transactions on Microwave Theory and Techniques, vol. MTT-22, No. 12, December 1974, pp. 1273-1280.
- Wu, T. K. and L. L. Tsai, "Electromathetic fields induced inside arbitrary cylinders of biological tissue," IEEE Transactions on Microwave Theory and Techniques, vol. MTT-25, No. 1, January 1977, pp. 61-65.
- Poggio, A. J. and E. K. Miller, Computer Techniques for Electromagnetics, edited by R. Mittra, Pergamon, New York, 1973, pp. 159-170.
- Wang, J. J. H., "Numerical analysis of three-dimensional arbitrarily-shaped conducting scatterers by trilateral surface cell modelling," <u>Radio Science</u>, vol. 13, No. 6, November-December 1978, pp. 947-952.
- Müller, C., Foundations of the Mathematical Theory of Electromagnetic Waves, Berlin, New York: Springer-Verlag, 1969.
- Chen, K. M., "General solution of Maxwell equations in terms of sources and surface fields" (unpublished manuscript).
- 15. Harrington, R. F., <u>Time-Harmonic Electromagnetic</u> <u>Fields</u>, McGraw-Hill <u>Co.</u>, New York, 1961, pp. 106-116.
- 16. Schelkunoff, S. A., <u>Electromagnetic Waves</u>, D. Van Nostrand Co., New York, 1943, pp. 158-159.
- Harrington, R. F., <u>Field Computation by Moment Methods</u>, Macmillan, New York, 1968.
- Guru, B. S. and K. M. Chen, "Experimental and theoretical studies on electromagnetic fields induced inside finite biological bodies," IEEE Transactions on Microwave Theory and Techniques, vol. MTT-24, No. 7, July 1976, pp. 433-440.
- Morita, Nagayoshi, "Surface integral representation for electromagnetic scattering from dielectric cylinders," IEEE Transactions on Antenna Propagation, vol. AP-26, No. 2, March 1978, pp. 261-266.





MICHIGAN STATE UNIV. LIBRARIES
31293100634959